Fire Behaviour of Self-Consolidating Concrete-Filled Double Skin Steel Tubular Columns

Hui Lu

MEng, BEng

Thesis submitted in fulfillment of the requirements of the degree of

Doctor of Philosophy

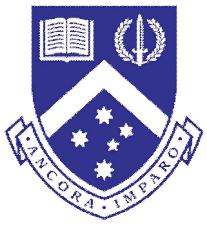

Department of Civil Engineering

Monash University

February 2010

ABSTRACT

The concrete-filled double skin tubular column (CFDST) is an innovative type of steel-concrete element which has potential for use as piers in bridges and columns in buildings. The use of self-compacting concrete (SCC) in CFDST is seen as a solution to resolve the challenge of concrete compaction in the columns. The behaviour of CFDST under static and cyclic loading at ambient temperature has been extensively studied. The fire performance of CFDST is crucial due to the direct fire exposure of the outer steel tube. Nevertheless, there is at present little information about the fire performance of CFDST. This thesis reports on research into the fire performance of SCC-filled CFDST columns. The research aims to understand the fundamental behaviour of SCC-filled CFDST columns under standard fire exposure by means of standard fire tests and finite element modelling and to develop guidance for fire resistance design of the columns.

Given the complexity in the responses of SCC-filled CFDST in fires, SCC-filled steel tubular stub columns (CFST), a specific type of CFDST without an inner steel tube, were selected for study in the first phase of the research program because of their simple configuration. Six SCC-filled CFST stub columns were prepared for standard fire tests and a finite element model to simulate the thermal and structural responses was developed. The main purpose of this phase of research was to develop a methodology for the further study of fire behaviour of CDFST columns by investigating how SCC affects the fire behaviour of composite columns and how steel tube affords confinement of the SCC to alter its behaviour at elevated temperature.

A series of standard fire tests for CFDST columns was conducted in the second phase of the research. Six CFDST columns and sixteen CFDST stub columns were prepared for standard fire tests. A further two CFDST stub columns were prepared as reference specimens to test the axial capacity at ambient temperature. The columns and stub columns in the tests represent slender and stub columns in authentic engineering practice in which the failure modes are buckling and compression failure respectively. Data obtained from the fire tests, i.e. temperatures, axial deformation, failure modes and fire resistance, were used to investigate the fire behaviour of the columns. Interaction among the three components in the columns during fire exposure was clearly shown in the tests. Such interaction is beneficial to the fire performance of CFDST columns.

Confinement of the tubes on the SCC prevents its spalling. Components which help each other through a load transfer mechanism are typical of the composite interaction in CFDST columns. Methods to enhance the fire resistance performance of CFDST, i.e. fire protection and steel fibre reinforced concrete, were also validated in the tests. In addition, the fire tests accumulated data to verify the numerical model in the subsequent research.

A finite element model was developed and used to study in detail the fire behaviour of CFDST columns and for the parametric study in the third phase of the research. An advanced finite element model which accounts for material and geometric non-linearity and the interaction of tubes and concrete was proposed to simulate the thermal and structural responses of CFDST columns under standard fire exposure. A concrete material model for confined concrete in CFDST at elevated temperature was developed accordingly. The model was then used to analyse the fire behaviour of the columns in terms of stress, strain and load share in components which cannot be obtained directly from fire tests. Yield of the inner steel tube was found to be a major cause of the final failure of the columns. The influence of a number of parameters on the fire resistance performance of the columns was investigated. The parameters which have significant influence on the fire resistance performance of the columns were identified.

Finally, guidelines for the fire resistance design of CFDST columns are proposed. These guidelines deal with how to appropriately select parameters for CFDST columns to ensure the columns achieve the anticipated fire resistance. Several practical design tables are also presented to illustrate how to use the guidelines to design CFDST columns to achieve a certain level of fire resistance.

PREFACE

This thesis is submitted to Monash University, Melbourne, Australia, in total fulfilment of the requirements for the degree of Doctor of Philosophy. The research work presented in this thesis was undertaken by the author in the Department of Civil Engineering as a PhD candidate during the period from June 2006 to January 2010 under the supervision of Prof. Xiao-Ling Zhao.

In accordance with Monash University Doctorate Regulations, the following original declarations are made:
To the best knowledge of the candidate, the thesis contains no material which has been accepted for the award of a degree or diploma in any university or institute, and no material has been published or written by another person, except where due reference is made in the text of the thesis.

The following papers, based on the research work presented in this thesis, have been jointly written with Prof. Xiao-Ling Zhao and Prof. Lin-Hai Han.

Journal papers

Lu H., Zhao X. L. and Han L. H., 2009, Fire behaviour of high strength self-consolidating concrete filled steel tubular stub columns, *Journal of Constructional Steel Research*, 65(10-11), pp. 1995-2010.

Lu H., Han L. H. and Zhao X. L., 2009, Fire performance of self-consolidating concrete filled double skin steel tubular columns: Experiments, *Journal of Fire Safety*, doi:10.1016/firesaf.2009.12.001.

Lu H., Zhao X. L. and Han L. H., submitted, Testing of self-consolidating concrete-filled double skin tubular stub columns exposure to fire, *Journal of Constructional Steel Research*.

Conference papers

Lu, H., Zhao, X.L. and Han, L.H., 2006, Fire resistance of SCC filled square hollow structural steel sections. In Proceedings of the *11th International Symposium on Tubular Structures*, Quebec, edited by Packer, J.A. and Willibald, S., (London: Taylor and Francis Group), pp. 403-410.

Lu, H., Zhao, X.L. and Han, L.H., 2007, Experimental investigation on fire performance of self-consolidating concrete (SCC) filled double skin tubular columns. In Proceedings of the *5th International Conference on Advances in Steel Structures*, Singapore, edited by Liew, J.Y.R. and Choo, Y.S. (Singapore: Research Publishing), pp. 973-978.

Lu H., Zhao X. L. and Han L. H., 2007, Finite element analysis of temperatures in concrete filled double skin steel tubes exposure to fires, In Proceedings of *the Fourth International Structural Engineering and Construction Conference (ISEC-4)*, Melbourne, edited by Xie Y. M. and Patnaikuni I., (London: Taylor & Francis Group), pp.1151-1156.

Lu H., Zhao X. L. and Han L. H., 2009, Tests on fibre reinforced SCC filled double skin tubular stub columns exposed to standard fire, In Proceedings of the *Fifth International Conference on Advances in Steel Structures*, Hong Kong, edited by Chen S. L., Chung K. F. and Wong Y. L., (Hong Kong: Hong Kong Institute of Steel construction), pp. 802-809.

Hui Lu

February, 2010

ACKNOWLEDGEMENTS

I am sincerely grateful to my supervisor Professor Xiao-Ling Zhao for his dedicated supervision, continuous support and encouragement, expert advice and friendship. His unending pursuit of excellence, hard work and a beautiful mind has been the main source of encouragement and inspiration for me. His academic excellence and scientific intuition have made him an exceptional academic to offer me invaluable advice and support in my research. Without his excellent expertise, this project would not have progressed. I am indebted to him more than he knows.

I gratefully acknowledge Professor Lin-Hai Han for his support, advice, recommendations, encouragement and friendship. As an expert in steel-concrete composite structures, he always provided insightful suggestions or comments when I had discussions with him, especially when he was a Visiting Professor at Monash University. Special thanks are due for his support for the experiments conducted in China through Project 50738005 from National Natural Science Foundation of China.

I would like to thank all the academic, administrative and technical staff in the Department of Civil Engineering and Engineering Faculty at Monash University. Many thanks go to Jenny Manson, Dominique Thomson and Jane Moodie. Thanks also go to Dr Alex Mcknight for providing assistance with proof-reading. Special thanks go to the technical staff in the Structures Laboratory, including Chris Power, the late Graeme Rundle, Long Kim Goh, Jeffrey Doddrell, Kevin Nievaart, Glenn Davis, Godwin Vaz and Mark Taylor, for their assistance in the experimental programme.

Similarly I would like to thank my postgraduate colleagues and friends in the department for their friendship, help and companionship. Thanks go to Hong-Bo Liu, Jimmy Haedir, Daniel Pang, Zhu Pang, Ren Zhao, Derek Chen, Tao Bai, Hayder Faleh and Siavash Hashemi.

I also gratefully acknowledge the support of Australian Tube Mills, Sika Australia Pty Ltd and Reoco Performance Fibres, for providing the materials used in the experimental

programme. The candidate also acknowledges Tianjin Fire Testing Laboratory in China to support fire tests of full size CFDST columns.

Last but no means least, I would like to convey my immense love to my dearest wife, Lin Jiang, my son, Si-Jie Lu and my parents. They often sacrificed their time during my candidature. Without the moral and emotional support of my family, this work would not have been possible.

Table of Contents

NOTATION

A_c	Cross-sectional area of concrete
$A_{concrete}$	Cross-sectional area of concrete in CFDST
$A_{c,nominal}$	Nominal cross-sectional area in CFDST ($A_{c,nominal} = \pi(D_o - 2t_o)^2/4$ for CHS CFDST and $A_{c,nominal} = (B_o - 2t_o)^2$ for SHS CFDST)
A_{inner}	Cross-sectional area of inner tube in CFDST
A_{outer}	Cross-sectional area of outer tube in CFDST
A_s	Cross-sectional area of steel in CFST
B	Width of SHS
B_i	Width of inner SHS in CFDST
B_o	Width of outer SHS in CFDST
c	Material specific heat
d	Distance form the inner surface of the outer tube
d_{max}	Maximum diameter of coarse aggregate (in mm)
D	Diameter of CHS
D_i	Diameter of inner CHS in CFDST
D_o	Diameter of outer CHS in CFDST
f'_c	Cylinder strength of concrete at ambient temperature
f_{ck}	Characteristic concrete strength (f_{ck}=0.67 f'_c for NSC)
f_y	Yield strength of steel at ambient temperature
$f_y(T)$	Yield strength of steel at elevated temperature
f_{yi}	Yield strength of inner steel tube at ambient temperature
f_{yo}	Yield strength of outer steel tube at ambient temperature
f_u	Ultimate strength of steel
G_f	Fracture energy of concrete at ambient temperature
G_{ft}	Fracture energy of concrete at elevated temperature
h_v	Heat convection coefficient
h_i	Heat contact conduction coefficient
k	Material thermal conductivity
K_c	Reduction factor on concrete strength
L	Length of a column
L_e	Effective length of a column
N_f	Load on column in fire test
N_u	Ultimate capacity of column at ambient temperature

q	Heat flux
r_f	Load level
t	Time or wall thickness of steel hollow section
t_i	Tube wall thickness of inner steel tube
t_o	Tube wall thickness of outer steel tube
t_{50}	The flow time from the sliding door to 50 cm away from the door in a L-box test
T	Temperature in Celsius
T_{cr}	Critical temperature
T_{limit}	Limiting temperature

α	Steel ratio for CFST column ($=A_s/A_c$)
σ	Stress or Stefan Boltzmann constant
ε	Strain
ε_f	Emissivity of fire
ε_m	Emissivity of steel
ξ	Confinement factor ($\xi = \frac{A_s \cdot f_y(T)}{A_c \cdot f_{ck}}$ for CFST and $\xi = \frac{A_s \cdot f_y(T)}{A_{c,nominal} \cdot f_{ck}}$ for CFDST)
λ_w	Heat for water vaporization
μ	Load level for CFST column
μ_0	Degree of utilization
ρ	Material density
χ	Cavity ratio for CFDST ($\chi= D_i/(D_o-2t_o)$ for CHS CFDST and $\chi= B_i/(B_o-2t_o)$ for SHS CFDST)

CFDST	Concrete filled double skin steel tubular column
CFST	Concrete filled steel tubular column
CHS	Circular steel hollow section
FRHSC	Fibre reinforced high strength concrete
HSC	High strength concrete
NSC	Normal strength concrete
SCC	Self-consolidating concrete
SHS	Square steel hollow section
SRC	Steel encased reinforced concrete column

Chapter 1

INTRODUCTION

1.1 BACKGROUND

Steel-concrete composite columns have been extensively used in buildings and other engineering structures. Traditionally, there have been two types of steel-concrete composite columns, namely steel-encased reinforced concrete (SRC) columns and concrete-filled steel tubular (CFST) columns. An SRC column is made up of a steel section fully or partially encased in concrete. A CFST column is formed by using concrete to in-fill a steel hollow section. In the last decades, a new type of steel-concrete composite column, known as the concrete-filled double skin steel tubular column (CFDST), has been proposed. CFDST columns consist of two concentrically-arranged steel hollow sections and concrete to fill the gap between the steel sections. CFDST columns originated from the idea of combining steel-concrete-steel sandwich panels and CFST columns to form an innovative steel-concrete composite column (Zhao and Han, 2006).

The composite action between the steel work and concrete in the sections results in SRC and CFST columns possessing high levels of structural performance, such as high load bearing capacity and seismic resistant ability. In addition, the bare steel sections in the columns offer support for the initial construction load and the concrete is cast around the steel section or the steel hollow section is in-filled later. This provides convenience in the construction process. Compared to SRC columns, CFST columns do not need formwork in construction and are more aesthetically appealing. Hence, CFST columns have received more attention than SRC columns since 1970s (Nethercot, 2004).

Many studies have been carried out to investigate the behaviour of CFDST columns under various loading conditions, as summarized in Zhao and Han (2006). The research results show that CFDST columns show behaviour similar to that of traditional types of composite columns, especially CFST columns. However, due to the additional inner tube and void in CFDST compared to CFST columns, there are a number of advantages for CFDST columns over CFST columns, such as lighter self-weight, better seismic performance in terms of high stiffness, ductility and energy dissipation ability, and higher local and global stability (Zhao and Han, 2006). Based on their structural performance, CFDST columns have potential for use as piers in bridges or viaducts over deep valleys or columns in high-rise and multistorey buildings.

One of the specific issues related to the construction of CFDST and CFST columns is the difficulty of compacting concrete in the columns. Self-consolidating concrete (SCC) is seen as a realistic option to resolve this difficulty. Several studies have been conducted to study the behaviour of SCC-filled CFST columns, beam-columns and beams (Han and Yao, 2004; Han et al, 2005; Han et al. 2006). It has been found that there are no significant differences in the behaviour of SCC and conventional concrete-filled CFST columns at ambient temperature. As with CFST columns, the issue of concrete compaction remains a challenge in CFDST columns during the construction process (Zhao and Han, 2006). The space to cast concrete in CFDST is more limited than that in CFST columns. Use of traditional concrete compaction methods, such as poker vibrators, may not achieve satisfactory concrete compaction in CFDST columns. Again, the use of SCC in CFDST columns is a promising and realistic solution to ensure that satisfactory concrete compaction is achieved in CFDST columns.

When investigating the structural performance of CFDST columns, one of the most important aspects is structural fire performance or fire resistance as the columns are to be used in buildings. Fire is one of the major risks to buildings. Current provisions in design codes require structural elements in a building to have a certain level of fire resistance to prevent the collapse of the building during evacuation and fire fighting. As a promising load-bearing element in buildings, CFDST columns should have adequate fire resistance to meet such requirements in design codes. CFDST columns are expected to have better fire performance compared to CFST columns due to the inner tube being well protected by the concrete (Zhao and Han, 2006). However, there is still a concern about the fire resistance performance of CFDST columns due to the direct fire exposure of the outer tube when the columns are in fires. Although the behaviour of CFDST columns under ambient temperature has been intensively studied, there is currently little information about the fire performance of CFDST available, as indicated in Zhao and Han (2006). It is therefore imperative to understand the fire performance of CFDST columns so that they can be used in buildings with confidence.

As SCC is used in CFDST columns, there is another concern in relation to how SCC affects the fire performance of the composite section. From the point of view of material mechanical properties, there are no significant differences between SCC and conventional concrete in the hardened state at ambient temperature (Holschemacher and Klung, 2002; Ouchi et al., 2003). Nevertheless, SCC is suspected to have a performance

different from conventional concrete under elevated temperature. Test results show that SCC tends to explosively spalling at elevated temperature, which is similar to the behaviour of high strength concrete (Persson, 2004; Noumowe et al., 2006). In CFDST columns, the concrete is enclosed by steel tubes. The steel tubes may provide confinement for the concrete to prevent the spalling of the SCC at elevated temperature. If spalling is prevented, SCC-filled CFDST columns are likely to have fire behaviour similar to conventional concrete-filled columns. All of these hypotheses need to be confirmed by in-depth investigation of the fire performance of SCC-filled CFDST columns.

Both CFST and CFDST columns have a steel tube at the exterior, which is directly exposed to fire when the columns are in fires. Such direct fire exposure will lead to temperatures in the exterior tube increasing more rapidly than the concrete and inner tube in CFDST columns and result in severe degradation in the mechanical properties and capacity of the exterior steel tube at elevated temperature. Research has demonstrated that CFST columns generally achieve a fire resistance of less than 30 min if there is no fire protection or other approach adopted (Han, 1998; Han, 2001; Han et al., 2003a; CIDECT, 1998; CIDECT, 1990). Three approaches currently exist in design codes or guidelines to enhance the fire resistance of CFST columns depending on the preference in different nations, i.e. the use of fire protection, steel fibre-reinforced concrete and reinforcement concrete in the columns (Eurocode 4, 2005; Kodur and Mackinnon, 2000; DBJ13-51, 2003). These approaches may also be applicable for CFDST with the exception of the reinforcement concrete approach. From the standpoint of engineering practice, the gap between the inner and outer tube in a CFDST section may not be able to offer enough space to conveniently install reinforcement in the section. Fire resistance of a column may be required up to 3h in buildings. Approaches to help CFDST columns to achieve anticipated fire resistance must be available. This is also an important component of the investigation of the fire performance of CFDST columns.

Many design solutions for the fire resistance of composite columns such as CFST columns have been proposed in design codes in various nations (Eurocode 4, 2005; Kodur and Mackinnon, 2000; DBJ13-51, 2003). Due to the similarity in the configuration between CFST and CFDST columns, these design solutions and guidelines can be use as references for CFDST columns, whereas they may not directly

apply to CFDST columns due to the unique configuration of CFDST columns. Relevant design solutions and guidelines for the fire resistance of CFDST columns need to be available.

1.2 OBJECTIVES

The ultimate goals of this research project are to understand the fundamental performance of SCC-filled CFDST columns under standard fire exposure and to develop design guidelines for the fire resistance design of CFDST columns.

The specific objectives of the research are as follows:

- To perform standard fire tests on SCC-filled CFST stub columns to investigate the effect of SCC on the fire performance of composite columns and develop a finite element model to simulate the fire behaviour of the columns. SCC-filled CFST stub columns are selected as the object of the preliminary research into the fire performance of SCC-filled CFDST columns.
- To perform standard fire tests on SCC-filled CFDST columns and stub columns to investigate the basic fire performance of the columns, in order to study the influence of certain parameters on fire performance, and to investigate how steel fibre reinforced concrete and fire protection affect the fire resistance performance of the columns.
- At the same time, to collect data from the fire tests to verify the numerical model used in the later study.
- To develop a finite element model to simulate the fire behaviour of CFDST columns. This model should be capable of simulating the thermal and structural responses of the columns under fire exposure.
- To develop a material mechanical property model for concrete in CFDST columns at elevated temperature.
- To verify the numerical model by comparing predicted results to the data from fire tests.
- To perform failure mechanism analysis using the proposed finite element model to discover the mechanism(s) causing the failure of the columns in fires. The outcomes of this analysis can be used to develop solutions to enhance the fire resistance performance of the columns.

- To perform parametric studies using the finite element method to identify parameters significantly affecting fire resistance performance.
- To develop design guidelines for the selection of appropriate parameters to ensure CFDST columns achieve certain fire resistance levels.
- To develop practical design tables for some typical CFDST columns and provide some typical examples of CFDST columns that can achieve fire resistance from 60 minutes to 180 minutes.

1.3 METHODOLOGY

The main methodologies used in the research are experiments and numerical modelling, briefly summarized as follows.

- Experiments

Standard fire tests were adopted as the experimental method in the current research. Standard fire testing is recommended by codes in many nations to determine the fire resistance of structural components, assemblies and structures. The standard fire tests in this research were adopted according to the provisions in AS 1534-1 (2005) which is equivalent to ISO-834 (1999). In addition to the fire resistance of the columns, other data such as failure modes, temperatures in the columns and axial deformation were obtained from the tests to investigate the fire performance of the columns.

- Numerical modelling

Finite element analysis was used as the numerical modelling method in the research. The finite element package ABAQUS (2008) was adopted in the modelling. This model is capable of simulating the thermal and structural responses of the columns. The finite element model was verified by the data from the fire tests, and the model was then employed to perform failure mechanism analysis and parametric studies.

1.4 OUTLINE OF THE THESIS

The chapters in this thesis are outlined as follows.

Chapter 1 contains an introduction to a new type of steel-concrete composite column, the CFDST column, and the significance of the use of SCC in CFDST columns is

briefly discussed. A gap in the knowledge of fire performance of CFDST columns is highlighted. The objectives and methodology of the research are also presented.

A review of the literature related to the current research is presented in Chapter 2, covering CFDST column behaviour at ambient temperature, structural fire safety, fire performance of CFST columns and properties of SCC. A gap to be filled in the knowledge of fire performance of SCC-filled CFDST columns is revealed and the significance of the research justified.

Standard fire tests of SCC-filled CFST stub columns and a finite element model to simulate the fire behaviour of the columns are presented in Chapter 3. Studies in this chapter are a preparation for the investigation of the fire performance of SCC-filled CFDST columns. Given the complexity of fire behaviour of CFDST columns, CFST columns are an appropriate starting point for the investigation of the effect of SCC on the fire behaviour of the CFDST because the CFST column is simpler in configuration than the CFDST. On the other hand, stub columns are preferred objects for the study of the effect of material properties on the performance of the columns due to the reduced effect of geometric non-linearity.

An experimental investigation into the fire performance of SCC-filled CFDST stub columns is presented in Chapter 4. The thermal and structural responses of the stub columns are obtained from standard fire tests. The fire behaviour of the columns and the composite action in the columns are studied by analysing the failure modes, critical temperature and fire resistance. Steel and polypropylene fibre SCCs are selected to enhance the fire resistance performance of the columns in the tests.

SCC filled CFDST columns under standard fire tests are presented in Chapter 5. The aim of the tests is to understand the fundamental fire behaviour of CFDST columns by analysing the failure modes, thermal and structural responses of the columns. The influence of a number of parameters on the fire performance is investigated. Fire protection coating is chosen as an approach to enhance the fire resistance performance of the columns in the tests.

A finite element model is proposed in Chapter 6 to simulate the thermal and structural responses of CFDST columns under fire exposure. A finite element package, ABAQUS,

is used in the modelling. Some key issues in the model are presented, such as material properties at elevated temperature, the steel and concrete interface and boundary conditions. The numerical model is verified by the fire test data presented in Chapters 4 and 5.

Chapter 7 presents detailed studies of the fire behaviour of CFDST columns with the aid of the proposed numerical model. Some data which cannot be obtained through fire tests, i.e. stress, strain, capacity and load share in the components, are thoroughly investigated. The failure mechanism of CFDST columns under fire exposure is then studied based on the above information.

Chapter 8 reports the results of a parametric study conducted using the finite element model. First, parameters which are likely to affect the thermal and structural responses of CFDST under fire exposure are identified. Then, the effect of these parameters on the thermal and fire resistance performance of CFDST columns is investigated. The purpose of this chapter is to identify those parameters significantly affecting the fire performance of CFDST columns.

Chapter 9 first summarizes those parameters which significantly influence the fire performance of CFDST columns, as revealed in Chapter 8. Then, design guidelines for the selection of appropriate parameters to ensure that CFDST columns achieve better fire resistance are presented. Finally, these design guidelines are used to develop practical fire resistance tables for several typical CFDST columns suitable for application in multi-storey and high-rise buildings.

Chapter 10 presents conclusions drawn from the main results and outcomes of this research. Recommendations and suggestions for further research are also proposed.

Chapter 2

LITERATURE REVIEW

2.1 INTRODUCTION

This chapter presents a review of current literature on the behaviour of CFDSTs at ambient temperature, structural fire safety, fire performance of concrete-filled steel tubular columns and the properties of SCC.

As an innovative type of composite member, concrete-filled double skin steel tubes (CDFST) have great potential to be used as piers and columns in construction. Knowledge of the structural behaviour and performance of CFDSTs under various loads, such as static, dynamic, earthquake and fire, is the basic foundation necessary for their engineering application. The first part of this chapter will summarize research on the behaviour of CFDST columns at ambient temperature under static and cyclic loading.

In addition to their behaviour under ambient temperature, the fire performance of CFDST columns needs to be understood before the columns can be used with confidence in buildings. The second part of the chapter reviews some general topics in structural fire safety including fire safety engineering, the behaviour of fire, and the material properties of steel and concrete at elevated temperature.

Little information is available about the fire performance of CFDST columns. However, CFDST is similar to CFST as both have a steel tube at the exterior of the component which is directly exposed to fire when the columns are under fire exposure. A review of research on the fire performance of CFSTs is the third part of this chapter which aims to discover information or methodologies helpful for the investigation of the fire performance of CFDSTs.

The use of self-consolidating concrete (SCC) in CFDSTs can provide convenience for construction and assurance of construction quality. SCC has unique characteristics different from conventional concrete. The final part of the chapter presents a review of the basic characteristics of SCC.

2.2 BEHAVIOUR OF CFDST UNDER AMBIENT TEMPERATURE

2.2.1 Steel and concrete composite columns

Concrete and steel are two of the most extensively-used construction materials in modern engineering structures. In most cases, these two materials work together as a structural element in engineering practice. The most common elements are reinforced concrete and steel-concrete composite structures. Steel-concrete composite structure refers to structures which use steel and concrete formed together into a component in such a way that the resulting arrangement functions as a single item (Nethercot, 2004).

A steel-concrete composite structure is a structural system which consists of one or more composite components. The typical composite components are composite beam, composite floor and composite column. The origin of composite beam, floor and column dates back to 100 years ago. With the development of construction technologies and research in composite structures, composite beams and floor systems were well accepted by the 1960s all over the world (Nethercot, 2004). However, the development of composite columns fell far behind. Even in the 1990s, most of the steel bridges and buildings in the USA were constructed with composite beams or girders, but only a few were built using composite columns (Galambos, 2000).

Composite columns originated from the idea of using concrete around the steel columns to provide fire protection for the columns (Nethercot, 2004; Uy, 1998). Their use became popular in multistorey buildings and bridge structures, and gained the name “steel reinforced concrete” or SRC (Narayanan, 1998; Nethercot, 2004). A typical cross-section of SRC columns is shown in Figure 2.1 (a). Apart from SRC columns, there is another type of composite column called a concrete filled steel tubular column (CFST) as shown in Figure 2.1 (b). The difference between SRC and CFST columns is the location of the steelwork. The steelwork located at the exterior surface of the column means that CFST columns have a more attractive appearance than SRC columns (Nethercot, 2004). In addition, there are many advantages of CFST columns compared to SRC columns. The most significant ones are that CFST columns do not need reinforced bars in the columns and temporary formwork during construction. Due

to these advantages, CFST columns have become a preferred option in structures to SRC columns.

(a) Steel reinforced concrete columns (b) Concrete-filled steel tubular columns

Figure 2.1 Typical cross-section of steel-composite columns

Before the 1950s, CFSTs were occasionally used as bridge piers or columns for industrial buildings. At that time, the bearing capacity of the composite columns was considered simply the sum of the in-filled concrete and the steel tubes. The composite action between these two materials was ignored. Extensive research into CFSTs began from the 1960s and 1970s. Several publications have reviewed and summarised the developments in research, design codes and engineering application of CFST columns. Shanmugam and Lakshmi (2001) reviewed the research into steel-concrete composite columns, including SRC and CFST columns. Kvedaras and Sapalas (1999) introduced the research into and practice of CFSTs in Lithuania. Han and Zhao (2003) reviewed the development of CFST in China. Galambos (2000) briefly reviewed the steel and steel-composite design and research in USA in recent years. Uy (1998) introduced the application of CFST box columns for multistorey buildings. Nishiyama and Morino (2004) studied the earthquake performance of CFSTs in a US-Japan cooperative research program.

Researchers have also tried to find approaches to further enhance the performance of CFST columns, such as the use of high strength and high performance steel and concrete (Gho and Liu, 2004; Uy, 2001; Uy and Patil, 1996; Varma et al., 2004; Young and Ellobody, 2006; Ellobody et al. 2006), or to extend the application range of CFST columns by the use of other metal material as the tube, such as stainless steel and aluminium (Ellobody and Young, 2006; Zhou and Young, 2008; Zhou and Young, 2009). The use of self-compacting concrete (SCC) in CFST columns is an innovative approach to the improvement of construction quality and thus to ensure the structural performance of CFST columns. In the construction procedure of CFST structures, the builder generally starts to build steel beams and unfilled steel tubes for several stories before concrete is placed into the hollow steel tubes to form CFST columns.

Compacting the concrete in the hollow steel tubes is difficult under such a construction procedure. SCC offers a solution to resolve this problem. In addition, SCC can reduce the environmental impact and labour costs. There has been some research on the behaviour of SCC CFST columns. The behaviour of SCC CFST columns has been found to be similar to that of normal concrete-filled columns under ambient temperature (Han and Yao, 2004). The fire performance of CFSTs filled with SCC is similar to that of CFSTs filled with high strength concrete (HSC) at elevated temperature (Lu et al., 2006).

In addition to the use of high strength and high performance materials to improve the behaviour of CFST columns, other innovative approaches have also been developed (Ge and Usami, 1992, Huang et al. 2002; Tao et al., 2005; Xiao et al., 2005). The concrete-filled double skin steel tubular column (CFDST) is one of them. CFDSTs originated from the idea of steel-concrete-steel sandwich panels (Zhao and Han, 2006). CFDSTs consist of two concentrated steel tubes and concrete to fill the gap between the two tubes. Typical profiles of CFDST columns are shown in Figure 2.2.

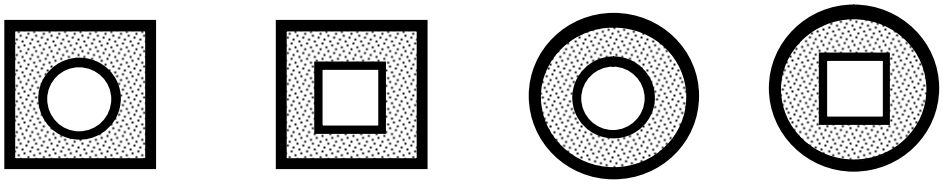

Figure 2.2 Typical profiles of CFDST columns

Due to its good performance, CFDST has great potential to be used as piers or columns in high-rise viaducts over deep valleys or in engineering structures, such as multistorey buildings and offshore structures (Zhao and Han, 2006).

2.2.2 Behaviour of concrete-filled double skin tubular columns at ambient temperature

Concrete-filled double skin tubes, as shown in Figure 2.2, are one type of double skin composite construction. Another type of double skin composite construction in this category is steel-concrete-steel sandwich double skin panels. Typical profiles of double skin panels are shown in Figure 2.3.

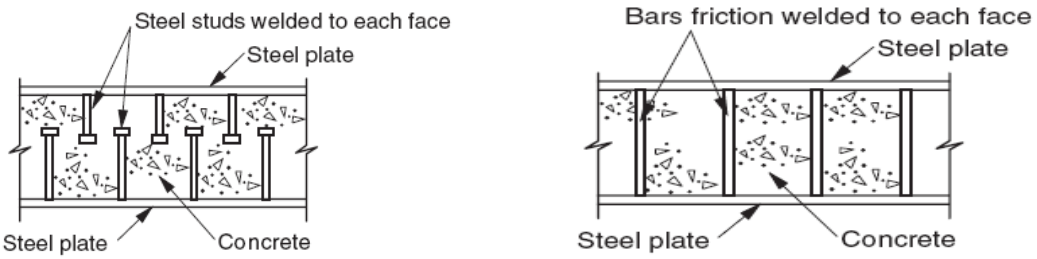

Figure 2.3 Typical profiles of double skin panels (Wright et al., 1991; Corus, 2006)

The origin of CFDSTs comes from the idea of combining double skin panels with CFSTs (Zhao and Han, 2006). However, CFDSTs and double skin panels have quite different mechanical behaviours. Double skin panels are mainly used as slabs, walls or cores in structures where the primary loads are flexural and shear forces. CFDSTs are potentially useful as columns, in which the load is axial compression.

In the early stage of application, CFDSTs have been used as vessels under high pressure in very deep water (Montague, 1975) and as compressive members in offshore structures (Wei et al., 1995b). CFDSTs have also been used as piers in high-rise bridge construction (Lin and Tasi, 2005; Nakanishi et al., 1999; Yagishita et al., 2000). In recent years, CFDSTs have been found to have great potential for use as columns in building structures (Zhao and Han, 2006). Many studies to date have concerned the behaviour of CFDSTs as columns or beam-columns.

It is well known that composite action exists in CFSTs (Han, 2007). Such interaction is also present in CFDSTs. When investigating polymer concrete-filled circular double skin tubular stub columns, it was found that the peak load of CFDST was greater than the simple sum of the capacity of the tubes and concrete (Wei et al., 1995b). Similar phenomena have been observed by other researchers (Tao et al., 2004; Zhao et al., 2002b). This indicates that there is a favourable interaction among tubes and concrete in CFDSTs which enhances their overall performance. In addition, concrete in CFDSTs changes the failure mode of the steel tubes in the columns. The failure mode of the outer tube is outward folding buckling, but the failure mode of the inner tube is either inward folding for circular hollow section (CHS) or inward and outward folding for square hollow section (SHS) (Elchalakani et al., 2002; Han et al. 2004; Tao and Han, 2006; Tao et al., 2004; Wei et al., 1995b; Zhao and Grzebieta, 2002; Zhao et al., 2002a; Zhao

et al., 2002b). This indicates that the core concrete provides strong support to the outer tube to change its failure mode, but concrete offers much less support to the inner tube.

Many studies have been conducted of CFDST stud columns to investigate their capacity (Elchalakani et al., 2002; Tao et al., 2004; Wei et al., 1995b; Zhao and Grzebieta, 2002; Zhao et al., 2002b; Zhao et al., 2010). Wei (1995a, 1995b) proposed a model to predict the strength of polymer concrete-filled double-skin stud columns (CHS for both inner and outer tubes). In this mode, no interaction between the concrete and inner tubes was considered and the interaction between concrete and outer tube was considered only when the tube had yielded. A simple formulation was proposed to predict the strength of CFDSTs (Zhao and Grzebieta, 2002; Zhao et al., 2002a; Zhao et al., 2002b; Zhao et al., 2010). A reduction factor of 0.85 was adopted for CFDSTs with RHS outer tube. In fact, this reduction factor is used to take into account the difference in the composite action for columns with CHS and RHS as inner and outer tubes. A plastic mechanism method was also proposed to predict the collapse behaviour of CFDSTs (Zhao et al., 2002a). A mechanics model for CFDSTs, similar to that used in CFSTs, has been proposed (Han et al. 2004; Tao and Han, 2003; Tao and Han, 2006; Tao et al., 2004) to predict the behaviour of CFDST columns. The interaction between the outer tube and concrete was considered in this model. Based on this model, formulations were also proposed to predict the capacity of CFDSTs (Han et al. 2004).

The materials to in-fill the gap between tubes can be cement-based concrete or other types of concrete, such as polymer concrete. The polymer concrete-filled CFDST has been found to have structural behaviour similar to the cement concrete-filled column (Wei et al. 1995a; Wei et al. 1995b). In addition, the outer tubes can be steel or other materials, such as FRP. The concept of hybrid FRP-concrete-steel tubular columns has been proposed (Teng et al., 2006). The outer FRP jacket cannot sustain any longitudinal load but provides confinement of the core concrete. The concrete is capable of delaying the occurrence of the local buckling of the inner steel tube in such a case. A confined concrete stress-strain model developed from FRP-confined concrete solid columns is applicable to this type of hybrid column (Teng et al., 2006).

The flexure behaviour of CFDST has been investigated by Zhao and Grzebieta (2002), Lin and Tasi (2005), Han et al. (2004) and Tao and Han (2006). The moment capacity of CFDSTs was found to be higher than CFSTs (Lin and Tasi, 2005). CFDST beams failed in a ductile way similar to CFST beams, but the local buckling of outer steel tube in CFDST beams was more significant than in CFST beams (Tao and Han, 2006). The failure mode of the steel tubes in CFDST beams is the same as CFDSTs in compression, outward folding buckling of the outer tube and inward folding buckling of the inner tube at the compressive zone (Han et al., 2005; Zhao and Grzebieta, 2002). A method to predict the ultimate moment capacity of CFDST beams has been proposed (Zhao and Grzebieta, 2002). An analytical model has also been proposed to analyse the behaviour of CFDST beams (Han et al., 2004; Tan and Han, 2003; Tao and Han, 2006; Tao et al., 2004). A simplified model to calculate the moment capacity of CFDST beams has also been proposed (Tao and Han, 2006). The flexural stiffness of CFDSTs has been compared to the relevant design codes (Han et al. 2006). The design codes AIJ (1997), AISC-LRFD (1999), BS5400 (1979) and Eurocode 4 (2005) overestimated the initial flexural stiffness of CFDSTs with CHS outer tubes, and reasonably predicted that of CFDSTs with SHS outer tubes with the exception of AIJ (1997). The flexural behaviour of hybrid FRP-concrete-steel composite beams has also been investigated (Teng et al., 2006; Yu, 2006). The outer FRP is orientated along the hoop direction and can only provide confinement on the concrete. The inner tube plays an important role in resisting the external load in such hybrid beams.

CFDST beam-columns have also been investigated (Han et al., 2006; Han et al., 2004; Nakanishi et al., 1999; Tao Han, 2006; Tao et al., 2004). Failure of CFDST beam-columns is usually overall buckling and normally no local buckling at the compressive zone of the specimens occurs (Han et al., 2004; Tao and Han, 2006; Tao et al., 2004). A mechanical model similar to that used to analyse CFDST stub columns and beams is proposed to analyse the behaviour of CFDST beam-columns. Based on the analytical analysis, simplified formulations to calculate beam-column capacity which account for M-N interaction have been developed. The behaviour of CFDST beam-columns is found to be generally similar to CFST beam-columns (Han et al., 2004; Tao and Han, 2006; Tao et al., 2004).

In order to investigate the capacity of CFDSTs to resist earthquake load, some specific performance features of CFDST, such as flexural stiffness, ductility, energy absorption ability and ability to resist cyclic load, have also been studied. Stub CFDST columns have very good ductility and energy absorption ability compared to empty steel tubes (Elchalakani et al., 2002; Lin abd Tasi, 2005; Zhao et al., 2002b). The stub column can retain 50% of the peak strength even when axial strain is as high as 0.03 (Han et al., 2004; Lin and Tasi, 2005; Tao and Han, 2006; Tao et al., 2004). Good energy dissipation capability and ductility have also been found in cyclic loading tests on CFDST columns (Han et al., 2006; Lin and Tasi, 2005; Nakanishi et al., 1999).

Research on CFDSTs under other types of load, such as resistance to the penetration of accidental local loading, has also been carried out (Corbett et al., 1990). Increasing the filler thickness or the inner tube stiffness significantly increases the ability to resist local penetration loading, such as collision.

It can be seen that the behaviour of CFDSTs has been intensively investigated. CFDST columns have been found have many advantages, such as light weight, high flexural stiffness, good energy absorption and ductility. However, almost all the research to date on CFDST columns has focused on their behaviour under ambient temperature. Very little information about the performance of CFDST columns under fire exposure is available. Fire is one of the major risks to building structures. Structural components in building structures are required to have sufficient fire resistance to ensure the fire safety of the structures. Therefore, the fire performance of CFDST columns should be understood before they can be confidently used in building structures.

2.3 STRUCTURAL FIRE SAFETY

2.3.1 Structural fire safety

Fire is one of the major threats to life and property. Statistical data from 16 industrial countries show that fires killed 1 to 2 in 100,000 inhabitants and damaged properties costing 0.2% to 0.3% of GNP in a typical year in the countries surveyed (The Concrete Centre, 2004). In order to prevent and reduce the losses caused by fires, an engineering discipline called fire safety engineering has been developed to investigate fires and the interactions between fire and the environment. Topics in fire safety engineering include

control of the ignition and spread of fire, control of means of escape, detection of fire and the prevention of structural collapse. These topics are briefly explained as follows.

- Control of the ignition and spread of fire

Control of the ignition of fire can be achieved by limiting flammable sources in structures and implementing fire risk management strategies such as bans on smoking. A traditional methodology to control the rapid spread of fire is to divide the space in the structures into compartments vertically, horizontally or a combination of the two (Purkiss, 2007).

- Control of means of escape

This can be achieved by the implementation of statutory requirements for the provision of escape routes and the training of occupants of the structures.

- Detection of fire

The main purposes of fire detection are to warn the occupants and aid the occupants to evacuate safely at the early stage of a fire. Therefore, the fire detection system generally consists of three systems; (i) a system to inform occupants to evacuate, (ii)a smoke-control system to eliminate toxic smoke so that the occupants can evacuate safely and (iii) a fire-fighting system enabled manually or automatically when fire occurs.

- Prevention of structural collapse

This topic concerns the prevention of the collapse of the structure for a sufficient period of fire exposure during the evacuation stage and fire fighting stage. To achieve this goal, elements in the structures must be designed to possess enough load capacity to prevent the collapse of the whole structure for a period of time. The period of the time in which a structural element can have enough capacity to resist load is the fire resistance of the element.

As can be seen from the outline above, fire safety engineering is a comprehensive discipline which covers a wide range of issues related to fire, people and structures. There is a sub-discipline, called structural fire engineering (safety), in fire safety engineering. Structural fire safety deals with specific aspects of passive fire protection by analysing the thermal effect of fires on buildings and designing members for adequate load bearing resistance and control of the spread of fire (Bailey, 2006).

Structural fire engineering (safety) is a discipline concerned with the prevention of collapse of structures. The structures or components in structures are subjected to both thermal actions from fire and external load. Therefore, the responses of the structures or structural components include thermal and structural responses.

There has been intensive research into the structural fire safety of various structures and structural components in concrete, steel and steel-composite structures (Bailey, 2002; Fabriel, 2000; Bennetts, 2002; Lawson, 2001; Plank, 2000; Sakumoto and Asito, 1995; Thomas and Bennetts, 1998; Wang, 2005). Due to the differences in the material properties of steel and concrete, the responses of concrete, steel or steel-concrete composite structures or structural components have their own typical characteristics. Concrete has lower thermal conductivity than that of steel. This allows concrete structures more easily to achieve better fire performance than steel structures. Steel-concrete composite structures have fire performance between the two. Steel-concrete structures have been seen as an approach to improve the fire performance of steel structures (Wang, 2005; Wang and Kodur, 2000).

A basic research methodology in structural fire safety is standard fire tests in which a structural component is tested under standard fire temperature (ISO-834, 1999). However, there are a number of drawbacks of the fire test method. For example, it is expensive and time consuming, there are limitations on specimens and it is not possible to consider the effects of various factors such as load level and constraints (Purkiss, 2006). In addition to experimental methods, numerical modelling has become a well-accepted methodology in research into structural fire safety (Wang, 2003). There are many advantages of numerical methods. The obvious ones are that such methods are cost-effective and are able to account for the effects of various factors. However, standard fire tests may still be necessary for a number of reasons, such as for the development and verification of the numerical methods.

Based on the research outcomes, design guidelines, recommendations and calculation methods have been proposed in design codes to design for or calculate the fire resistance of structural components and structures (Eurocode 2, 2005; Eurocode 3, 2005; Eurocode 4, 2005; ECCS, 1983; ECCS, 1988). A prospective approach is generally

used in these design codes or recommendations. This approach is based on interpreting data from standard fire tests on structural components or assemblies. Therefore, the fire resistance of a structure is based on the consideration of the fire resistance of individual components. If each component is adequate for a given level of fire resistance, the whole structure is deemed to be safe. Generally, there are design guidelines for the selection of parameters for a structural component and calculation methods to calculate the thermal and structural responses of the component in order to design a structural component to achieve a given level of fire resistance in the prospective approach. This is a simple and practical methodology to assess or design structures to achieve a given level of fire resistance. However, there are also a number of drawbacks for this methodology. One of the drawbacks is that the interaction among components has been ignored. This may lead to a conservative or uneconomic result. In addition, standard fire temperature may not represent real fire severity in structures. Due to the prospective approach being based on the outcomes from standard fire tests, it may not be able to realistically predict the fire performance of a component in a real fire situation.

In recent years, with developments in structural fire safety, the concept of performance-based structural fire safety has been proposed and has attracted the attention of researchers (Johann et al., 2006; Meacham, 1997; Wang, 2003). The performance-based approach aims to overcome drawbacks in the prospective approach to offer safer and more economic solutions for the fire safety of structures. The performance-based approach involves modelling of fire in the structure, and thermal and structural analysis of the structure. The performance-based approach is more complicated than the prospective approach. It requires theoretical knowledge, empirical information, and analytical capability and technology (Johann et al., 2006). However, it can offer tailored fire safety solutions for structures.

2.3.2 Behaviour of fire

As discussed in the above section, fire compartment is a traditional method used in fire safety engineering to prevent the spread of fires in buildings. Therefore, fire in a building generally occurs in an enclosed space in a building that is separated from other parts of the building. Hence, fires in buildings are generally referred to as compartment fires in fire safety engineering. The course of a compartment fire can be divided into several stages in terms of fire temperature and the fire exposure time relationship.

Figure 2.4 shows an idealized fire temperature versus time relationship in a compartment fire (Karlsson and Quintiere, 2000). As can be seen, the whole course of a compartment fire is divided into the following stages, ignition, growth, flashover, fully developed fire and decay.

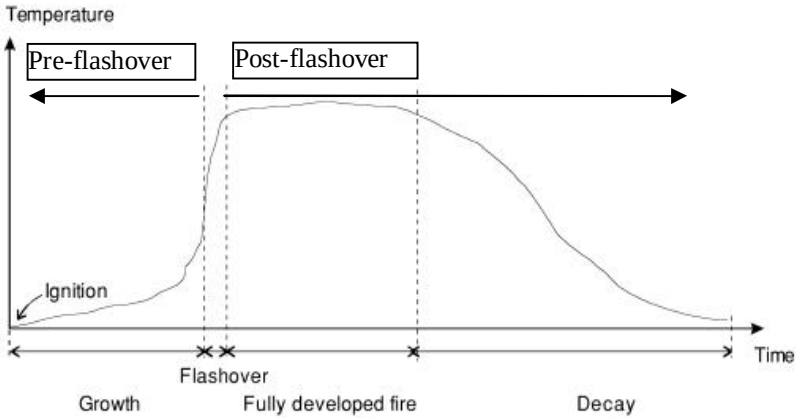

Figure 2.4 Idealized temperature and fire exposure time relationship in compartment fire (Karlsson and Quintiere, 2000)

Ignition is an exothermic action accompanied by the combustion process. In the growth period the fire can grow at a slow or fast rate, depending on a series of factors (Karlsson and Quintiere, 2000). The temperature increases dramatically in a short time in the flashover period with the compartment temperature reaching 500-600^{o}C. The temperature reaches the highest value and remains almost constant in the fully developed fire period. Then the temperature begins to decrease in the decay period as the fuel depletes gradually.

From the point of view of fire safety engineering, the course of a compartment fire can be divided into two broad stages, pre-flashover and post-flashover plus a transition stage, flashover, as shown in Figure 2.4. In the pre-flashover fire stage, the growth of fire may be accompanied by smoke while the temperature remains low. What is of most concern in this stage is the safety of human beings. Fire detectors, alarm systems, smoke control systems and sprinklers are expected to activate to help the occupants evacuate safely. The post-flashover stage in a compartment fire includes the fully developed fire and decay periods. Temperatures can reach as high as 1000 ^{o}C in the post-flashover fire stage which may last for hours. In this stage, structural stability is the issue that is of

most concern. (Karlsson and Quintiere, 2000). Hence, the post-flashover stage of compartment fire is related to structural fire safety.

In order to assess the structural fire safety of a building, the course of a compartment fire's temperature must be known. Several numerical models have been proposed to predict the post-flashover stage of compartment fires, such as the one-zone (Purkiss, 2006), two-zone (Florian Kettner, 2006; Karlsson and Quintiere, 2000) and CFD models (Karlsson and Quintiere, 2000). Based on numerical modelling, formulations to describe the relationship of fire temperature and fire exposure time in the post-flashover stage can be developed (SFPE, 2002). Parameters related to the compartment and source of fire, such as the geometric properties of the compartment, openings and the thermal properties of boundary materials, are required in the formulations. The fire temperature versus fire exposure time relationship obtained by this method is generally called a parametric fire (Karlsson and Quintiere, 2000).

As discussed in the previous section, one of the basic methodologies in the study of structural fire safety is to perform standard fire testing. Standard fires refer to fires defined by different national standards organizations in terms of fire temperature versus time relationship. For example, ISO-834 fire (AS-1530.4, 2005; ISO-834, 1999) is the standard for furnace tests of structural components, assemblies or structures. Standard fire tests aim to reasonably represent temperatures attained in most building fires. However, it should be noted that standard fires neither represent the fire behaviour likely to be experienced nor the most severe fire conditions in practice (Margaret, 1986). Despite their limitations, standard fire tests offer a great amount of data to establish a prescriptive approach for the assessment or design of structural fire safety in design codes. In addition, a performance-based approach for structural fire safety has also been developed based on the results and observations from standard fire resistance tests (Bailey, 2006). The prospective approach in the codes of various nations remains a well-accepted methodology to assess the fire safety of structures although it may produce conservative results. Hence, the standard fire test is still needed at the current stage (Lie, 1992).

Because the severity of standard fires cannot realistically reflect that of real compartment fires, approaches have been proposed to equate the severity of standard fires to that of real compartment fires (Harmathy, 1978; Purkiss, 2006). Purkiss (2006) summarized several of the approaches, such as a time equivalence approach based on the same temperature rise in the element, and a time equivalence approach based on the consideration of equivalence in heat input. In such a way, the fire resistance of a structural component obtained from standard fire tests can be approximately equivalent to that in a real compartment fire which has fire severity different from that of the standard fire.

2.3.3 Material properties of concrete and steel at elevated temperature

2.3.3.1 Thermal properties

The thermal response of structural members in fires follows energy conservation laws. Material density, thermal conductivity and specific heat of materials are three material thermal properties involved in the laws. These material thermal properties are necessary input data in the thermal analysis of structural members in fires (Lie, 1992).

When concrete or steel is exposed to fires, chemical and physical changes may occur. Such changes cause variation in the thermal and mechanical properties of concrete and steel at the elevated temperatures.

The crystalline structure of carbon-based structural steel undergoes transformation during exposure to fires. The transformation in structural steel is believed to occur at a temperature at and above $600^{o}C$ (Harper, 2004). This transformation affects the mechanical properties of steel more severely than the thermal properties.

The density of steel can normally take its density at ambient temperature (Purkiss, 2006). The thermal conductivity and specific heat of structural steel are temperature-dependent. There have been several models proposed to describe the temperature-dependence of thermal conductivity and specific heat of structural steel. In the models of Eurocede 3 (2005) and Lie and Irwin (1995), the conductivity of the steel decreases

with the increase of temperature until the temperature reaches 800 to 900^{o}C and then remains constant. In the BSI models (1990), thermal conductivity is independent of temperature. The specific heat of steel increases with an increase in the temperature (ECCS, 1983; Eurocode 3, 2005; Lie and Irwin, 1995), but there is a peak value of specific heat at around 730^{o}C in the models of Eurocode 3 (2005) and Lie and Irwin (1995), at which temperature phase change of steel occurs.

The thermal properties of concrete are more complex than those of steel because concrete is a composite material which consists of cement, aggregate, water and other chemical ingredients. The thermal properties of concrete depend on the properties of every ingredient, their proportion in the mixture, moisture content and movement of the moisture during elevated temperatures, and physical and chemical changes of the ingredients at elevated temperature. When the temperature elevates from ambient temperature to 1200 ^{o}C, concrete experiences a series of chemical and physical changes (Bazant and Kaplan, 1996). Such changes lead to variation in the thermal properties of concrete.

Several models to describe concrete's thermal properties have been proposed such as those in Eurocode 2 (2004) and proposed by Lie and Caron (1988) and Lie and Chabot (1998). The conductivity of concrete tends to decrease when the temperature increases. The conductivity of high strength concrete is higher than normal-strength concrete due to the denser microstructure in high strength concrete. There is an obvious difference in the thermal properties of the concrete with different coarse aggregates, i.e. siliceous and carbonate aggregates. Eurocode 2 (2004) provides a unique formulation to calculate the specific heat of concrete regardless of what type of aggregate and whether normal or high strength concrete is used. The models proposed by Lie and colleagues (Lie and Caron, 1988; Lie and Chabot, 1998) take into account the effect of aggregate type and normal/high strength concrete on the thermal properties of the concrete.

2.3.3.2 Mechanical properties

Like the material mechanical properties at ambient temperatures, material properties such as yield stress, ultimate stress, modulus of elastic, stress-strain relationship are used to describe the mechanical behaviours of materials at elevated temperatures. Of

them, the stress-strain relationship is the most comprehensive. Other mechanical properties can be derived from this relationship.

Unlike at ambient temperature, the deformation of steel and concrete at elevated temperatures is not only caused by stress, but also by thermal expansion and concrete incompatibilities between mortar and aggregate in concrete (Purkiss, 1986). The total strain of steel and concrete at elevated temperatures may consist of the following sub-strain (Li and Purkiss, 2005; Purkiss, 1986),

$$\varepsilon_t = \varepsilon_{th}(T) + \varepsilon_{\sigma}(\sigma, T) + \varepsilon_{cr}(\sigma, T, t) + \varepsilon_{tr}(\sigma, T) \tag{2.1}$$

where, ε_t is the total strain, σ is the corresponding stress, T is the temperature, and t is time. ε_{th} is the thermal strain induced by thermal expansion, ε_{σ} is stress-related strain, ε_{cr} is the classic creep strain, and ε_{tr} is the transient strain. Transient strain is induced by the incompatible deformation in the ingredients in concrete. Therefore, transient strain exists only in concrete.

In all sub-strain components, as thermal strain is the only one which is independent of stress, it is usually treated individually and excluded from the stress-strain relation. There are two types of stress-strain models available for concrete and steel, called general and detailed here. The general model implicitly incorporates all the sub-strain components into a comprehensive stain component in the stress-strain model, whereas the detailed model explicitly expresses the relationship between stress and each sub-strain component.

Many general stress-strain models for structural steel at elevated temperature have been proposed. Ramberg-Osgood (1943) proposed a three parameter stress-strain model. A model to describe the stress-strain relation of steel at elevated temperature was proposed by Lie and Irwin (1995) for the investigation of the fire behaviour of CFSTs. Eurocode 3 (2005) provides a stress-strain model for structural steel at elevated temperature. Chen and Young (2006; 2007) investigated the mechanical properties of cold-formed steel material at elevated temperature and a stress-strain model was proposed for the corner parts of cold-formed steel sections. Chen and Young (2006a) also conducted research on the mechanical properties of stainless steel at elevated temperature. In a study of

conventional strength steel S355, Outinen et al. (1997) found that Eurocode 3 (2005) can predict the mechanical properties well; however Ramberg-Osgood's model (Ramberg-Osgood, 1943) cannot predict the stress-strain-temperature relationship well.

Detailed models have been proposed for the stress-strain relation of structural steel at elevated temperatures. There are two sub-strain components in the models, stress related strain and creep strain components (Anderberg, 1988; Poh, 1998; Poh, 1997).

Creep of steel at elevated temperatures can be generally divided into three periods: primary, secondary and tertiary creep stages (Poh, 1998; Zeng et al., 2003). Creep strain increases with time significantly in the primary stage and increases dramatically in the tertiary stage, but is relatively stable in secondary stage which lasts for a long time. The creep of steel was found to be obvious only when the temperature rises above 450^{o}C (Twilt, 1988). Although the explicitly detailed model for steel is highly recommended for structural fire analysis (Bennetts, 2002; Poh, 1998), it has been found that the use of detailed models is not necessary for structural elements under standard fire conditions (Twilt, 1988).

Due to concrete being an inhomogeneous material, the mechanical properties of concrete are affected by a number of factors, for example, the type of coarse (Lie and Caron, 1988; Lie and Chabot, 1998). Normal strength concrete (NSC has mechanical performance different from that of high strength concrete (Phan and Carino, 1998).

There is a transient strain component in formulation (2.1), which is only available for concrete. Until Anderberg and Thelandersson (1976) conducted transient state tests on concrete with constant stress, it has been found that transient strain was an important sub-strain components in concrete at elevated temperature (Purkiss, 1986). There are several factors which are considered as causes of transient strain, including incompatibilities in mortar and aggregate, the application of instantaneous loading during test, and the imposition of temperature gradient during heating (Purkiss, 1986). Ignoring transient strain at significant axial compressive load at high temperature, such as the case of columns, may cause unsafe results in numerical modelling (Li and Purkiss, 2005).

Many stress-strain models have been proposed for concrete at elevated temperatures (Anderberg and Thelandersson, 1976; Eurocode 2, 2004; Khoury, 1995; Khoury et al., 1986; Lie, 1992; Schneider, 1986). All sub-strain components specified in Eq. 2.1 except thermal strain are included in these concrete stress-strain models either explicitly or implicitly. In stress-strain models for concrete, some of the models explicitly express each strain component (Anderberg and Thelandersson, 1976), some combine two strain components together (Khoury, 1995; Khoury et al., 1986; Schneider, 1986) and others express the result as a total strain (Eurocode 2, 2004; Lie, 1992). Li and Purkiss (2005) compare several stress-strain models and point out that Anderberg and Thelanderson's and Schneider's models are more applicable to predict the behaviour of concrete at elevated temperature when strain softening occurs in the strain history. In addition, the model in Eurocode 2 (2004) might cause unsafe results in some cases (Li and Purkiss, 2005).

2.4 FIRE BEHAVIOUR OF CONCRETE-FILLED STEEL TUBULAR COLUMNS

There is little information available about the fire performance of CFDST columns. However, CFDST columns are similar to CFST columns because both types have an exterior steel tube which is directly exposed to fire and concrete behind the exterior steel tubes. Hence, the research results for the fire performance of CFST columns can be used for reference for CFDST columns. Since the 1980s, intensive research into the fire performance of CFST columns has been conducted in European, North American and Asian countries. Design guidelines, tables, diagrams and formulations have been proposed for the fire resistance design of CFSTs..

2.4.1 Research in European countries

Researchers in the UK conducted a series of tests on fire performance in the 1980s. A design methodology for fire endurance of CFST columns was proposed for unprotected and protected CFST columns. The use of reinforcements or steel fibre reinforced concrete was recommended for columns without fire protection to help the columns achieve better fire resistance performance. The load level was identified as an important factor influencing the fire performance of the columns. Fire insulation was recommended as another option to enhance the fire performance of the columns (British Steel Tubes and Pies, 1990; British Steel, 1990).

Hass reported on fire tests of 43 circular and square CFST specimens with plain and reinforcement concrete and proposed a numerical method to calculate fire endurance (1991). Klingsch (Klingsch, 1985; Klingsch, 1991) reported tests on about 100 CFST specimens at elevated temperatures, in which reinforcements were used. There was no protection for the specimens. A numerical model was proposed to predict the thermal and structural responses of the columns under fire exposure. The simulated results were conservative compared to the test results. The interaction between concrete and steel at elevated was not considered in the numerical model.

Wang (1997; 1999; 2000) used numerical methods to calculate the fire endurance of CFSTs and proposed a simplified method to calculate the fire endurance of circular CFSTs (Wang and Orton, 2008). Ding and Wang (2008) proposed a finite element model to simulate the fire behaviour of CFST columns. The predicted results match the test results well. The effect of constraints on the fire behaviour of the CFST columns was also studied (Wang and David, 2003; Ding and Wang, 2006).

A series of investigations into the fire resistance of CFSTs was completed by CIDECT (CIDECT, 1988; CIDECT, 1990; CIDECT, 1998; CIDECT, 2000; CIDECT, 2004a; CIDECT, 2004b). Reinforcement and steel fibre was used as means to improve the fire performance of the CFST columns without fire protection. The fire performance of high strength concrete (HSC) filled CFSTs was also investigated. The use of HSC in CFST columns was found to negatively affect the fire performance of the columns. A FE model with updated Lagrange description was proposed to simulate the behaviour of CFSTs at elevated temperatures. Geometrical and material non-linearity and interaction of steel and concrete were considered in the model. The predicted results are consistent with the test results (CIDECT, 2004b; Renaud et al., 2003).

Based on the research conducted in European countries, design tables, diagrams and formulations for calculating the fire resistance of CFST columns were proposed and incorporated into design codes and recommendations in Europe, such as ECCS-Technical Committee 3 and Eurocode 4 (ECCS, 1988, Twilt et al., 1996; Eurocode 4, 2005). No fire protection is recommended for CFST columns in Europe. Instead,

reinforcement is recommended as a method to help the columns to achieve a certain level of fire resistance. Load level, cross-section dimension, reinforcement ratio and concrete cover for the reinforcement are factors which determine the fire resistance of CFST columns in the simple design tables. In addition, the use of advanced methods, such as numerical modelling, is recommended as an option to analyse the fire performance of CFST columns.

2.4.2 Research in North American

From the 1980s, a series of standard fire tests of CFST columns was carried out in Canada to investigate the fire behaviour of the columns. At the early stage of research, the CFST columns were filled with plain concrete (Lie and Chabot, 1992a; Lie and Stringer, 1994). The fire resistance of the CFST columns filled with plain concrete can achieve 1 to 2h if the load on the columns is limited at a low level. The type of coarse aggregate in the concrete was found to affect the fire resistance of CFST columns (Lie and Caron, 1988; Lie and Chabot, 1998). CFST columns filled with carbonate aggregate concrete generally have a fire resistance 10% higher than columns filled with siliceous aggregate concrete (Kodur, 1999). For columns at high load level or which need greater than 2h fire resistance, two methods to enhance the fire endurance of CFST columns were employed in later research. These were the use of reinforcement or steel fibre in the concrete (Kodur and Lie, 1996; Lie, 1994; Lie and Irwin, 1995; Lie and Kodur, 1996a; Lie and Stringer, 1992). These two methods can effectively improve the fire resistance of CFST columns. Columns filled with reinforcement concrete can achieve higher fire resistance than columns filled with steel fibre-reinforced concrete. The fire resistance of CFST columns filled with high strength concrete was found to be worse than the columns filled with normal concrete (Kodur, 1997; Kodur et al., 2004a).

A numerical model was proposed to study the behaviour of CFST columns at elevated temperatures (Anchor et al., 1986; Kodur and Lie, 1996; Lie, 1994; Lie and Chabot, 1990; Lie and Irwin, 1995; Lie and Kodur, 1996a; Lie and Stringer, 1994). This model is a simplified model to predict the temperature distribution and the axial deformation of CFST columns under fire exposure. The fire resistance of the columns can also be obtained through the axial deformation versus fire exposure time curves. In order to use the numerical model to predict the fire behaviour of CFST columns, models to describe temperature dependent on the thermal and mechanical properties of concrete (normal strength , high strength and steel fibre-reinforced concrete) and steel were also proposed

(Kodur and McGrath, 2003; Lie and Kodur, 1996b). The interaction of the steel and concrete was not considered in the numerical model.

The numerical model was then used to study the influence of parameters on the fire resistance performance of CFST columns (Kodur, 1998; Lie & Kodur, 1996). Several parameters which have significant influence on fire resistance performance have been identified. Based on the parametric studies, simplified formulations to predict the fire resistance of CFST columns and design guidelines were proposed (Kodur, 1998a; Kodur, 1998b; Kodur, 1999; Kodur and Machinnon, 2000). These formulations and guidelines were incorporated into design codes or recommendation in Canada and USA (Kodur and Machinnon, 2000). For columns filled with plain concrete, fire resistance may achieve 1 to 2 h if the load on the columns is limited at a low level. For columns with high load level or which need higher fire resistance, bar-reinforced or steel fibre-reinforced concrete should be used (Kodur and Lie, 1997; Kodur and Machinnon, 1998; Kodur and Machinnon, 2000; Kodur, 2005).

2.4.3 Research in Asia

Countries in Asia, such as Japan, South Korea, Australia and China, have carried out extensive research into the fire resistance of CFSTs.

Patterson et al. (1999) conducted fire resistance tests on circular and square CFSTs filled with high strength concrete. A numerical model proposed by BHP Research has been used for parametric studies (BHP Research, 1991). Load ratio, slenderness, size, load eccentricity and initial imperfection were identified as primary factors which affect the fire endurance of CFST (BHP Research, 1991; O'meagher et al, 1991).

In South Korea, Kim et al., (2000) conducted fire resistance tests on 8 circular and square CFSTs and proposed a numerical method for predicting fire endurance.

Investigations into the fire resistance of CFST columns have been carried out in Japan (Okada et al., 1991; Sakumoto et al., 1994). The steel for the steel tubes was normal structural steel and fire-resistant steel. The fire resistance performance of CFST columns with fire-resistant steel was found to be better than CFST columns with normal

structural steel. It was also found that eccentric load has an adverse influence on the fire endurance of CFST columns compared to concentrically loaded columns.

A Rankine method was proposed to analysis the fire resistance of RC and CFST columns (Tan and Tang, 2004). It was found that the proposed method was able to predict the fire endurance of RC and CFST columns.

Comprehensive research on fire resistance of CFST has been conducted in China (Han, 1998; Han, 2000; Han, 2001; Han et al., 2003, 2003a, 2003b, 2003c, 2003d; Han et al., 2007). A number of standard fire tests were carried out for CHS, SHS and RHS CFST columns. The concrete used was normal strength concrete, high strength concrete and SCC. Instead of using reinforcement or steel fibre reinforced concrete to enhance the fire resistance of CFST columns, fire protection coating was used. The load ratio for columns was generally greater than 0.6 and both concentric and eccentric load cases were included in the fire tests. A simplified numerical model was proposed to predict the fire behaviour of CFST columns. In this numerical model, a temperature-dependent constitutive model for concrete was also proposed. Unlike other material property models for concrete in CFST columns, this concrete constitutive model considers the confinement of the steel tube on the concrete, which results in the concrete having a higher peak load, larger strain corresponding to the peak load and a more gradually descending branch in the stress-strain curves at elevated temperature. This influence weakens as the temperature increases. Parametric studies were carried out with the aid of the numerical model. Parameters significantly influencing the fire resistance of CFST columns were identified. Finally, based on the parametric studies, simplified formulations were proposed to calculate the fire endurance of CFST columns with and without fire protection. For CFST columns without fire protection, the load level on the columns is recommended to be limited to a certain value so that the fire resistance can achieve a certain level of fire resistance, normally less than 1h. However, for columns with fire protection, the fire resistance of the columns is achieved by selecting an appropriate thickness of fire protection coating.

2.4.4 Summary

After reviewing relevant research conducted by researchers in different nations, some findings can be summarized as follows:

- Fire resistance performance of CFST columns is better than steel tubes alone. Plain concrete-filled CFST columns may achieve 1 to 2 h fire resistance if the load on the columns is limited at a low level.
- There are options to improve the fire resistance performance of CFST columns if the load level is high or high fire resistance performance is needed. In European countries, the use of reinforcement in CFSTs is recommended in the design codes. In North America, the use of steel fibre concrete or reinforcements in CFST is recommended to enhance the fire resistance performance of the columns. In China, fire protective coating is the preferred option to improve the fire resistance performance of the columns.
- The methodology to investigate the fire behaviour of CFST columns consists of experiments and numerical modelling. Standard fire tests are the basic experimental method in the studies. Simplified and finite element analysis numerical models are two approaches in numerical modelling.
- Several material property models for steel and concrete at elevated temperature have been proposed. Confinement of steel tube on the concrete is neglected in some models, whereas some material models consider the influence of confinement on the mechanical properties of concrete.
- The proposed numerical models have been used to carry out parametric studies to identify the influence of various parameters on the fire resistance performance of CFST columns.
- Data from parametric studies have been used to develop practical formulations, tables and diagrams for the fire resistance design of CFST columns. Related design guidelines have been proposed accordingly.

2.5 PROPERTIES OF SELF-CONSOLIDATING CONCRETE

Self-consolidating concrete is a concrete which has the ability to fill formwork by its weight without the aid of external forces. The concept of self-compacting or consolidating concrete was originally proposed by Professor Hajime Okamura of Kochi University in 1986. The first publication about SCC was presented at the 2nd East-Asia

and Pacific Conference on Structural and Construction in 1989 (Okamura and Ouchi, 2003; Vachon, 2002). Since that time, research into and applications of SCC have spread around the world.

2.5.1 Mixture of SCC

The unique behaviour of SCC is its high deformability, passing ability and ability to resist segregation at the fresh and plastic states before hardening (Hwang et al., 2006). In order to achieve the goal of self compaction, the amount of the coarse aggregate in the concrete mixture has to be reduced in order to decrease friction and collision in the aggregates, whereas the amount of paste has to be increased to improve fluidity and achieve enough viscosity to avoid the blockage of coarse aggregate when passing through obstacles (Okamura and Ouchi, 2003). A diagram comparing a typical mixture of SCC and conventional concrete is shown in Figure 2.5, where W represents water, C represents cement, S represents sand and G represents coarse aggregate.

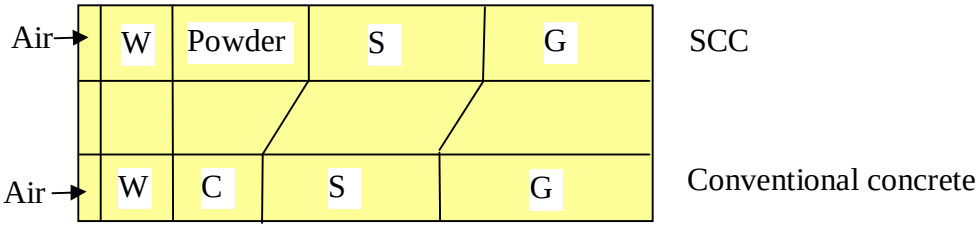

Figure 2.5 Comparison of mix proportion between SCC and conventional concrete (Okamura, 1997)

Several SCC mixture design methods have been proposed. One of the methods used is the so-called Japanese method suggested by the Japanese academics who proposed the concept of SCC. In this mixture design method, workability of the concrete is achieved by reducing the amount of aggregate and increasing the amount of powder in the mixture. At the same time, superplasticizer is used to maintain moderate viscosity and low shear stress in the concrete to resist segregation (Okamura, 1997). A large amount of powder materials and low water-powder ratio are characteristics of the SCC mixture developed by this method.

A simple mix design method for SCC with small amounts of powder has been proposed by Chinese academics. This is the so-called Chinese method (Su et al., 2001; Su and

Miao, 2003). The main idea in this method is to use binder to fill the voids of the aggregate piled loosely (Su et al., 2001). A parameter called the packing factor was proposed to link aggregate content to concrete workability. The SCC developed from this method generally has lower amounts of cement and powder in the mixture. As a result, the strength of the SCC developed from this method is generally in the medium strength range, 30 to 60 MPa.

In Europe, a mixture design method has been developed using the packing theory (Brouwers and Radix, 2005). Concrete was thought of as consisting of water and solids. Here solids include not only coarse and fine aggregates, but also cement, flay ash and furnace blast slag. The amount of aggregate and binder can be determined by selecting an appropriate grading curve (Brouwers and Radix, 2005).

2.5.2 Methods for test workability of SCC

The workability of fresh SCC is the most unique characteristic of the concrete. In order to evaluate the workability of fresh SCC, several new test methods have been developed. Among them, the slump flow, L-box, V-Funnel and J-Ring test methods are well-accepted because of their convenience for both laboratory and in-situ tests. Schematic diagrams of these apparatus are shown in Figure 2.6.

In addition to the test methods to evaluate the workability of the SCC, indexes corresponding to these test methods have also been proposed by organizations in different nations, such as EFNARC (2002), PCI (TR-63, 2003), JSCE (1999), RILEM (Skarendahl and Petersson, 2001), SCA (Association, 2002) and ACI (2007). Hwang et al., (2006) summarize the workability indexes for SCC in different guidelines. After further investigation, Hwang et al (2006) found that a combination of two test methods shown in Figure 2.6 was sufficient to evaluate the workability of SCC (Hwang et al., 2006), such as the combination of the slump cone test and the L-Box test.

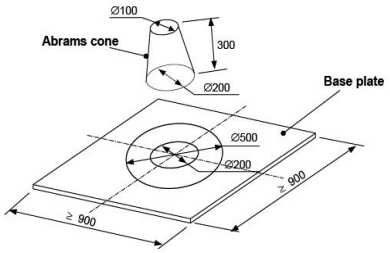

(a)Slump flow test

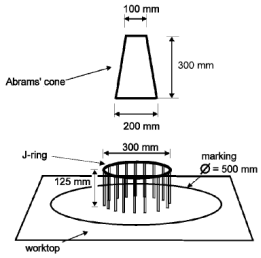

(b) J-Ring test

(c) L-Box test

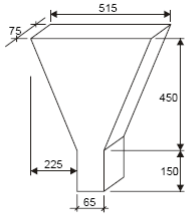

(d) V-Funnel test

Figure 2.6 Schematic diagram of apparatus for test workability of SCC (Schtter, 2005; ACI,2007)

2.5.3 Behaviour of hardened SCC

The properties of hardened SCC have been found to be similar to those of conventional concrete. Typical behaviour of hardened SCC is summarized as follows:

- Compressive strength

SCC compressive strength at 28 days is not significantly different from that of conventional concrete when their mix proportions are similar (Holschemacher and Klung, 2002; Ouchi et al., 2003).

- Tensile strength

The tensile strength and the tensile/compressive ratio of SCC is in the same order of magnitude as conventional concrete, but it is generally higher than that of conventional concrete when the compressive strength is the same (Brouwers and Radix, 2005; Dehn et al., 2000, Holschemacher and Klung, 2002; Ouchi et al., 2003).

- Elastic modulus

The ratio of elastic modulus to compressive strength of SCC follows the rule for conventional concrete (Ouchi, 2003; Persson, 2001), but the elastic modulus is a little lower than that of conventional concrete (Bonen and Shah, 2005; Holschemacher and Klung, 2002; Ouchi et al., 2003; Persson, 2001).

- Bond strength

The bond strength of SCC and reinforcements is generally higher than conventional concrete (Dehn et al., 2000; Ouchi, 2003).

- Shrinkage

Shrinkage of hardened SCC is either similar to (Persson, 2001) or higher than conventional concrete (Bonen and Shah, 2005).

2.5.4 Fibre reinforced SCC

In recent years, several studies of fibre-reinforced self-consolidating concrete (FRSCC) have been conducted (Grunewald and Walraven, 2001; Nehdi and Ladanchuk, 2004). The aim of these studies is to develop FRSCC in order to enhance the performance of SCC (Grunewald and Walraven, 2001) under elevated temperature conditions.

The use of fibre in SCC adversely affects the workability of the concrete (Grunewald and Walraven, 2001; Nehdi and Ladanchuk, 2004). The type of fibre (steel or/and Polypropylene), shape and size of the fibre, and the amount of fibre in concrete are key factors affecting the workability of fibre-reinforced SCC. By optimizing these factors, it is possible to obtain a fibre-reinforced SCC which can meet the workability requirements and have better mechanical performance.

2.5.5 Behaviour of SCC at elevated temperature

Some research has been conducted on the performance of SCC at elevated temperature (Blontrock and Taerwe, 2002; Noumowe et al., 2006; Persson, 2004; Reinhardt and Stegmaier, 2006). Some behaviours of SCC exposed to fire have been confirmed consistently, whereas remain controversial as outlined in the following section:

- Spalling

Persson (2004) and Noumowe et al. (2006) found that SCC has a higher risk of spalling under fire exposure compared to conventional concrete. However, no obvious differences in spalling behaviour of SCC and conventional concrete under fire exposure were observed by Blontrock and Taerwe (2002) and Reinhardt and Stegmaier (2006).

- Effect of polypropylene fibre on spalling of SCC

The use of polypropylene fibre in SCC can effectively reduce the risk of spalling in SCC.

2.6 CONCLUSIONS

Based on the foregoing review of research in the fields of steel-concrete composite columns, concrete-filled double skin tubes, structural fire safety, fire resistance of concrete-filled steel tubular columns and the properties of self-compacting concrete, some findings can be drawn.

- The concrete-filled double skin steel tube (CDFST) is an innovative kind of composite member which has great potential to be used as piers and columns in construction. CFDST columns have the advantages of light weight, high flexural stiffness, high energy absorption ability, high ductility and better fire resistance when compared to concrete-filled steel tubes and steel members (Zhao and Han, 2006).
- The behaviour of concrete-filled double skin tubes at ambient temperature has been intensively studied. Formulations to predict the capacity of the columns have been proposed. The composite action between the steel tubes and concrete in CFDSTs is the key factor which contributes to the good performance of the element. Due to the specific configuration of CFDSTs, compaction of the concrete in the columns may be difficult during construction. The use of SCC is a practical option to resolve this problem. SCC not only offers convenience in construction but also provides assurance of construction quality by ensuring that the composite action is able to develop well in the columns.
- Compared to the comprehensive studies conducted on the behaviour of CFDSTs at ambient temperature, little information about the performance of CFDST under fire exposure is currently available. Fires are one of the major risks for buildings. Structures are required to have sufficient fire resistance in the case of fires. Therefore, the fire performance of CFDSTs needs be understood before they can be used in buildings with confidence.
- Standard fire tests are one of the fundamental methodologies in the study of structural fire safety, although there are drawbacks to this method. In addition, standard fire tests are the foundation of prospective approaches in current design codes to assess or design the structural fire safety of structures.

Numerical modelling is another well-accepted methodology in this field. The numerical modelling method offers a possibility to investigate the objects over a broader range which cannot be achieved by fire tests. Material properties at elevated temperature critically affect the fire performance of structures under fire exposure. A model to describe such temperature-dependent material properties is an important part of the numerical modelling.

- Due to the similarities in the profiles of CFSTs and CFDSTs, the methodologies and outcomes of the research into the fire performance of CFSTs can be used as reference points to investigate the fire performance of CFDSTs. CFST columns have better fire resistance performance than steel tubes alone and are seen as a way to improve the fire resistance of steel tubes alone. Several options have also been proposed to enhance the fire resistance of CFSTs when higher fire performance is required, namely the use of steel fibre concrete, reinforcement and fire protection. However, it should be borne in mind that there are also differences between the profiles of CFDST and CFST columns. The behaviour of CFDSTs may be more complicated then CFSTs due to the increased number of components in CFDSTs. It is important to reveal the unique characteristics of CFDSTs under fire exposure.
- The major differences between SCC and conventional concrete are in the fresh stage of the concrete. The concrete mixture of SCC is dissimilar to that of conventional concrete so that SCC can have increased workability. Guidelines have been proposed to design mixtures of SCC. The mechanical properties of SCC in the hardened stage are generally similar to conventional concrete at ambient temperature. However, it is generally believed that SCC has a higher risk of spalling like high strength concrete at elevated temperature than conventional normal strength concrete, although this is a controversial point of view. When SCC is used in CFST or CFDST columns, a concern may arise over whether the use of SCC affects the fire performance of the composite columns. Hence, special attention needs be paid to the fire performance of SCC-filled CFST and CFDST columns.

Chapter 3

Fire Behaviour of High Strength Self-Consolidating Concrete (SCC)-Filled Steel Tubular Stub Columns

3.1 OVERVIEW

There have been many studies of the fire resistance of concrete-filled steel tubular (CFST) columns. However, almost all the studies have been related to slender CFST columns. The typical failure mode of slender CFST columns is buckling of the entire column both at ambient and elevated temperatures, whereas the typical failure mode of CFST stub columns at ambient temperature is compression failure. Nevertheless, there is limited study into the fire behavior of CFST stub columns at elevated temperature. Self-consolidating concrete (SCC) has become a popular solution for engineers in reinforced concrete and steel-concrete composite structures. The fire behaviour of SCC-filled CFST therefore requires research.

This chapter presents an investigation into the behaviour of high-strength SCC-filled steel tubular stub columns exposed to standard fire. A series of tests were carried out to obtain the temperature distribution, axial deformation, limiting temperature of steel and fire endurance of the SCC-filled steel tubular stub columns. In addition, a finite element analysis (FEA) model was proposed and used to simulate the fire behaviour of the columns. The verified FEA model was used to analyse the structural behaviour of the columns under fire exposure and finally to gain insight into the failure mechanism of the columns.

The CFST stub can be used as a reference object for later research on CFDST columns. In addition, the FEA model proposed in this chapter can be further extended and revised to simulate the fire behaviour of CFDST columns.

3.2 EXPERIMENTAL PROGRAM

3.2.1 Material Properties

3.2.1.1 Steel

Cold-formed C350L0 square hollow sections (SHS) were used in the testing program. The sizes (width and thickness of the SHS) are given in Table 3.1. The SHS was manufactured using the cold-forming process in accordance with Australian Standard AS1163 (1991). A typical manufacturing process involves five steps: (1) uncoiling and joining coils to ensure a continuous production; (2) forming the steel strip into a circular

shape using a series of rollers; (3) welding using ERW (Electric Resistance Welding) to form a circular hollow section (CHS); (4) sizing and shaping using a series of rollers to turn the CHS tube into a square or rectangular hollow section (SHS or RHS); and (5) cutting and bundling. A detailed description of each step can be found in Zhao et al (2005).

Table 3.1 Parameters of specimens

Specimen	Width (mm)	Thickness (mm)	Load Eccentricity (mm)	Load (kN)	Ultimate capacity (kN)	Load level μ	Fire Endurance (min)	Predicted fire endurance (min)	T_{lim} (^{0}C)
S1R2E0	150	5.0	0	486	2787	0.17	>90	92	920
S1R4E0	150	5.0	0	1216	2787	0.44	26	23	521
S1R4E2	150	5.0	25	808	2049	0.39	55	57	819
S2R3E0	200	6.0	0	1226	4702	0.26	55	80	649
S2R4E0	200	6.0	0	1800	4702	0.38	43	46	595
S2R4E1	200	6.0	25	1350	3702	0.36	43	49	637

The mechanical properties of steel, i.e. elastic modulus, yield stress and ultimate stress, were obtained through tensile coupon tests according to Australian Standard AS 1391 (2007). The coupons were cut from the flat face of the SHS along the longitudinal direction of the section. The measured mechanical properties of the steel are summarized in Table 3.2.

Table 3.2 Mechanical properties of steel

Steel Hollow Section	Elastic modulus (GPa)	Yield stress (MPa)	Ultimate tensile strength (MPa)
150×150×5	197	486	558
200×200×6	199	467	544

3.2.1.2 Self-consolidating concrete

The most important characteristic of SCC is its high workability in the fresh state. In order to obtain such high workability, the mixture of SCC is designed different from conventional concrete. Besides, some unique test methods are used to check the flow

ability of SCC. Mixture of the SCC in the test program is shown in Table 3.3. The coarse aggregate was basalt.

Table 3.3 Mixture proportion of self-consolidating concrete (kg/m3)

Water	Cement	Fly ash	Sand	Coarse aggregate	Superplasticizer
178	380	170	776	831	11

There are several techniques available for testing the workability of fresh SCC such as slump cone, L-Box and J-Ring. Slump cone and L-Box tests were used in this investigation. The schematic diagram of L-Box and the test of SCC sample in L-Box are shown in Figure 3.1. The flow time from the sliding door to 40cm ($T40$) away from the door, the flow speed, and other data were recorded. The fresh properties of the SCC mixture are summarized in Table 3.4.

Table 3.4 Workability of the self-consolidating concrete

Slump (mm)	Slump flow (mm)	T_{50} (s)	T_{40} (s)	H_1 (mm)	H_2 (mm)	Flow speed (mm/s)
273	694~740	3.1	3.6	530	60	110.5

Concrete cylinders were also prepared to determine the compressive strength of the concrete. Some of the cylinders were cured in standard conditions for testing the standard strength at 28 days. Some were cured in the same conditions as that of CFST specimens and tested on the same day when the CFST specimens were tested. The cylinder compressive strength of the concrete at 28 days and the average cylinder strength in the days of the CFST specimens testing were 90 and 99 MPa, respectively.

(a) Slump flow test of SCC

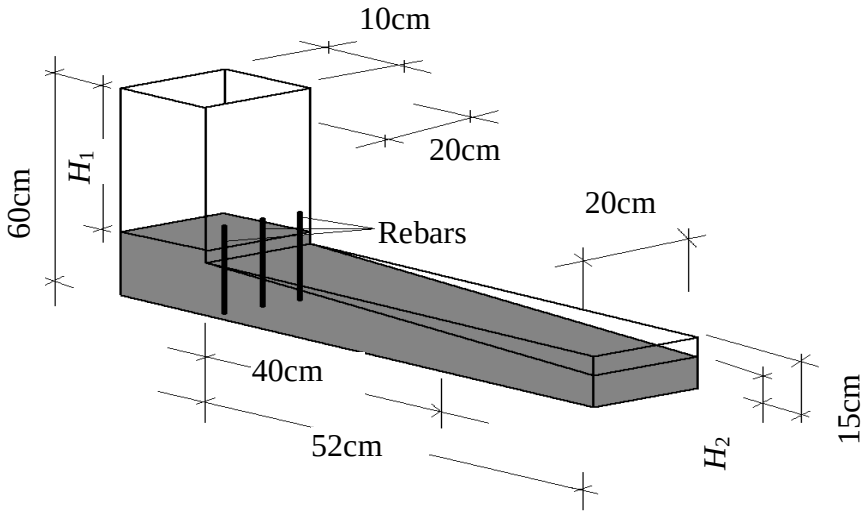

(b) Schematic diagram of L-Box

(c) Test of SCC in L-Box

Figure 3.1 Tests to determine the workability of SCC

3.2.2 Specimens

Six high strength SCC filled square stub columns were prepared. Parameters of the specimens are shown in Table 3.1. The total length of all specimens was 760 mm. Several factors which were found sensitive to the fire endurance of conventional concrete filled CFST columns were chosen as variable parameters, i.e. cross section size, load case and load level. Two cross section sizes of the steel hollow sections were prepared for the specimens. Load cases were either concentric or eccentric load. The load level or degree of utilization (μ) in Twilt et al. (1996) is defined as the ratio of load applied in fire test to ultimate capacity of a column at ambient temperature. Design guidance on minimum load level was given in Twilt et al. (1996) for μ of 0.3 to 0.7. Considering high strength concrete was used, the load level in the columns was likely lower than that specified in Twilt et al. (1996). The load level was chosen ranging from 0.17 to 0.44 in the current tests.

3.2.3 Experimental Procedure

Firstly, the steel hollow sections were cut to the designated length. A hole for ventilating vapour in the concrete at elevating temperature was drilled at the middle height of every steel hollow section. In order to acquire temperatures in the specimens, three thermocouples were installed in every specimen. The position of the thermocouples in the specimens is shown in Figure 3.2. One was located at the interface of the steel and concrete, the other two were at the 1/4 width and at the centre of the section. The steel hollow section was placed vertically on plywood and attached to the plywood by silica glue. Then, the self-consolidating concrete was placed into the steel hollow section from the top side without any vibration.

Specimens were tested in Civil Engineering Laboratory at Monash University. The fire test set up is shown in Figure 3.3, which consists of gas furnace, control unit, reaction frame, loading system and data acquisition system. The control system controls the temperature in the furnace according to certain provision. The specimens were bolted to the steel cylinder extension at the left hand side which was connected to the reaction frame as shown in Figure 3.3(b). On the right hand side, the steel cylinder extension is connected to a strong end plate which can move along the axial direction of the specimen by wheels at the bottom of the plate (see Figure 3.3(b)). Load was applied to the specimen by hydraulic jacks between the strong steel end plate and the reaction

frame. The maximum load capacity is 500 tons. The loading system was manually controlled to compensate variation in load due to the axial deformation of the specimens at elevating temperature. The axial deformation and temperatures were recorded by the data acquisition system.

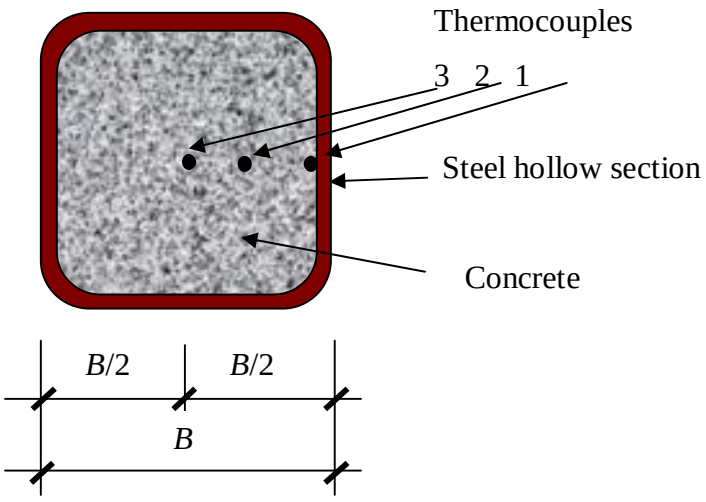

Figure 3.2 Positions of thermocouples

The fire test conformed to AS 1530.4 (1997). Specimen was loaded to the designated load level before it was heated up. The standard ISO fire temperature was followed, which can be expressed as AS 1530.4 (1997):

$$T_t - T_0 = 345\log(8t + 1) \tag{3.1}$$

where, T_t and T_0 are furnace temperature at time t and initial furnace temperature in degree Celsius and t is fire exposure time in minutes.

All the specimens were tested until failure. The failure provisions were either the axial deformation or the deformation rate specified in AS 1530.4 (1997).

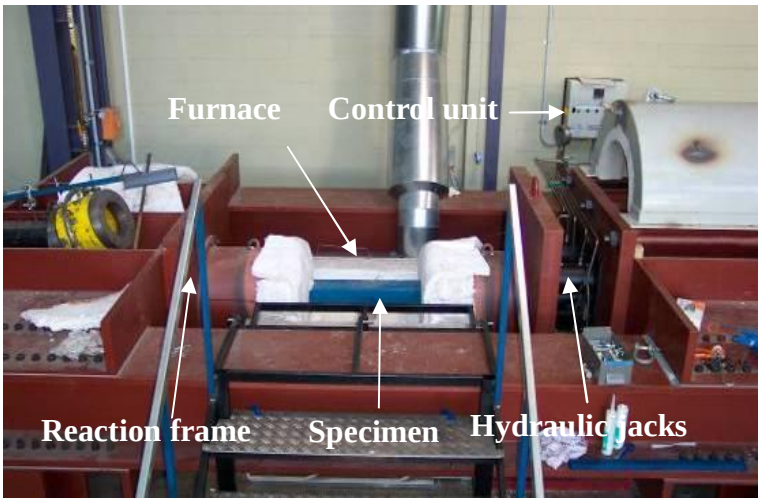

(a) Test set up

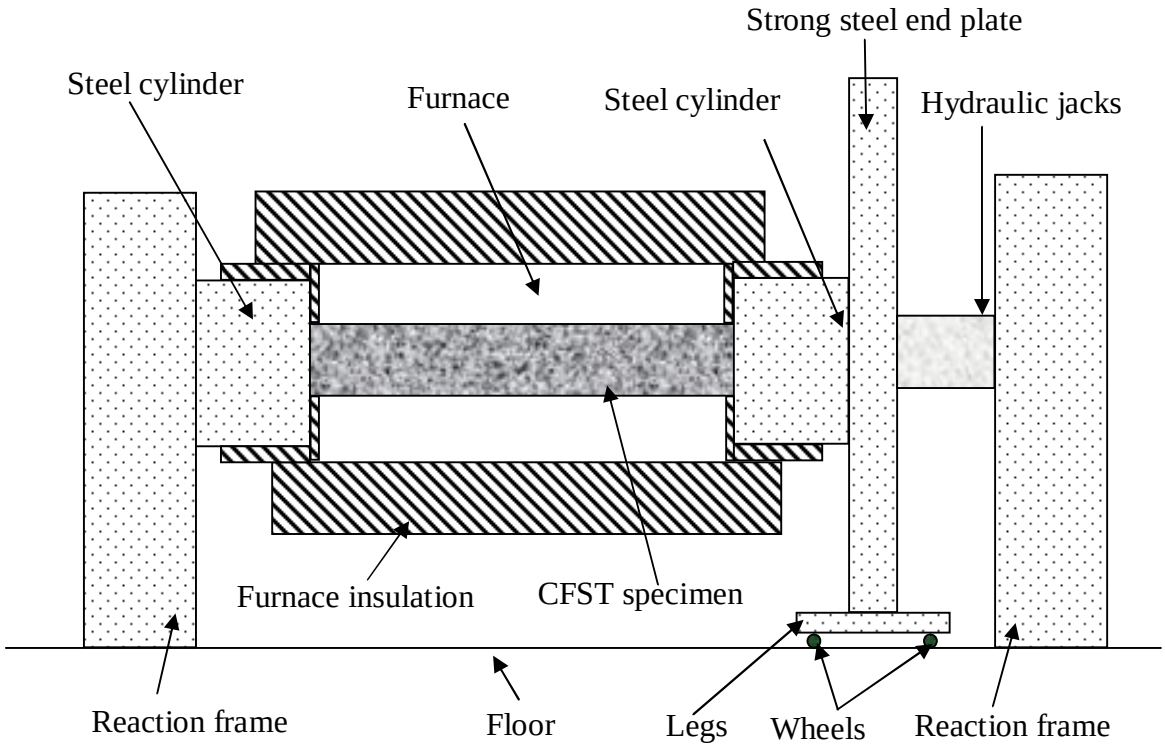

(b) Schematic elevation view

Figure 3.3 Test set up

3.3 TEST RESULTS

3.3.1 Temperature

The temperature in specimens was measured using thermocouples installed in the specimens. The position of the thermocouples is shown Figure 3.2. Temperatures versus fire exposed time curves are shown in Figure 3.4. As shown in the figure, temperature

in the concrete increases with the increase in the fire exposure time. In addition, temperature at point 1 which is at the steel and concrete interface is much higher than temperatures in the inner part of the concrete (i.e. point 2 and 3), whereas the difference in temperature at point 2 and 3 is not so notable. There is dramatic variation in temperature in the outer part of the concrete (i.e. between point 1 and 2) and much less variation in the temperature in the inner part of the concrete becomes (i.e. between point 2 and 3).

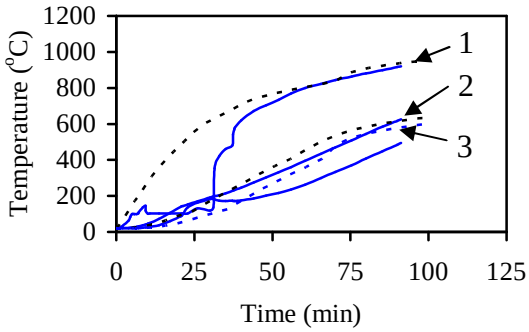

(a) S1R2E0

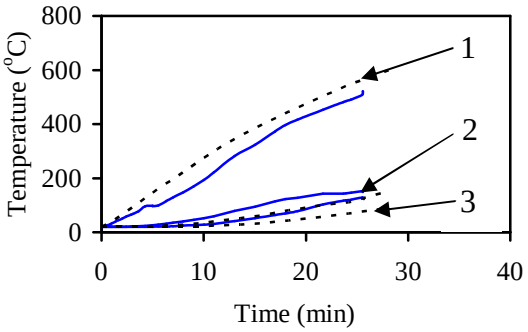

(b) S1R4E0

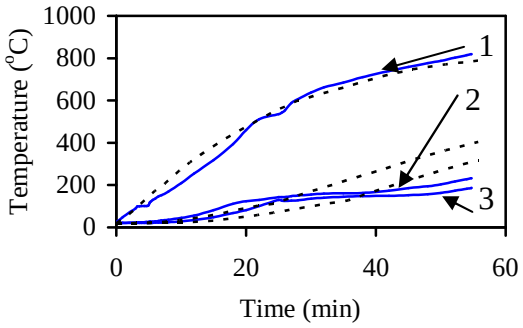

(c) S1R4E2

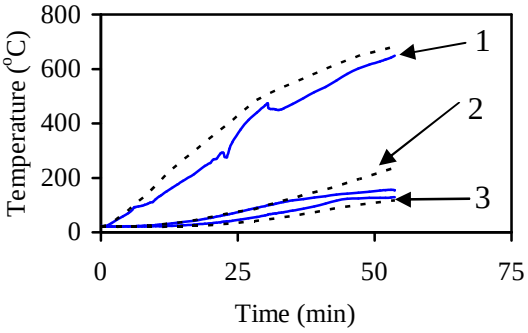

(d) S2R3E0

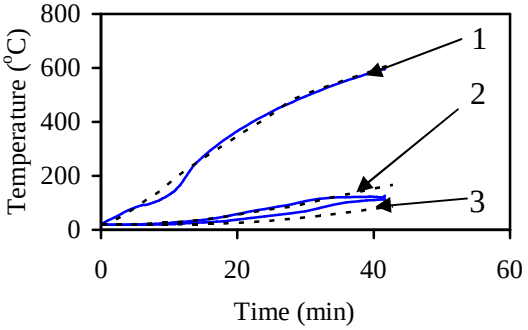

(e) S2R4E0

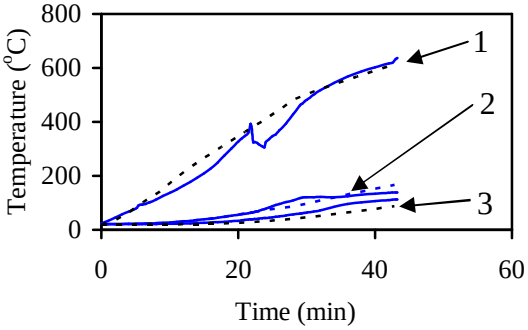

(f) S2R4E1

– – – – – Predicted ——— Test

Figure 3.4 Temperatures in specimens

3.3.2 Axial deformation

The curves of axial deformation versus fire exposure time are shown in Figure 3.5. Based on the axial deformation curves, the fire endurance for each specimen was determined as shown in Table 1. It should be pointed out that the maximum temperature elevation time was set to be 90 minutes before testing. The test stopped by the control unit if the time reached 90 minutes even if the specimen had not failed yet. This was what happened to the specimen S1R2E0.

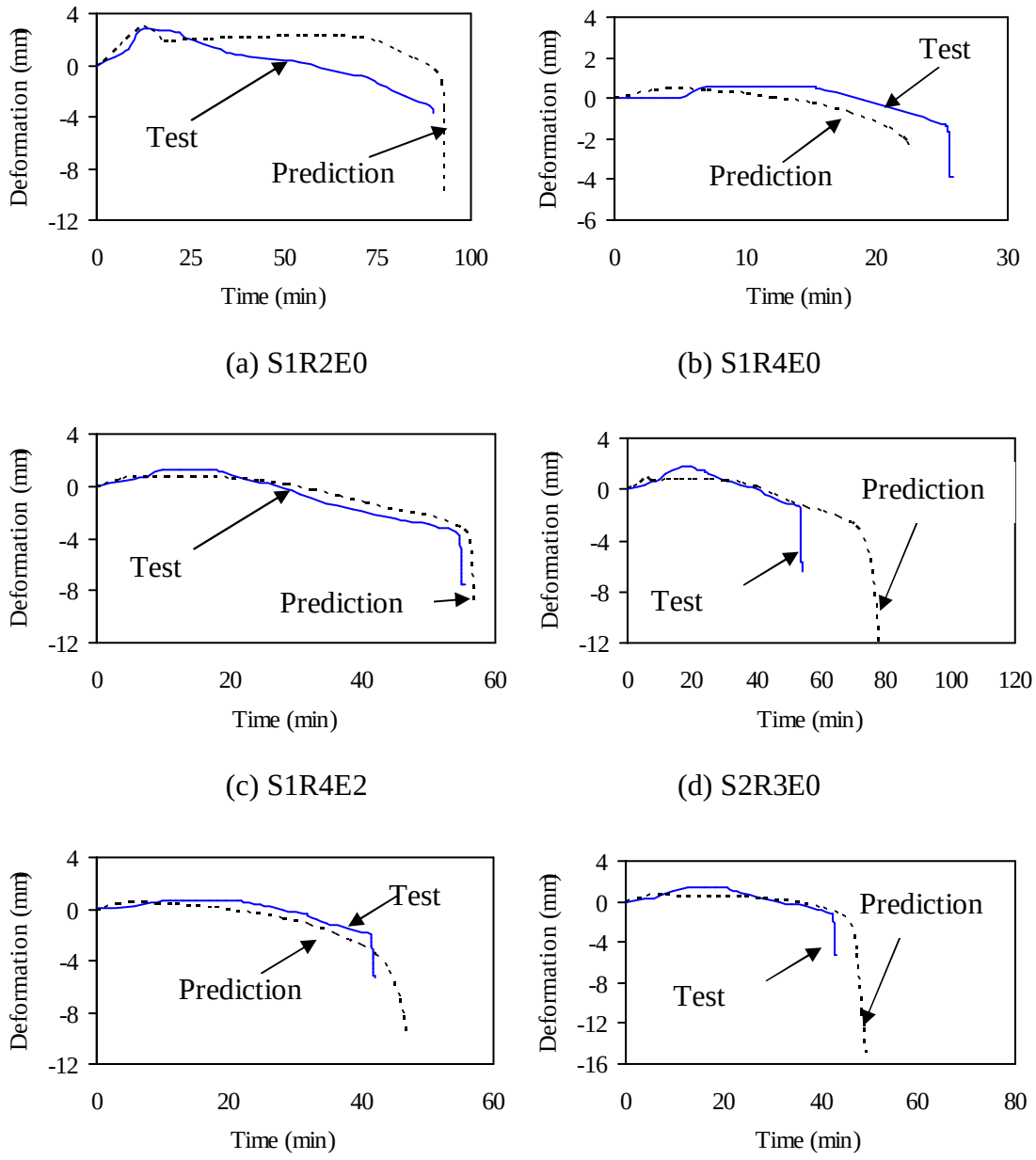

Figure 3.5 Axial deformation

As can be seen in Figure 3.5, axial deformation of the specimens experiences a tensile deformation at the early stage of the fire exposure and then turns to compressive deformation. Finally, the compressive deformation increases sharply which indicates that the specimens loss capacity.

3.3.3 Failure modes

In order to investigate the failure mechanism and interaction of the concrete and steel in the composite columns, the failure modes of the entire specimens and core concrete were observed after test. The failure modes in Figure 3.6 show that there are outward bulges on each face of the square steel hollow sections. A typical failure mode of the concrete is shown in Figure 3.7. As shown in this figure, concrete crushes at the mid-height of the specimens and there are longitudinal cracks on the concrete surface.

(a) S1R2E0

(b) S1R4E0

(c) S1R4E2

(d) S2R3E0

(e) S2R4E0

(f) S2R4E1

Figure 3.6 Failure modes of the specimens

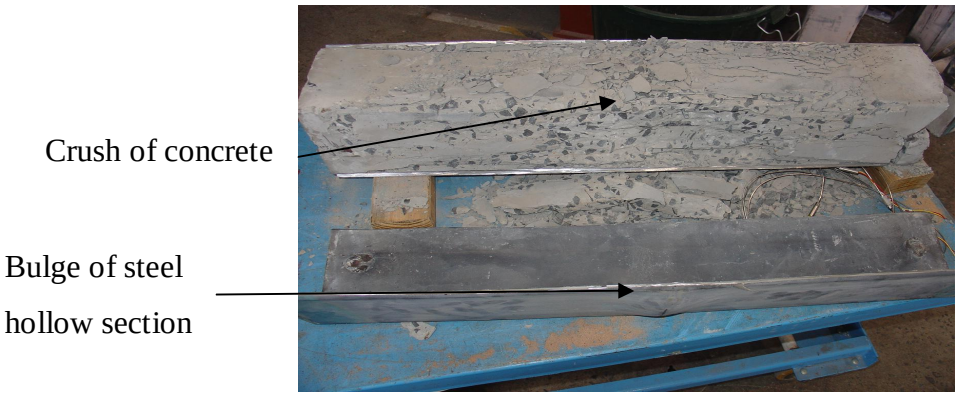

Figure 3.7 Typical failure mode of core concrete

3.3.4 Limiting temperature of steel

The limiting temperature of steel is defined as temperature in steel when the specimens reach fire endurance (Han et al., 2003a). The limiting temperatures which vary from 521 ^{o}C to 920 ^{o}C are listed in Table 4.1. Four of the specimens have limiting temperature within the range of 521 to 649 ^{o}C and limiting temperature for the other two specimens is between 819 and 920 ^{o}C.

3.4 DISCUSSION OF TEST RESULTS

3.4.1 Axial deformation

It is clear from Figure 3.5 that axial deformation of the specimens can be divided into three stages. A schematic view of the deformation versus fire time is shown in Figure 3.8. As can be seen in Figure 3.8, expansion dominates the deformation in the first stage (from A to B). In the second stage (from B to C), the compressive deformation overcomes the expansion and gradually increases. This is mainly due to the deterioration in the mechanical properties of the steel and concrete at elevated temperatures. In the third stage (from C to D), the compressive deformation sharply increases in a very short time interval beyond the turning point (C). At this moment, the specimens can no longer withhold the load and attain the fire endurance due to the successive and rapid axial deformation. The deformation history of the specimens illustrates that the specimens behave in a very ductile manner. The deformation behaviour of the high strength SCC filled stub columns is similar to that of columns filled with NSC, HSC and FRHSC (Kodur, 1998; Kodur, 1998a; Han et al., 2003a; Han et al., 2003b).

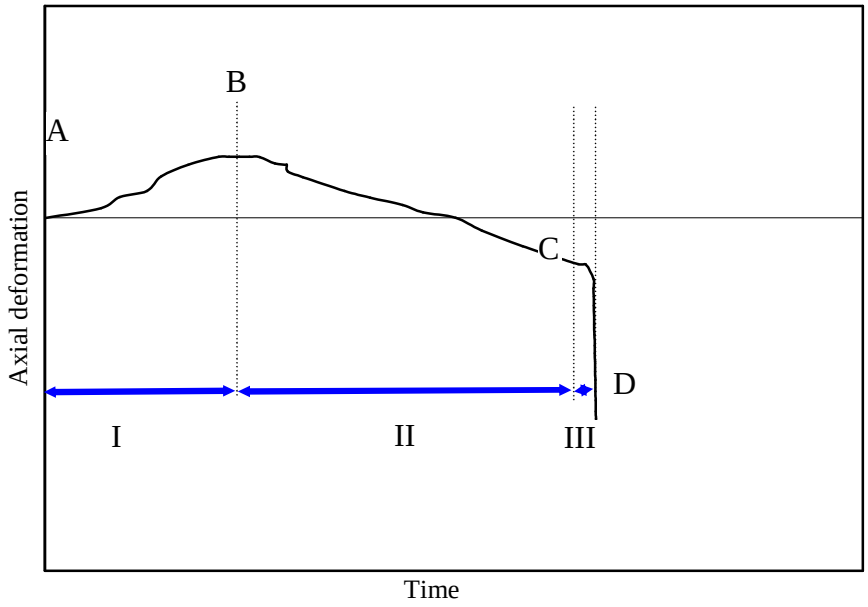

Figure 3.8 Typical axial deformations versus time relationship of CFST stub columns

3.4.2 Failure mode

The primary failure mode of the specimens was the outward bulges of the hollow steel section as shown in Figure 3.6. There was no obvious lateral deflection observed. This implies that failure of the stub columns is induced by compressive failure rather than overall buckling which is the usual failure mode of slender CFST columns exposed to fire (Kodur, 1998; Kodur, 1998a; Han et al., 2003a; Han et al., 2003b; Wang, 1999; Tan and Tang, 2004; Uy and Bradford, 1995). It is well known that the presence of concrete in CFST columns changes buckling mode and behaviour of steel hollow section at ambient temperature (Uy, 1998). The present stub column test shows that concrete also changes the buckling mode and behaviour of the steel hollow section in the CFST stub columns at elevated temperature. The buckling mode of the steel hollow section in the CFST stub columns at elevated temperature is similar to that at ambient temperature. In addition, it was found that specimens retained integrity and there was no separation between the concrete and steel hollow sections after test. These imply that there is an interaction between the steel and concrete in the CFST columns during the whole course of temperature elevation.

The steel hollow sections were cut and taken away to observe the failure mode of the core concrete after fire testing. There was a bond between the concrete and steel hollow section when the cut steel hollow sections were taking away. As can be seen in Figure 3.7, the outer concrete at the middle height of the specimen crushed, which was

corresponding to the outward bulge of the steel hollow section. There was also longitudinal cracking on the surface of the concrete. There was neither spalling of the SCC nor obvious tangential slipping between the concrete and steel interface observed. Obviously, the possible spalling of the SCC is avoided by the confinement of the steel hollow section. Local buckling of the steel hollow section and crush of the outer concrete are among factors which lead the columns loss the load capacity.

3.4.3 Limiting temperature

The limiting temperatures in steel are between 521 to 920 ^{o}C with the load level varying from 0.17 to 0.44, as shown in Table 3.1. Most of the limiting temperatures are from 521 to 649 ^{o}C. The range of the limiting temperatures in the current test is similar to that of the CFST columns with load level of 0.7, from 530 to 590 ^{o}C (Han et al., 2003a). It should be noted that specimens in Han et al (2003a) are different from those in the current test in column slenderness, type of concrete and load level.

The fire resistance of steel structural members can be determined in temperature domain (Eurocode3, 2005). Critical temperature, similar to limiting temperature in this chapter, is used to calculate the fire resistance of steel structural members. The critical temperature of steel members depends on degree of utilization μ (i.e. load level in this chapter), ranging from 526 to 711 ^{o}C when degree of utilization decrease accordingly from 0.7 to 0.22 (Eurocode3, 2005). The critical temperatures calculated from Eurocode 3 (2005) are 604, 623, 685, 627 and 636 ^{o}C respectively for specimens in Table 3.1. It is clear that there is no significant difference between the critical temperature provision in Eurocode 3 (2005) and the limiting temperatures of the CFST columns acquired from the current test and Han et al (2003a). However, the fire resistance of CFST columns is proved better than void steel hollow section (Kodur, 1998; Kodur, 1998a; Han et al., 2003a; Han et al., 2003b; Wang, 1999). This indicates temperature elevation in the steel hollow section of the CFST columns is much slower than that in the void steel hollow section. On the other hand, comparing the results from the current test and the previous tests (Kodur, 1998; Kodur, 1998a; Han et al., 2003a; Han et al., 2003b; Wang, 1999), it can also be clearly seen that the limiting temperature of steel in CFST columns is independent of type of core concrete and failure modes of entire columns.

3.4.4 Effect of load level

Load level has been found as one of the important factors that affect the fire endurance of CFST columns (Han et al., 2003a). Figure 3.9 shows the relation of the fire endurance to load level (μ) for the specimens. The fire endurance of the SCC filled stub columns generally decreases with the increase of the load level. Higher load level in the CFST columns results in higher stress in concrete and steel in the composite columns. Therefore, fire endurance of the columns decreases when the load ratio increases.

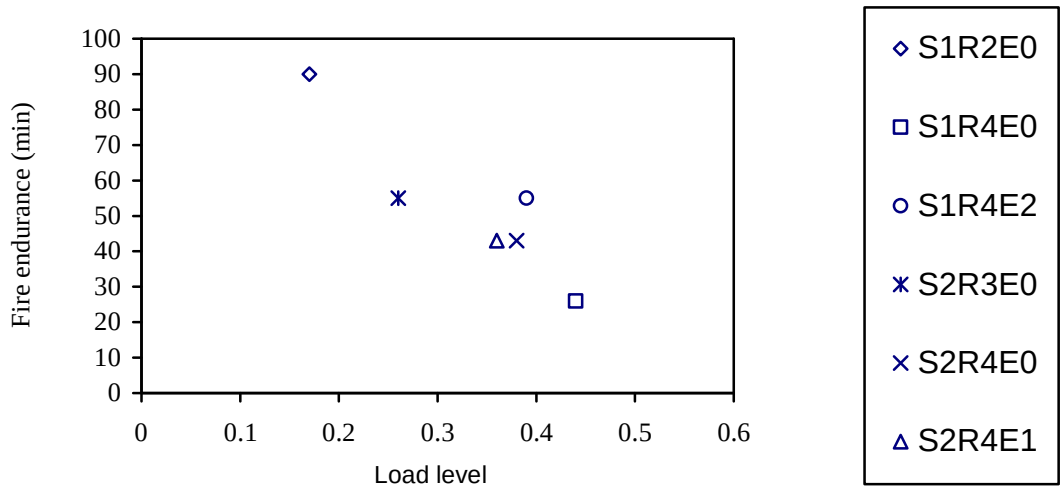

Figure 3.9 Fire endurance versus load level

3.4.5 Effect of load eccentricity

It has been shown in the literature (e.g. Han et al, 2003a) that load eccentricity has moderate influence on the fire resistance of slender CFST columns. However, comparing the fire endurance of S2R4E0 and S2R4E1 shown in Table 3.1, the load eccentricity has little effect on the fire resistance of the stub columns. This is mainly because the failure mode of the stub columns under fire does not involve overall buckling of the entire columns.

3.5 FINITE ELEMENT ANALYSIS

A finite element analysis (FEA) model was proposed in this investigation to analyse the fire behaviour of the high strength SCC filled stub columns, such as temperature, stresses, displacement and fire endurance. The commercial FEA program, ABAQUS (2008), was used in the analysis.

3.5.1 Analysis procedure

The structural response of CFST columns at elevated temperatures depends on not only the mechanical properties of material, but also the temperature in the CFST columns, whereas the thermal response of the CFST columns is independent of the structural response. Based on the relationship of the thermal and structural responses in CFST columns exposed to fire, a sequentially coupled thermal-stress analysis procedure in ABAQUS (2008) was used in this investigation. It is assumed that the stress/displacement depends on the temperature field but there is no reverse dependency in this procedure. Therefore, this analysis procedure was divided into two steps, a pure heat transfer analysis step and a stress/displacement analysis step which read temperature from the result of the heat transfer analysis.

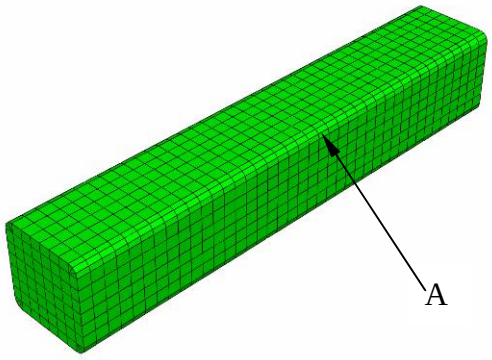

(a) FEA model for heat transfer analysis

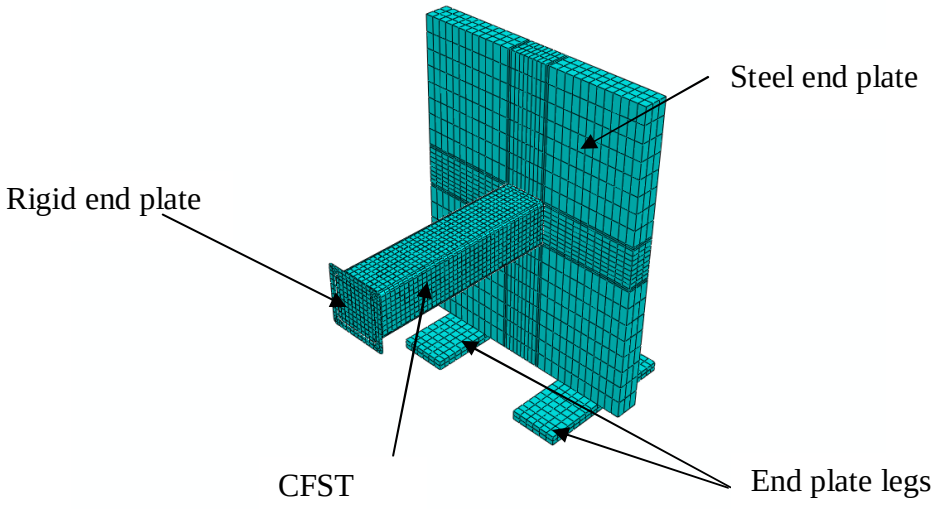

(b) FEA model for stress and displacement analysis

Figure 3.10 Finite element mesh for CFST stub columns

Due to different issues are dealt with in these two steps, the FEA model, such as boundary conditions, material property and type of element, is different in each step. Therefore, there should have some consistent requirements in the model between the two steps so that data can be transferred from one step to another effectively. So identical discretized mesh was chosen for both steps and the elements in two steps were from the same element family. Density of the mesh was determined by trial convergent calculation. A typical mesh for the CFST stub columns is shown in Figure 3.10.

3.5.2 Material property model

There are two types of material properties required, which are corresponding to the two steps of analysis in the FEA model, thermal and mechanical properties which are both temperature dependent.

Material thermal properties used in the analysis were thermal conductivity and specific heat. In the previous research, thermal properties of HSC were found suitable to predict the temperature in SCC filled columns under fire exposure (Lu et al., 2005). In this analysis, the thermal property model for high strength concrete proposed by Kodur (2007) was used. Influence of water vaporization in concrete at elevated temperature was incorporated into the concrete thermal properties by transforming the heat required for water vaporization into specific heat of the concrete (Lu et al., 2007). The free water was assumed 5% in the concrete and the water was assumed to vaporize between 100 and 115 ^{o}C. Thermal property model for steel was the one proposed by Kodur (2007).

Mechanical models for steel and concrete at elevated temperature are available from material library in ABAQUS (2008). There are metal and concrete models in the library at ambient temperature. Another parameter, temperature, was incorporated into the models to consider the temperature dependence of the material properties. There are elastic and plastic material properties in each model. The elastic property includes elastic modulus and Poisson's ratio. The plastic properties normally include uni-axial non-linear stress-strain relationship, yield function to define yield of the material at multi-axial stress, and flow criterion to define plastic flow. Besides, thermal expansion is also another important material property. Thermal expansion models for steel and concrete in the analysis were those proposed by Lie (1994).

Uni-axial stress-strain relationship for steel at elevated temperature in the analysis was from Lie (1994). A classic metal material model in ABAQUS (2008) was chosen to describe the behaviour of the steel at multiple stresses state. This model follows Misses yield and associated flow criterion under multiple stresses. The Poisson's ratio was 0.3, which was assumed independent of temperature. The elastic modulus of steel at elevated temperature was taken as scant elastic modulus at zero stress point.

The concrete damaged plasticity model in ABAQUS (2008) was used for concrete. The yield (or failure) surface of this model is controlled by two equivalent plastic strains in tension and compression respectively so as to reflect different failure mechanism of concrete in tension and compression. A Drucker-Prager hyperbolic flow potential function is used to define the plastic flow. Both uni-axial compressive and tensile stress-strain relations are necessary for the model due to the difference in failure mechanism in tension and compression.

It is believed that confinement of steel hollow section on the core concrete in CFST columns can enhance the strength and ductility of the core concrete at ambient temperature. However, it is difficult to observe such confinement for CFST columns under fire exposure. Kodur (1998a) proposed a mechanical model for compressive concrete in CFST columns at elevated temperature, which ignored the confinement of steel hollow section. Another model for compressive concrete was proposed by Han et al. (2003b), which took into account the confinement of steel hollow section at elevate temperature. These models were all initially developed for simplified numerical analysis model. The concrete compressive uni-axial stress-strain relation in this FEA analysis was based on the model proposed by Han et al. (2003b). This stress-strain-temperature relation is:

$$\begin{aligned} y &= 2x - x^2 \qquad (x \le 1) \\ y &= \frac{x}{\beta(x-1)^{\eta} + x} \qquad (x > 1) \end{aligned} \tag{4.2}$$

where, $x = \varepsilon / \varepsilon_0$; $y = \sigma / \sigma_0$; $\sigma_0 = f'_c / [1 + 1.986(T-20)^{3.21} \times 10^{-9}]$;

$\varepsilon_0 = (1300 + 12.5 f'_c + 800 \cdot \xi^{0.2}) \cdot 10^{-6} \cdot (1.03 + 3.6 \times 10^{-4} \cdot T + 4.22 \times 10^{-6} \cdot T^2)$;

$\eta = 1.6 + 1.5/x$; $\beta = \dfrac{f_c^{'0.1}}{1.2\sqrt{1+\xi}}$.

In the equations, ξ is a parameter relating to the confinement of steel hollow section on the concrete. It is defined as follow:

$$\xi = \frac{A_s \cdot f_y(T)}{A_c \cdot f_{ck}} \tag{4.3}$$

where, A_s and A_c is the cross sectional area of the steel hollow section and concrete respectively; f_{ck} is the characteristic strength of concrete which equals to 0.67f'c. $f_y(T)$ is defined as:

$$f_y(T) = \begin{cases} f_y & (T < 200°C) \\ \dfrac{0.91 f_y}{1 + 6.0 \times 10^{-17} \cdot (T-10)^6} & (T \geq 200°C) \end{cases} \tag{4.4}$$

The tensile uni-axial stress-strain relationship can be defined as stress-strain or fracture energy-displacement relationship in the concrete damaged plasticity model. Use of fracture energy is effective in calculation because it can resolve the mesh sensitive problem due to the cracking of the concrete. There is no experimental data on fracture energy of concrete at elevated temperature. It was assumed that tensile strength of concrete and fracture energy decreases linearly from 100% at 20°C to 10% at 1000°C. The influence of fracture energy and tensile strength of concrete on predicting the fire performance of CFST columns will be discussed later. Fracture energy of concrete was defined as a material property in the model. The fracture energy of concrete at ambient temperature was calculated by the following equation (CEB-FIP, 1993):

$$G_f = \gamma \left(\frac{f'_c}{10}\right)^{0.7} \times 10^{-3} \quad \text{(N/mm)} \tag{4.5}$$

where, $\gamma = 1.25 d_{\max} + 10$; $d_{\max}$ is the diameter of coarse aggregate.

The Poisson's ratio of concrete is taken as 0.2. The elastic modulus of concrete at elevated temperature was taken as scant elastic modulus at the point where stress is equal to 40% of the peak stress.

3.5.3 Temperature field analysis

Temperature elevation in CFST columns is governed by general heat transfer principle. Numerical methods are the most common way to solve the nonlinear and transient heat transfer differential equations. The model employed in this investigation used a hybrid method to solve the equations, i.e. discrete finite elements in the geometric domain and finite difference division in the time domain.

In the heat transfer analysis, heat transfer from the fire temperature to CFST columns out surface by radiation and convection. The heat convective coefficient and resultant heat emissivity was taken as 25 (W/m^2K) and 0.56 respectively (Han et al, 2007). Besides, there is a heat resistance between the steel and concrete interface because two materials are not in perfect contact at the interface. Several models have been proposed to calculate such heat resistance. All proposed models were found quite well predicting the temperature in CFST columns in the previous study (Lu et al., 2007). A heat contact conductance parameter in ABAQUS was used to describe the heat resistance in the interface. The heat contact conductance was taken as 100 (W/m^2K).

Typical temperature distribution in the specimens is shown in Figure 3.11 and 3.12. The predicted temperature confirms the temperature measuring in the test which showed that temperature at the outer part of the concrete is much higher than that in the inner part of the concrete. In addition, the highest temperature in the whole section occurs at the corner of the square section. Moreover, temperature in the larger specimens is lower than that in the smaller one, for example temperature at the centre of 200 mm and 150 mm width specimens at 120 minutes of fire exposure is 532 and 636 ^oC respectively.

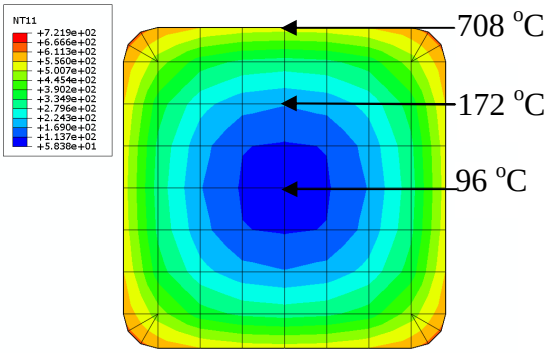

(a) t=30 minutes

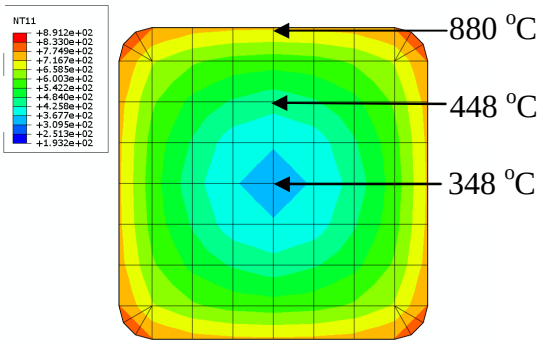

(b) t=60 minutes

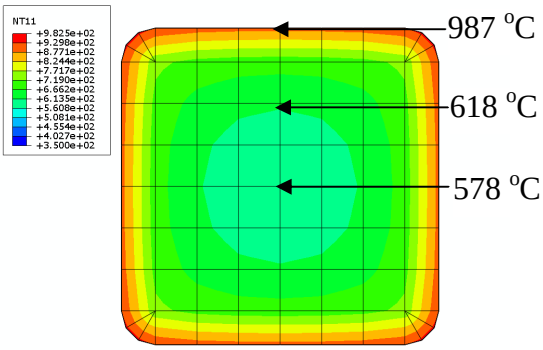

(b) t=90 minutes

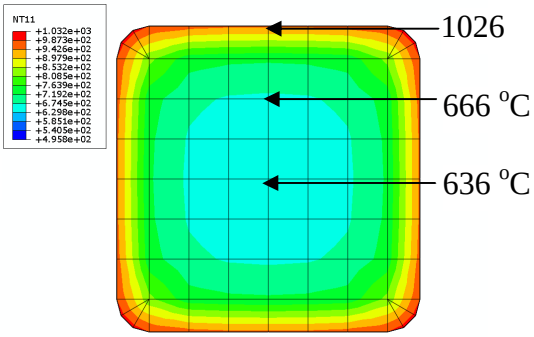

(c) t=120 minutes

Figure 3.11 Temperatures in specimens with width of 150 mm

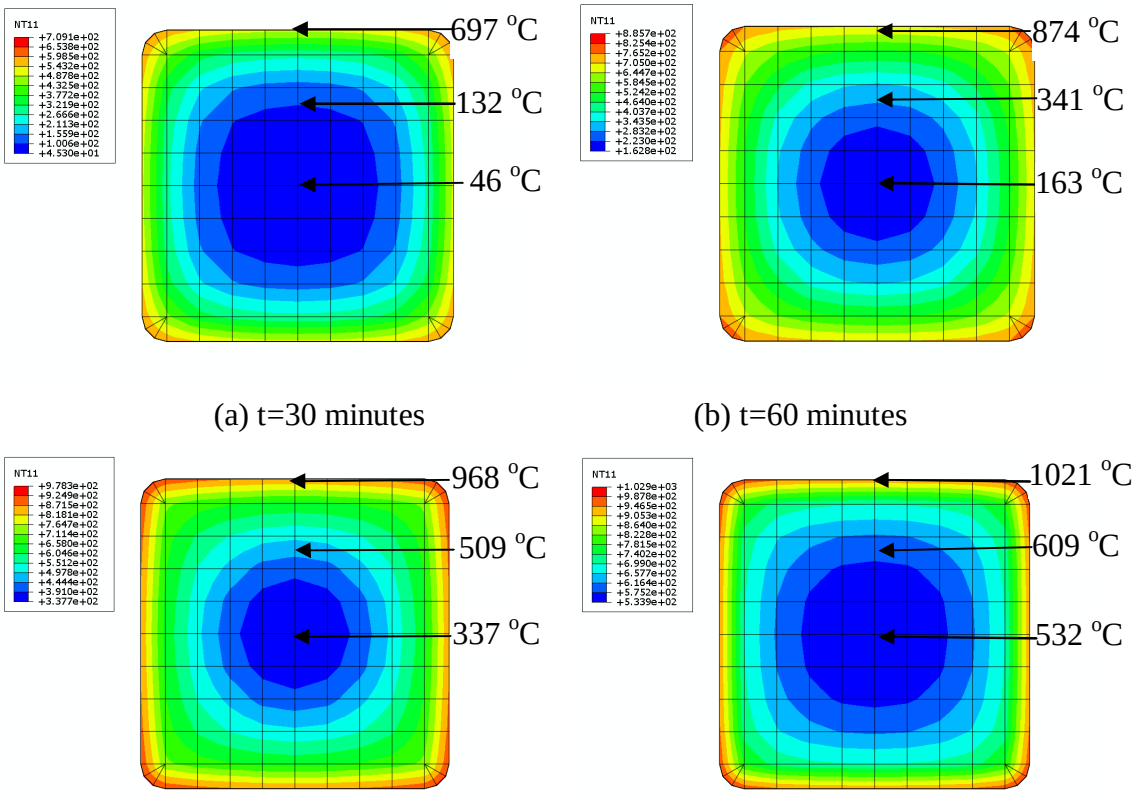

(a) t=30 minutes (b) t=60 minutes

(c) t=90 minutes (d) t=120 minutes

Figure 3.12 Temperatures in specimens with width of 200 mm

3.5.4 Stress and displacement analysis

The FEA model in the subsequent stress and displacement analysis can be developed from the model of the thermal analysis by altering the material property, boundary conditions, interface interaction property in steel and concrete and type of element.

The material mechanical properties for steel and concrete were used to replace the thermal properties in the analysis. The linear reduced-integration 3D solid element (C3D8R) with 8 nodes was used for concrete and the linear reduced-integration 4 nodes shell element (S4R) was utilized for the steel hollow section. There are three translation degrees of freedom for nodes in the solid element and three translation and two rotation degrees of freedom for nodes in shell element.

The interaction of steel and concrete was simulated by contact interaction in ABAQUS (2008). The surfaces of the concrete and steel in contact were defined as a contact pair, one as master surface and the other as slave surface. Two surfaces may contact each other or separate from each other. The mechanical properties of the contact pair are

defined in normal and tangential direction respectively. The “hard contact” behaviour was selected for the normal direction. In this behaviour, the contact pair transmits no contact pressure unless the nodes of the slave surface contact with the master surface. There is no limitation to the magnitude of contact pressure transmitted when the surfaces are in contact (ABAQUS, 2008). A Coulomb friction model was used for the tangential behaviour of the contact pair. A friction coefficient of 0.25 was found suitable to predict CFST columns at ambient temperature (Han et al, 2007). In the current model, a friction coefficient of 0.18 was utilized to consider deterioration in the stiffness of the steel and concrete at elevated temperature. The bond between steel and concrete interface was not considered at this stage. The effect of bond will be discussed in section 3.5.2.

The boundary condition at the right hand side, which is shown in Figure 3.3(b), can not be simply defined as fixed or pinned. So, the whole strong steel plate with legs was included in the FEA model as shown in Figure 3.10(b). Boundary conditions were applied on the bottom of the legs to allow the strong steel plate move freely along the axial direction of the specimens to simulate the real boundary conditions.

The analysis procedure is similar to that in the fire test. The columns were loaded to the prescribed load under ambient temperature, then temperature elevated in the columns until failure of the columns. Temperatures in the columns which derived from the temperature analysis are used in this subsequent analysis.

3.5.5 Sensitivity analysis

As discussed in the above sections, the tensile property of concrete, bond and friction of the steel and concrete at interface are some of the material or mechanical properties required for the FEA modelling. These mechanical properties also degrade at elevated temperatures. However, there is not enough information available to quantify these properties at elevated temperatures. In this investigation, these properties were determined based on their properties at ambient temperature and extrapolated to elevated temperatures. The following sensitivity analysis is used to justify the reliability of the extrapolation. One of the stub columns in Table 3.1, S1R2E0, was used for the FEA modelling.

3.5.5.1 Concrete fracture energy

Three cases were used to analyse the influence of concrete fracture energy on the fire performance of the CFST column. They were:

Case 1: The fracture energy is equal to its value at ambient temperature and remained unchanged at elevated temperature;

Case 2: The fracture energy linearly decreased from 100% at 20 ^{o}C to 10% at 1000 ^{o}C;

Case 3: The fracture energy linearly decreased from 100% at 20 ^{o}C to 10% at 200 ^{o}C and then remained as 10% till 1000 ^{o}C.

The predicted axial deformation of the CFST stub column in standard fire exposure using different concrete fracture energy models is shown in Figure 3.13. When fracture energy is selected as case 3, the predicted fire endurance is slightly lower than other models; however, such difference is not significant. Finally, the fracture energy model in case 2, fracture energy decrease linearly with increase of temperature, was used in the further FEA modelling.

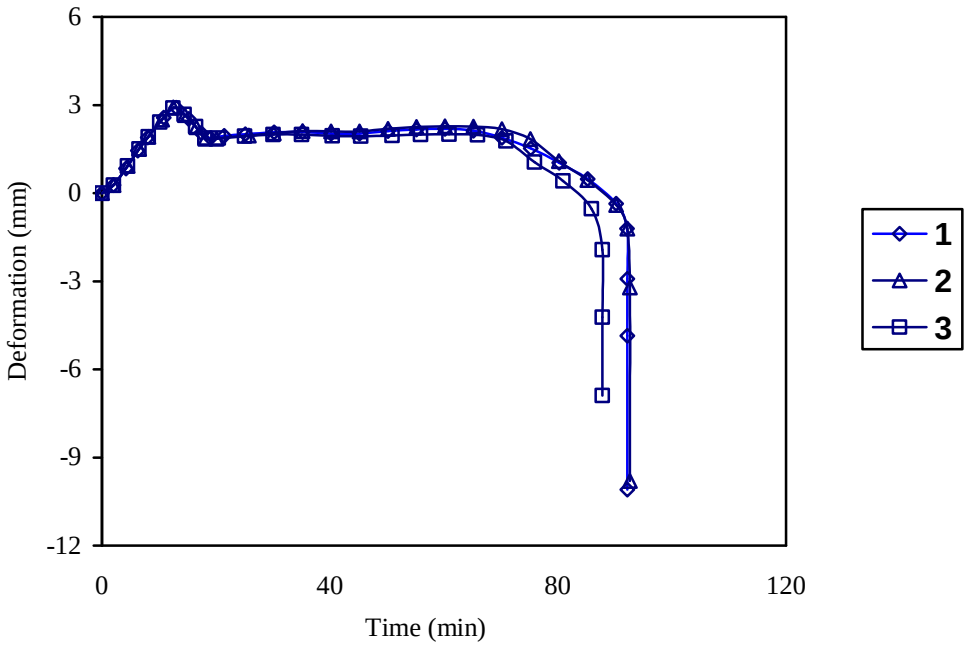

Figure 3.13 Influence of concrete fracture energy on fire performance

3.5.5.2 Contact property of steel and concrete interface

The mechanical properties required in simulating the interaction of concrete and steel at interface are the bond and slip of the concrete and steel. When the tangential stress at

the interface is less than the bond strength, no slip occurs at the interface. If the tangential stress is greater than the bond stress, there is a relative slip at the interface. The relative slip is resisted by friction at the interface, which can be defined by a friction coefficient at the interface.

Three cases were considered to investigate the influence of bond strength:

- Bond strength taken as that at ambient temperature;
- Bond strength taken as one-fourth of that at ambient temperature;
- Bond strength taken as zero.

The friction coefficient used in the FEA modelling of CFST columns at ambient temperature is generally between 0.25 and 0.6 (Han et al., 2007). Therefore, friction coefficients of 0.6, 0.18 and 0 were used in the sensitivity analysis.

The influence of bond strength and friction property on the fire performance of the CFST stub column is shown in Figures 3.14 and 3.15 respectively. It can be seen there is no significant difference in the mechanical responses of the stub column if the contact properties vary in the above range.

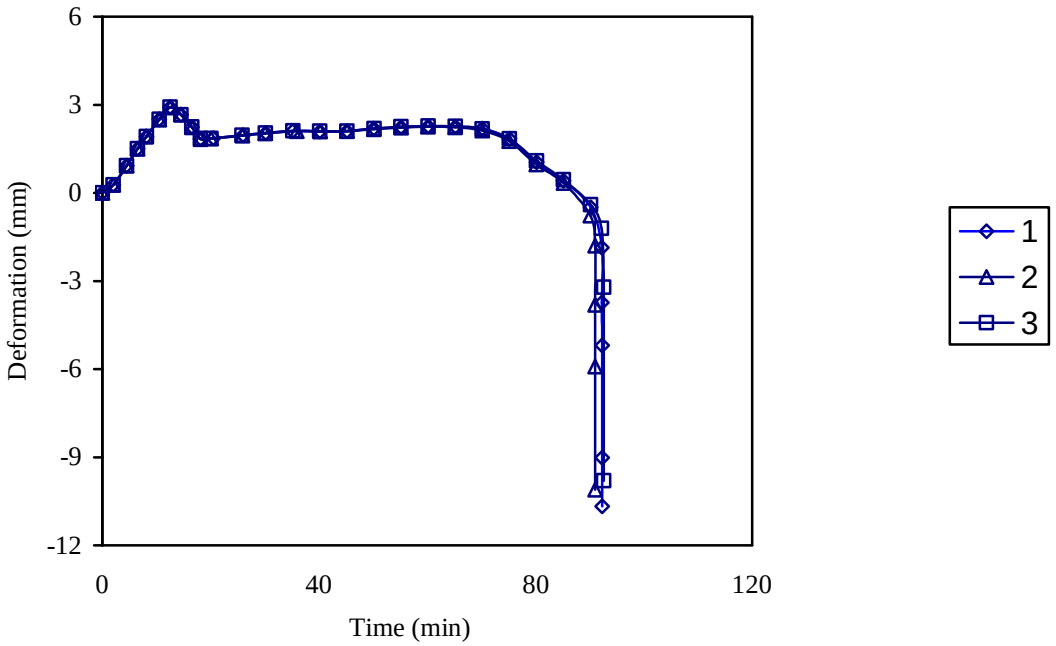

Figure 3.14 Influence of bond strength on fire performance

Bond strength in concrete and steel interface reduces when such separation starts to occur. As discussed above, interaction in concrete and steel was simulated by contact

which had different properties defined along normal and tangential directions of the interface. It seems that the contact property along tangential direction has insignificant effect on the structural response of the composite columns. Similar phenomenon was also observed by other researcher in modelling the fire resistance of CFST columns (Ding and Wang, 2008).

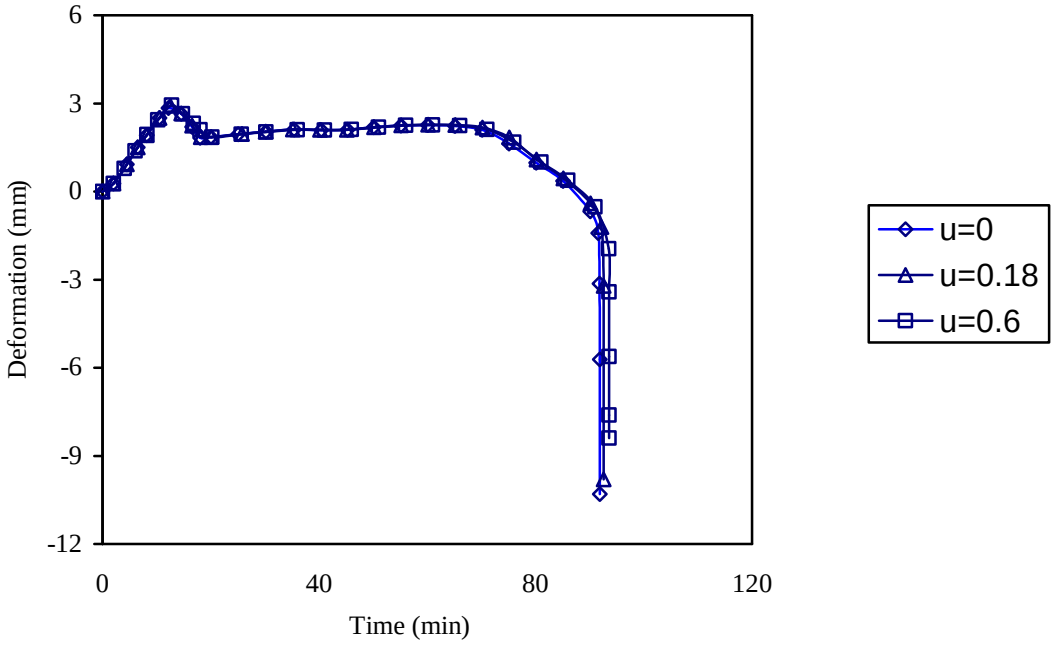

Figure 3.15 Influence of interface friction on fire performance

Hence for the further FEA modelling in this investigation, the bond strength was neglected and a friction coefficient of 0.18 was used.

3.5.6 Verification of the FEA model

The predicted temperatures in the CFST specimens comparing to the test results are shown in Figure 3.4. It can be seen that the prediction generally well agree with test results. This indicates that thermal properties of HSC are applicable to predict the temperatures in the high strength SCC filled columns. The predicted axial deformation and fire endurance of the specimens are shown in Figure 3.5 and Table 3.1 respectively. The prediction generally well agrees with the test result except the specimen S2E3E0.

Typical predicted failure mode of the CFST stub column is shown in Figure 3.16. The predicted failure mode generally agrees with the actual failure modes for specimens shown in Figure 3.6.

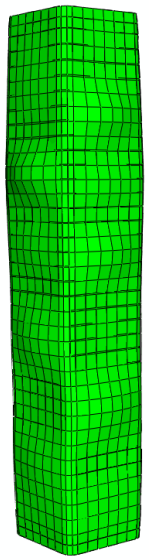

Figure 3.16 Typical predicted failure mode

3.6 STRUCTURAL BEHAVIOUR AND FAILURE MECHANISM

CFST columns under fire exposure are subjected to both thermal and mechanical actions. The behaviour of the columns can be divided into thermal and structural responses. The thermal response of the columns can be conveniently observed in tests by installing thermocouples in the columns. However, the only information about the structural response of the columns that can be acquired from the fire tests is the axial deformation of the CFST columns due to the difficulty of measuring the stress or strain of the CFST columns at high temperatures. Other structural behaviours are almost not able to be explicitly observed in fire tests or analysed by simplified numerical models. Therefore a more comprehensive numerical model, for example FEA model, is required to study in detail the structural behaviour of the columns during fire exposure.

The verified FEA model was used to analysis the structural behaviour of the CFST stub columns under fire exposure, such as stress, strain, load shared by the steel and concrete and buckling of the steel hollow section, and finally to establish the failure mechanism of the columns. Two of the specimens, S1R2E0 and S1R4E0 with load level of 0.17 and 0.44 respectively, were selected as examples in the analysis. The axial deformation of the columns, one of the most important structural responses of the columns, was

measured in the fire tests and predicted by the modelling as well. The predicted deformation versus fire exposure time relationship curves of S1R2E0 and S1R4E0 are shown in Figure 3.17. As discussed in section 3.4.1, the three distinct stages of the axial deformation of the CFST columns: (I) expansion; (II) gradual compression; and (III) sharp reduction, can be seen in Figure 3.17. In order to understand the structural behaviour of the columns in detail, these three stages are used to analyse other structural behaviours of the columns under fire exposure.

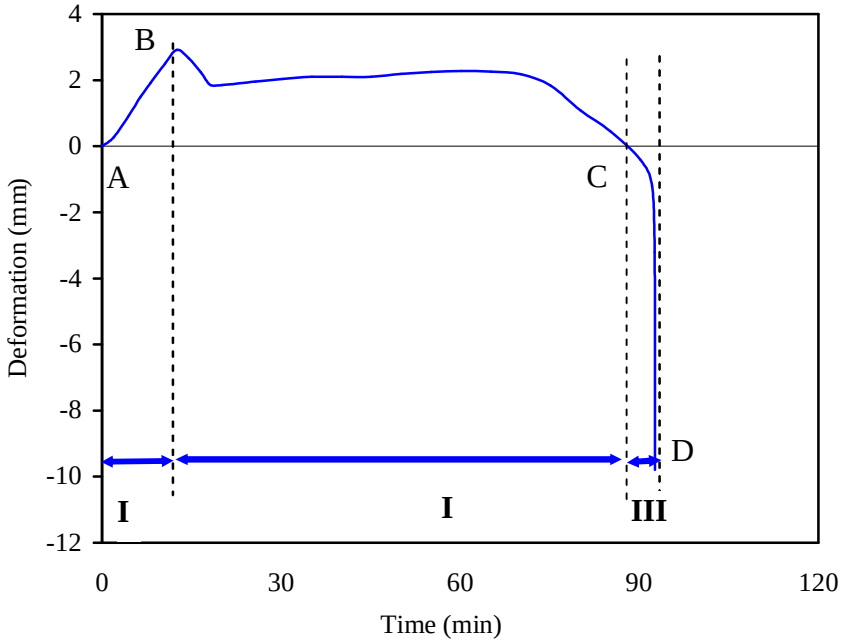

(a) S1R2E0

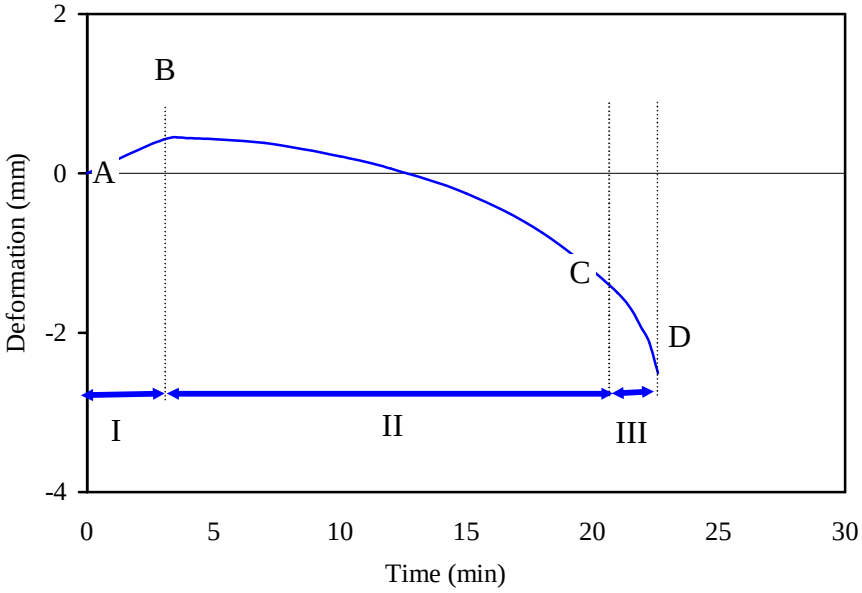

(b) S1R4E0

Figure 3.17 Predicted axial deformation

3.6.1 Structural behaviour

3.6.1.1 Load shared by steel and concrete

The load ratio of steel and concrete during fire exposure is shown in Figure 3.18 which gives an indication how the steel hollow section and concrete share the load in the three stages of fire exposure. As can be seen in Figure 3.18, there is a load and a unload process in the steel and concrete before the axial deformation of the CFST columns reaches peak tensile deformation. There is a period for specimen S1R2E0 in which load ratio of steel and concrete remains relatively constant and steel takes almost all the load. Then load ratio for steel decreases and load ratio for concrete increases moderately until the column reaches fire endurance. The turning point of the load and unload in the steel and concrete for S1R2E0 occurs after tensile deformation has reached peak point (point B) and this turning point coincides with point B for S1R4E0. After this turning point, the load in the steel and concrete in both columns almost linearly decreases and increases respectively.

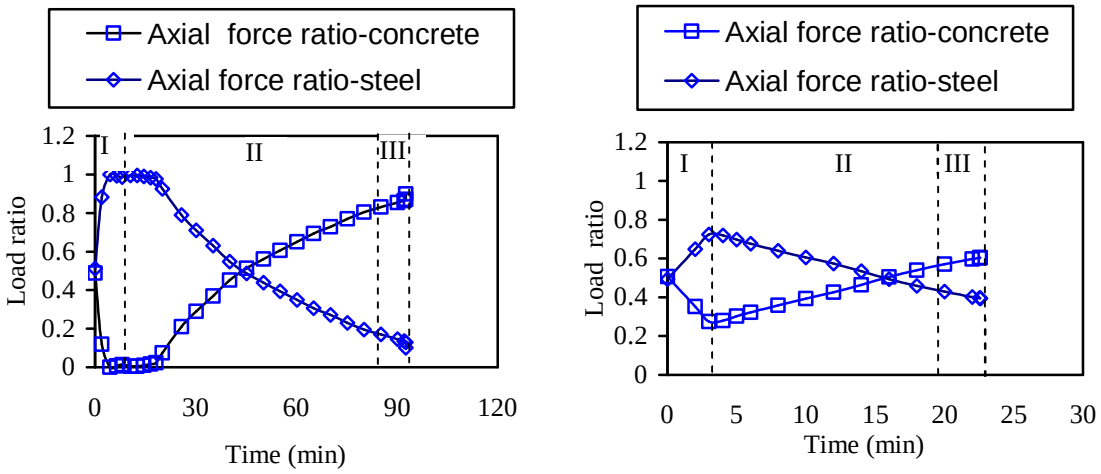

(a) S1R2E0 (b) S1R4E0

Figure 3.18 Axial load ratio in CFST stub columns

3.6.1.2 Strain

Strain of steel and concrete at elevated temperature generally consists of instantaneous stress induced strain, creep strain and thermal strain. The strain components of the steel at the corner of mid-span section are shown in Figure 3.19. The stress induced strain can be further divided into elastic and inelastic strain, in which the former is induced by variation in elastic modulus and the latter is induced by non-linearity in material stress-

strain relationship. It should be pointed out that creep strain is implicitly incorporated in the steel mechanical property model (Lie, 1994).

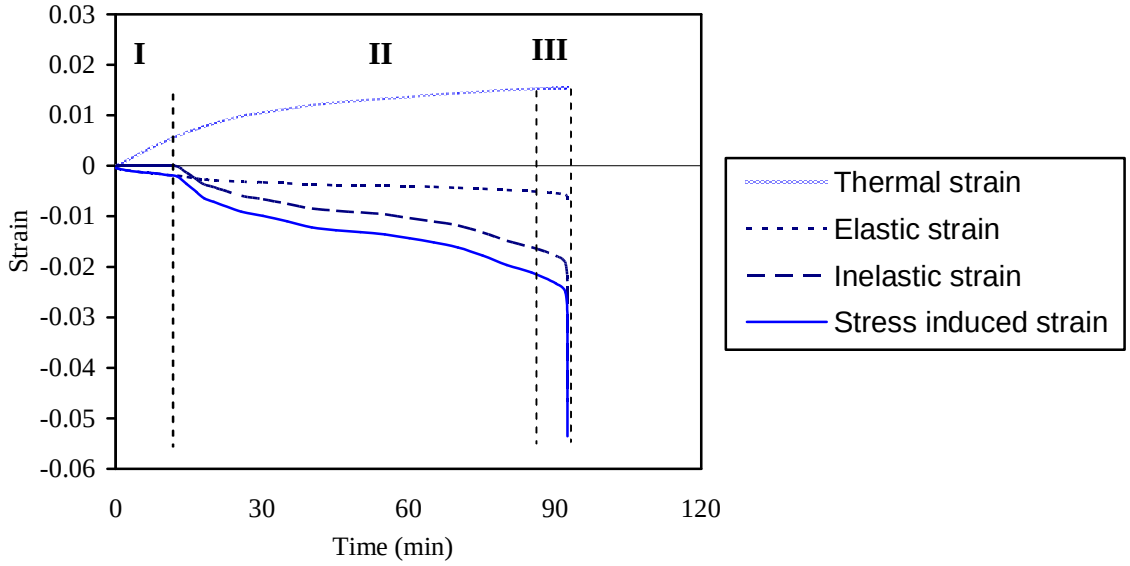

(a) S1R2E0

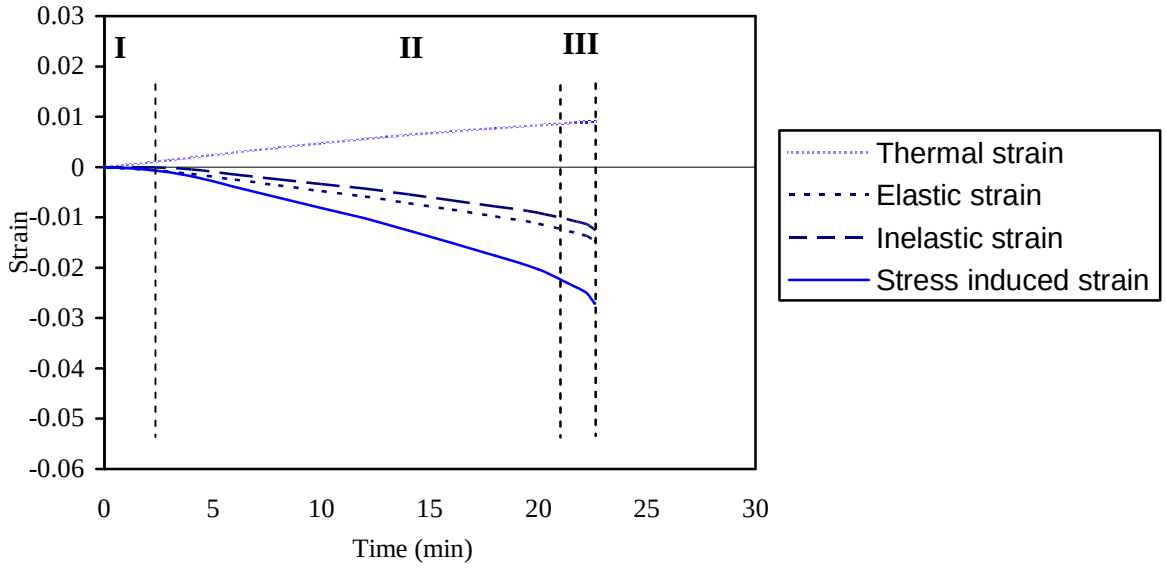

(b) S1R4E0

Figure 3.19 Strain in steel tube

As can be seen in Figure 3.19, the thermal strain gradually increases in all stages of the fire exposure. The stress induced strain increases slowly in the first stage of fire exposure (stage I in Figure 3.17), moderately in the second stage of fire exposure (stage II in Figure 3.17) and then increases dramatically in the third stage of fire exposure

(stage III in Figure 3.17). The thermal strain is higher than the stress induced strain until the beginning of the second stage of fire exposure, then the stress induced strain overcomes the thermal strain until failure of the CFST columns. So, the entire CFST columns behave in tensile deformation until the beginning of the stage II and then in compressive deformation until failure. Then, both the inelastic strain and stress induced compressive strain increase steadily in stage II and increase dramatically when the columns close to fire endurance.

The axial deformation of the CFST columns is constrained by the constant compressive load, which forces the concrete and steel in the column deforming consistently in the axial direction. This also leads to variation in proportion of load taken by the steel and concrete. In the first stage of the fire exposure, the stress induced strain is dominated by elastic strain which can be clearly seen in Figure 3.19, or the CFST column behaves elastic in this stage. The steel which has higher temperature and thermal expansion property will increase its load proportion due to its free tensile deformation is constrained. Inelastic strain of the steel begins to increase in the second stage of the fire exposure (stage II in Figure 3.17). Material non-linearity of the steel starts significantly influence the behaviour of the CFST column from stage II. Increase in the compressive strain of the steel will not results in proportional increase in the stress of the steel and the core concrete tends to resist the compressive axial deformation. This macroscopically leads the drop in the load taken by steel and increase in the load taken by concrete as shown in Figure 3.18.

3.6.1.3 Stress and strength

The ratio of Mises stress of the steel at the corner of the mid-span section to the yield stress of the steel is shown in Figure 3.20. The yield stress of the steel is taken as stress in the stress-strain-temperature model (Kodur, 2007) at strain of 0.02. It can be clear seen in Figure 3.20 that the stress ratio increases rapidly in the first stage of fire exposure. Then, this ratio increases steadily for S1R4E0 until failure of the column, but it increases steadily in the second stage of fire exposure and then increases dramatically in the third stage of fire exposure for S1R2E0. The Mises stress of the steel is almost equal to the yield stress of the steel when the CFST columns reach fire endurance.

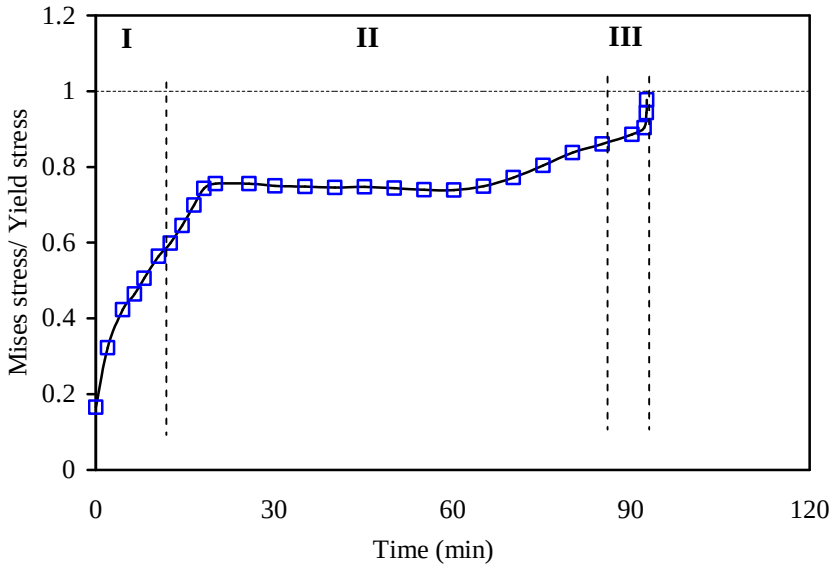

(a) S1R2E0

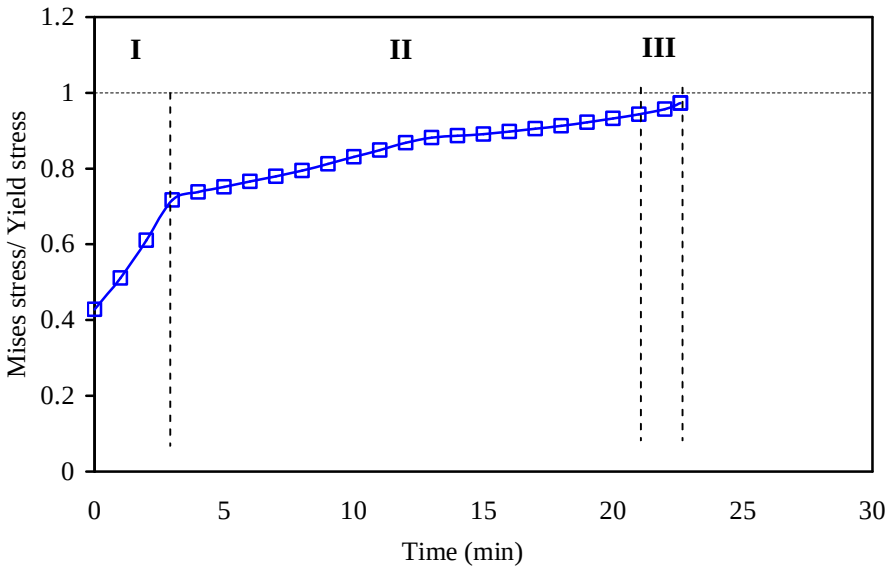

(b) S1R4E0

Figure 3.20 Mises stress to yield stress ratio in steel tube

The stress in the concrete and the degradation in the concrete compressive strength is complex due to the non-uniform temperatures in the concrete. The ratio of the axial stresses in the concrete which is corresponding to point 1, 2 and 3 in Figure 3.2 at the mid-height section to the compressive strength of the concrete is shown in Figure 3.21. As shown in the figure, the stress ratio at the outer part of the concrete (point 1)

decreases in the first stage of the fire exposure and increases steadily until the third stage. There is a clear drop of the stress ratio at point 1 as the CFST columns close to fire endurance. It is also interesting to find out that the stress ratio at point 1 is greater than one near the end of the second stage of the fire exposure. This means that there is a lateral restraint from the inner part of concrete and steel on this part of concrete. The stress ratio in the inner part of the concrete (points 2 and 3) is lower than that in the outer part of concrete (point 1). The stress ratios at points 2 and 3 are higher in the specimen S1R2E0 due to its longer fire exposure time.

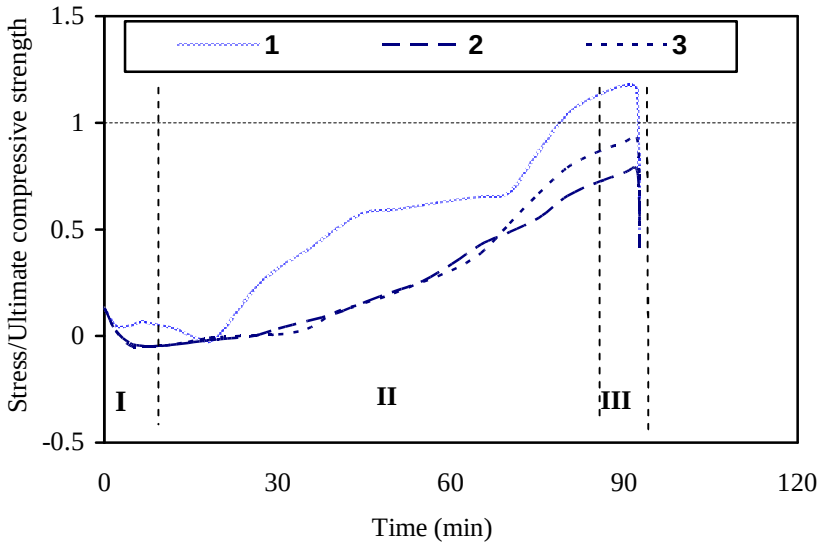

(a) S1R2E0

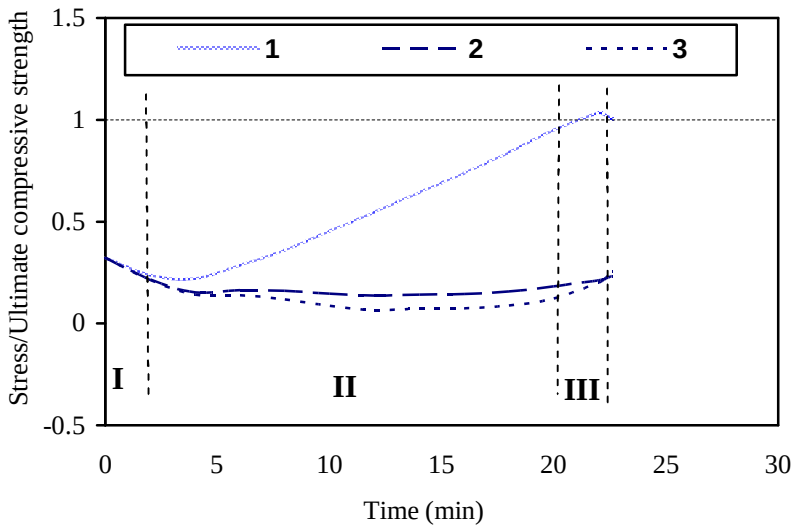

(b) S1R4E0

Figure 3.21 Axial stress to ultimate compressive strength ratio at typical points in concrete

3.6.1.4 Local buckling of the steel hollow section

Local buckling of the steel hollow section at elevated temperatures occurs far before the columns reach the fire endurance, i.e. in stage II shown in Figure 3.17. The buckling of the steel hollow section has not been found heavily influence the behaviour of the columns. The in-filled concrete prevents inwards buckling of the steel hollow section and the steel hollow section is forced to bulge outwards as shown in Figure 3.22(a). Outwards bulging in the steel hollow section develops from one bulge to several bulges gradually. Concrete provides support to the steel hollow section at positions between bulges where the steel hollow section contacts with the concrete. The reaction force, R_c, from concrete to steel hollow section at these positions is schematic shown in Figure 3.22(b). Steel plates at each face of the steel hollow section become multi-span plates supported by the concrete. Number of the bulges increases causes increase in the number of span and decrease in the span between bulges. In this way, the buckling load of the steel hollow section can retain relatively stable. Thus, the buckling of steel hollow section does not result in dramatically reduction in the capacity of the steel hollow section. As a result, behaviour of the columns is not significant influence by the buckling of the steel hollow section.

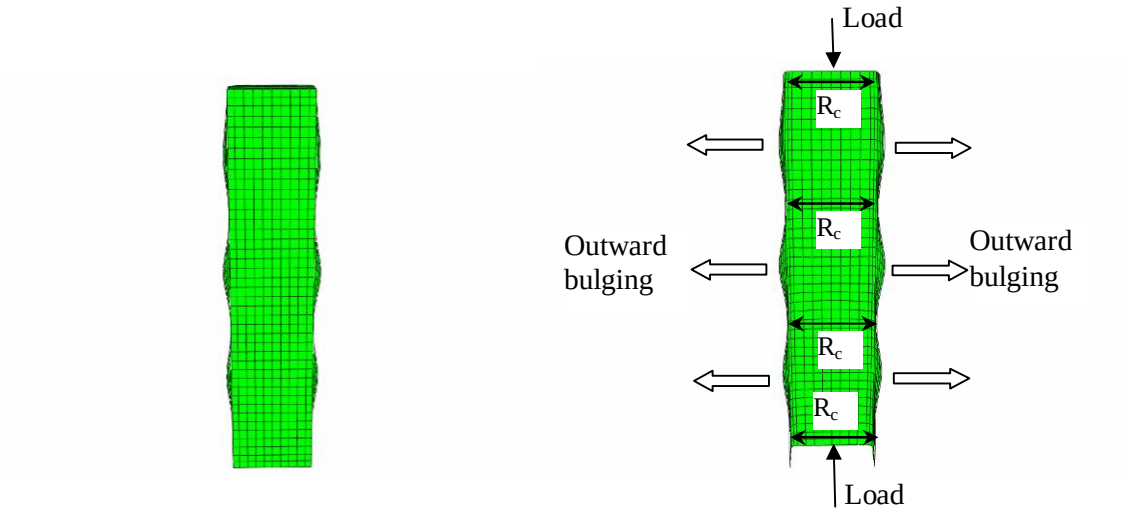

(a) Buckling of steel tube (b) Lateral support of concrete to steel tube

Figure 3.22 Lateral support of concrete to steel tube after buckling

3.6.2 Failure mechanism

From the above analysis, it is clear that there is a load transfer between the steel and concrete in the CFST columns during fire exposure. Ultimate compressive strength of the concrete in the inner part of the core concrete degrades slowly due to the slow

temperature elevation in this part of concrete. The core concrete can continuously take compressive load transferred from the steel hollow section until the outer part of the concrete reaches its compressive strength. On the other hand, the concrete provides lateral support for the steel hollow section so as it can retain its load capacity to some extent when the steel hollow section buckles locally. The interaction between the steel and concrete in the composite columns is a key factor responsible for the good fire performance of the columns.

Yield of the steel is the major cause for the CFST columns loss its capacity during fire exposure. Yield of the steel should have resulted in excessive axial deformation in the steel hollow section, whereas the core concrete resists such excessive deformation by sharing the load from the steel hollow section. The compressive stress of concrete is not even because of the non-uniform temperature distribution. The outer part of the concrete is the most vulnerable in the whole concrete which is in higher temperature and compressive stress and lower strength. This part of the concrete crushes first and let the inner part of the concrete alone to resist the load. Buckling of the steel hollow section and crushing of the outer part of the concrete have greatly reduced the confinement on the inner part of concrete. This leads reduction in the capacity of the inner part of the concrete. Thus, the column fails when the core concrete can not further resist the load transmitted from the steel hollow section.

3.7 CONCLUSIONS

The behaviour of high strength SCC filled CFST columns exposed to standard fire was investigated experimentally. In addition, a FEA model was proposed to simulate the behaviour of the columns. The verified FEA model was further used to analyse the structural behaviour of the CFST stub columns under fire exposure. Several conclusions can be drawn based on the study in this chapter:

- The behaviour of high strength SCC filled stub columns exposed to standard fire is almost the same as that of conventional concrete filled columns.
- All stub columns fail in a ductile way. Specimens retained integrity after testing despite of local bulge of the steel hollow section and local crush of the concrete. These observations are strong evidences of the interaction of the concrete and steel in the CFST columns during the whole process of fire exposure.

- The limiting temperature in the steel of the SCC the filled stub columns ranged from 512 to 819 ^{o}C which is comparable to that of conventional concrete filled columns.
- The proposed FEA model was used to predict the temperatures, fire endurance and failure mode which generally well agree with the test results. Thermal properties of the HSC are applicable to represent those of SCC in calculating the temperatures of the high strength SCC filled columns. The material mechanical model, which was originally developed for normal and high strength concrete in CFST columns, suits to represent that of the high strength SCC in the stub columns. The FEA model could be used to predict the fire behaviour of large CFST stub columns in buildings.
- The FEA modelling was used to analyse the structural behaviour of the CFST stub columns to gain insight into the failure mechanism. The interaction between the steel and concrete in the columns is found to be a key factor responsible for the good fire performance of the composite columns. The yield of the steel hollow section is a major cause of the failure which occurs when the concrete can not further sustain the load transferred from the steel hollow section.

[Blank page]

Chapter 4

EXPERIMENTAL INVESTIGATION INTO FIRE BEHAVIOUR OF SCC-FILLED DOUBLE SKIN STEEL STUB COLUMNS

4.1 OVERVIEW

The behaviour of CFDST columns at ambient temperature has been intensively studied, and CFDST columns exhibit behaviour similar to or even better than that of CFST columns at ambient temperature. However, the fire behaviour of CFDST columns remains unknown. When CFDST columns are used in buildings, fire resistance is one of the major concerns which need to be addressed. The susceptible fire performance of CFDST columns is due to the direct fire exposure of the outer steel tube. Thus, the fire behaviour of CFDST columns needs to be understood before they can be used in buildings with confidence.

Similar to CFST columns, CFDST columns can be classified as stub and slender columns which have different behaviours at ambient temperature. The behaviour of CFDST stub and slender columns at elevated temperature is also likely to differ. At the same time, CFDST columns are a construction type for which SCC has great potential application because SCC can offer convenience in construction and ensure quality and structural performance of the composite columns. Therefore, the fire behaviour of SCC-filled CFDST columns is a significant topic which needs investigation.

This chapter focuses on an experimental investigation into the fire performance of SCC-filled CFDST stub columns. A total of eighteen stub columns were prepared, two of which were reference specimens which were tested under ambient temperatures, while the remainder were for standard fire tests. Different types of concrete, normal SCC, steel fibre-reinforced SCC and both steel and polypropylene fibre-reinforced SCC were used to research their effects on the fire performance of the composite columns. In addition, the influence of certain parameters, such as load level and profile size, on the fire behaviour was also studied. The tests were carried out on relatively small specimens due to the load capacity limitation of the test rig. The primary purpose of the test was to obtain some basic fire performance data for the columns, such as temperature distribution and failure mode, and to establish reference points for the calibration of the finite element analysis model in the subsequent study.

4.2 EXPERIMENTAL PROCEDURE

4.2.1 Material Properties

4.2.1.1 Property of SCC

In the current study, a combination of ACI recommended mixture design method (ACI, 2007) and a method proposed by Su et al. (2001) was used to design the SCC mixture. The amount of aggregate was firstly determined by selecting an appropriate packing factor. The amount of cement and water/cement ratio was determined based on the anticipated strength of the concrete. Then, the amount of fly ash and/or slag was determined to allow enough paste and mortar in the mixture to reduce friction in the aggregate. Finally, superplasticizer was used to further improve the workability and avoid segregation of the concrete.

Steel fibre or steel/polypropylene fibre reinforced SCC was obtained through modifying the mixture of the SCC without fibre by adjusting the amount of superplasticizer in the mixture. Either the steel or polypropylene fibre was found seriously influence the workability of SCC in the current test. Similar phenomenon has been observed by other researchers (Nehdi and Ladanchuk, 2004).

After trails, the mixtures of the SCC were finally determined as shown in Table 4.1. The expected concrete cylinder strength was between 40 to 70 MPa, which was common strength of SCC in engineering applications (Domone, 2006). The coarse aggregate was crushed basalt with size ranging from 10 to 15 mm. The aspect ratio of the steel fibre was 35 (30 mm long and 0.85 mm thick). The polypropylene fibre was monofilament polypropylene fibre. The steel and polypropylene fibres are shown in Figure 4.1.

Table 4.1 SCC and fibre-reinforced SCC mixture (per m3)

Concrete type	Cement (kg)	Fly ash (kg)	Slag (kg)	Water (kg)	Fine aggregate (kg)	Coarse aggregate (kg)	SP (l)	Steel fibre (kg)	Polypropylene fibre (kg)
SCC1	125	157	157	160	865	817	2.77	0	0
SCC1SF	125	157	157	160	865	817	2.83	42	0
SCC2	380	170	0	178	776	831	2.85	0	0
SCC2SF	380	170	0	178	776	831	3.08	42	0
SCC2SPF	380	170	0	178	776	831	3.62	42	0.9

(a) Steel fibre

(b) Polypropylene fibre

Figure 4.1 Steel and polypropylene fibres in the tests

In order to test the workability of SCC, unique testing methods have been proposed, such as slump flow test, J-ring, L-box and column segregation test (ACI, 2007). In this study, the slump flow and L-box tests were used to evaluate the workability of the SCC. Typical slump flow and L-box tests of the SCC sample are shown in Figure 4.2.

(a) Slump cone test

(b) L-box test

Figure 4.2 Test the workability of SCC sample

The flow ability index of SCC can vary in a reasonable range due to the diverse application of the concrete. Generally, slump flow is required between 450 and 760 mm,

t_{50} not more than 2 to 5 seconds and the block ratio greater than 0.8 (ACI, 2007). The flow ability of the SCC sample in this test is summarized in Table 4.2. As shown in the table, the slump flow and t_{50} generally meet the above mentioned requirements, whereas the block ratio is somewhat lower than the recommended value. Blockage of the fibres by the reinforcements in the L-Box was the main cause of the low block ratio of the SCC with fibres. However, SCC is a performance based concrete. Its workability can be determined by the application situations (Hwang et al., 2006). Considering the concrete to be used in CFDST columns without reinforcements, there is an enough gap to allow concrete to flow. It seems that block ratio may not be a critical index for the workability of SCC to be used in CFDST columns. Therefore, the workability shown in Table 4.2 was deemed to satisfy the requirement of SCC use in CFDST columns. Such judgment on the workability of the SCC was later proven appropriate because no blockage of the SCC was observed during placing the concrete into the CFDST columns.

Table 4.2 Workability of SCC

Concrete type	Slump flow (mm)	t_{50} (sec)	Block ratio
SCC1	570	1.53	0.64
SCC1SF	580	1.41	0.58
SCC2	640	1.84	0.83
SCC2SF	590	1.06	0.57
SCC2SPF	560	2.83	0.44

Besides tests on the workability of the concrete, concrete cylinders were prepared to determine the strength of the concrete. Some of the cylinders were cured under standard condition to test the strength of the concrete at 28 days. Others were cured under conditions similar to the concrete in the CFDST specimens so as to obtain more realistic concrete strength as shown in Figure 4.3. Table 4.3 summarizes the concrete strength at 28 days and the average concrete strength obtained during the testing period of CFDST specimens. As can be seen in the table, the concrete strength can be divided into two groups (SCC1 and SCC2), i.e. 46.6 to 48.6 MPa and 61.2 to 63.4 MPa.

Table 4.3 Cylinder strength of concrete (MPa)

Concrete type	Fibre used	28 day Standard curing	28 day CFDST curing	Average strength during test
SCC1	None	50.6	42.7	46.6
SCC1SF	Steel	53.5	41.8	48.6
SCC2	None	65.9	60.8	63.4
SCC2SF	Steel	58.9	56.1	61.2
SCC2SPF	Steel and polypropylene	64.4	61.5	62.5

Figure 4.3 Curing of the concrete

4.2.1.2 Property of steel

Both circular and square tubes used for the CFDST columns are cold-formed tubes manufactured to AS 1163 (1991). In order to obtain mechanical properties of the steel, tensile coupons were cut longitudinally from each type of the tubes. Steel coupons were cut from the flat face of the square tube adjacent to the face with weld seam. For circular tube, steel coupons were cut at the position 90^o away from the weld seam. The longitudinal coupons taken from circular steel hollow sections were not flattened in the parallel length in which the deformation was measured but the gripped ends were flattened for gripping in the testing machine. Two strain gauges were installed on each side of the coupons. The average readings of the strain gauges were used to represent the deformation of the coupons to eliminate the effect of any bending in the coupons. Three coupons were prepared for each tube. The average of the test results was used to represent the mechanical properties of the steel. The yield stress and ultimate tensile strength are shown in Table 4.4. The 0.2% proof stress was adopted as the yield stress since no obvious yield point exists for cold-formed tubes (Zhao et al., 2005).

Table 4.4 Steel properties

Tube label	Profile of the section	B (D) $\times t$ (mm)	f_y (MPa)	f_u (MPa)
C1	Circular	406×8	401	458
C2	Circular	219.1×5	426	469
C3	Circular	165.1×3	399	470
C4	Circular	101.6×3.2	426	476
S1	Square	350×8	514	564
S2	Square	200×6	506	591
S3	Square	150×5	504	539
S4	Square	89×3.5	506	545

4.3 Specimens

CFDST columns can have tubes with different profiles as inner and outer steel tubes, such as circular, square or rectangular tubes. In this study, the inner and the outer tubes have the same shape (either circular or square) as shown in Figure 4.4. The total length of the specimens was 800 mm. Other parameters of the specimens are given in Table 4.5. The specimen label in Table 4.5 is arranged as 'outer tube-inner tube-type of concrete' in which the outer and inner tubes are represented by the tube labels shown in Table 4.4 and the type of concrete is given in Table 4.3.

Table 4.5 Parameters of the specimens

Specimen label	Cavity ratio (χ)	Load (kN)	Load level (r_f)	Fire endurance (min)	Critical temperature (^oC)
C1-C3-SCC2	0.42	4100	0.37	62	726
C1-C3- SCC2SF	0.42	4000	0.37	138	937
C1-C3- SCC2SFP	0.42	3400	0.31	>122	963
C2-C4- SCC2	0.49	1821	0.5	30	563
C2-C4- SCC2SF	0.49	1785	0.5	39	696
C2-C4- SCC2SFP	0.49	1821	0.5	27	623
S1-S3- SCC2	0.45	4420	0.35	79	856
S1-S3- SCC2SF	0.45	4420	0.36	128	918
S1-S3- SCC2SFP	0.45	4420	0.35	88	844
S2-S4- SCC2	0.47	1900	0.4	42	711
S2-S4- SCC2SF	0.47	1860	0.4	53	861
S2-S4- SCC2SFP	0.47	1900	0.4	44	710
C2-C4- SCC1	0.49	1923	0.6	24	566
C2-C4- SCC1SF	0.49	1964	0.6	26	563
S2-S4- SCC1	0.47	2567	0.6	18	461
S2-S4- SCC1SF	0.47	2615	0.6	18	400
C2-C4- SCC1-Ref	0.49	3333*	N/A	N/A	N/A
C2-C4- SCC1SF-Ref	0.49	3289*	N/A	N/A	N/A
Note: *Load capacity at ambient temperature for reference specimens.					

Totally eighteen specimens were prepared, sixteen of them for standard fire test and the other two as reference specimens at ambient temperature. The purpose of the reference specimens was to find out any difference in the capacity of the columns filled with SCC and steel fibre reinforced SCC. Cavity ratio (χ) in the table is defined as:

$$\chi = B_i /(B_o - 2t_o) \quad \text{or} \quad D_i /(D_o - 2t_o) \tag{4.1}$$

where B_i is the width of the inner tube, B_o is the width of the outer tube, D_i is the diameter of the inner tube, D_o is the diameter of the outer tube, to is the thickness of the

outer tube. Load level (r_f) or called degree of utilization (μ_o) is the ratio of load on the columns in the fire tests to ultimate capacity of the columns at ambient temperature.

Steel tubes were cut into 800 mm length. Then, the inner and outer tubes were concentrically welded to a 5 mm thick mild steel end plate. A 20 mm diameter hole was drilled on the outer tube for releasing vapour in the concrete at elevated temperatures. In order to monitor the temperatures in the CFDST columns, three thermocouples were installed in each specimen, as shown in Figure 4.4. The concrete was placed into the gap between the tubes (see Figure 4.5) without vibration. The concrete was cured for two weeks and then air dried until testing.

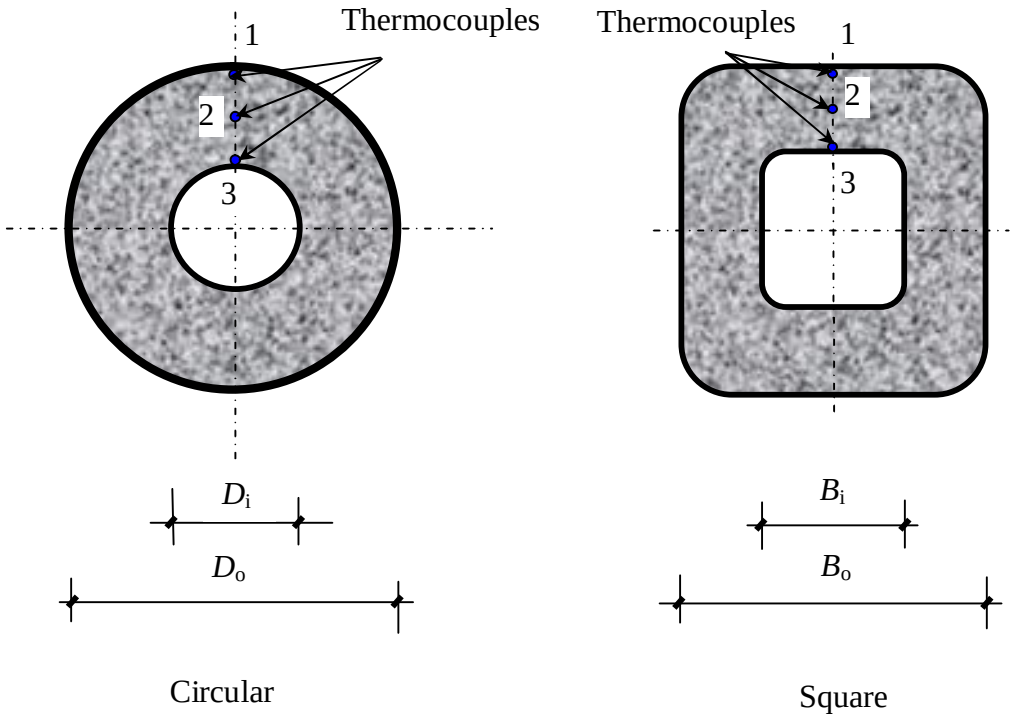

Figure 4.4 Profile of CFDST specimens

Figure 4.5 Placing concrete in CFDST specimens

4.4 Test conditions

The specimens were tested in a furnace located in Civil Engineering Laboratory at Monash University. The setup consists of a gas furnace, a load reaction frame, a loading system with maximum capacity of 5000 kN, a fire temperature control unit and data acquisition system. Details of the setup and test procedure are similar to those reported in Chapter 3. The fire temperature in the current tests followed the fire temperature versus time relationship specified in AS 1530.4 (1997).

4.5 TEST RESULTS

4.5.1 Temperature Distribution

Temperatures measured from the thermocouples in the CFDST specimens are shown in Figure 4.6. Temperature curves noted as 1, 2 and 3 in Figure 4.6 are corresponding to temperatures measured by thermocouples 1, 2 and 3 shown in Figure 4.4. As can be seen in Figure 4.6, the temperature is not uniform in CFDST specimens. Temperature in the outer tube (point 1) is significantly higher than that in the inner tube (point 3), whereas the temperatures at the middle of the concrete (point 2) is close to that on the external surface of the inner tube (point 3). The highest temperature in the outer tube varies from 400 to 963 ^{o}C and the corresponding temperature in the inner tube varies from 59 to 197 ^{o}C.

There is a relative stable stage of the temperature values in the concrete when the temperature is about 100 ^{o}C. This phenomenon is caused by state change of water in the concrete. At this moment, most of the heat is used to change the state of the water rather than to elevate the temperature in the concrete.

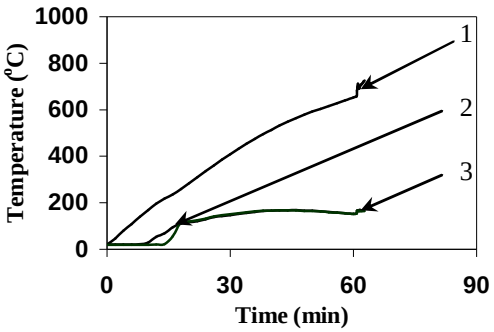

(a) C1-C3-SCC2

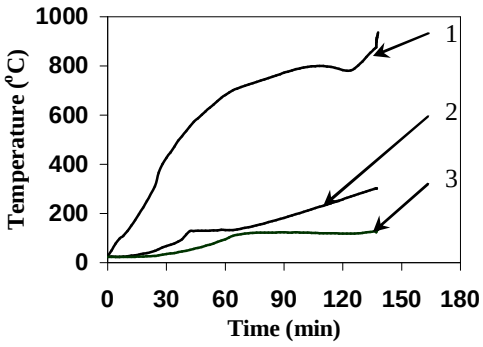

(b) C1-C3- SCC2SF

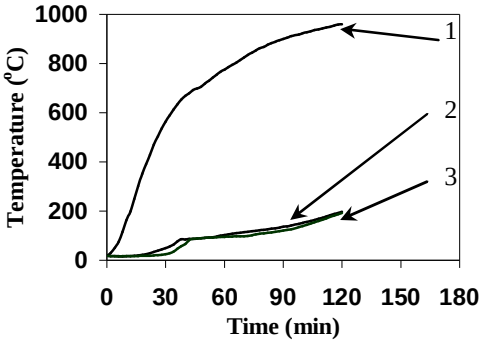

(c) C1-C3-SCC2-SFP

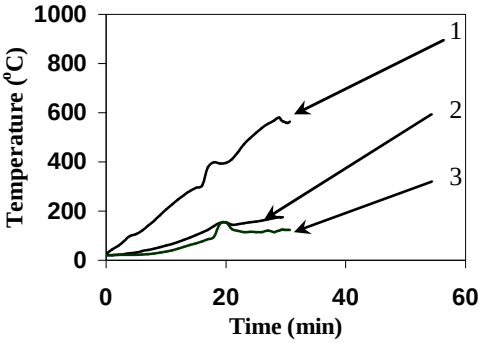

(d) C2-C4-SCC2

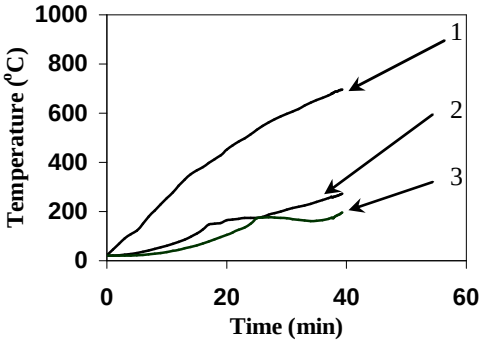

(e) C2-C4-SCC2-SF

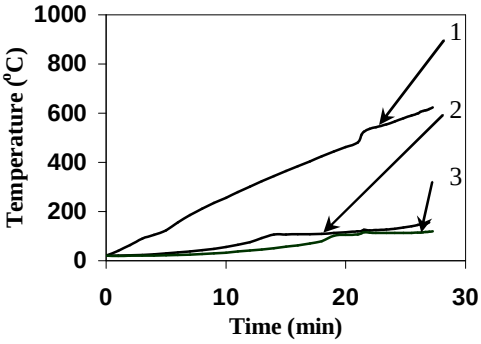

(f) C2-C4-SCC2-SFP

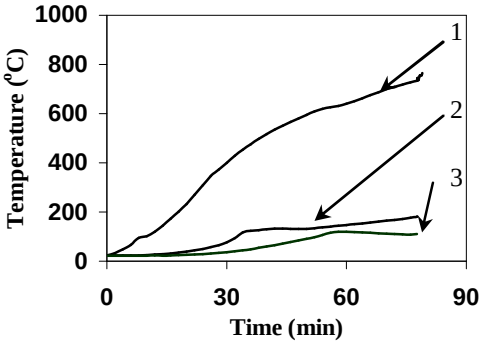

(g) S1-S3-SCC2

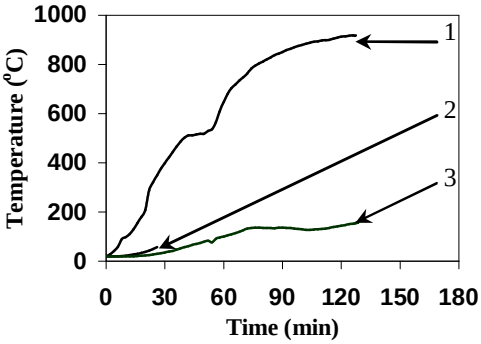

(h) S1-S3-SCC2SF

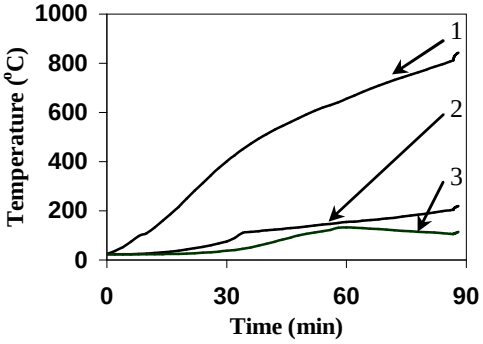

(i) S1-S3-SCC2-SFP

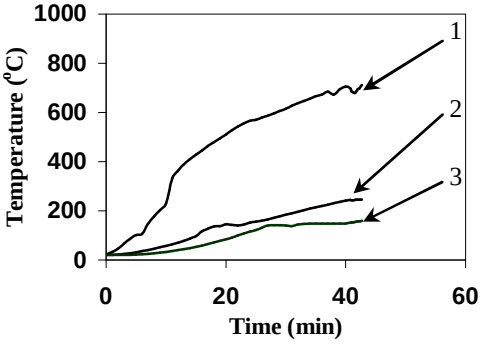

(j) S2-S4-SCC2

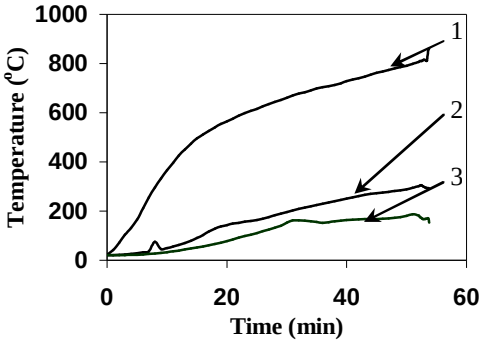

(k) S2-S4-SCC2SF

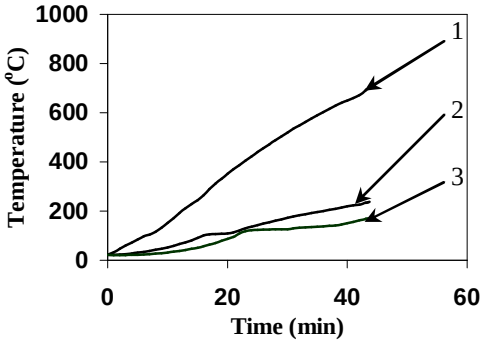

(l) S2-S4-SCC2-SFP

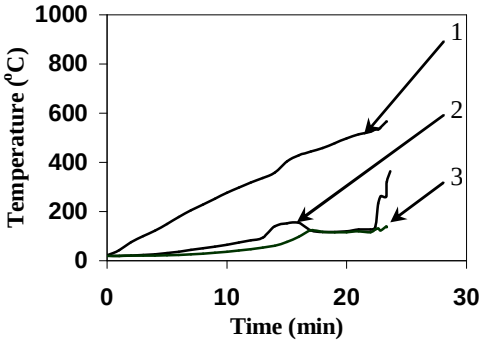

(m) C2-C4-SCC1

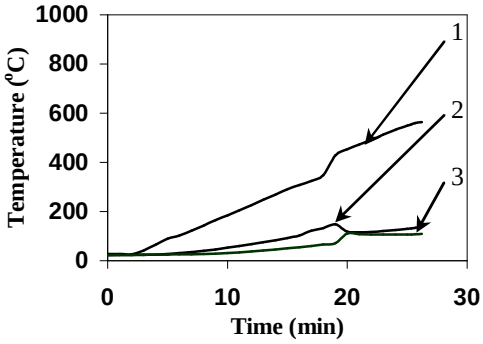

(n) C2-C4-SCC1SF

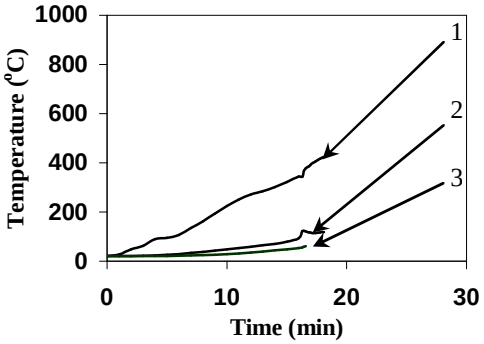

(o) S2-S4-SCC1

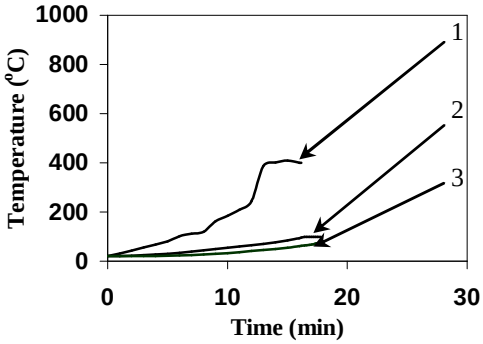

(p) S2-S4-SCC1SF

Figure 4.6 Temperatures in the CFDST specimens

4.5.2 Axial Deformation

The axial deformation for the stub columns is shown in Figure 4.7. Similar to the axial deformation of CFST columns under fire exposure (Lu et al., 2009; Han et al., 2003c; Kodur, 1998a), the axial deformation of the CFDST stub columns has three distinct stages. The first stage is the early stage of fire exposure. There is a little axial deformation which is generally a tensile deformation for most of the specimens in this stage. Then in the second stage, the tensile deformation changes to compressive deformation and the deformation gradually increases. Finally in the third stage, the axial

deformation dramatically increases in a very short time and the stub columns can no longer sustain the applied load. It should be noted that specimen C1-C3-SCC2-SFP had not tested to failure due to some insulation problems and the test had to be stopped at 122 minutes.

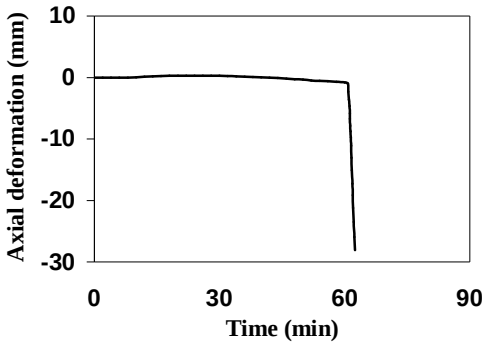

(a) C1-C3-SCC2

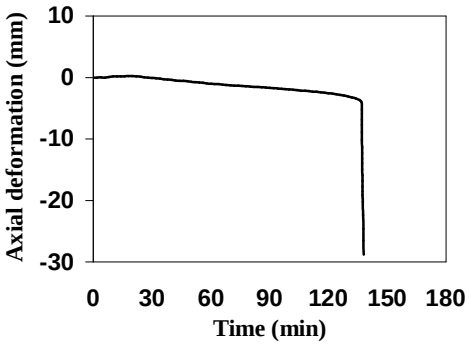

(b) C1-C3- SCC2SF

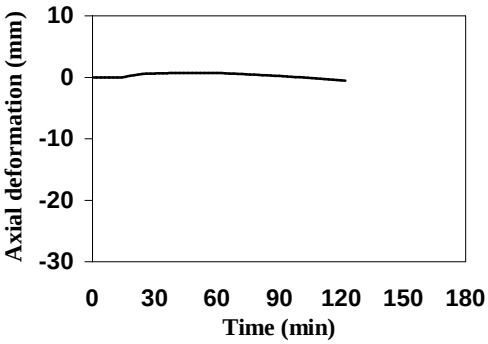

(c) C1-C3-SCC2-SFP

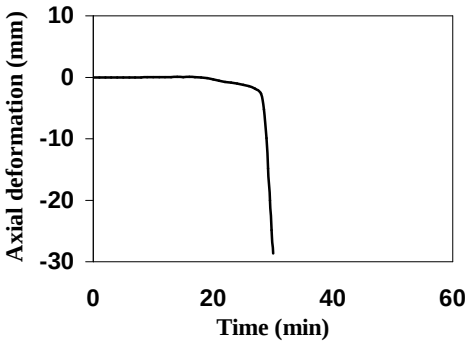

(d) C2-C4-SCC2

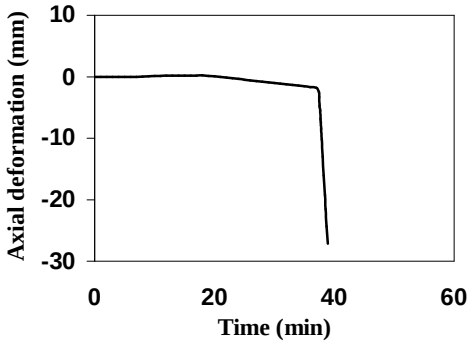

(e) C2-C4-SCC2-SF

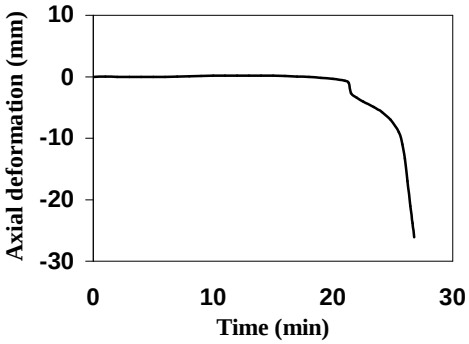

(f) C2-C4-SCC2-SFP

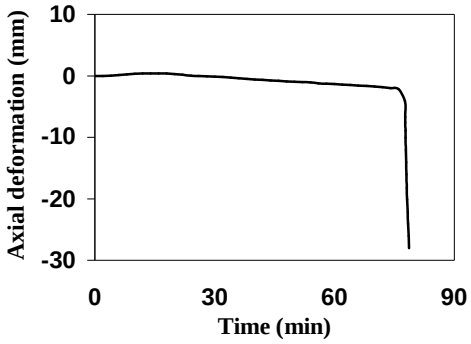

(g) S1-S3-SCC2

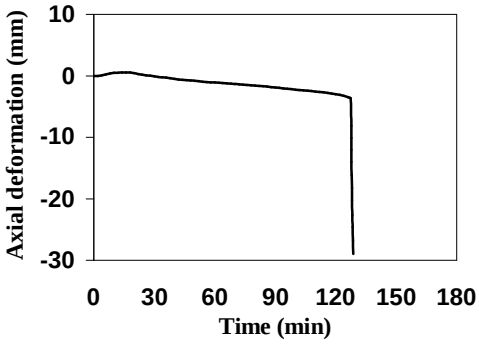

(h) S1-S3-SCC2SF

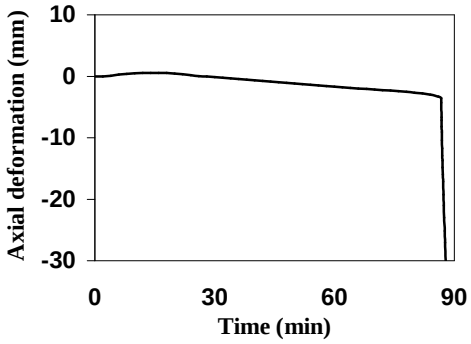

(i) S1-S3-SCC2-SFP

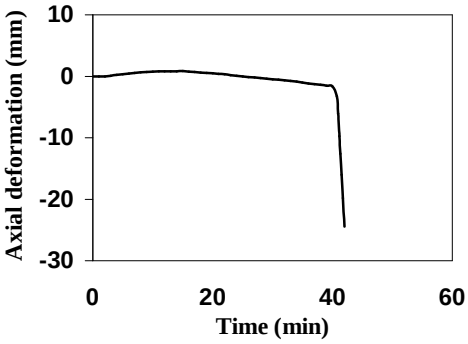

(j) S2-S4-SCC2

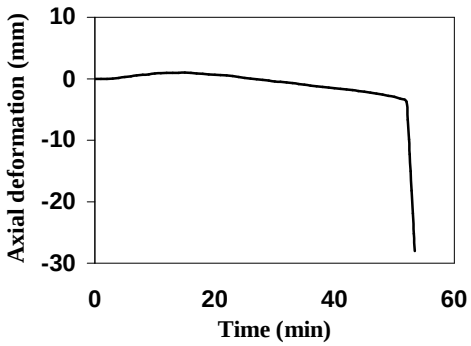

(k) S2-S4-SCC2SF

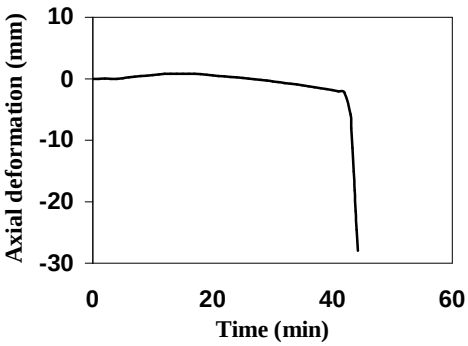

(l) S2-S4-SCC2-SFP

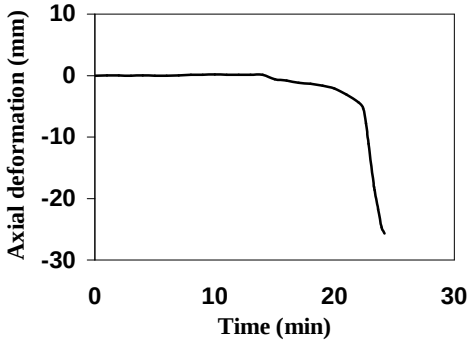

(m) C2-C4-SCC1

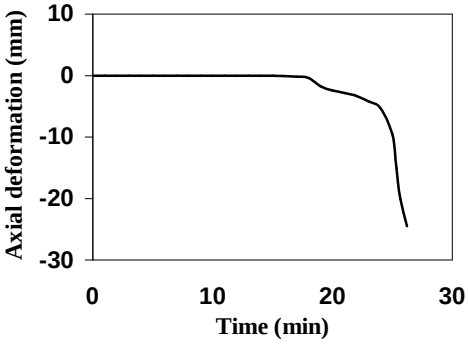

(n) C2-C4-SCC1SF

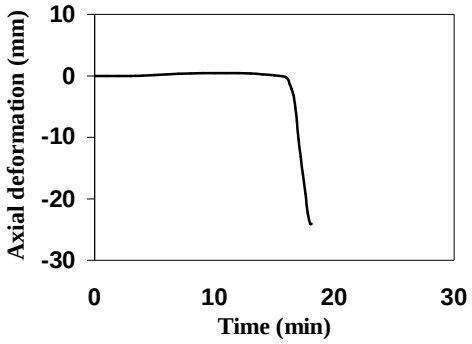

(o) S2-S4-SCC1

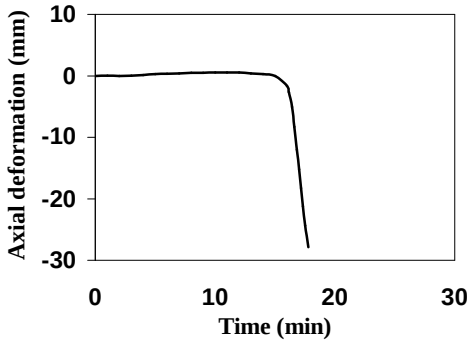

(p) S2-S4-SCC1SF

Figure 4.7 Axial deformation of the CFDST specimens

4.5.3 Fire Resistance

Fire resistance of the stub columns was determined by the axial deformation versus the fire exposure time relationship. The failure criteria are either total axial compressive deformation or deformation rate reaching the values specified in AS-1530.4 (1997). Most of the specimens reached the compressive deformation rate provision earlier than the compressive deformation provision. The fire resistance of the columns which varies from 18 to 138 minutes is shown in Table 4.5. As can be seen in this table, the large size columns have longer fire resistance than the small size columns. The use of fibre in the SCC can effectively increase the fire resistance of the columns. In addition, load level has significant influence on the fire resistance of the columns. More discussions are given in section 4.6.

4.5.4 Failure Modes

Figure 4.8 shows typical failure modes of the stub columns, inner steel tube and concrete. Failure mode of the whole specimens is a typical compression failure without overall buckling, as expected for short columns. The failure mode of the outer tube is outwards bulge as that observed for CFST columns. Failure mode of the inner tube is consecutively inwards and outwards local bulging, which is similar to the failure mode of unfilled tubes. Crush of the concrete occurs at positions corresponding to severe outwards bulge of the outer steel tube. There are also longitudinal cracks in the concrete. Concrete in the large specimens has lighter color compared to that for the small specimens. This is because that the larger specimens have experienced a longer fire exposure time and thus experienced a higher temperature (see Figure 4.6). The temperature near the outer steel tube could be as high as 700 ^{o}C. Decomposition of the

ingredients in concrete, such as calcium hydroxide, calcium silicate hydrate and calcium carbonate, has occurred under such temperature.

(I) Failure mode of specimen

(II) Failure mode of inner tube

(III) Failure mode of concrete

(a) Specimen S2-S4-SCC2SF

(I) Failure mode of specimen

(II) Failure mode of inner tube

(III) Failure mode of concrete

(b) Specimen S1-S3-SCC2SFP

(I) Failure mode of specimen

(II) Failure mode of inner tube

(III) Failure mode of concrete

(c) Specimen C2-C4-SCC1

(I) Failure mode of specimen

(II) Failure mode of inner tube

(III) Failure mode of concrete

(d) Specimen C1-C4-SCC1SF

Figure 4.8 Typical failure modes of the CFDST specimens after fire tests

4.6 Test Results of Reference Specimens

Two reference specimens, C2-C4-SCC1-Ref and C2-C4-SCC1SF-Ref, were tested to failure at ambient temperature. The load versus axial deformation curves of the columns are shown in Figure 4.9. The capacity of the columns listed in Table 4.5 is defined as the peak load in the curves. As shown in Figure 4.9, there is no significant difference in the load versus axial deformation curves of the two specimens.

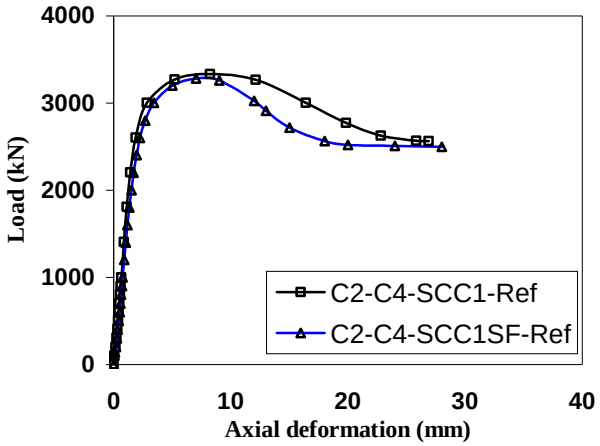

Figure 4.9 Load versus axial deformation of the reference specimens

The failure mode of two reference specimens is shown in Figure 4.10. Comparing the failure modes of the stub columns in fire and those at ambient temperature reveals that there is no significant difference in the failure modes of the inner and outer tubes under the two conditions.

Figure 4.10 Failure modes of the reference CFDST stub columns at ambient temperature

4.7 DISCUSSIONS

4.7.1 Capacity at ambient temperature

When determining the load level of the CFDST columns in fire tests, capacity of the columns under ambient temperature should be known in advance. There are equations to calculate capacity of CFDST columns proposed by several researchers, which were summarized in Zhao and Han (2006). In this testing program, the concrete used to fill the CFDST stub columns were both SCC and fibre reinforced SCC. However, the capacity formulations proposed by other researchers were derived from studies in plain concrete (without fibre) filled CFDST columns. Influence of the fibre on the capacity of the CFDST stub columns is unknown. Therefore, two reference specimens were prepared to investigate the influence of steel fibre on the capacity of the CFDST stub columns.

The major difference in the behaviour of steel fibre reinforced and plain concrete is ductility. Steel fibre reinforced concrete has higher ductility compared to plain concrete. The difference in the ductility of the concrete mainly affects the behaviour of concrete after it has reached peak stress value. However, when concrete is confined by steel tubes, the difference in peak load and ductility for cases with or without fibres is not significant as shown in Figure 4.9. In addition, polypropylene fibre is generally used to improve the crack resistance of concrete due to shrinkage and has little influence on the strength of concrete. Therefore, equations proposed in Zhao and Han (2006) which were based on plain concrete were used to determine the capacity of the stub columns in this testing program. Capacity of the columns is the summation of the capacity of each component in the CFDST columns shown as follows (Zhao and Han, 2006),

$$P_{CFDST} = P_{outer} + P_{concrete} + P_{inner} = A_{outer} f_{yo} + k_c A_{concrete} f_c + A_{inner} f_{yi} \quad (4.2)$$

where A_{outer}, A_{inner} and $A_{concrete}$ is the cross-sectional area of the outer tube, inner tube and concrete, f_{yo} and f_{yi} is the yield stress of the outer and inner steel tubes, fc is the concrete strength, k_c is reduction factor on concrete strength taken as 0.85 except when both outer and inner tubes are CHS where k_c is taken as 1.0 (Zhao and Han, 2006).

The capacity predicted by Eq. 4.2 for the reference specimens is 3127 kN which agrees well (within 6.5%) with the test results of the columns shown in Table 4.5, i.e. 3333 kN for C2-C4-SCC1-Ref and 3298 kN for C2-C4-SCCSFRef.

4.7.2 Temperature Distribution

4.7.2.1 Effect of fibre on the temperature distribution

The primary purpose of adding steel and polypropylene fibres in concrete is to improve the mechanical behaviour of the concrete. Steel fibre can increase toughness of the concrete. Polypropylene fibre can prevent shrinkage crack of concrete at ambient temperature and explosive spalling of concrete at elevated temperature. However, the effect of these two types of fibres on the thermal property of concrete is less significant. Research conducted by Kodur et al (2003) showed that steel fibre did not affect temperature in concrete and polypropylene fibre could slightly slow down temperature elevation in concrete. The melting point of polypropylene fibre is about 160 ^{o}C. Melting of polypropylene fibre absorbs heat in concrete thus potentially slows down temperature elevation in concrete.

Comparing temperatures in the CFDST specimens with different types of concrete in the current testing program (e.g. SCC2 series versus SCC2SF series), there is no significant difference between temperatures in the CFDST specimens filled with SCC and filled with steel fibre reinforced SCC when exposed to fire for the same period of time. This further confirms the fact that steel fibre does not alter the thermal property of concrete nor the temperature distribution in concrete. The temperatures in the specimens filled with both steel and polypropylene fibres are not significantly different from those filled with plain SCC. This is mainly due to the fact that only small quantity of polypropylene fibre (9 kg/m3) was added to the concrete. Such small amount of polypropylene fibre can not alter the thermal property of the concrete nor the temperature distribution in the CFDST columns.

4.7.2.2 Effect of concrete thickness and perimeter of the outer tube on temperature distribution

Concrete has lower heat conductivity and higher heat capacity than steel. Thus, temperature elevation in concrete is slower than that in steel. The presence of concrete in the CFDST columns slows down temperature elevation in the composite columns and results in non-uniform temperature distribution in the CFDST columns as can be seen in Figure 4.6. Therefore, concrete thermal mass is a major parameter influencing the temperature distribution in the CFDST columns. Concrete thickness and perimeter of

outer tube are selected as two parameters to reflect the concrete thermal mass in the CFDST columns.

In order to investigate the effect of the concrete thickness and outer tube perimeter on the temperature distribution in the CFDST stub columns, the measured temperatures at 15 and 30 minutes of fire exposure are extracted from Figure 4.6 and shown in Figure 4.11 and 4.12.

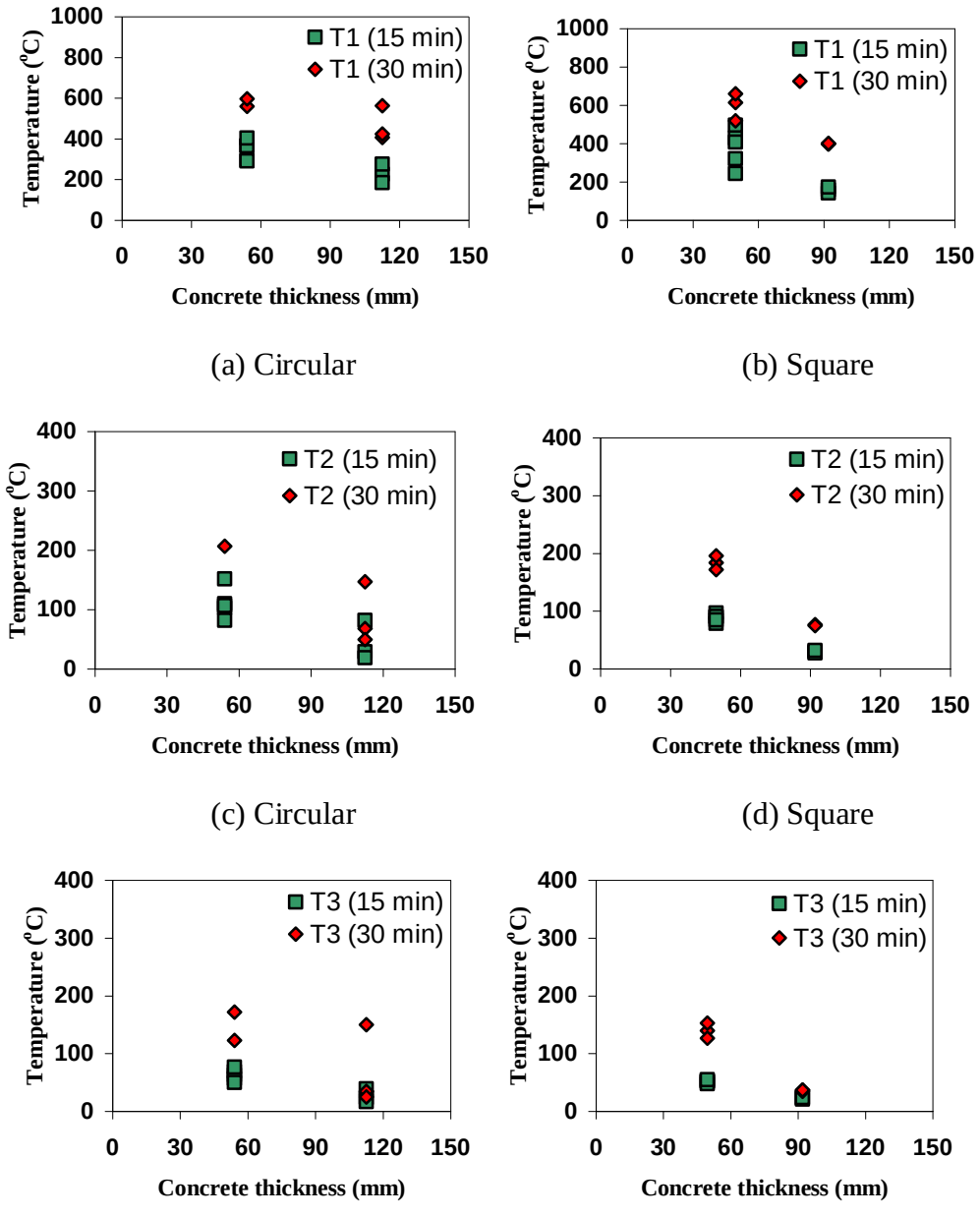

(a) Circular (b) Square

(c) Circular (d) Square

(e) Circular (f) Square

Figure 4.11 Effect of concrete thickness on temperatures in CFDST specimens

The terms T1, T2, and T3 are corresponding to the temperatures measured by thermocouples 1, 2 and 3 shown in Figure 4.4. It can be clearly seen from the figures

that both concrete thickness and outer tube perimeter have significant effect on the temperature distribution in the CFDST columns. The thicker the concrete is and/or the longer the outer tube perimeter is, the lower the temperature in the CFDST columns is.

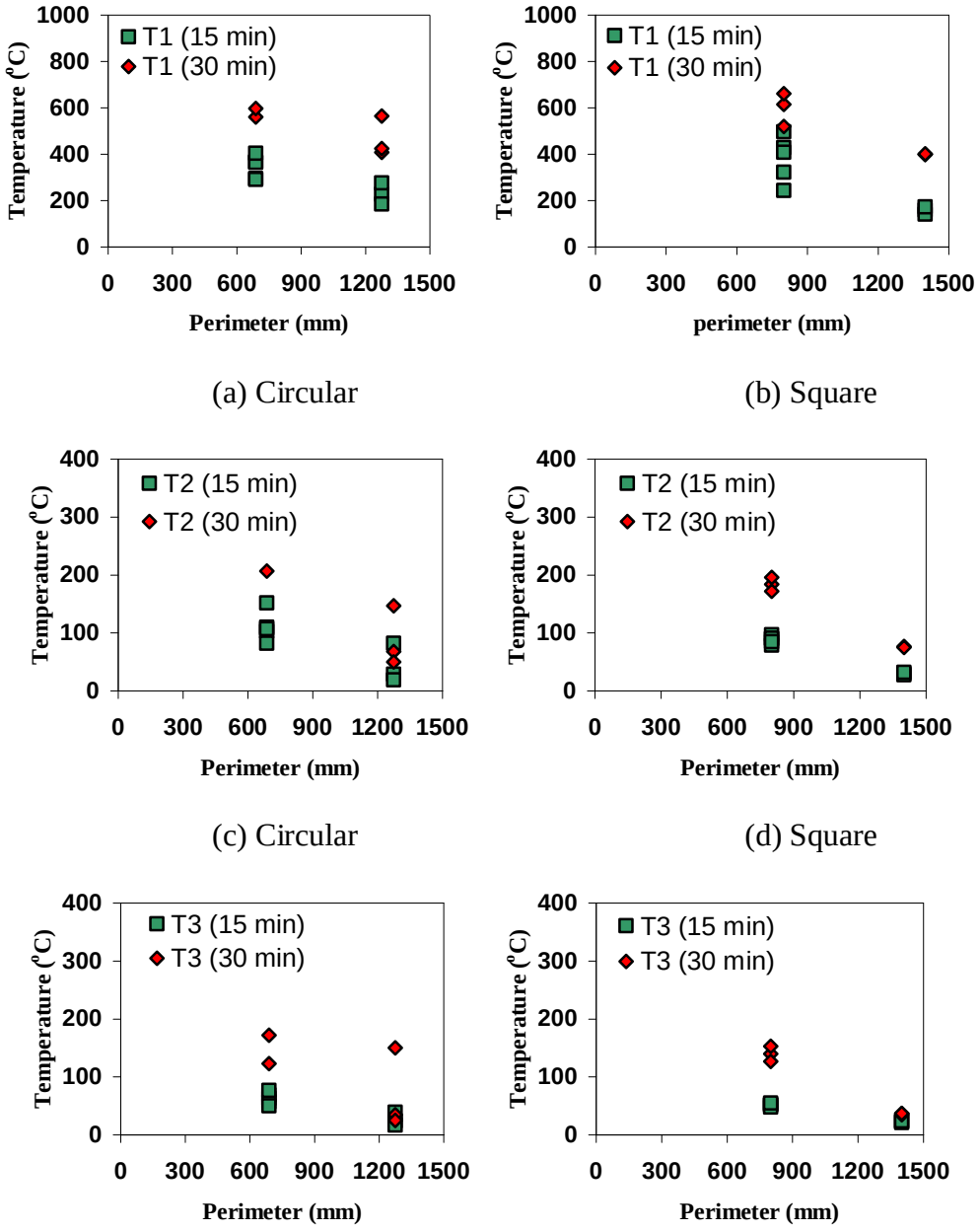

(a) Circular (b) Square

(c) Circular (d) Square

(e) Circular (f) Square

Figure 4.12 Effect of outer tube perimeter on temperatures in CFDST specimens

4.7.3 Critical or Limiting Temperature

Fire resistance of steel members alone can be determined in the temperature domain by critical temperature of the steel. The term “critical temperature” is used in Eurocode 3 (2005) whereas the term “limiting temperature” is used in AS4100 (1998). When

temperature reaches critical temperature, the steel members are deemed to lose their capacity or to reach the fire resistance. The critical temperature (T_{cr}) or limiting temperature (T_{limit}) depends on the degree of utilization (μ_o) or the load level (r_f). The formulae for T_{cr} in Eurocode 3 (2005) and T_{limit} in AS 4100 (1998) for steel members alone is given in Eq. (4.3) and Eq. (4.4), respectively.

$$T_{cr} = 39.19 \cdot \ln\left(\frac{1}{0.9674\mu_0^{3.833}} - 1\right) + 482 \tag{4.3}$$

$$T_{limit} = 905 - 690 r_f \tag{4.4}$$

The limiting temperature of the steel tube in CFST columns was found very close to that of an unfilled steel tube, but the temperature elevation in the steel hollow section of CFST columns is much slower than that in an unfilled steel tube (Lu et al., 2009).

In the CFDST columns, the limiting temperature refers to that in the outer tube which is directly exposed to fire. The limiting temperature concept does not apply to the inner tube because the inner tube does not directly expose to fire and the temperature in the inner tube is very low (below 200^{o}C) when the CFDST columns reach the fire resistance.

The limiting temperatures of the outer steel tube in the CFDST columns are plotted in Figure 4.13 against the load level. The predicted T_{cr} and T_{limit} from Eq. (4.3) and Eq. (4.4) are also plotted in Figure 4.13. It is clear from Figure 4.13 that the limiting temperature in CFDST columns is also load level dependent. Higher load level leads to lower limiting temperatures. The critical temperature of the steel decreases almost linearly with the increase of the load level. It is encouraging to observe that the limiting temperature in CFDST is much higher than that given in Eq. (4.3) and Eq. (4.4) for steel members alone, when the load level is below 0.6.

The corresponding temperature in the inner tube is also shown in Figure 4.13. It can be seen that the corresponding temperatures in the inner tube are around 150 to 200 ^{o}C which is significant lower than the critical temperatures because the inner tube is well insulated by the concrete. The inner steel tubes do not lose much strength and stiffness in this temperature range. Due to limited number of specimens in this program, no equations are proposed for the critical or limiting temperature of CFDST columns. The critical or limiting temperature may also depend on the combination of the outer tube

and the inner tube. More research is needed before an accurate formula could be recommended.

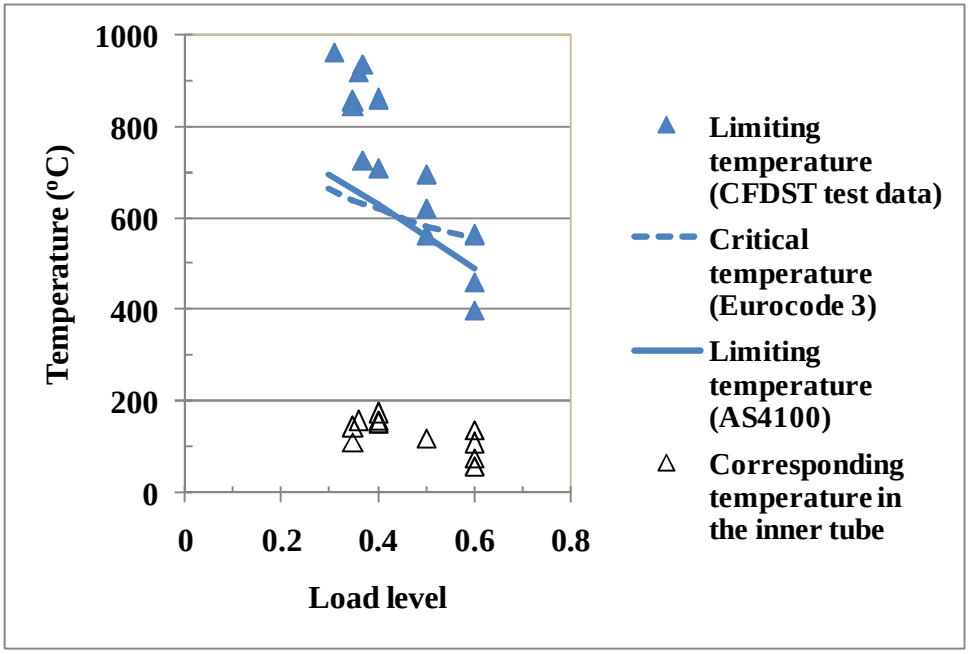

Figure 4.13 Limiting and critical temperatures versus load level

4.7.4 Fire Resistance

4.7.4.1 Effect of load level on fire resistance

The relationship of the fire resistance of the CFDST columns and the load level is shown in Figure 4.14. As can be seen in the figure, load level has significant effect on the fire resistance of the CFDST columns. Generally, the fire resistance of the columns increases with the decrease in load level. Such influence is much more obvious when the load level is less than 0.4. The fire resistance of columns filled with fibre reinforced SCC is more sensitive to the variation in the load level. When load level is less than 0.5, those columns filled with fibre reinforced SCC gain more increase in fire resistance than columns filled with plain SCC.

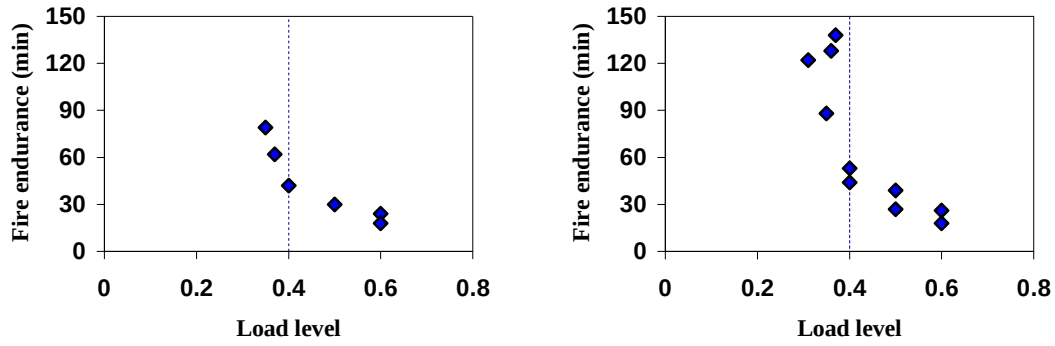

(1) CFDST filled with SCC (2) CFDST filled with fibre reinforced SCC

Figure 4.14 Fire endurance versus load level

4.7.4.2 Effect of the type of concrete on fire resistance

Comparison of the fire resistance of the CFDST specimens filled with different types of concrete is shown in Figure 4.15. As can be seen in the figure, the use of fibres in the SCC can dramatically increase the fire resistance of the CFDST stub columns except for those with high load level (e.g. 0.6). It was also found that adding both steel and polypropylene fibres in SCC does not show any further increase in fire resistance of CFDST columns.

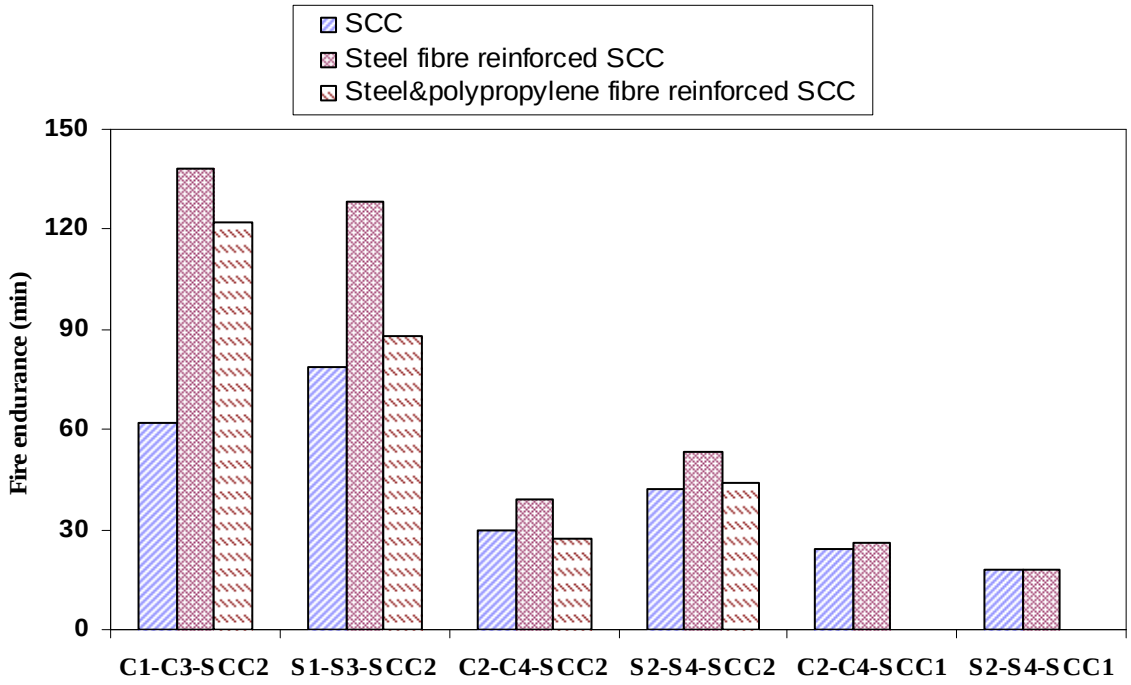

Figure 4.15 Fire resistance of CFDST columns filled different types of concrete

4.7.5 Composite Action in the CFDST Stub Columns

Composite action has been recognized as the cause of the higher level structural performance of the steel and concrete composite elements (Nethercot, 2004). Composite action in CFST and CFDST columns at ambient temperature relies on interaction between the concrete and steel tube in the columns. The bond and friction at the interface of steel and concrete contributes to the composite action to a certain extent, whereas the interaction along the direction perpendicular to the interface makes more significant contribution to the behaviour of the columns. Confinement of the steel tube on the concrete enables the concrete to achieve higher compressive strength and ductility. At the mean time, the support from the concrete alters the failure mode of the steel tubes leading to a higher level of performance.

Under fire exposure, there is doubt about the confinement of the tube to the concrete in CFST or CFDST columns because steel has higher thermal expansion than concrete. However, the typical failure modes of the columns shown in Figure 8 reveal that there is no obvious separation or slip between outer steel tube and concrete. For CFDST columns, the inner steel tube is an important component in the composite action especially because of its low temperature under fire condition. Future research is needed to maximize the composite action by considering different combinations of the three components (the outer tube, the inner tube and the concrete), e.g. using a thicker inner tube.

4.8 CONCLUSIONS

Based on the limited experimental studies presented in this chapter, several conclusions can be drawn:

- The use of steel fibre in the SCC did not affect the capacity of the CFDST stub columns at ambient temperature when compared to the columns filled with plain SCC. The existing formulae for plain SCC filled CFDST could be applied to fibre reinforced SCC filled CFDST.
- Temperature in the inner tube was very low (less than 200^{o}C) even when the fire resistance was reached.
- The thermal mass of concrete, namely concrete thickness and perimeter of the outer tube has significant influence on the temperature distribution in the CFDST columns.

- The critical or limiting temperature of CFDST columns is much higher than those for unfilled steel tubes when the load level is below 0.6. The critical or limiting temperature depends on the load level and may be on the different combination of the outer and inner tubes.
- The fire resistance of CFDST columns increases with the decreases in load level especially for those filled with fibre reinforced SCC. The use of steel fibre in the SCC can significantly increases the fire resistance of CFDST columns when the load level is below 0.6.

[Blank page]

Chapter 5

EXPERIMENTAL INVESTIGATION INTO FIRE BEHAVIOUR OF SCC-FILLED DOUBLE SKIN STEEL TUBULAR COLUMNS

5.1 OVERVIEW

As discussed in Chapter 4, the failure modes of stub and slender CFDST columns are different under ambient temperature. The failure mode of stub columns is generally compressive failure, while slender columns are generally dominated by overall buckling. Therefore, the behaviours of stub and slender CFDST columns are quite different due to their different failure modes. The failure mode of CFDST stub columns under fire exposure has been found to be primarily compressive failure. The fire behaviour of CFDST stub columns and the influence of certain parameters on their fire behaviours have been studied through fire tests of the CFDST stub columns as reported in the last chapter. However, the fire behaviour of slender CFDST columns remains unknown.

This chapter investigates the fire performance of SCC-filled CFDST slender columns by means of full size slender column fire tests. The tests aim to understand the fundamental fire performance of slender composite columns and to investigate the influence of a number of parameters on their fire performance. Test results, such as failure modes, temperatures, deformation and fire resistance, are obtained from fire tests. The fire performance of CFDST columns is investigated through analysis of the thermal and structural responses of the columns. The thermal response of the columns includes the limiting temperatures of the specimens and the influence of fire protection on the temperature distribution. The structural response of the columns focuses on the effects of several key parameters on the fire endurance of the composite columns. In addition, the composite action of steel and concrete and its effect on fire behaviour is also analysed.

5.2 EXPERIMENTAL PROCEDURE

5.2.1 Specimens

Six full size CFDST columns were tested, four were unprotected and another two were protected by spray fire resistant coating. Profiles of the specimens are shown in Figure 5.1. The specimens were designed to enable the effect of various parameters on the fire performance of the CFDST columns to be studied. The profile of outer tube and cavity ratio in the CFDST columns are among factors that affect the behaviour of CFDST at ambient temperature (Zhao and Han, 2006). On the other hand, load and load case are important factors affecting the fire resistance of CFST columns (Tao and Han, 2006).

So, in the experimental program, the variable parameters selected were load ratio (n), cavity ratio (χ), load case and the profile. Load ratio and cavity ratio are defined as follows:

$$n = \frac{N_f}{N_u} \tag{5.1}$$

$$\chi = B_i /(B_o - 2t_o) \quad \text{or} \quad D_i /(D_o - 2t_o) \tag{5.2}$$

where, B_o and B_i are width of outer and inner SHS, D_o and D_i are diameter of outer and inner CHS, t_o and t_i are thickness of the outer and inner steel tubes, N_f is the load applied in the fire test and N_u is the ultimate capacity at ambient temperature respectively. Formulae to determine N_u can be found in Zhao and Han (2006). The parameters of the specimens are shown in Table 5.1.

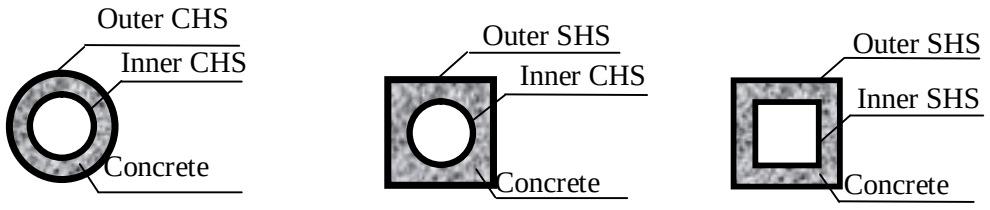

(a) CHS plus CHS (b) SHS plus CHS (c) SHS plus SHS

Figure 5.1 Profiles of CFDST specimens

The total length of each specimen is 3810 mm as shown in Figure 5.2. Steel tubes for specimens were all fabricated from mild steel sheet. The square tubes were fabricated from four sheets with butt welding along the corners. The steel sheet was curved to the required circular section and butt weld longitudinally to form a CHS.

There were two semi-circular holes with diameter of 25 mm drilled on the outer steel tube at the upper and bottom end of the specimens for ventilation of vapor in concrete at elevated temperature.

Two end plates with bolt holes which were used to fix the specimen to the loading system of the test rig were welded to the tubes. One of the endplates was welded before the concrete was poured into the specimens. Before the fire test, epoxy mortar was used to compensate any shrinkage at the open end and another endplate was welded to the tubes. The geometric centre of the steel tubes corresponded to the centre of the endplate for concentric load specimens, whereas, for eccentrically loaded specimens the

geometric centre of the steel tubes located away from the centre of the endplate by the distance equal to the load eccentricity. In order to monitor the temperatures in the CFDST specimens, three thermocouples were installed in each specimen. One was at the middle of the core concrete and the other two were at the outer surface of the inner tube and inner surface of the outer tube. The schematic view of the specimens is shown in Figure 5.2 and position of the thermocouples is shown in Figure 5.3.

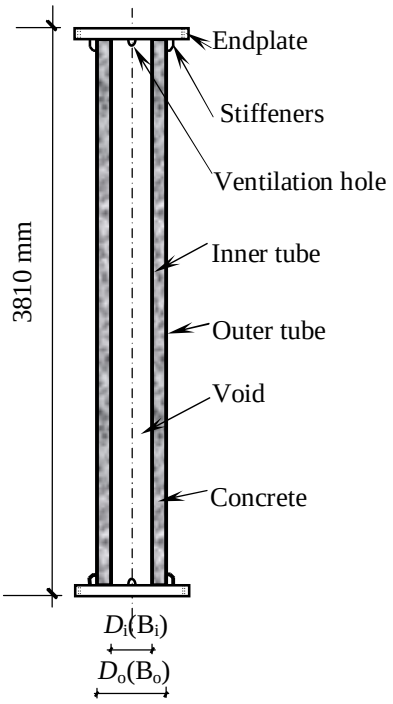

Figure 5.2 Schematic view of the specimens

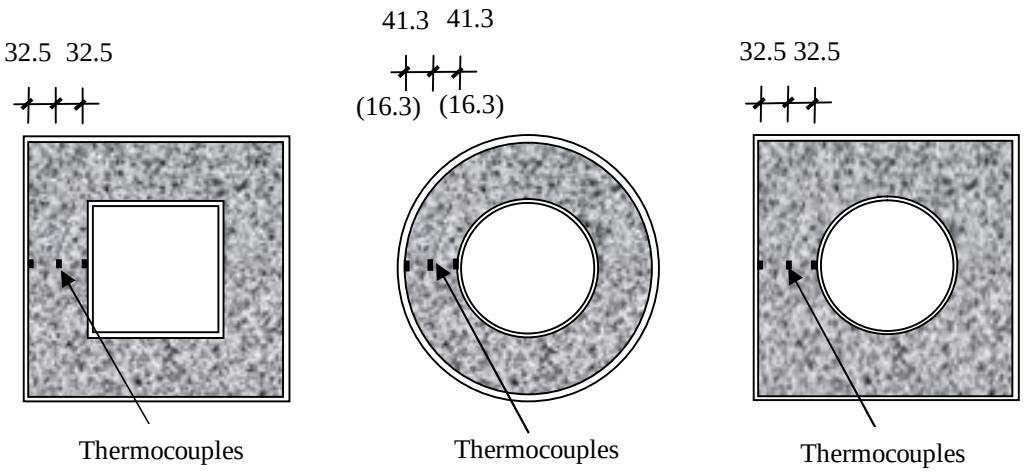

(a) SS1 and SS2 (b) CC1, CC2, CC3 (c) SC1

Figure 3 Position of thermocouples (unit: mm)

Table 5.1 Basic parameters for specimens

No	Specimen label	Outer tube (mm)	Inner tube (mm)	Cavity ratio	Load eccentricity (mm)	Load (kN)	Load ratio	Fire protection thickness (mm)	Fire endurance (min)	Failure criterion	Failure mode
1	CC1	CHS300×5	CHS125×5	0.43	0	1810	0.54	10	240	/	Buckling
2	CC2	CHS300×5	CHS125×5	0.43	75	570	0.31	0	97.5	1	Buckling
3	CC3	CHS300×5	CHS225×5	0.78	0	2000	0.65	0	40	2	Buckling
4	SC1	SHS280×5	CHS140×5	0.52	0	2050	0.55	0	82	2	Buckling
5	SS1	SHS280×5	SHS140×5	0.52	0	1200	0.32	0	115	2	Buckling
6	SS2	SHS280×5	SHS140×5	0.52	75	1100	0.50	10	165	2	Buckling
Note: Failure criterion 1 corresponding to axial deformation exceeding 0.01H mm and failure criterion axial deformation rate exceeding 0.003 H mm/min.											

For specimens with spray coating, the fire resistant coating was sprayed several weeks before the fire tests. Firstly, the external surface of the outer tube was cleaned and rust was removed. Then, three layers of protective coating were sprayed on the surface. The subsequent layers of coating were sprayed after the previous layer had hardened. A polypropylene mesh was wrapped around the surface after the first layer of coating had been sprayed to prevent possible spalling of the coating at elevated temperature. Finally, the outer surface of the coating was plastered to ensure the total thickness of the coating meets the specified thickness.

5.2.2 Material Properties

Steel coupons at ambient temperature were taken from the steel sheet along the same direction as the longitudinal direction of the specimens. The yield stress was found to be 320 MPa.

Normal strength self-consolidating concrete was used in the test. The mixture proportion of the self-consolidating concrete is shown in Table 5.2. The mixture of concrete was designed to meet the requirement of anticipated strength and workability of SCC as well. Two methods were adopted to test the workability of the SCC, slump cone and L-Box test.

The workability of the fresh SCC is shown in Table 5.3, which generally satisfied the requirements of SCC (ACI, 2007). Concrete cubes, with dimension of 100×100×100 mm, were prepared to test the strength of the concrete, some cured under standard conditions to test the standard strength at 28 days and the others cured under the same condition as the concrete in the CFDST specimens to test a more realistic strength of the concrete in the CFDST columns. The 28 days cube strength and elastic modulus was 26 and 1.77×10^4 MPa and the average cube strength and elastic modulus were 38 and 2.1×10^4 MPa at the time when the CFDST specimens were tested.

Table 5.2 Mixture of SCC to in-fill the CFDST (kg/m^3)

Water	Cement	Fly ash	Sand	Coarse aggregate	Superplasticizer
171	370	170	810	915	5.13

Table 5.3 Workability of fresh self-consolidating concrete

Slump (mm)	Slump flow (mm)	Flow speed in L-Box test (mm/s)
225	610	8.5

The spray coating is cement mortar based material incorporating light weight filler which has low thermal expansion behaviour at elevated temperature so that the coating can effectively adhere to the steel surface during the fire exposure. Furthermore, the coating is non-combustible and has good thermal properties to delay the temperature increase in the specimens. The thermal properties of the coating material are shown in Table 5.4. The spray coating has much lower strength compared to normal strength concrete. Therefore, the spray coating has little contribution to the capacity of the columns and its effect on the structural response of the columns is negligible.

Table 5.4 Thermal properties of the protection material

Density (kg/m^3)	Conductivity (W/m·K)	Specific heat (J/kg·K)
500	0.0907	1.047×10^3

5.2.3 Test Set-up

The CFDST specimens were tested in the column furnace at Structural Fire Resistance Laboratory in Tianjin Fire Research Institute, China. The whole set-up consists of furnace, reaction frame, loading system, air and fuel supply system, and control and data logging system. The maximum allowed length is 4 m. The furnace chamber is 2.6 m by 2.6 m in square section and 3 m in height. The test rig is shown in Figure 5.4.

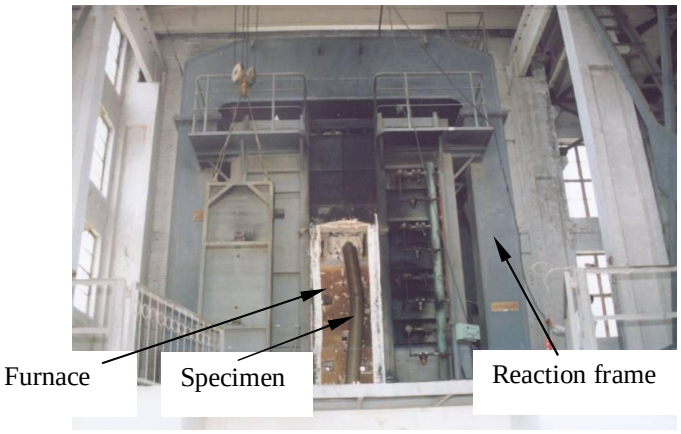

Figure 5.4 A general view of the test set-up

There are three burners along the height of each side of the chamber. This arrangement of the burners allows air and fuel to circulate around the chamber to generate a uniform fire temperature in the furnace. The furnace can produce a test environment specified by standards (ISO-834, 1999; AS-1534-4, 2005), such as requirements in temperature elevation, pressure, loading, and fire exposure condition. There are also several observation holes at each side of the chamber for observation the specimen during the fire test. A servo controlled hydraulic jack is at the bottom of the rig which can automatically compensate deformation of the specimen and retain the load in a stable state. The maximum load capacity of the jack is 500 tons.

The specimens were fixed to the load frame by bolts. The boundary condition at one end is fixed while the other end is pinned. There was a displacement transducer at the front of the jack to monitor the axial deformation of the columns. There was another displacement transducer along the side of the furnace to measure the lateral deflection of the specimens. A molybdenum wire, which has a high melting point and low thermal expansion at high temperature, was bound to the specimen at the mid-height and attached to a displacement transducer outside the furnace through an observation hole. The lateral deflection measured in such manner was reasonable because of the very limited expansion of molybdenum wire.

5.2.4 Test Conditions and Procedure

The specimens were installed in the furnace and bolted to the reaction frame. Then, thermocouples and displacement transducers were connected to the data logging system. Load was applied on the column 30 minutes before the ignition of fire. The axial deformation before ignition was recorded as a relative initial deformation of the column in the fire testing.

The fire temperature in this test was according to fire temperature and fire exposure time relationship prescribed in ISO-834 (1999). There are several thermocouples in the furnace to monitor the temperatures in the chamber. The monitoring data feed back to the control system so that the system can control the average temperature in the furnace to match the desired temperature-time curve.

During the fire test, the load applied on the column remained constant through the servo controlled hydraulic jack. All the specimens except CC1 were tested to failure: CC1

was tested to 240 minutes. The failure criteria are those prescribed in ISO-834 (1999), i.e. either axial deformation exceeding 0.01*H* mm or the deformation rate exceeding 0.003*H* mm/min where *H* is the height of the columns in millimetres.

5.3 TEST RESULTS

5.3.1 Failure Modes

Failure modes of the specimens are shown in Figure 5.5. As can be seen, failure of the specimens is overall buckling. For eccentrically loaded specimens a more severe lateral deflection was experienced than for the concentrically loaded specimens. It was observed during the fire test that buckling of the specimens only became obvious at the stage close to the fire endurance.

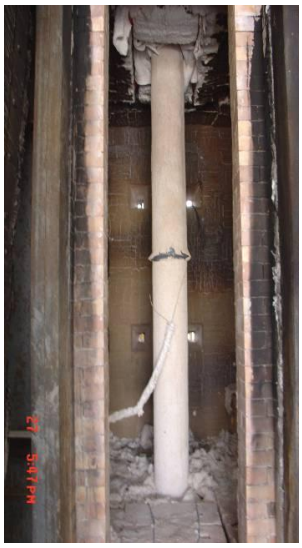

(a) CC1

(b) CC2

(c) CC3

(d) SC1

(e) SS1

(f) SS2

Figure 5.5 Failure modes of overall specimens

For specimens with circular outer tubes, no cracks were observed in the outer tubes as shown in Figure 5.6. There was a bulge around the outer circular tube at the mid-height section of the specimen in CC1. It was observed that the spray coating at this position cracked after the specimen was exposed to fire for about 80 minutes and then the coating gradually flaked off from 100 minutes. Then this part of outer steel tube was exposed to fire directly. The temperature in this part of steel tube was obviously higher than those protected by the spray coating. This induced quicker degradation in the mechanical properties and finally caused local buckling of the steel tube. There was also a local bulge on outer steel tube around the circular section near the mid-height of specimen in CC3. However, the bulge in CC3 was far less severe than that in CC1.

(a) CC1

(b) CC2

(c) CC3

(d) SC1

(e) SS1

(f) SS2

Figure 5.6 Local failure modes of the specimens

For specimens with square outer steel tubes, severe local buckling and corner cracking were observed in the outer square steel tubes. Weld cracking at the corners of the outer square tubes was found at the position corresponding to the most serious bulge of the tubes. The bulges of the outer steel tubes were all outward because the concrete prevents them bulging inward. It was observed during fire tests that corner cracking occurred much later than the bulging of outer steel tubes. As can be seen in Chapter 4, there is no such weld cracking in CFDST columns with square cold-forming steel hollow sections in which the weld is at the flat surface, whereas weld at the corner of fabricated hot-rolling steel hollow section is probably a critical position which potentially has adverse influence on the fire performance of CFDST columns.

After testing, the outer steel tubes were removed to observe the failure mode of the concrete as shown in Figure 5.7. Local concrete crushing was found at positions corresponding to serious local outward bulges of the outer tubes for specimens with square outer tubes. However, most of the concrete was still intact for all specimens. There is obvious cracking along the longitudinal direction of the specimens, and some transverse cracking can be seen in the concrete for eccentrically loaded specimens. No slipping between the outer steel tubes and the concrete was observed.

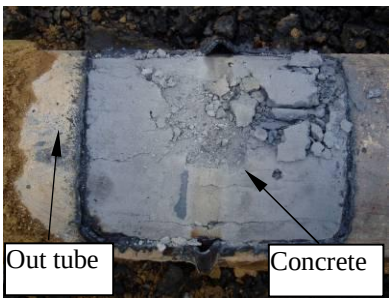

(a) CC1

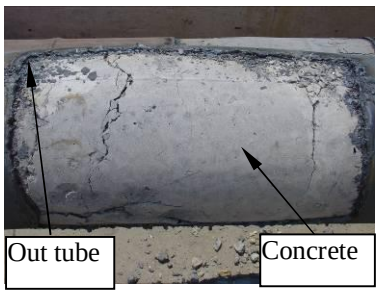

(b) CC2

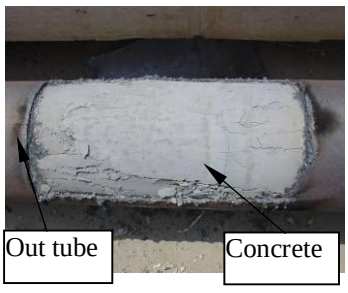

(c) CC3

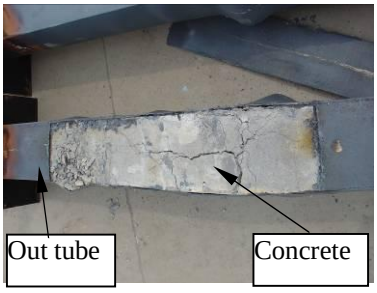

(d) SC1

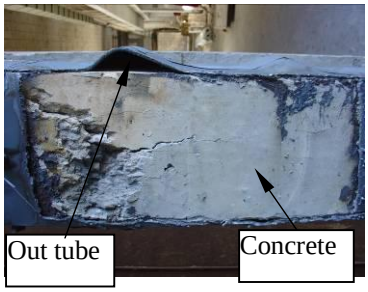

(e) SS1

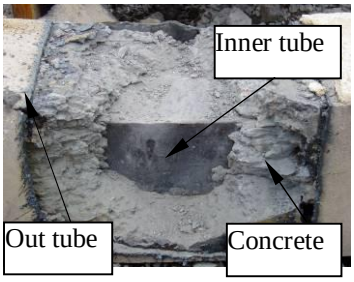

(f) SS2

Figure 5.7 Failure mode of the concrete

It should be noted that the in-filled concrete in this test is self-consolidating concrete. Although there are still controversial findings on fire performance of SCC (Persson, 2004; Moumowe et al., 2006; Reinhardt and Stegmaier, 2006), it is generally believed that the behaviour of SCC under fire exposure is similar to that of high strength concrete, i.e. higher possibility of explosive spalling. It is found that steel tube in CFST can effectively prevent the spalling of high strength concrete (Kodur, 1998a). It is clear from this test, steel tubes in the CFDST columns can also prevent the spalling of SCC in concrete filled double skin steel tubular columns.

The failure modes of inner steel tubes are shown in Figure 5.8. As can be seen, there is no local buckling on inner steel tubes for specimens with circular outer tubes. However, there is local buckling in all specimens with square outer tubes. There is an inward bulge on the inner circular tube of SC1. There are bulges on inner square steel tubes in SS1 and SS2. The buckling mode in the square inner tubes in SS1 and SS2 is outward bulge in one facet and inward bulge in the adjacent facet. The location of the local buckling of the inner steel tube corresponds to local buckling of the outer tubes.

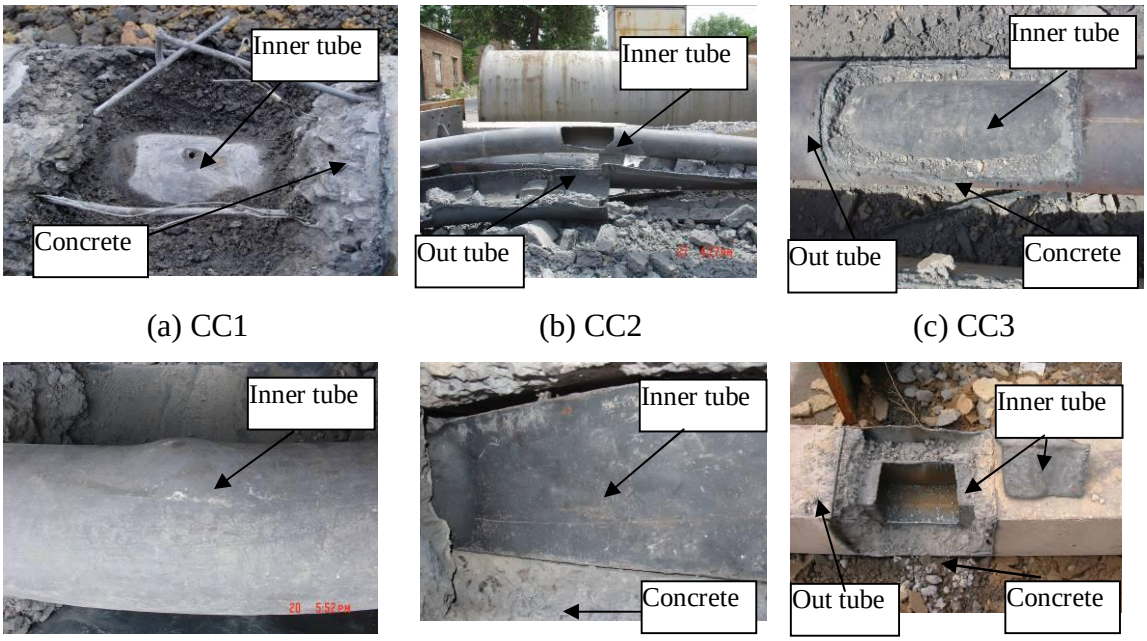

(a) CC1 (b) CC2 (c) CC3

(d) SC1 (e) SS1 (f) SS2

Figure 5.8 Failure modes of inner tubes

5.3.2 Temperature Distribution

Temperatures in CFDST specimens are shown in Figure 5.9. Although there were 3 thermocouples in each specimen, some of the thermocouples were not working in the

fire tests. However, the trend in temperatures in the CFDST specimens can still be found. The temperatures in the outer steel tube generally develop rapidly at the early stage of fire exposure. There is a relatively stable stage for temperatures in the concrete and inner tubes when the temperatures are above 100 ^{o}C. This is mainly due to evaporation of the free water in the concrete absorbing a great deal of heat for transformation. It can also be seen that the temperatures in the inner tubes are generally below 450 ^{o}C and maximum temperature at the outer tubes is about 940 ^{o}C.

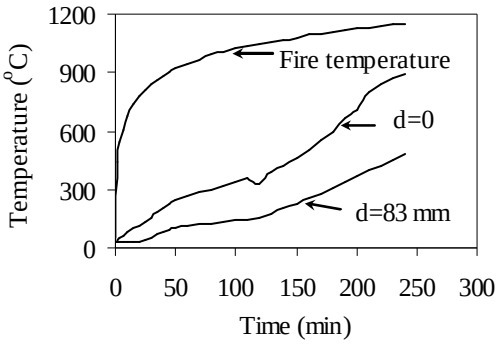

(a) CC1

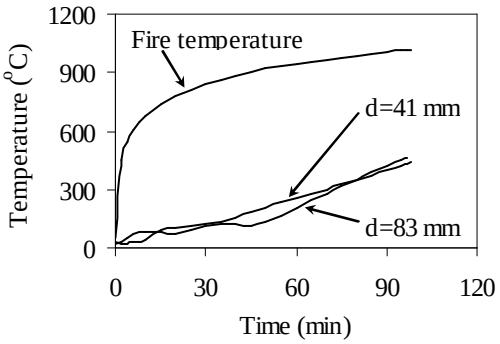

(b) CC2

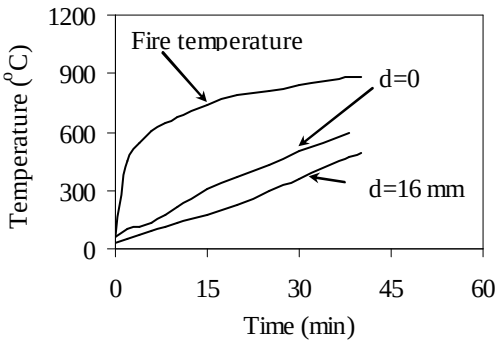

(c) CC3

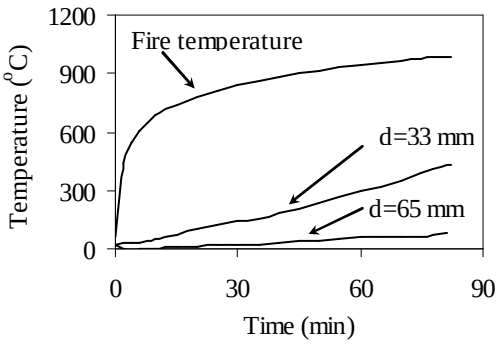

(d) SC1

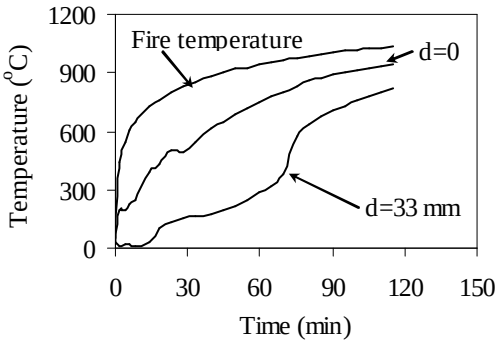

(e) SS1

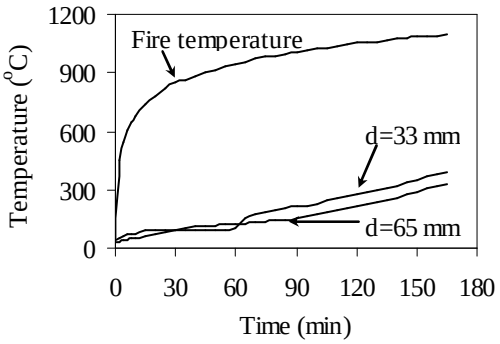

(f) SS2

Figure 5.9 Temperatures in specimens

5.3.3 Deformation and Fire Resistance

The axial deformation of the specimens, which is used to determinate the fire endurance of the specimens, is shown in Figure 5.10. For specimen CC1, the fire exposure time was set to 4 hours in the test by the control system. The specimen still had the ability to sustain the applied load at 4 hours fire exposure. All other specimens were tested to failure, unable to sustain the applied load. The fire endurance of the specimens which is determined through the relationship between axial deformation and fire exposure time is shown in Table 5.1.

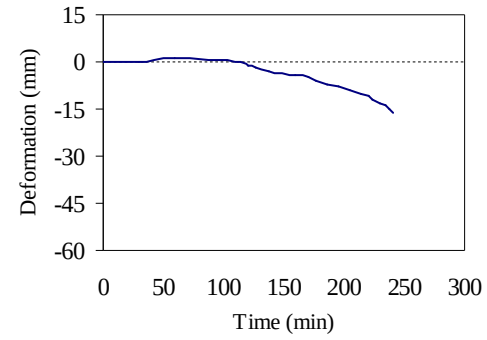

(a) CC1

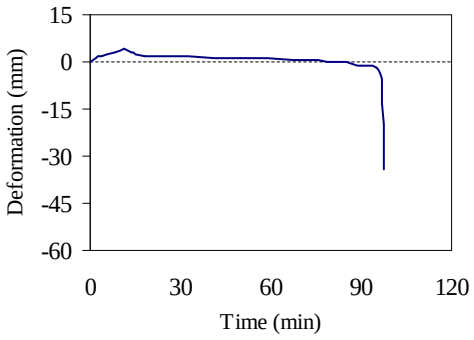

(b) CC2

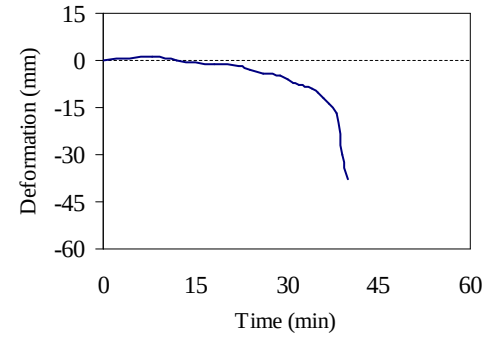

(c) CC3

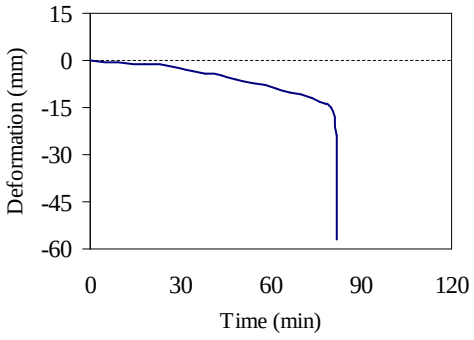

(d) SC1

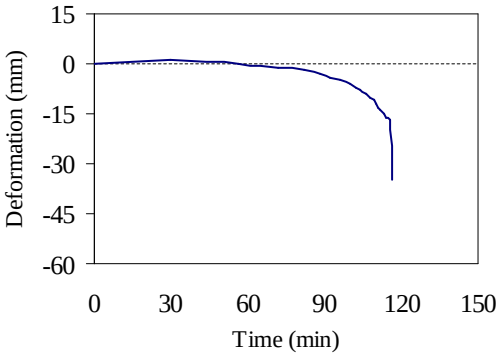

(e) SS1

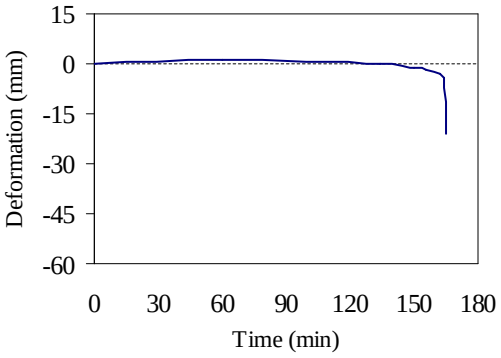

(f) SS2

Figure 5.10 Axial deformation

Axial deformation of the CFDST specimens generally consists of three stages, (I) expansion, (II) gradual development of compression deformation and (III) compression deformation increase dramatically in a short time. However, if the load ratio is high, such as in SC1, there is no expansion stage for the CFDST specimens. For concentrically loaded specimens, the compression deformation develops gradually for a relative long time before the collapse of the specimens, whereas for eccentrically loaded specimens (CC2 and SS2), collapse of the columns occurred not long after the expansion stage. It is found that the axial deformation of the CFDST specimens is generally similar to that of CFST columns (Han et al., 2003c).

Examples of lateral deformation of the specimens (SC1 and CC3) are shown in Figure 5.11. Lateral deformation of the specimens generally increases moderately with the increase in fire exposure time. Then, there is a turn point which is very close to the fire endurance of the specimens. The lateral deformation increases dramatically after the turning point. Buckling of the CFDST columns occurred beyond this turning point. It can be seen from Figures 5.10 and 5.11 that both axial and lateral deformations increase sharply when the specimens are approaching their fire endurance.

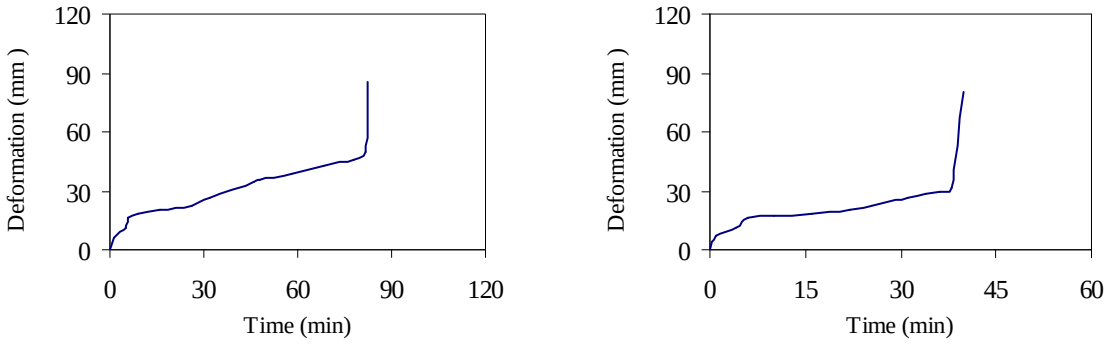

(a) SC1 (b) CC3

Figure 5.11 Examples of lateral deformation

5.4 DISCUSSIONS OF THE EXPERIMENTAL RESULTS

5.4.1 Limiting Temperatures

The limiting temperature (T_{cr}) in the outer steel tubes is defined as temperature of the outer tube when the CFDST specimens reached fire endurance. This temperature is similar to the critical temperature or limiting temperature defined in structural fire design of steel structures (Eurocode 3, 2005; AS 4100, 1998). It is well known that

structural fire design of steel components can be completed in the temperature domain. Critical temperature or limiting temperature is the upper limit for structural fire safety, or beyond this temperature the steel components lose their capacity. Load ratio is the key factor affecting the critical temperature or limiting temperature.

The limiting temperatures for specimens CC1, CC3 and SS1 are 896, 590 and 942 ^{o}C respectively. T_{cr} was not recorded for the other specimens due to the failure of thermocouples in the fire test. The limiting temperatures of the CFDST specimens in this test are compared to the critical temperatures or limiting temperature derived from design codes and fire test results of CFST.

The load ratios for specimens in this test are between 0.31 and 0.65. Critical temperatures for steel components under same range of load ratio from design codes are 711 to 496 ^{o}C in Eurocode3 (2005) and 645 to 531 ^{o}C in AS4100 (1998). Comparison of the limiting temperatures in the specimens to those predicted by design codes is shown in Figure 5.12. It can be seen that limiting temperatures in CC1 and SS1 are significantly higher than the critical temperatures for steel alone. The outer steel tube loses capacity when its temperature reached the critical temperature. However, the limiting temperature of the outer steel tube can be as high as 942 ^{o}C. This indicates that there is a load transfer mechanism in the CFDST columns when the outer tube reaches the design critical temperature.

The limiting temperatures of CFST columns have been found generally between 530 and 590 ^{o}C for a load ratio of 0.77 in fire tests (Han et al., 2003c). The critical temperature of CC1 (896 ^{o}C) is significantly higher than those in the CFST columns and the critical temperature of CC3 (590 ^{o}C) is comparable to the limiting temperatures in the CFST columns. The load ratio for CC1 (0.54) and CC3 (0.65) is lower than that of the CFST columns. As discussed above, lower load ratio should lead higher limiting temperature in the CFDST columns compared to the CFST columns. It is true that CC1 has higher limiting temperature. Nevertheless, CC3 has limiting temperature comparable only to those in the CFST columns. The effect of another factor, the difference in the configurations between CFDST and CFST columns, needs be investigated.

CFST columns have a better performance in thermal response than CFDST columns based on the fact that CFST columns possess thicker concrete than CFDST columns. However, such difference in the configurations may also affect the structural response of the columns. When the steel tube in CFST or the outer tube in CFDST reaches critical temperature and the tubes starts to lose load bearing capacity, there is only one load transfer path for CFST columns, i.e. from the tube to the core concrete, whereas load can transfer to both the concrete and inner tube in CFDST columns. As can be seen in the current tests, the maximum temperature in the inner tube of CC1 is 484 ^{o}C. Although strength and stiffness of the inner tube have degraded to some extent due to the elevated temperature, it may still have the capability to sustain part of the load transferred from the outer tube. The additional load transfer path to the inner tube in the CFDST column is one of the important factors which results in the column possessing higher limiting temperature than that in CFST columns. It should be noted that concrete thickness in CC1 is 82.5 mm compared to 37.5 mm in CC3. Hence, temperature at the inner steel tube in CC3 is much higher than in CC1. This greatly weakens the contribution of the inner steel tube to the structural performance of CC3 at elevated temperature. Therefore, CC3 cannot achieve a higher limiting temperature compared to CFST columns.

5.4.2 Composite Action between Steel and Concrete

Composite action between steel and concrete in CFDST columns is a prominent characteristic of the composite columns. It is well-known that such interaction has great influence on the behaviour of the CFDST column at ambient temperature (Zhao and Han, 2006). Composite action between concrete and steel in CFDST at elevated temperatures is more complicated due to both thermal and mechanical action incorporated in the procedure. It is difficult to quantitatively estimate the effect of steel-concrete composite action on the fire performance of the composite columns based on the test results. However, composite action between steel and concrete can be qualitatively recognized.

Concrete in the CFDST column can serve as heat sink to absorb heat because of its low heat conductivity and high heat capacity. Presence of concrete in the composite column can delay temperature elevation in the concrete and more importantly work as insulation for the inner tubes as well. As can be seen, the temperatures in the inner tubes are less than 500 ^{o}C in the tests even when the temperatures in the outer tubes are as high as

about 900 ^{o}C. Concrete is an effective insulation for the inner steel tube in the thermal action of the CFDST columns, which will finally benefit the structural fire performance of the columns.

In the analysis of the limiting temperature in the CFDST columns, the existence of a load transfer mechanism in the columns exposed to fire has been indentified. Such load transfer is a typical phenomenon of steel-concrete interaction in the composite columns. The temperatures in the outer steel tubes are much higher than those in the concrete and inner steel tubes. Thus, thermal expansion of the outer steel tubes is higher than the concrete and inner tubes. At the early stage of the fire exposure, stress in the outer steel tubes increases due to the extra thermal expansion over concrete and inner tubes. At the same time, the mechanical property of the steel in the outer steel tubes degrades as temperature elevated. As soon as the increasing stress in the outer steel tubes reaches the yield stress, the outer steel tubes start to lose their capacities. Load has to transfer from outer tubes to the concrete and inner tubes. At this moment, the temperature in the inner tubes is quite low. The yield stress for structural steel is almost the same as that at ambient temperature when the temperature is less than 400 ^{o}C (Eurocode 3, 2005). The inner steel tube still has ability to take over the load transfer from the outer steel tube together with the concrete.

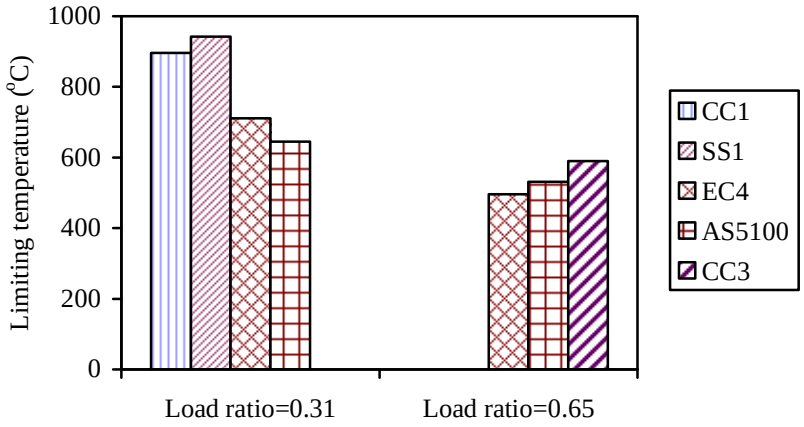

Figure 5.12 Comparison of limiting temperatures

Besides load transfer in the CFDST column, interaction of steel tubes and concrete can be found through the failure modes of concrete and steel tubes. The outer steel tube provides confinement on the concrete even after yielding. It effectively prevents spalling of the concrete and possible disaggregation of the concrete at elevated

temperature. This can be clearly seen in Figure 5.7, most concrete remains intact although it is seriously cracked. On the other hand, it is clear that the concrete changes the failure mode of the outer steel tubes, buckling of the outer steel tubes is all outward. The failure modes of the inner tubes in specimens with square outer tubes are similar to that of unfilled tubes. This phenomenon is also observed for CFDST stub column tests at ambient temperature (Zhao and Han, 2006). For CFDST specimens with both inner and outer SHS tubes, there are several bulges induced by local buckling on the inner RHS tube surfaces, whereas there is only a major bulge on CHS inner tube for specimen with SHS outer tube and CHS inner tube. However, there is no local buckling observed in the inner tube in specimens with CHS outer tube. In CFDST columns, CHS can offer uniform confinement on the concrete, whereas SHS has strong confinement only at the corners. Hence, concrete in turn provides stronger support around the circumference of the CHS to prevent local buckling of the steel tubes. However, such support to the SHS is weaker on the faces of the tubes and unable to prevent local buckling. Therefore, no obvious local buckling occurs on CHS while severe local buckling appears on SHS of the CFDST specimens.

Through analysis the composite action of steel and concrete in CFDST, it shows that such interaction benefits the fire performance of the composite columns. More research is needed to optimize the design to maximize the composite action.

5.4.3 Fire Resistance

Fire resistance of the specimens is summarized in Table 5.1. Fire resistance of unprotected CFDST varies from 40 to 115 minutes, while the protected ones are 165 and 240 minutes respectively. It is clear that the fire resistant spray coating is very effective at increasing the fire resistance of the CFDST columns even though the thickness of the coating is only 10 mm, comparing to the case of steel structural components with fire resistance of 1 hour, where the required thickness of such spray coating is 15 mm (ECS 24, 1990). This implies that CFDST columns have superior fire resistance to unfilled steel hollow columns.

Load ratio is one of the key factors affecting the fire endurance of the CFST column (Han et al., 2003c). Here, the load ratio is also found to significantly affect the fire endurance of the CFDST columns. Comparing the fire endurance of SC1 and SS1, the

fire endurance increases from 82 to 115 minutes as the load ratio decreases from 0.55 to 0.32.

The fire resistance of SC1 and CC3 is 82 and 40 minutes respectively, the former is more than twice the latter. There are several factors which may cause the difference in the fire endurance of the columns, load ratio, profile, outer cross section size and cavity ratio. Load ratio for SC1 is 10% lower that of CC2. The fire endurance of SC1 is supposed to be higher than CC2 in term of load ratio. However, such a small difference in the load ratio is unlikely to explain such a large difference in the fire resistance of the columns. SC1 has an outer SHS and inner CHS, but CC2 has both inner and outer CHS. Hence, the average thickness of the concrete in SC1 is greater than that in CC2. It is likely that the lower temperature in SC1 is the reason why higher fire endurance is achieved.

The perimeter of the outer steel tube is a factor which has significant influence on the fire endurance of CFST columns. A CFST column with longer outer perimeter means it possesses greater cross section area or thicker concrete in the column, thus, temperature rise is slower and its fire endurance is higher (Han et al., 2003c). Similar to CFST columns, the outer tube perimeter is also one of the parameters influencing the concrete thickness in CFDST columns. The perimeter of outer steel tube of SC1 is greater than that of CC2. This is likely one of other factors responsible for the longer fire resistance of SC1. However, effect of another factor which is unique for CFDST columns, i.e. the cavity ratio, should be considered.

Cavity ratio, defined in Eq. 4.2, is a factor considering the void in the inner tube and the thickness of the concrete in the CFDST columns. A high value of the cavity ratio implies a reduced thickness of concrete between tubes in the CFDST columns. So, cavity ratio affects temperature in CFDST columns and will consequently affect the fire resistance of the columns. The outer perimeter and cavity ratio are the main factors contributing to the increased fire resistance of SC1 over CC3, in which outer perimeter accounts for the absolute cross section size and cavity ratio represents the relative thickness of the concrete. Both these factors have relatively significant effects on the fire resistance of the CFDST columns.

5.5 CONCLUSIONS

Based on the test results reported in this chapter, several conclusions can be drawn:

(1) SCC filled double skin tubular columns can have higher limiting temperatures on outer steel tubes than unfilled and concrete filled steel tubular columns. This implies CFDST columns can have better fire endurance than unfilled and concrete filled steel tubular columns.

(2) There is strong evidence to support the existence of composite action between steel and concrete in the composite columns during fire exposure. Such composite action is of benefit to the higher level fire performance of the columns.

(3) The effect of a number of parameters on the fire endurance of the CFDST columns has been identified. Cavity ratio which is unique for CFDST columns affects the fire endurance of the composite columns.

[Blank page]

Chapter 6

FINITE ELEMENT MODEL AND VERFICATION

6.1 INTRODUCTION

The fire behaviour of structural elements has been traditionally studied by means of standard fire tests. Although fire testing is a straightforward method to investigate the fire behaviour of elements, fire tests are generally conducted on limited numbers of elements under specific conditions due to their high cost and time-consuming nature. Another methodology which has become well-accepted in the study of the fire behaviour of structural elements is numerical modelling, as one of the obvious advantages of the numerical method is its cost-effectiveness.

Many numerical models have been proposed to study the fire behaviour of steel-concrete composite elements, most of which have been simplified models. In recent years, the finite element method has been used to analyse the fire behaviour of CFST columns. The finite element method is a general numerical modelling methodology which does not need any simplification assumptions as required in the simplified models. In addition, the finite element method can provide more detailed information on the analysed objects to enable insights into the behaviour of the objects under complex load conditions.

This chapter describes the use of a finite element model to simulate the fire behaviour of CFDST columns. A finite element package, ABAQUS, was used for modelling. A sequentially coupled thermal-stress analysis procedure in the package was selected, which consists of thermal and stress/displacement analysis steps. Some key aspects in the finite element model are introduced in this chapter. Finally, the proposed model is verified by the fire test results presented in the previous chapters.

6.2 FINITE ELEMENT ANALYSIS PROCEDURE

There are two types of action simultaneously applied to CFDST columns under fire exposure, i.e. elevated temperature and axial load. In the current study, a finite element analysis package, ABAQUS (ABAQUS, 2008), was used to simulate the non-linear behaviour of the columns under both thermal and mechanical actions.

In the ABAQUS package (ABAQUS, 2008), two procedures are available for thermal-stress analysis: fully-coupled and sequentially-coupled thermal-stress analyses. The

former is capable of analysing the stress/displacement and temperature field simultaneously. It is generally used in cases where thermal and mechanical solutions strongly affect each other (ABAQUS, 2008). The advantage of this procedure is that it can simulate thermal and mechanical actions simultaneously acting on objects. However, this procedure involves high cost in calculation because of the need to resolve thermal-stress coupled non-linear equations. Sequentially-coupled thermal-stress analysis is utilized in cases where the stress/displacement solutions are dependent on a temperature field but there is no inverse dependency (ABAQUS, 2008). This procedure generally consists of two analysis steps. Thermal analysis is conducted first to obtain the temperature distribution in the objects, followed by a stress/displacement analysis step in which temperature elevation in the objects is obtained from the thermal analysis step. The advantage of the sequentially-coupled analysis procedure is that it is more efficient in the calculation.

For CFDST columns under fire exposure, the structural response of the columns depends on the thermal response because the mechanical properties are all temperature-dependent. The structural response may or may not affect the thermal response of the columns. However, such influence can simply be incorporated in the thermal response analysis by appropriately adjusting the thermal properties of the material. Hence, the sequentially-coupled thermal-stress analysis procedure in the package was used to study the fire behaviour of the columns. As indicated above, this procedure consists of two consecutive steps, thermal and mechanical analysis which is shown schematically in Figure 6.1. Temperatures in the CFDST columns are obtained through thermal analysis and stored in the hard drive in the computer as a function of fire exposure time. Then, in the structural response analysis, the columns are loaded at ambient temperature and temperatures are read as a predefined filed. Temperatures in the columns elevate with the increase of time in fire in the structural analysis step until the failure of the columns.

There are some requirements in creating the finite element model so that temperatures obtained in the thermal analysis step can be transferred to the structural analysis step. First, the type of elements should come from the same element families. In the current study, 3D solid elements were selected for concrete and shell elements were selected for the steel tubes in the CFDST columns. The 3D solid elements for thermal and structural analysis were DC3D8 and C3D8R respectively. The shell elements for thermal and structural analysis were DS4 and S4R respectively. Second, the time in the thermal

analysis step should match the time in the structural analysis step so that the temperatures in both steps have the same meaning. In addition, the finite element mesh should be selected to be identical in two steps so that data can be transferred more efficiently between steps.

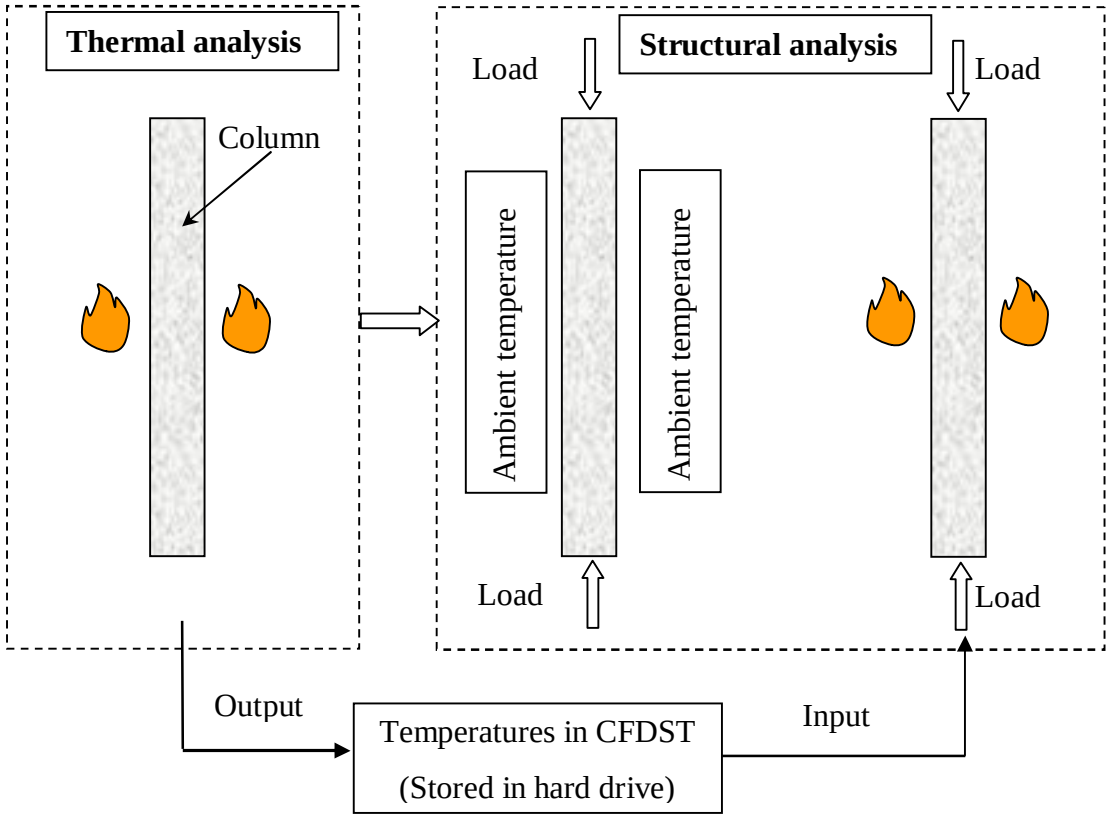

Figure 6.1 Schematic view of sequentially coupled thermal-stress analysis procedure

As the CFDST columns in this study use either CHS or SHS as inner and outer tubes, the columns are symmetrical in geometry. In addition, the fire temperature around the columns and load on the columns are also symmetrical. Therefore, only half of the columns were used in the modelling and the symmetrical boundary conditions were applied on the symmetric edges and surfaces. A typical finite element mesh for columns is shown in Figure 6.2. In the thermal response analysis, only the columns were used in the modelling, whereas two rigid end plates were added to the model in the structural response analysis for the purpose of applying load and assigning column-end boundary conditions to the columns.

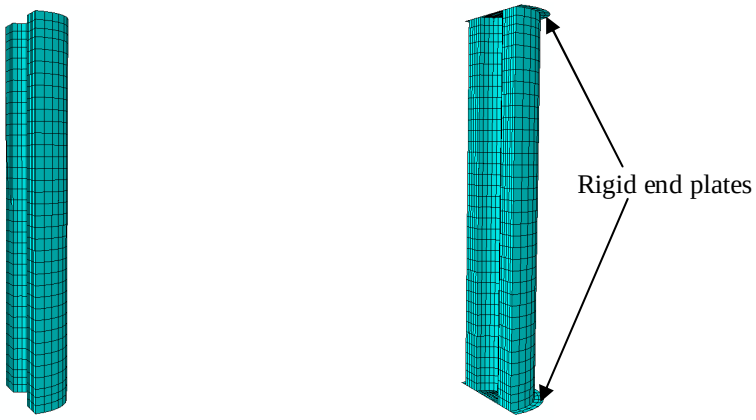

For thermal analysis For structural analysis

(a) CHS CFDST

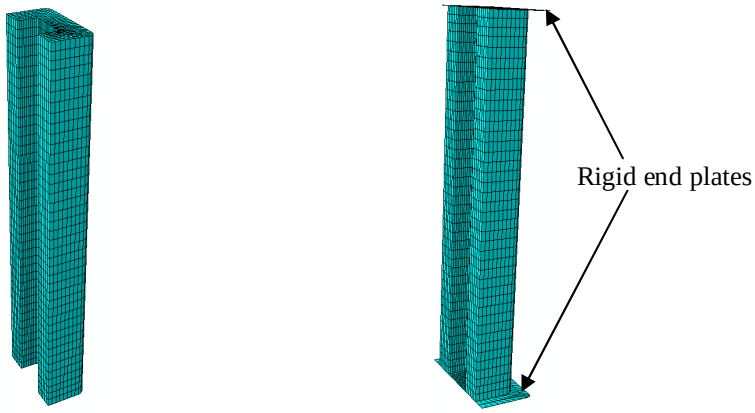

For thermal analysis For structural analysis

(b) SHS CFDST

Figure 6.2 Typical finite element meshes for CFDST columns

6.3 THERMAL RESPONSE ANALYSIS

6.3.1 Heat transfer in CFDST columns exposed to fire

The thermal response of CFDST columns under fire exposure is actually a transient heat transfer problem in which the heat of the fire transmits to the exterior surface of the outer tube and then conducts into the inner tubes. The heat transfer problem is governed by Green and Naghdi's energy balance law and the heat conductance is governed by Fourier's law (ABAQUS, 2008). For the transient heat transfer problem, the laws can be expressed by the following differential equation:

$$\rho c \frac{\partial T}{\partial t} = k\left(\frac{\partial^2 T}{\partial^2 x} + \frac{\partial^2 T}{\partial^2 y} + \frac{\partial^2 T}{\partial^2 z}\right) \tag{6.1}$$

where, ρ is the material density, c is the specific heat, k is the thermal conductivity, T is the temperature and t is the time. The numerical method used to solve this equation in

ABAQUS comprises procedures of spatial discretization, time integration and solving non-linear equations.

An unconditionally stable backward difference algorithm was chosen for time integration with the balance of accuracy and reducing oscillations. The modified Newton method was used to solve the nonlinear equations. The time increment is controlled automatically by the time stepping algorithm in the package (ABAQUS, 2008).

Heat is transmitted from the fire to the exterior surface of the outer tubes by convection and radiation. When the fire temperatures are available, the heat can be input by convection and radiation respectively in the ABAQUS package. Heat flux for convection and radiation can be expressed by the following equations:

$$q_{convection} = h_v(T_f - T_s) \tag{6.2}$$

$$q_{radiation} = \varepsilon_f \varepsilon_m \sigma[(T_f - T_0)^4 + (T_s - T_0)^4] \tag{6.3}$$

where, q is the input heat flux, T_f, T_s and T_0 is the temperature of fire, exterior surface of outer tube and absolute zero respectively, h_v is heat convective coefficient, ε_f and ε_m is emissivity of fire and steel surface, σ is the Stefan Boltzmann constant. For the standard fire condition, h_v=25 (W/m^{2}K), ε_f = 0.8 and ε_m =0.7 are recommended by Eurocode 4 (2005) for composite elements. These values were used in the current analysis.

Apart from the fire-exposed surface of the outer tubes, there is another boundary condition for CFDST which is at the inner surface of the section. The heat may radiate in the void within the inner tube when the temperature increases in the inner tube. But for the CHS and SHS CFDST columns, the cross-sections are symmetrical. In this case, there is no heat radiation in the inner void of the CFDST. This boundary condition can be simulated by a free heat boundary condition, which means that no heat boundaries apply on the interior surface of the inner tube.

6.3.2 Material thermal properties

Material thermal properties are necessary input data in the calculation, namely density, specific heat and thermal conductivity. Several thermal property models are available

for structural steel and concrete (Lie, 1994; Eurocode 4, 2005). The thermal properties of concrete are mainly affected by the mixture, type of aggregate and moisture content. In this study, a concrete thermal model proposed by Lie (1994) was used, in which the effect of aggregate type on the thermal properties of concrete is considered. The steel thermal property model used is also that proposed by Lie (1994). To consider the effect of the moisture content on the thermal properties of concrete, the thermal properties of water are incorporated into the thermal properties of concrete as shown in Eq. 6.4.

$$\begin{cases} \rho_c' c_c' = (1-\phi)\rho_c c_c + \phi\rho_w c_w & (T < 100°C) \\ \rho_c' c_c' = (1-\phi)\rho_c c_c + \phi\rho_w' c_w' & (100°C \le T \le 200°C) \\ \rho_c' c_c' = \rho_c c_c & (T > 200°C) \end{cases} \tag{6.4}$$

where, ρ_c', c_c' and ρ_c, c_c is the density and specific heat of concrete after and before modification, ϕ is the percentage of moisture in concrete, and ρ_w, c_w and ρ_w', c_w' is the density and specific heat of water when the temperature is below 100°C and between 100°C and 200°C respectively.

In addition, the transformation of water from liquid to vapour was considered. In order to reduce the convergent difficulty in calculation, the water was assumed to vaporize between 100 and 200°C. The heat required for water vaporization is $\lambda_w = 2.3\times10^6$ (J/kg). This required heat can be converted into the specific heat of the water, as illustrated in Figure 6.3. The specific heat of water increases greatly when the temperature is between 100 and 200°C. This means that much heat will cause water vaporization rather than increase in the temperature of the concrete.

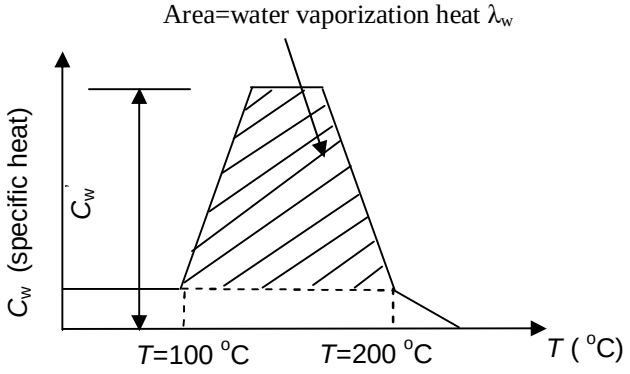

Figure 6.3 Relationship of heat for water vaporization and specific heat (Lu et al, 2007)

6.3.3 Thermal resistance in steel and concrete interface

In CFDST columns, the interface of steel and concrete is not a perfect contact when observed in a microscopic view. There are some areas of the interface that are void and contain water or steam during elevated temperatures (Ghojel, 2004). In addition, the differences in the heat expansion rates of steel and concrete may also cause small gaps in the concrete and steel interface when the columns are at elevated temperatures. When heat transmits through the steel and concrete interface, there is a thermal resistance. This thermal resistance in the steel and concrete interfaces can be expressed by the heat contact conductance concept, as shown in the following equation.

$$q = h_i\left(T_s - T_c\right) \tag{6.5}$$

Several heat contact conduction coefficients for CFST columns have been proposed (Ghojel, 2004; Han et al., 2003c; CIDECT, 2004b). The heat contact conductance coefficient proposed by CIDECT (2004b) is 100 (W/m^2K). Other models to calculate the contact conduction coefficient have been proposed by Ghojel (2004) and Han (2003c) which are shown in Eq. 6.6 and 6.7 respectively. Ghojel's model is based on experiments and heat reverse analysis. CIDECT's model was obtained through trial analyses of CFST temperature fields in fires (CIDECT, 2004b). The conductance of Ghojel's model is controlled by the temperature of the steel. Han's model is a function of time in fire, while CIDECT's model is independent of temperatures or other factors.

$$h_i = 160.5 - 63.8exp\left(-339.9T_s^{-1.4}\right) \tag{6.6}$$

$$h_i = \sqrt{k_s c_s \rho_s / \pi t} \tag{6.7}$$

where, k_s, c_s, ρ_s is the conductivity, specific heat and density of steel respectively, t is time to fires and T_s is the temperature at steel.

Ghojel (2004) found that the differences in predicted temperatures are not significant if the heat contact conductance coefficient varies between 10% and 100% of the value calculated by the Ghojel's model. The maximum difference in the heat contact conductance coefficients calculated by CIDECT's, Han's and Ghojel's models is within that range. Therefore, all the models may be applicable to predict temperatures in CFDST columns at elevated temperature with minimal differences in the predicted temperatures in the columns (Lu et al., 2007).

Ding and Wang (2008) used CIDECT's model to analyse the temperatures in CFST columns. A parametrical analysis was also performed by changing the value from zero to 100 (W/m^2K). The results show that the thermal resistant coefficient of 100 (W/m^2K) can achieve a better correlation to the test results. Hence, CIDECT's model was selected in this study.

6.4 STRUCTURAL RESPONSE ANALYSIS

As shown in Figure 6.2, the structural response analysis is divided into two sub-steps. In the first sub-step, the columns are loaded through two rigid endplates at ambient temperature. In the second sub-step, temperatures are read from the solutions of thermal analysis to simulate the action of fire while the load is maintained until the failure of the columns. The structural response analysis involves resolving nonlinear equations. The full Newton method was chosen to solve the nonlinear equations to obtain the structural response of the columns. To resolve nonlinear equations, each analysis sub-step was divided into increments. In each increment, a series of iterations was performed to find an equilibrium solution. In order to implement structural response analysis, some related parameters needed to be established for the finite element model, such as material mechanical properties, interaction of concrete and steel tubes and boundary conditions.

6.4.1 Material mechanical properties

During the structural response analysis, material mechanical properties at elevated temperature are the basic input data for the finite element analysis. Material properties required in the analysis generally include elastic and inelastic mechanical properties and elongation. For concrete and steel, all these mechanical properties are temperature-dependent at elevated temperature. Elastic modulus and Poisson's ratio are two basic parameters related to the elastic mechanical properties of material in ABAQUS. A uni-axial stress-strain relationship, a yield function and a plastic flow rule to describe material behaviour under multi-axial stress state are required to represent the inelastic properties of material. In the ABAQUS package, different types of material models are available, such as models for classic metal and concrete. In these material models, the yield function and plastic flow rule have been predefined. Hence, inelastic material

properties can be determined by selecting an appropriate material model and uni-axial stress-strain relationship.

The elongation of steel and concrete used in this analysis is the model proposed by Lie (1994). The expansion ratio of the steel and concrete of this model is illustrated in Figure 6.4. As can be seen, the expansion ratio of steel and concrete increases with the increase in the temperature.

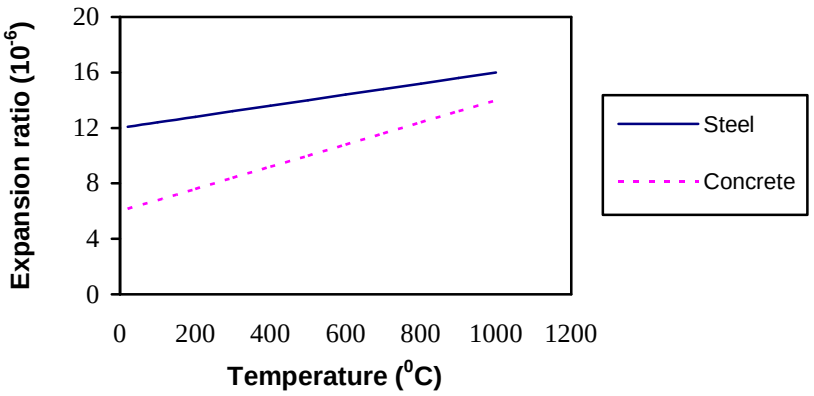

Figure 6.4 Expansion ratio of steel and concrete at elevated temperature (Lie, 1994)

The stress-strain relationship for steel used in the analysis is also that proposed by Lie (1994). Elastic modulus of steel is taken as the initial secant elastic modulus in the stress-strain curve. A classic metal material model in ABAQUS is chosen for steel. This model follows von Misses' yield function and associated plastic flow rule. Typical stress-strain curves for steel at elevated temperatures from Lie's model are shown in Figure 6.5. The hardening of steel has been considered in this model.

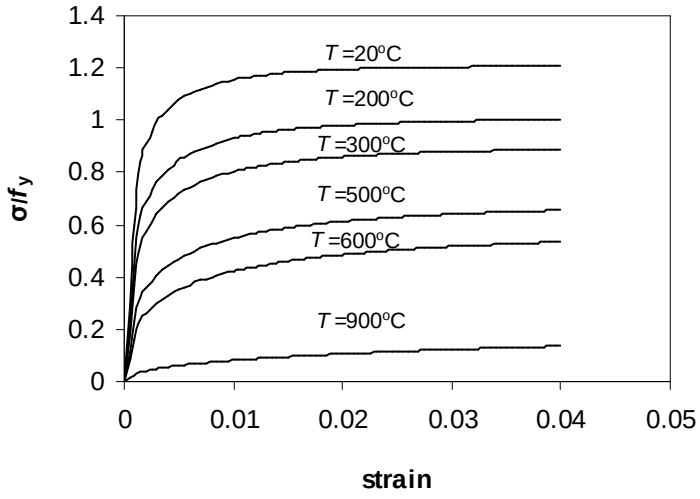

Figure 6.5 Typical steel stress-strain curves at elevated temperature (Lie, 1994)

A concrete damaged plasticity model in ABAQUS was used for the constitutive relationship of concrete in this study. This model uses concepts of isotropic damaged elasticity in combination with isotropic tensile and compressive plasticity to represent the inelastic behaviour of concrete, and consists of a combination of non-associated multi-hardening plasticity and scalar (isotropic) damaged elasticity to describe the irreversible damage that occurs during the fracturing process (ABAQUS, 2008). Concrete has different behaviours and failure mechanisms under compression and tension. Therefore, the stress-strain relationship for concrete needs to be defined in compression and tension separately.

It is well known that there is an interaction between the steel tubes and concrete in CFDST columns. Such interaction can lead the concrete to achieve better performance at ambient temperature. However, this interaction may weaken when the columns are under fire exposure due to the rapid degradation in the mechanical property of the outer tube at elevated temperature. The concrete compression stress-strain relationship in this study is a modification of that proposed by Han (2003c) for CFST columns. The original stress-strain relationship was proposed to predict the structural response of CFST columns under fire exposure by using the fibre model method. The compressive stress-strain relationship for SCC and steel fibre reinforced SCC is defined by the following equations:

$$y = \begin{cases} 2x - x^2 & (x \le 1) \\ \dfrac{x}{\beta(x-1)^{\eta} + x} & (x > 1) \end{cases} \tag{6.8}$$

where; $x = \varepsilon / \varepsilon_0$ and $y = \sigma / \sigma_0$.

For SCC

$$\sigma_0 = \begin{cases} f'_c / \left[1 + 1.986 \times 10^{-9} (T-20)^{3.21}\right] & (f'_c \le 55MPa) \\ f'_c / \left[1 + 9.45 \times 10^{-8} (T-20)^{2.66}\right] & (f'_c > 55MPa) \end{cases}; \tag{6.9}$$

$$\varepsilon_0 = \left(1300 + 12.5 f'_c + 800 \cdot \xi^{0.2}\right) \cdot 10^{-6} \cdot \left(1.03 + 3.6 \times 10^{-4} \cdot T + 4.22 \times 10^{-6} T^2\right); \tag{6.10}$$

$\eta = 4$;

$$\beta = \begin{cases} 0.1 & (T \le 100°C) \\ 6.45 \times 10^{-4} T + 0.087 & (100°C < T \le 400°C) \\ 0.345 & (T > 400°C) \end{cases} \text{ and } \beta \ge \left(0.0338 - 0.00125\xi\right) \cdot f'^{\,0.5}_c \tag{6.11}$$

For steel fibre reinforced SCC

$$\sigma_0 = \begin{cases} f'_c / \left[1 + 1.2\times10^{-9}(T-20)^{3.21}\right] & (T \le 150°C) \\ 1.05 f'_c / \left[1 + 1.2\times10^{-9}(T-20)^{3.21}\right] & (150°C < T \le 450°C); \\ f'_c / \left[1 + 1.2\times10^{-9}(T-20)^{3.21}\right] & (T > 450°C) \end{cases} \quad (6.12)$$

$$\varepsilon_0 = \left(1600 + 12.5 f'_c + 800 \cdot \xi^{0.2}\right) \cdot 10^{-6} \cdot \left(1.005 + 8\times10^{-3} \cdot T + 1.8\times10^{-5} T^2\right) \quad (6.13)$$

$$\eta = \begin{cases} \left(1.4767 + 1.1628\times10^{-3} T\right) & (T \le 450°C) \\ 2 & (T > 450°C) \\ \left(0.8035 + 2.3256\times10^{-4} T\right) \cdot (1.6 + 1.5/x) & (T \le 450°C) \\ 1.6 + 1.5/x & (T > 450°C) \end{cases} \begin{matrix} \\ \\ (\text{CHS CFDST}) \\ \\ (\text{SHS CFDST}) \end{matrix}; \quad (6.14)$$

$$\beta = \begin{cases} (2.36\times10^{-5})^{[0.25 + (\xi - 0.5)^7]} \cdot (f'_c)^{0.5} \cdot 0.5 \ge 0.12 & (\text{for CHS CFDST}) \\ \dfrac{f_c'^{0.1}}{1.2\sqrt{1+\xi}} & (\text{for SHS CFDST}) \end{cases}; \quad (6.15)$$

In the equations, ξ is a parameter relating to the interaction of steel tubes and concrete. It is defined as:

$$\xi = \frac{A_{s,out} \cdot f_{y,out}(T)}{A_{c,no\min al} \cdot f_{ck}} \quad (6.16)$$

where, $A_{s,out}$ is the cross-sectional area of outer steel tube; $A_{c,nominal}$ is the nominal cross-sectional area of concrete which is equal to the void area enclosed by the outer tube; f_{ck} is the characteristic strength of concrete which equals to $0.67f'_c$ and $f_y(T)$ is defined as:

$$f_y(T) = \begin{cases} f_y & (T < 200°C) \\ \dfrac{0.91 f_y}{1 + 6.0\times10^{-17} \cdot (T-10)^6} & (T \ge 200°C) \end{cases} \quad (6.17)$$

There are several options in the concrete damaged plasticity model to define the tensile stress-strain relationship of concrete. A traditional tensile stress-strain relationship for concrete may cause convergent problems in the finite element model if the concrete is seriously cracking. The concept of fracture energy to define the tensile behaviour of concrete is a better solution to achieve a convergent result. Therefore, the tensile property of concrete at elevated temperature is defined as a stress and fracture energy relationship provided in the concrete damaged plasticity model. The fracture energy of concrete at elevated temperature is defined as:

$$G_{ft} = G_f \cdot \left(0.2882 + 8\times10^{-4} T - 1\times10^{-6} T^2\right) \quad (6.18)$$

where G_f is the fracture energy of concrete at ambient temperature which is calculated by the following equation (N/mm):

$$G_f = \begin{cases} \alpha \cdot (\frac{f_c'}{10})^{0.7} \cdot 2.5 \times 10^{-3} & \text{(for SCC)} \\ \alpha \cdot (\frac{f_c'}{10})^{0.7} \cdot 5 \times 10^{-3} & \text{(for steel fibre reinforced SCC)} \end{cases} \quad (6.19)$$

where, f_c' is the concrete cylinder strength at ambient temperature in MPa, α=1.25d_{max}+10, d_{max} is the maximum diameter of corse aggregate in millimetre.

6.4.2 Steel and concrete interface properties

In finite element modelling, the steel tubes and concrete are modelled as individual parts. Although steel tubes and concrete have geometry interfaces in the finite element model, they are independent parts and deform independently unless the interaction between tubes and concrete is defined. In the actual situation, interaction between tubes and concrete has been recognized as a factor which significantly influences the behaviour of the columns. Hence, interaction between tubes and concrete needs to be considered in the modelling.

An approach of contact interaction in ABAQUS (ABAQUS, 2008) is used to simulate the interaction of tubes and concrete in this study. The surfaces of concrete and tube at the interface are defined as a contact pair, one as master surface and the other as slave surface. The master and slave surfaces may contact each other or remain separate. A node-to-surface formulation is used in the simulation. The contact condition is established if nodes in the slave surface effectively interact with a group of points in the master surface. The mechanical properties of the contact pair are defined along normal and tangential directions to the interface respectively. "Hard contact" was selected for the normal directional behaviour. When a contact pair is in contact, there is pressure between the master and slave surfaces, whereas two contact surfaces separate as the pressure comes to zero. A Coulomb friction model was used to simulate the tangential behaviour of the contact pair. When the shear stress in the interface is smaller than a certain value or the bond strength between surfaces, no slipping occurs, otherwise slipping occurs between surfaces. When two contact surfaces have relative slipping, there is frictional or shear stress between surfaces. This stress is determined by the frictional coefficient and the pressure between surfaces. Therefore, a friction coefficient and the bond strength between surfaces are two parameters to determine the mechanical behaviour along the tangential direction. A friction coefficient of 0.2 has been found to be satisfactory in analysing the fire behaviour of CFST columns (Ding and Wang, 2008). In the current study, this value was chosen to be 0.2. The bond between tubes and

concrete was ignored, based on the consideration that bond strength in the interface may degrade quickly at elevated temperatures.

From the above definition of contact properties, it is clear that confinement of steel tubes on the concrete is simulated by the normal contact property, whereas the tangential contact behaviour simulates the transmission of shear force in the surfaces.

6.4.3 Boundary conditions and initial eccentricity

As shown in Figure 6.2, only half of an actual CFDST column is used to create a finite element model. There are two rigid end plates, on the top and bottom of the column, which are used to apply load and assign column-end boundary conditions on the column. Fixed, pinned or other constraining boundary conditions can be applied on the end plates to simulate the actual boundary conditions. In addition to column-end boundary conditions, symmetry boundary conditions need to be defined on the symmetry faces and edges. The symmetry boundary conditions and load on the columns are illustrated in Figure 6.6.

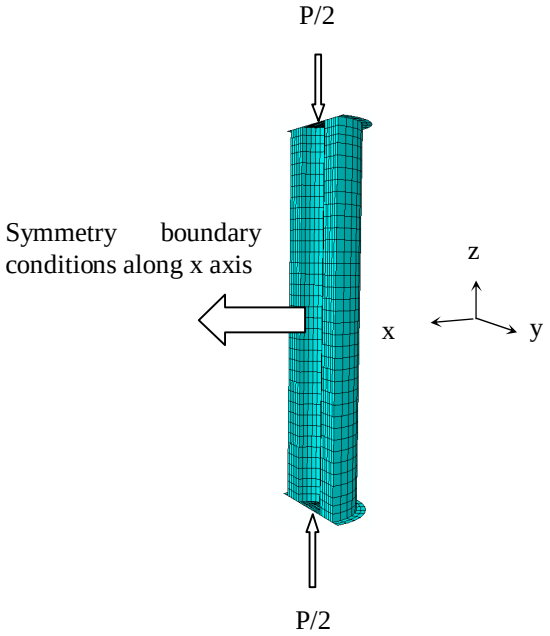

Figure 6.6 Symmetry boundary conditions and load on the model

During analysis of the behaviour of columns under axial load, imperfection in the straightness of the columns is one of the parameters which should be considered in the modelling. Ding and Wang (2008) conducted a sensitive analysis to investigate the

initial straightness imperfection on the fire behaviour of CFST columns. The initial straightness imperfection was converted into load initial eccentricity at the ends of the columns. This study showed that initial eccentricity has a minimal influence on the fire behaviour of the CFST columns when the initial eccentricity varies from $L/2000$ to $3L/1000$, where L is the length of the columns, and an initial eccentricity of $L/1000$ was used in the analysis. In the current study, the initial eccentricity was taken as $L/1000$.

6.5 FINITE ELEMENT MODEL VERIFICATION

The finite element model proposed above was used to predict the fire behaviour of the CFDST columns and stub columns in Chapters 4 and 5. The predicted temperatures, axial deformation, failure modes and fire resistance were compared to those from the fire tests to verify the finite element model.

6.5.1 Temperatures

Comparisons of the predicted temperatures to the temperatures gained from the fire tests for the CFDST columns and stub columns in Chapters 4 and 5 are shown in Figures 6.7 and 6.8 respectively. In these figures, the solid lines represent the temperatures measured in the fire tests and dashed lines represent the predicted temperatures. The denotations, 1, 2 and 3, for curves in the Figure 6.8 correspond to the locations for measurement of the temperatures in the CFDST stub columns in Chapter 4.

As can be seen, the predicted temperatures are generally consistent with the temperatures measured in the fire tests. It should be noted that a revised thermal property for the fire protection coating was used to predict the temperature of SS2 shown in Figure 6.7(f) to consider the effect of local buckling of the outer SHS on the integrity of the fire protection system. Further discussion is provided in the following section.

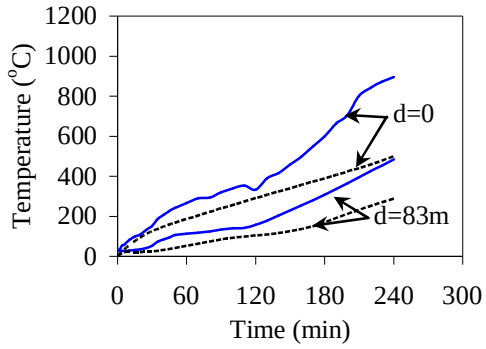

(a) CC1

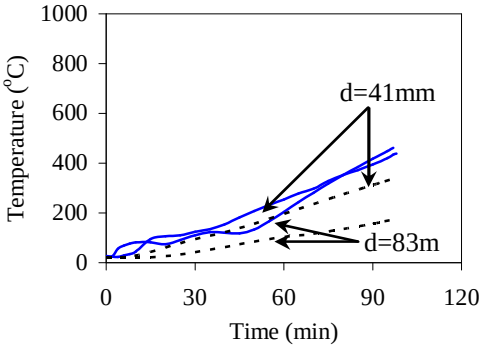

(b) CC2

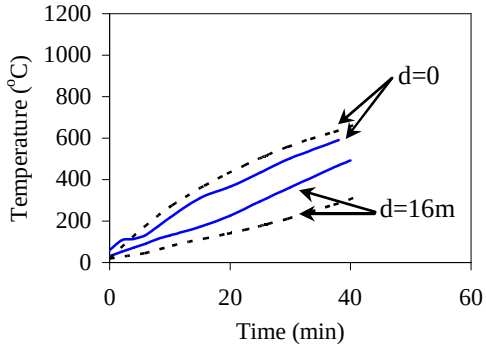

(c) CC3

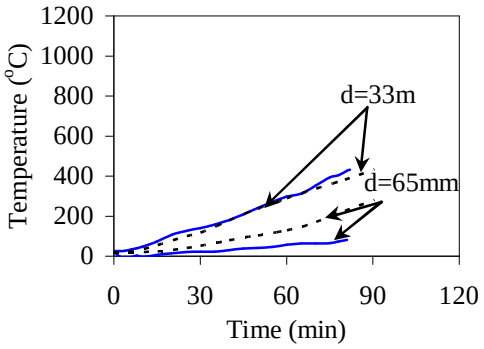

(d) SC1

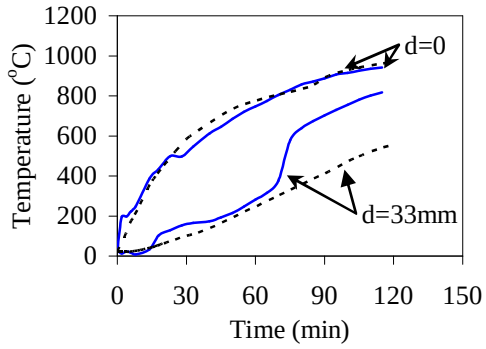

(e) SS1

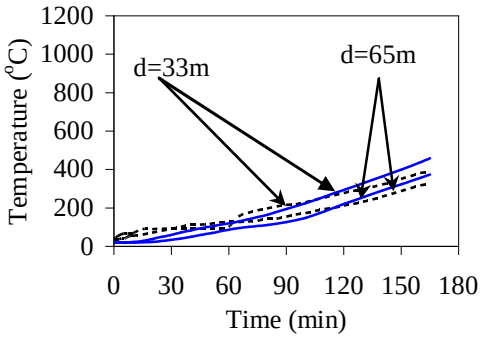

(f) SS2

Figure 6.7 Comparison of predicted and measured temperatures in CFDST columns

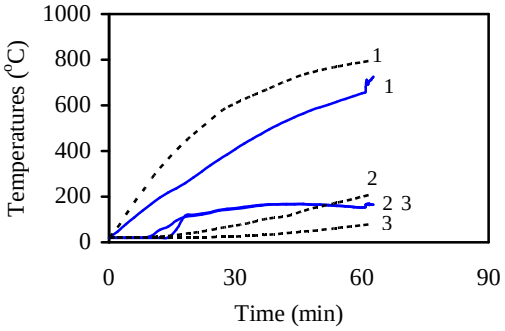

(a) C1-SC2-C

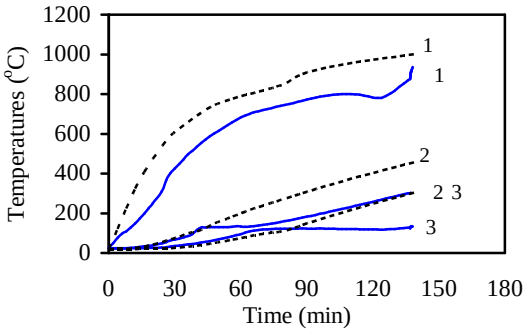

(b) C1- SC2-CS

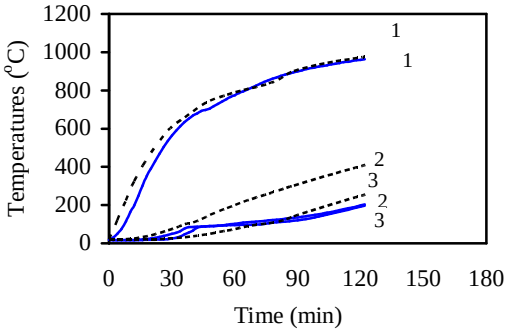

(c) C1- SC2-CSP

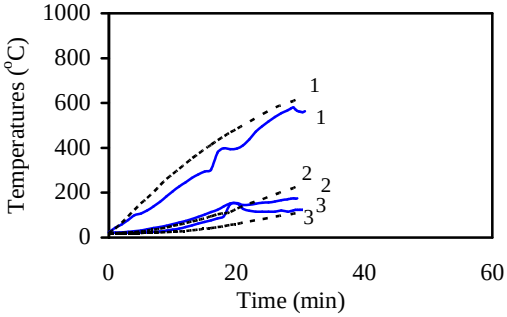

(d) C2- SC2-C

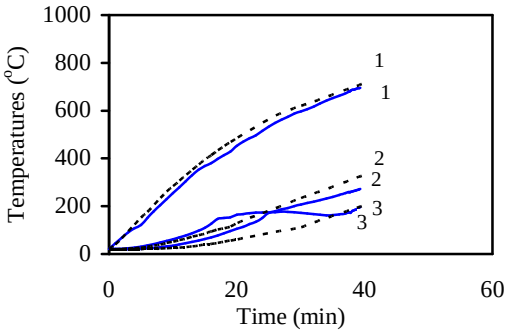

(e) C2- SC2-CS

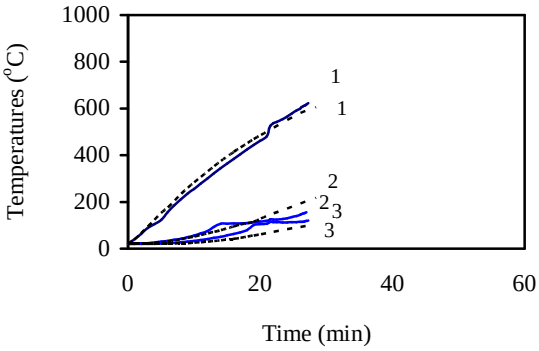

(f) C2- SC2-CSP

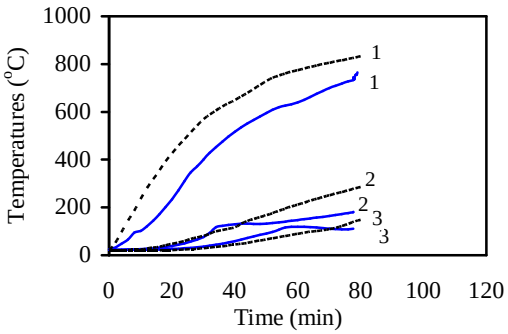

(g) S1- SC2-C

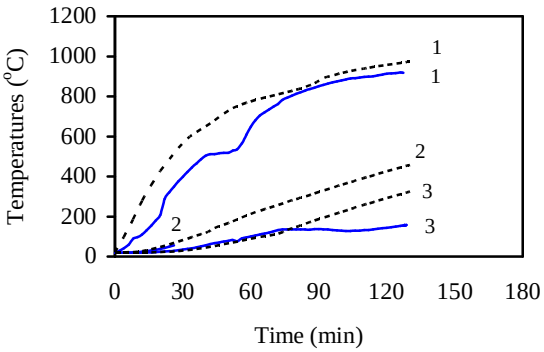

(h) S1- SC2-CS

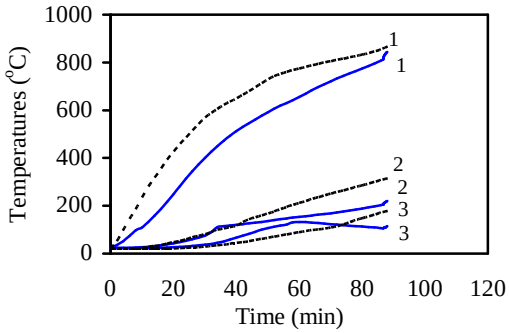

(i) S1- SC2-CSP

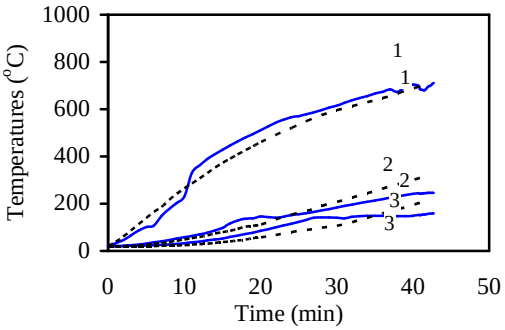

(j) S2- SC2-C

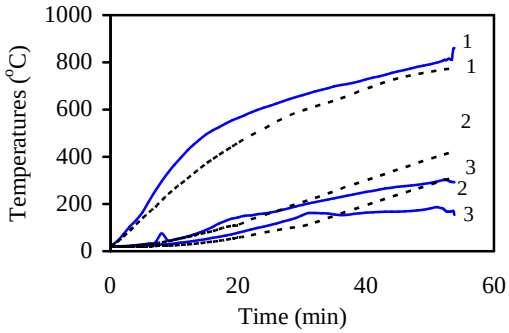

(k) S2- SC2-CS

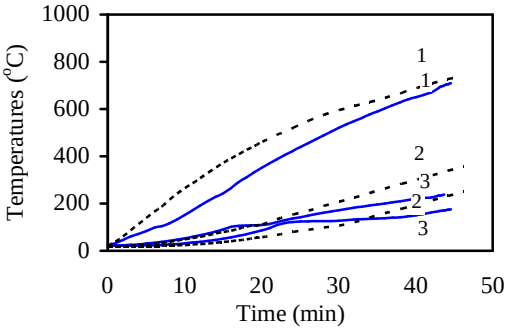

(l) S2- SC2-CSP

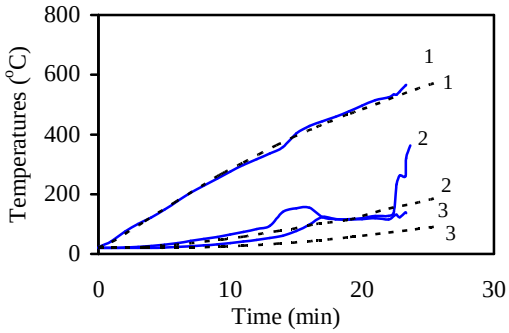

(m) C2- SC1-C

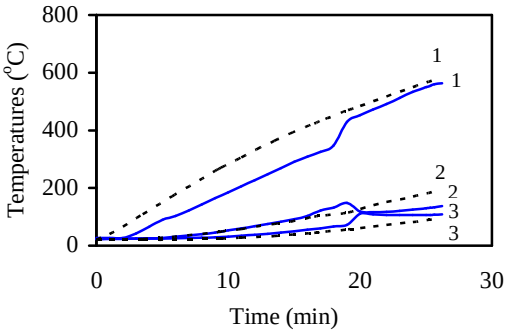

(n) C2- SC1-CS

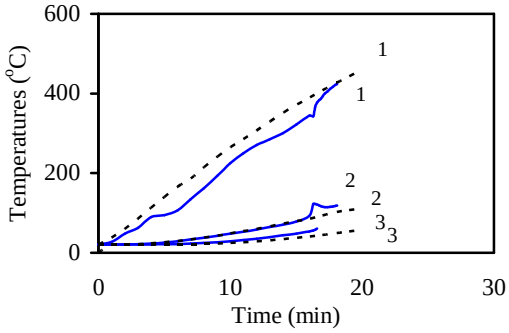

(o) S2- SC1-C

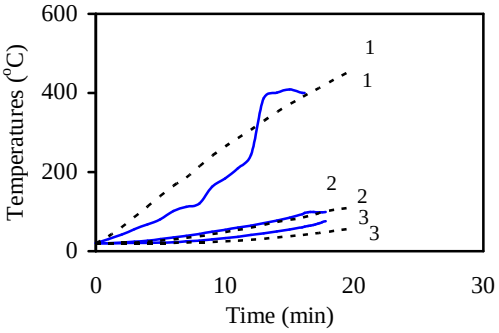

(p) S2- SC1-CS

Figure 6.8 Comparison of predicted and measured temperatures in CFDST stub columns

6.5.2 Axial deformation

The comparison of the predicted and measured axial deformation for the CFDST columns and stub columns in Chapters 4 and 5 is shown in Figures 6.9 and 6.10 respectively.

Most of the predicted axial deformation is consistent with the measured values. As presented in the last section, the effect of local buckling of the outer steel tube in SS2 on the thermal insulation system has been considered in the modelling. As discussed in Chapter 4, during the fire tests, it was observed that local buckling of the outer tube occurred long before the columns reached fire resistance for the CFDST columns with SHS as outer tube. Buckling of the outer tube causes serious cracking in the insulation coating and consequently affects the integrity of the insulation coating. To consider such influence in the finite element model, the thermal properties of the insulation coating were adjusted to appropriate values after local buckling occurred at the outer steel tube in the thermal response analysis step. For SS2, the thermal conductivity of the insulation coating increased to 2.5 times of its original value after 100 minutes of fire exposure. The predicted temperatures in SS2 matched the measured temperatures well after such adjustment had been implemented in the finite element model as shown in Figure 6.7 (f). Then, the predicted temperatures shown in Figure 6.7 (f) were used to calculate the structural response of the column. The predicted axial deformation for SS2 is shown in Figure 6.9 (f). As can be seen, the predicted deformation was quite consistent with the measured axial deformation.

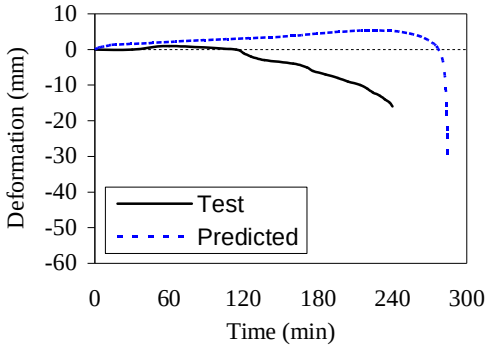

(a) CC1

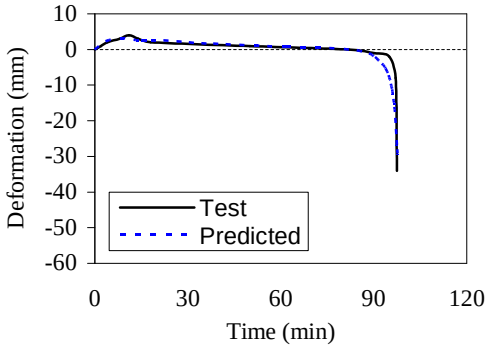

(b) CC2

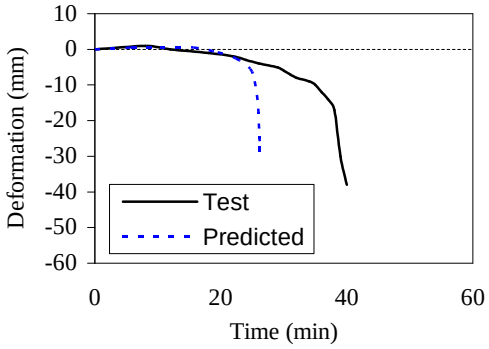

(c) CC3

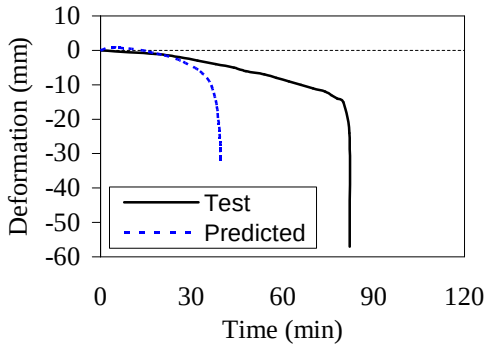

(d) SC1

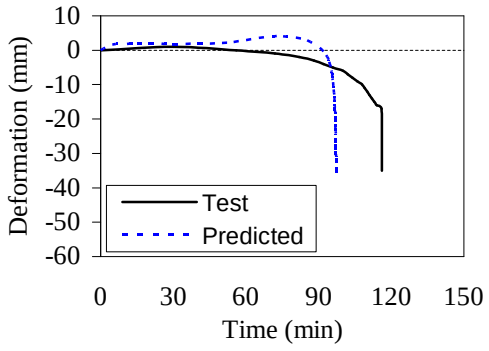

(e) SS1

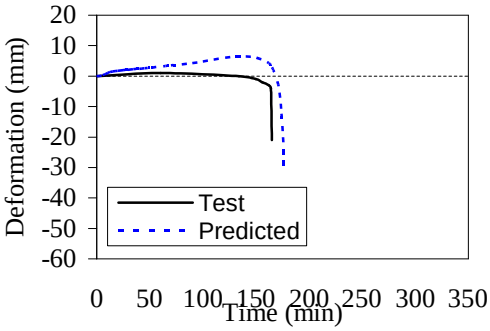

(f) SS2

Figure 6.9 Comparison of predicted and measured axial deformation of CFDST columns

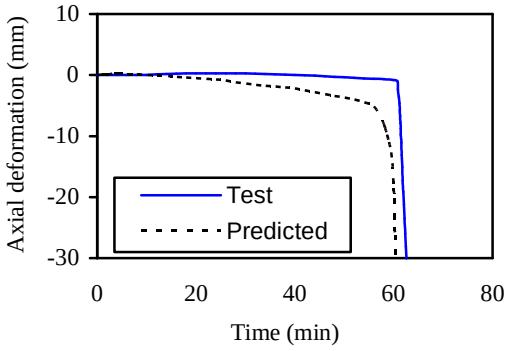

(a) C1-SC2-C

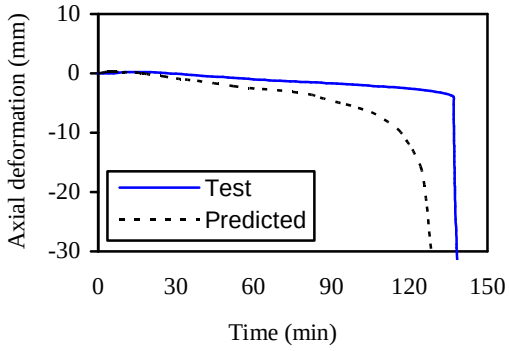

(b) C1- SC2-CS

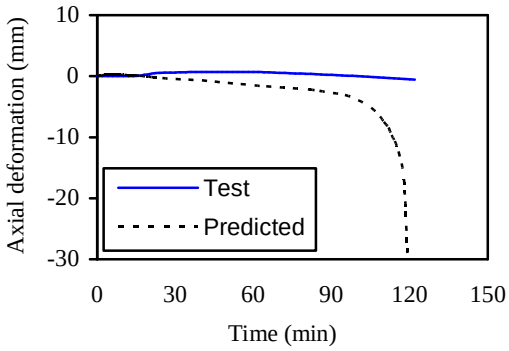

(c) C1- SC2-CSP

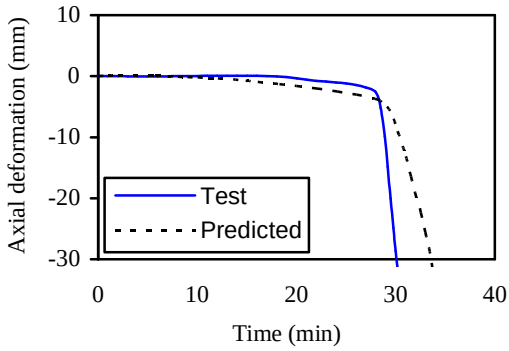

(d) C2- SC2-C

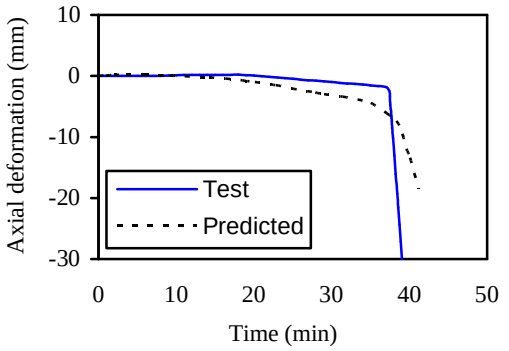

(e) C2- SC2-CS

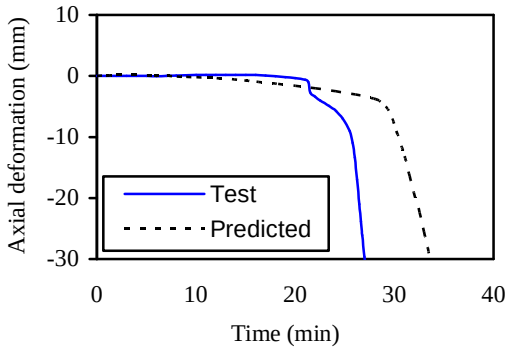

(f) C2- SC2-CSP

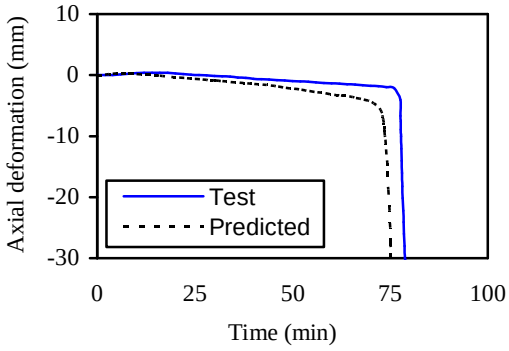

(g) S1- SC2-C

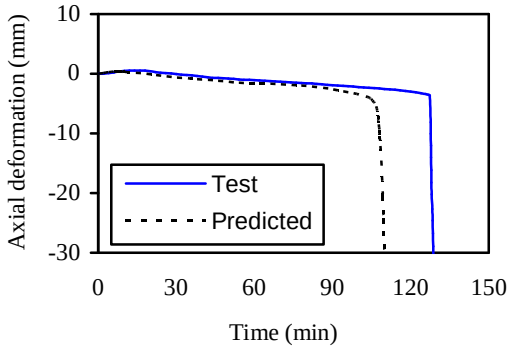

(h) S1- SC2-CS

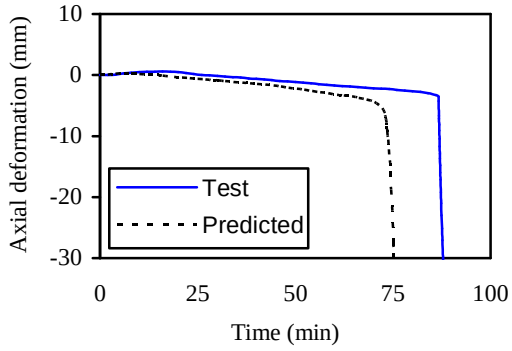

(i) S1- SC2-CSP

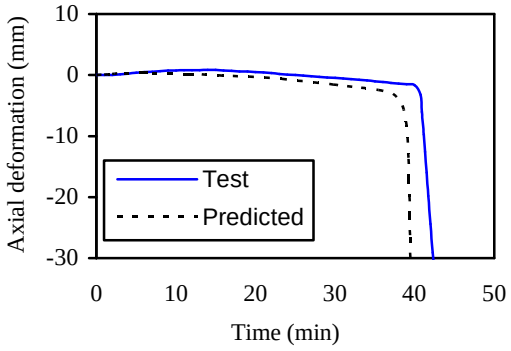

(j) S2- SC2-C

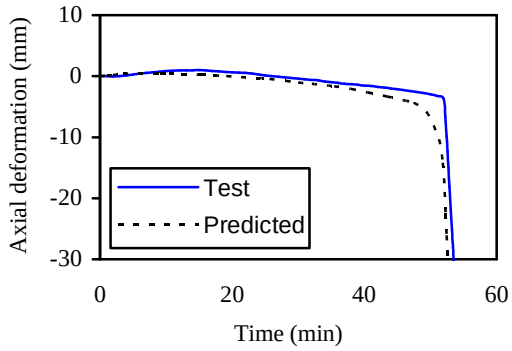

(k) S2- SC2-CS

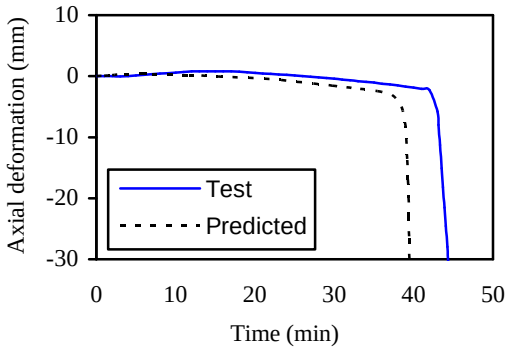

(l) S2- SC2-CSP

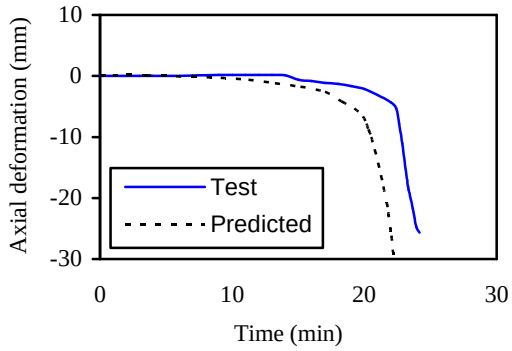

(m) C2- SC1-C

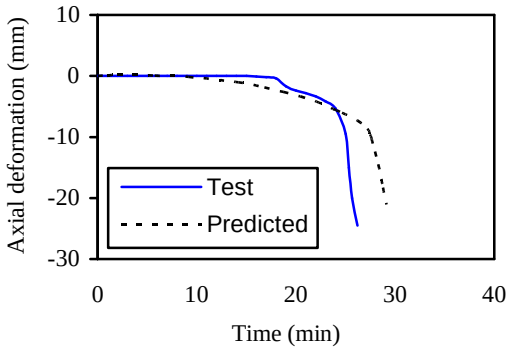

(n) C2- SC1-CS

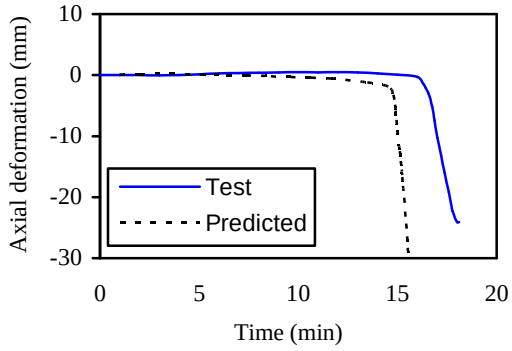

(o) S2- SC1-C

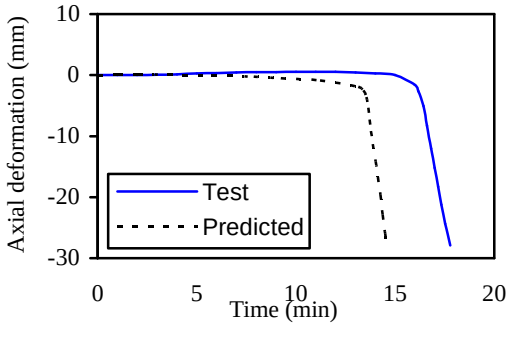

(p) S2- SC1-CS

Figure 6.10 Comparison of predicted and measured axial deformation of CFDST stub columns

6.5.3 Failure modes

Typical predicted failure modes of a CFDST column and a CFDST stub column were used to contrast the observed failure modes to illustrate the capability of the finite element model to predict the failure modes of CFDST columns under fire exposure.

The predicted failure mode of SS2 when the column reaches fire endurance and the corresponding failure mode of the outer and inner tubes are shown in Figure 6.11 (a) to (c). There is an obvious lateral deflection in the column. This suggests that the column failed due to the combination of local and overall buckling. Local buckling occurred in the outer tube and the most serious local buckling appeared at the position corresponding to where maximum lateral deflection occurred. Local buckling also appeared in the inner tube at the position corresponding to where maximum lateral deflection was present. Comparison of the predicted failure mode in Figure 6.11 (a) and the observed failure mode shown in Chapter 4 confirms that the finite element model can predict the failure mode of the columns well.

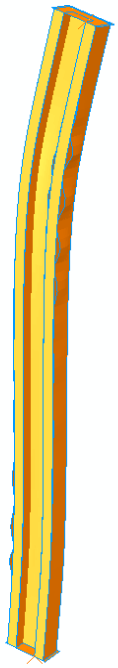

(a) Overall column

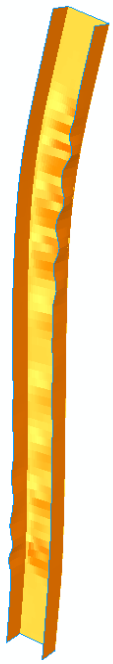

(b) Outer tube

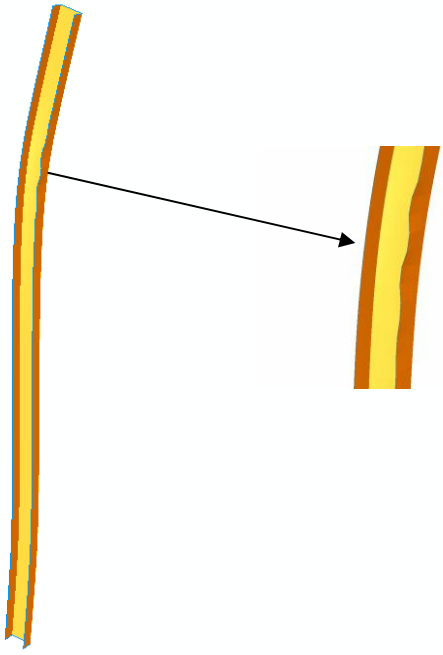

(c) Inner tube

Figure 6.11 Predicted failure mode of SS2

The observed failure mode of a CFDST stub column, C1-SC2-CS, was further used for comparison with the predicted failure mode as shown in Figure 6.12 (a) to (b). As can be seen, there is an obvious outward bulge in the outer tube. However, there is no

obvious lateral deflection in the column. This is a typical compression failure mode for CFDST stub columns. The outer tube is forced to outward bulging because of the presence of the concrete. In contrast, the inner tube is forced to inward bulging by the concrete as shown in Figure 6.17 (c) and (d). Again, the finite element model can well predict the failure modes of the CFDST stub columns and steel tubes.

(a) Failure mode of the stub column

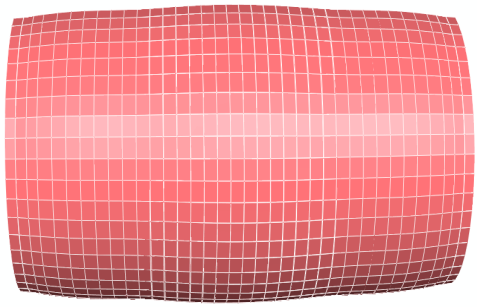

(b) Predicted failure mode of the stub column

(c) Failure mode of the inner tube

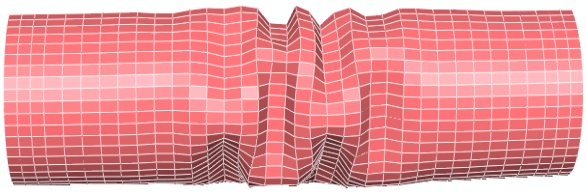

(d) Predicted failure mode of the inner tube

Figure 6.12 Comparison of failure mode for C1-SC2-CS

The failure modes shown in Figures 6.11 and 6.12 represent two types of failure mechanisms for CFDST columns under fire exposure: overall buckling and compression failure. The finite element model can truly predict the failure modes of the columns which fail under different failure mechanisms.

6.5.4 Fire resistance

The comparison between the predicted and measured fire endurance of the CFDST columns and stub columns is shown in Figure 6.13. As can be seen, the finite element model can well estimate the fire endurance of the CFDST columns.

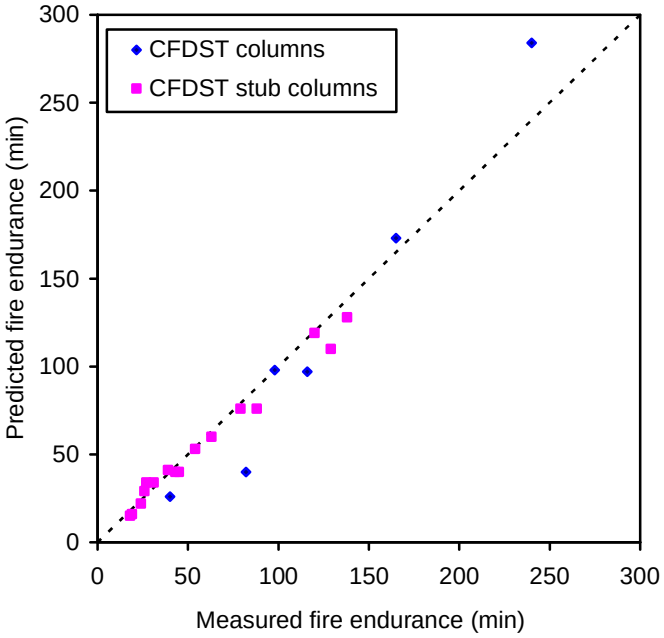

Figure 6.13 Comparison of measured and predicted fire endurance

6.6 CONCLUSIONS

A finite element model using the finite element package, ABAQUS, to simulate the fire behaviour of the CFDST columns has been proposed. A two-step sequentially-coupled thermal-stress analysis procedure was utilized in the model.

In the thermal response analysis, the effect of water on the temperatures in CFDST columns has been considered by incorporating the thermal properties of water into those of the concrete. Thermal resistance at the interface of concrete and steel was also considered.

A concrete mechanical property model at elevated temperature has been proposed for the analysis of the structural response of the columns. This material property model can be used for both plain concrete and fibre-reinforced concrete.

The proposed finite element model has been verified by the fire tests results presented in the previous chapters. The predicted temperatures, axial deformation and fire endurance are consistent with the test results. In addition, the predicted failure modes of the columns and steel tubes are also consistent with the observed failure modes. Hence, the proposed finite element model can predict the fire behaviour of CFDST columns well.

Chapter 7

MODELLING THE FIRE BEHAVIOUR OF CFDST COLUMNS

7.1 INTRODUCTION

The fire behaviour of CFDST columns is complex due to the simultaneous thermal, structural and composite actions acting on the columns. Generally, fire tests cannot provide sufficient direct evidence to analyse in detail the fire behaviour of CFDST columns, whereas numerical modelling offers the possibility of achievement of this goal.

In this chapter, the finite element model proposed and verified in Chapter 6 is used to analyse the fire behaviour of CFDST columns. The analysis is divided into two parts, thermal and structural response analysis. The thermal response of CFDST columns has been extensively discussed in the previous chapters. Here, the complementary discussion focuses on the thermal response of the outer steel tubes. In the structural response, deformation, strain, stress, strength and load share in each component of CFDST columns are discussed. Then, the failure mechanism of CFDTS columns under fire exposure is illustrated, based on the above information on the thermal and structural responses of the columns. Understanding of the fire behaviour and failure mechanism of CFDST columns is the foundation upon which methods to enhance the fire performance of the columns can be based.

7.2 THE FE MODEL AND COLUMNS FOR ANALYSIS

7.2.1 FE model

The finite element model introduced in Chapter 6 is used for the parametric studies. In order to enhance modelling efficiency, ¼ of the actual columns are used in the modelling. Symmetric boundary conditions are applied on the symmetric planes as shown in Figure 7.1.

The fire temperature prescribed in AS 1530-4 (2005) is used in the thermal response analysis. The steel thermal properties model and the concrete thermal properties for normal strength concrete with carbonate aggregate proposed by Lie (1992) are used in the analysis.

The steel mechanical property model proposed by Lie (1992) and the concrete mechanical property model presented in Chapter 6 are used in the structural response analysis.

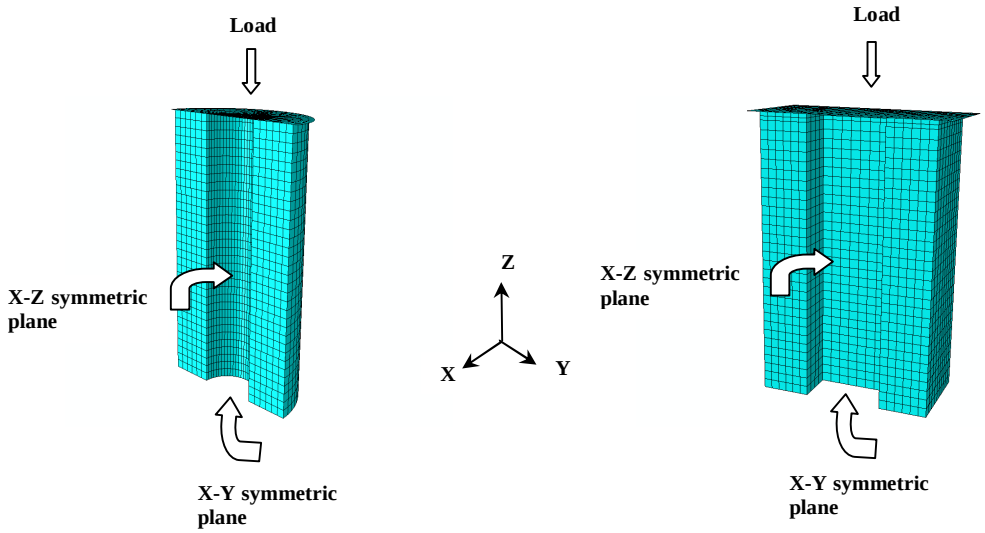

Figure 7.1 Symmetric boundary conditions for the FE models

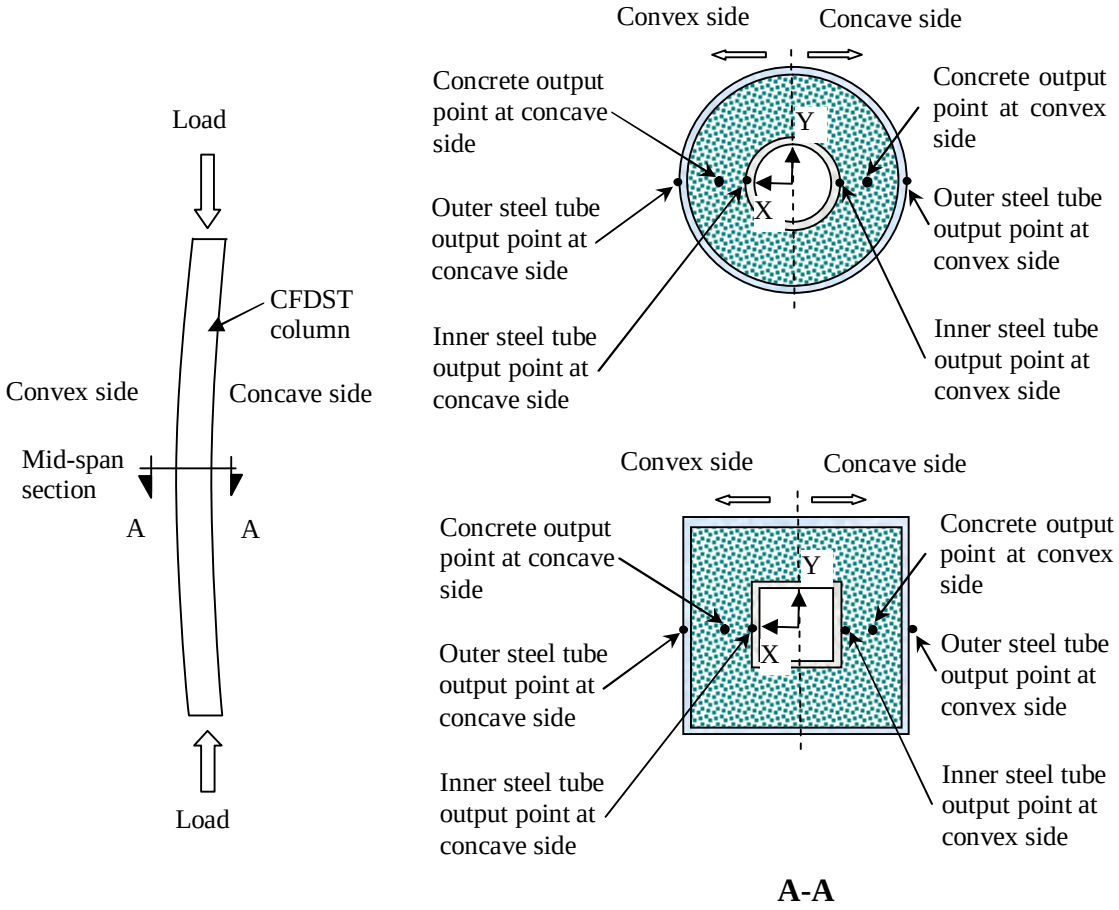

Figure 7.2 Typical output points and stress direction

The FE analysis procedure and model are the same as those described in Chapter 6. Stress and strain values at some typical points in the mid-span section of the CFDST columns are selected for analysis. The positions of these typical points and direction of the stress and strain are shown in Figure 7.2.

7.2.2 CFDST columns for analysis

Four typical CFDST columns are selected for analysis. The parameters of the columns are shown Table 7.1. As can be seen, these columns include slender and stub columns with sizes similar to columns used in high rise and multistorey buildings.

Table 7.1 Basic parameters for CFDST columns

No	Outer tube ($D_o \times t_o$) (mm)	Inner tube ($D_i \times t_i$) (mm)	Length L (mm)	L/D_o	f_{yo} (MPa)	f_{yi} (MPa)	f_c (MPa)	Load (kN)	Load level	Boundary conditions
1	CHS700×25	CHS300×20	4200	6.0	350	350	40	21945	0.5	Pin-Pin
2	CHS1200×40	CHS500×25	3500	2.9	350	350	40	62990	0.5	Pin-Pin
3	SHS700×25	SHS300×20	4200	6.0	350	350	40	26278	0.5	Pin-Pin
4	SHS1200×40	SHS500×25	3500	2.9	350	350	40	74846	0.5	Pin-Pin

7.3 THERMAL RESPONSE

For columns under fire exposure, the fire temperature is assumed to be uniform along the axial direction. Hence, the thermal response of the CFDST columns depends on the profile and cross-sectional sizes. Two of the CFDST columns in Table 1, No 1 and No 3, are used as examples to analyse the thermal responses of the columns. The relationships between the temperatures and fire exposure time at typical points corresponding to the points shown in Figure 2 in the outer tubes, concrete and inner tubes are shown in Figure 7.3. The temperature distributions in the column cross-sections at different fire exposure times in the columns are shown in Figures 7.4 and 7.5 respectively.

As shown in the figures, temperature distribution in the CFDST columns is non-uniform, the outer steel tubes experiencing a much higher temperature than the inner steel tubes. The outer part of the concrete also experiences a higher temperature than the inner part of the concrete. Due to the symmetry, temperatures in the circular CFDST are uniform

along the circumference. However, for square CFDST, temperatures at the corners are significantly higher than elsewhere.

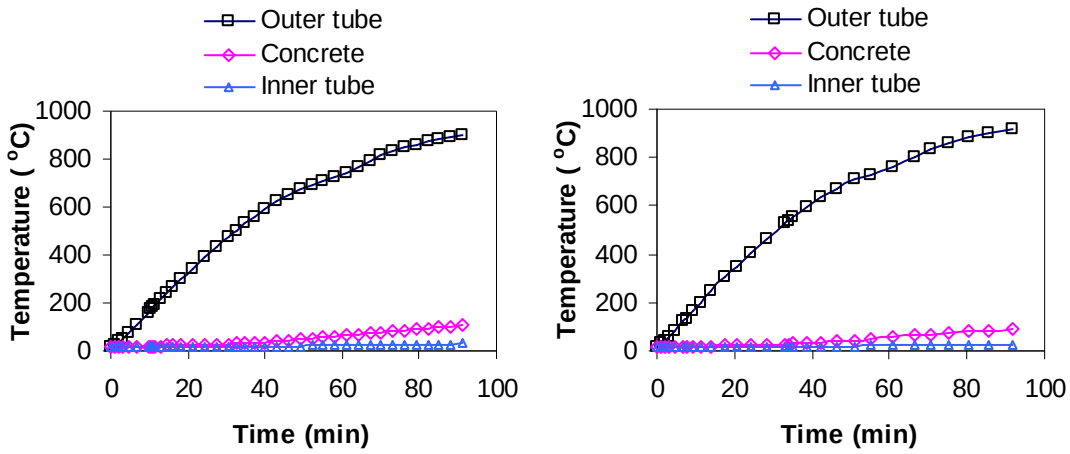

(a) CHS CFDST (No.1 in Table 1) (b) SHS CFDST (No.3 in Table 1)

Figure 7.3 Temperatures in typical points in the CFDST columns

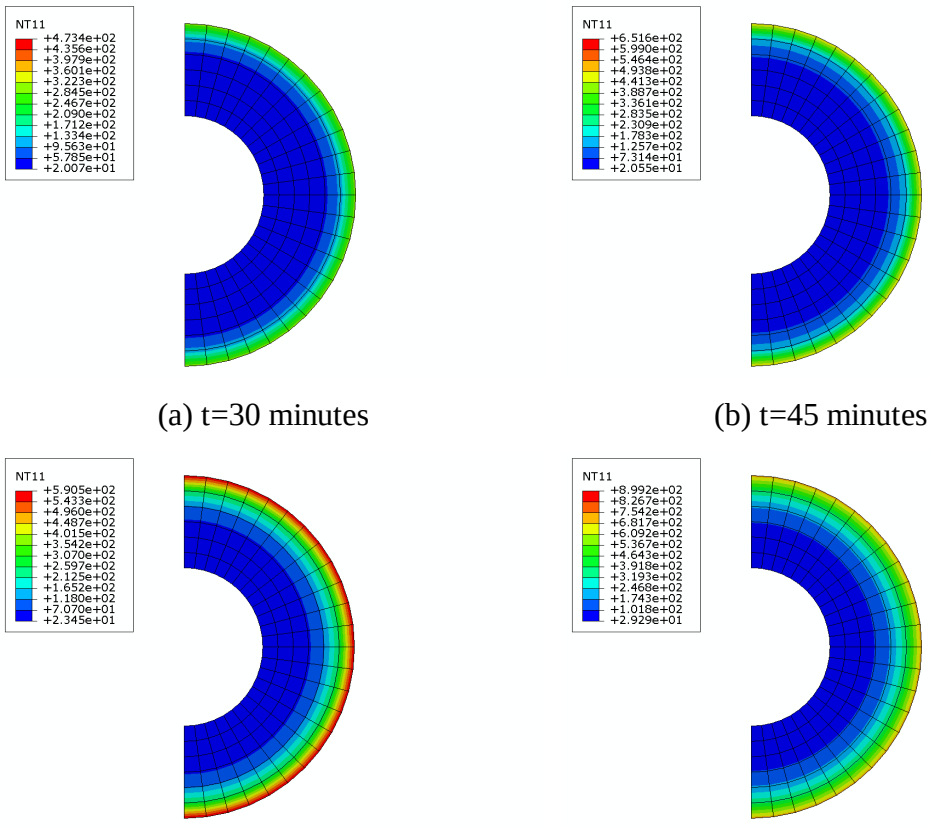

(a) t=30 minutes (b) t=45 minutes

(c) t=60 minutes (b) t=90 minutes

Figure 7.4 Temperature distribution in a circular CFDST column (No.1 in Table 1)

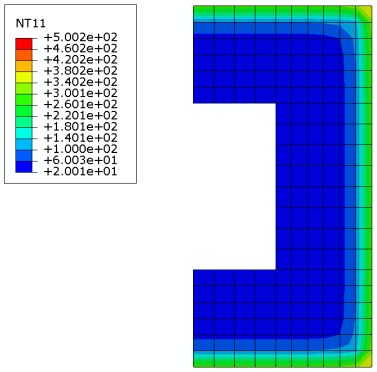

(a) t=30 minutes

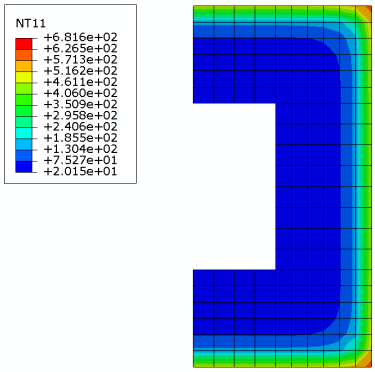

(b) t=45 minutes

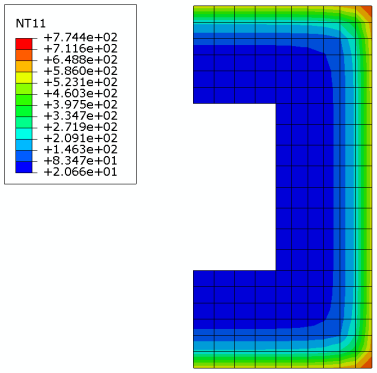

(c) t=60 minutes

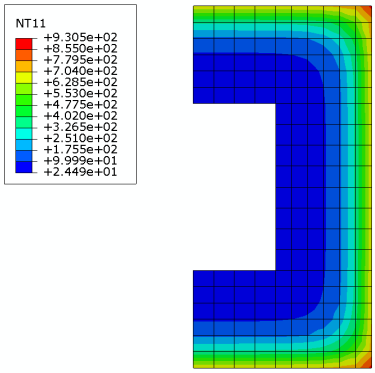

(b) t=90 minutes

Figure 7.5 Temperature distribution in a square CFDST column (No.3 in Table 1)

Non-uniform temperature distribution in the CFDST is primarily caused by the good thermal resistance ability of the concrete, which serves as an effective insulation for the inner steel tubes and results in temperature gradient in the concrete. As can be seen in Figure 7.3, the temperature of the outer steel tube is about 900 ^{o}C, while the temperature of the inner steel tube is less than 60 ^{o}C at 90 minutes of standard fire exposure. Such a significant difference in the temperatures between the outer and inner steel tubes has also been observed in the fire tests reported in Chapters 4 and 5. However, the effect of concrete on the temperatures of the outer steel tubes has not been evident from the fire tests.

The first column in Table 7.1 is selected as an example to investigate the effect of the concrete on the temperature of the outer steel tubes. Temperatures in a circular unfilled CHS which has the same size as the outer steel tube of this CFDST column to exposes to the same fire temperature is also calculated for comparison. The temperatures at the exterior and interior surfaces of the outer steel tube in the CFDST and unfilled CHS versus the fire exposure time are shown Figure 7.6.

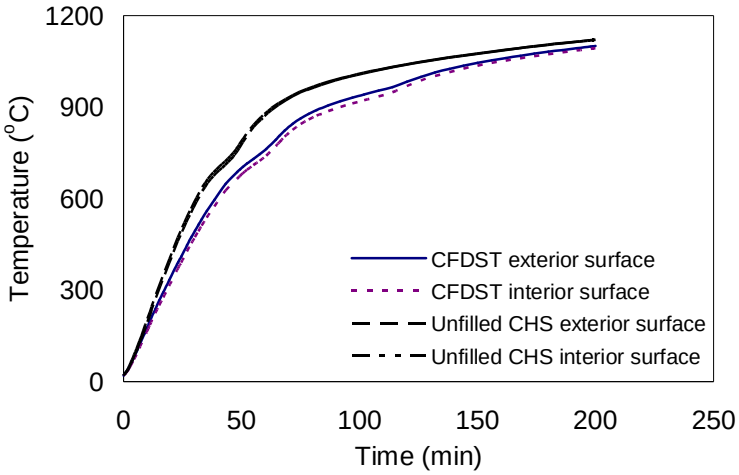

Figure 7.6 Comparison between temperatures in outer steel tube and corresponding unfilled CHS

As shown in Figure 7.6 above, the temperatures in the outer steel tube of the CFDST are lower than the temperatures in the corresponding unfilled CHS. In addition, the difference in the temperature between the exterior and interior surface of the outer steel tube in the CFDST is also larger than that in the unfilled CHS. This means that the concrete in CFDST columns can not only work as heat insulation for the inner steel tubes, but also serves as a heat sink to absorb heat from the outer steel tubes to slow down temperature elevation in the outer steel tubes.

7.4 STRUCTURAL RESPONSE

7.4.1 Failure mode

Failure modes of the CFDST columns are shown in Figure 7.7. As can be seen, there is obvious lateral buckling of the slender columns. However, lateral buckling is not obvious for the stub columns. There is no obvious local buckling in the steel tubes of the circular CFDST columns, whereas local buckling occurs at the outer steel tubes of the square CFDST columns.

The failure modes of the columns are generally similar to those observed from the fire tests reported in Chapters 4 and 5. However, there is an obvious difference between the failure modes of the columns in Figure 7.7 and those in the tests as local buckling does not occur in the inner steel tubes. This is due to the differences in the temperature

distribution and magnitude of the axial deformation between those in the fire tests and the columns in this analysis. For the slender columns in this analysis, the temperatures in the inner steel tubes are close to ambient temperature as the columns fail. However, the temperatures in the inner steel tubes of the CFDST columns in the fire tests in Chapter 5 were much higher than ambient temperature. The stub columns in the fire tests shown in Chapter 4 experienced a significant axial deformation, the total axial deformation being about 40% of the original column length. However, the failure modes of the stub columns in Figure 7.7 correspond to the columns which have experienced axial deformation of about 15% of the column length.

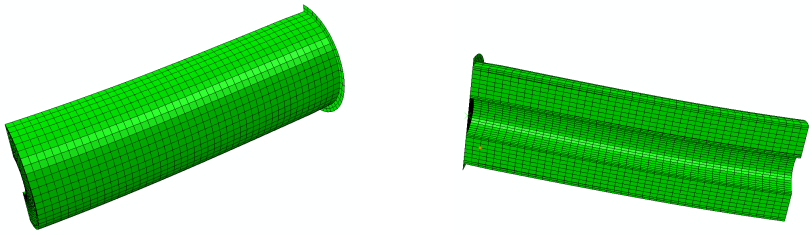

(a) CHS CFDST slender column

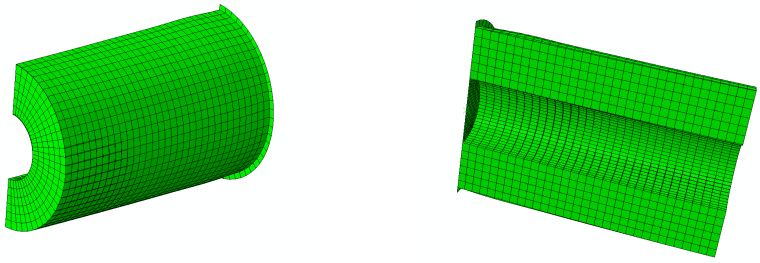

(b) CHS CFDST stub column

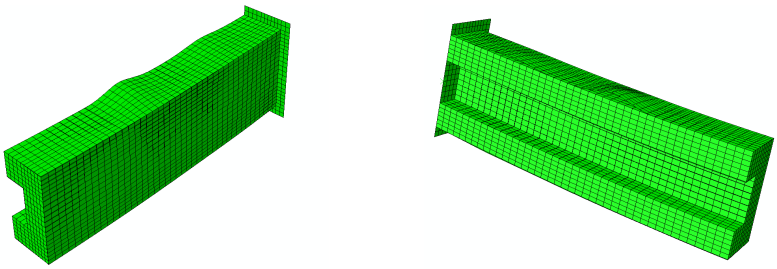

(c) SHS CFDST slender column

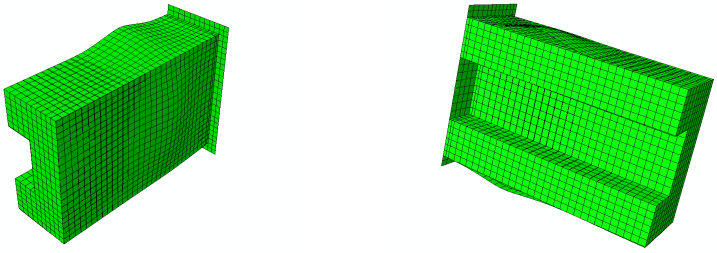

(d) SHS CFDST stub column

Figure 7.7 Failure modes of the CFDST columns

7.4.2 Deformation

The relationship of axial deformation and lateral deflection at the mid-span section and the time to fire is shown in Figure 7.8. As discussed in Chapters 4 and 5, the deformation of the columns under fire exposure can be divided into three stages as shown in the figure. In the first stage, both the axial and lateral deformations are small and relatively stable at the beginning of the fire exposure. Then in the second stage, the deformations increase moderately. In the last stage, both of the deformations increase markedly in a short time. Although the trend of the deformation develops in a similar way for all the columns, there are differences between the deformation of the CFDST slender and CFDST stub columns. In the second stage shown in the figure, axial deformation in the stub CFDST columns develops more quickly than lateral deformation, whereas lateral deformation develops more quickly than axial deformation for the CFDST slender columns. In addition, the values of the lateral deformation are far greater than the values of the axial deformation in the CFDST slender columns as the columns reach fire endurance. Nevertheless, the values of the lateral deformation are slightly smaller than the values of the axial deformation in the CFDST stub columns when the columns reach fire endurance.

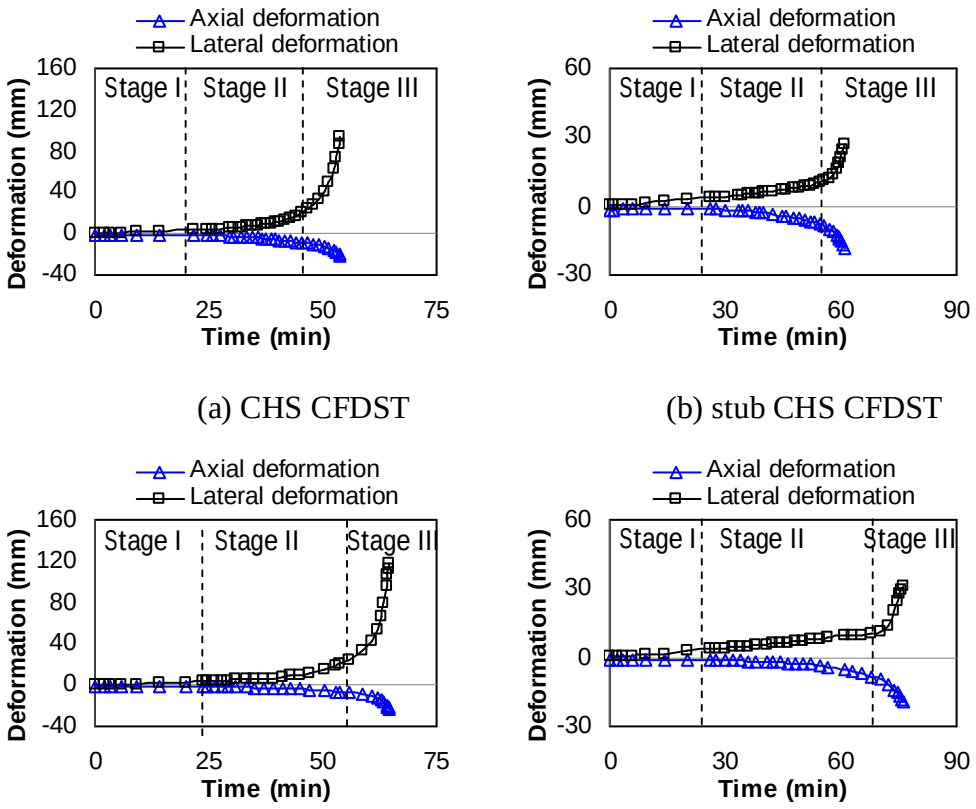

(a) CHS CFDST (b) stub CHS CFDST

(c) SHS CFDST (d) stub SHS CFDST

Figure 7.8 Axial and lateral deformation versus fire exposure time

As shown in Figure 7.8, all the slender columns exhibit considerable lateral deformation as the columns reach fire endurance. This is clear evidence of buckling failure of the columns. Therefore, the final failure mode of the slender columns is overall buckling as shown in Figure 7.7. The axial deformation of the stub columns is more severe than the lateral deflection. Therefore, the stub columns fail in axial compression failure mode. The lateral deflection in the stub columns is induced by the initial imperfection in the columns. In the analysis, the initial imperfection in straightness is transferred as a load eccentricity at both ends of the columns. Failure of the CFDST columns is induced by both the axial load and the moments at the ends of the columns. As can be seen in Figure 7.8, the lateral deflection of the slender columns is several times the axial deformation. The second order effect has more profound influence on the slender columns and finally causes buckling failure of the slender columns. In contrast, the stub columns fail by excessive axial deformation in the columns, i.e. compressive failure. Then, the stiffness of the columns decreases as compression failure occurs. The lateral deflection develops subsequently by the action of the moments at the ends of the columns.

7.4.3 Strain

7.4.3.1 Strain in steel tubes

Strains at the typical points in the outer and inner steel tubes are shown in Figures 7.9 to 7.12. Strains at concave and convex sides are the strains at the utmost fibres of the steel tubes in the mid-span section at the concave and convex sides of the columns. The total strain consists of the thermal strain and the stress-induced strain. Thermal strain is induced by thermal expansion and stress-induced strain is induced by the load on the columns.

As can be seen from the figures, the thermal strains in the outer steel tubes increase steadily with the increase in the time of exposure to fire, whereas there are minimal thermal strains in the inner steel tubes. This is due to the nature of the temperature distribution in the CFDST columns. The outer steel tubes are directly exposed to fire and thus have much higher temperatures than the temperatures in the inner steel tubes which are about 30 ^{o}C until the columns reach fire resistance.

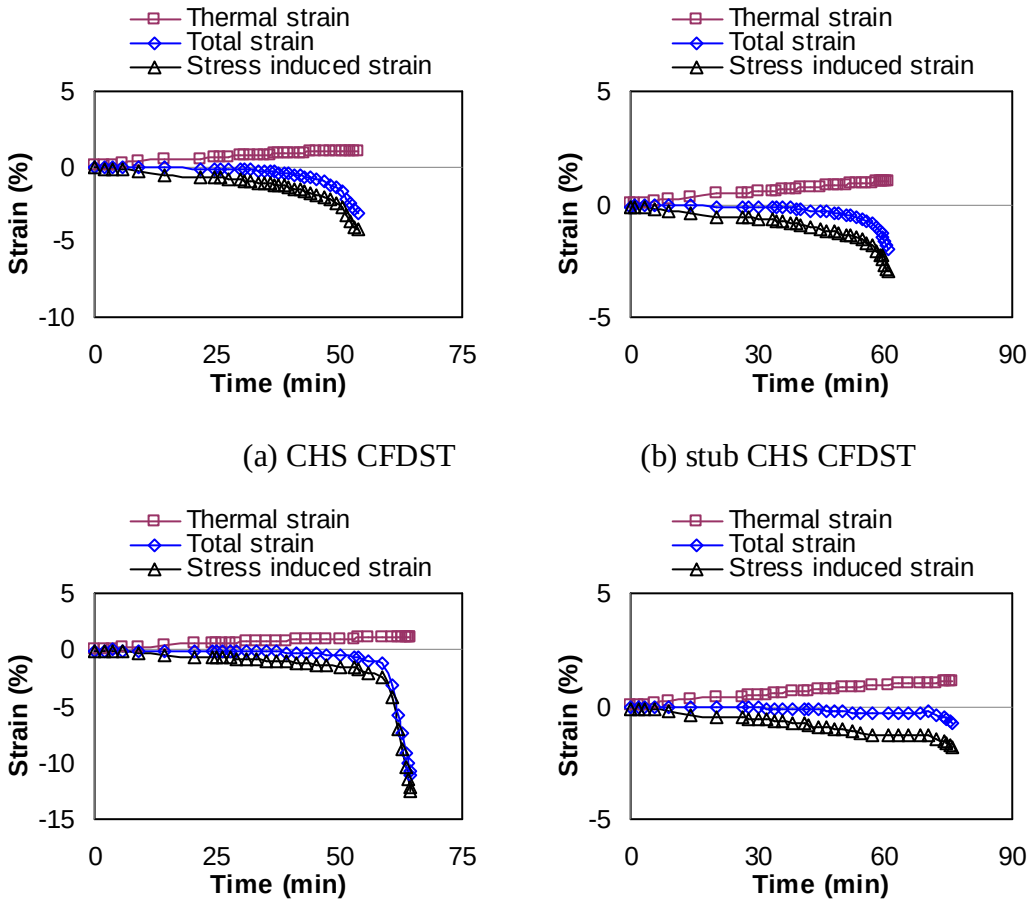

(a) CHS CFDST (b) stub CHS CFDST

(c) SHS CFDST (d) stub SHS CFDST

Figure 7.9 Strain at outer steel tube (concave side)

The values of the stress-induced strain in the outer steel tubes are larger than those in the inner steel tubes. In addition, steel tubes at the concave side experience a higher level of straining than at the convex side. It should be noted that the stress-induced strains at the convex side of the CFDST slender columns decrease as the columns approach fire endurance. This results in the total strains at this position becoming tensile when the columns are close to failure as shown in Figure 7.10 (a) and (c).

The outer steel tubes of the CFDST columns experience much higher temperatures than the inner steel tubes. Therefore, degradation in the material properties, i.e. strength and stiffness, of the outer steel tubes is more serious than in the inner steel tubes. This is the major cause of more severe strain in the outer steel tubes. Considering the temperature in the inner steel tubes is as low as about 30 ^{o}C when the columns reach fire endurance, the stress-induced strains arising in the inner steel tubes are not caused by thermal attack but by load transfer from the outer steel tubes and/or concrete. Load transfer among the three components in the CFDST columns will be further discussed later.

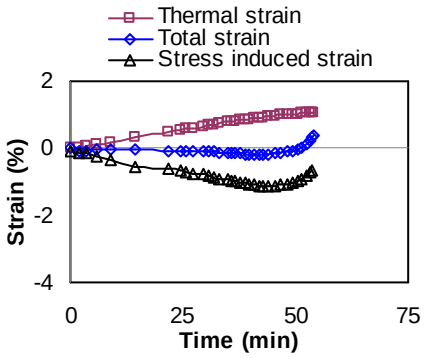

(a) CHS CFDST

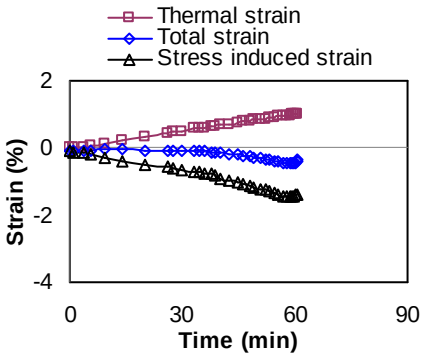

(b) stub CHS CFDST

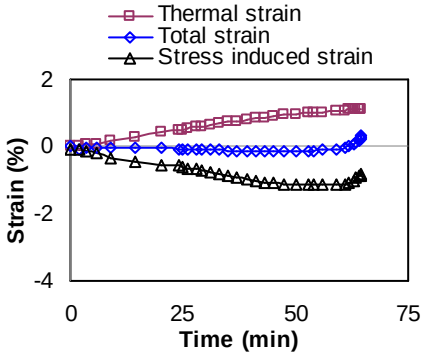

(c) SHS CFDST

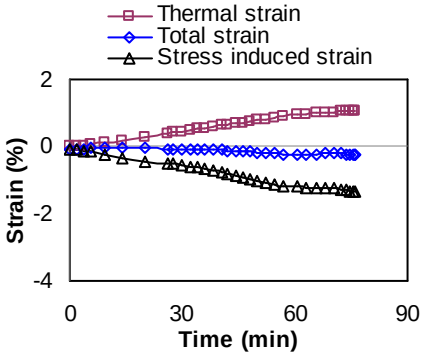

(d) stub SHS CFDST

Figure 7.10 Strain at outer steel tube (Convex side)

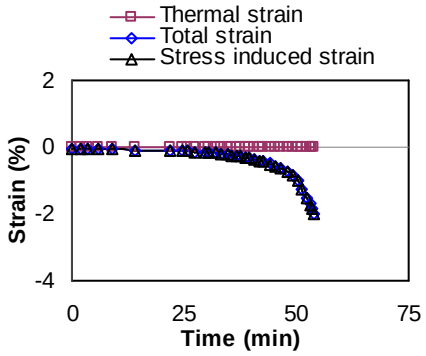

(a) CHS CFDST

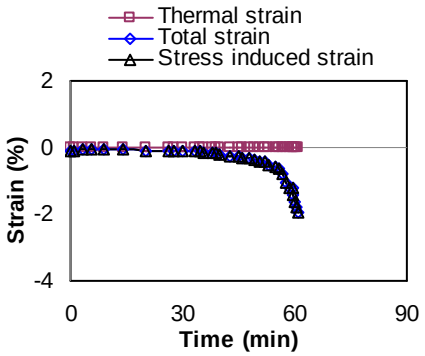

(b) stub CHS CFDST

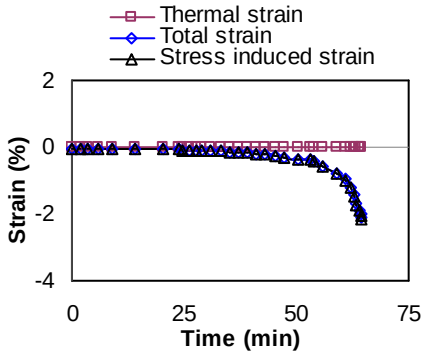

(c) SHS CFDST

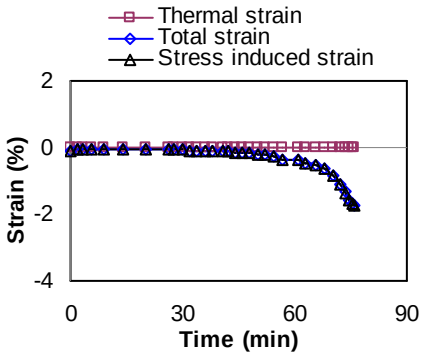

(d) stub SHS CFDST

Figure 7.11 Strain at inner steel tube (concave side)

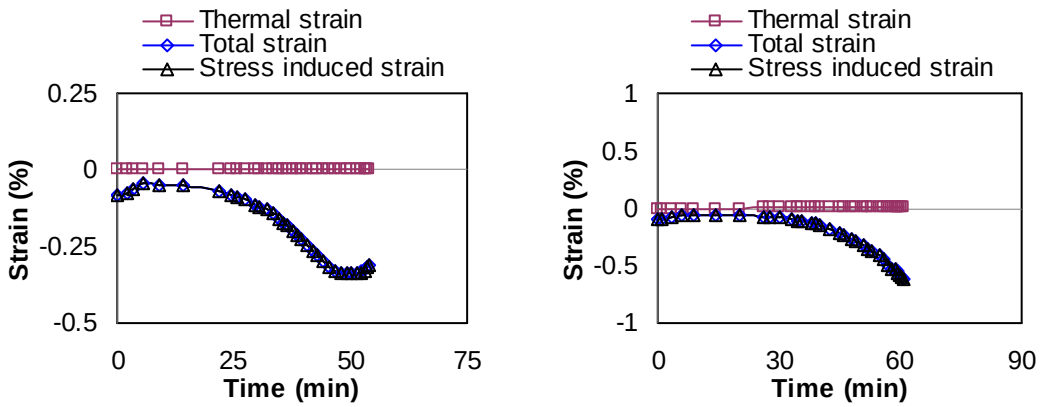

(a) CHS CFDST (b) stub CHS CFDST

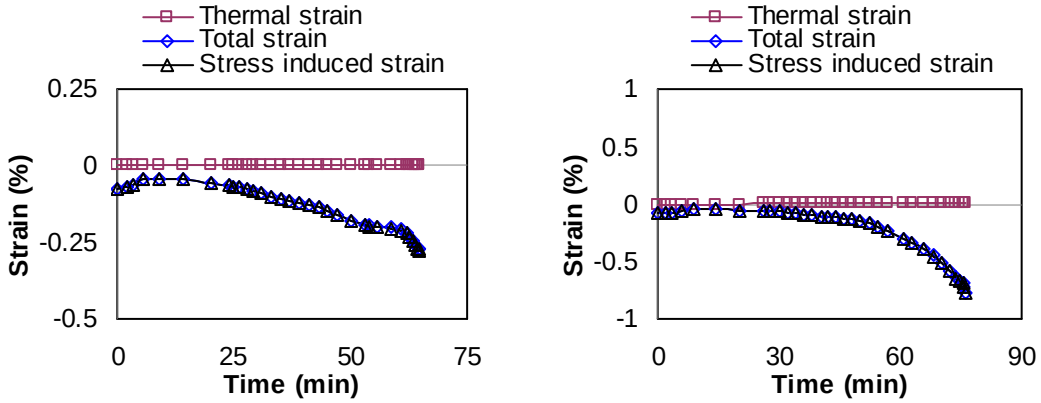

(c) SHS CFDST (d) stub SHS CFDST

Figure 7.12 Strain at inner steel tube (Convex side)

7.4.3.2 Strain in concrete

Longitudinal strains at typical points at the concave and convex sides of the concrete are shown in Figure 7.13. The thermal strains are very small compared to the stress-induced strains, while the stress-induced strains at the concave side are greater than those at the convex side. For CFDST slender columns, the total strains at the convex side become tensile as the columns approach fire endurance.

Variation in the stress-induced strains in the concrete is caused by both degradation in the mechanical properties of the concrete at elevated temperature and load transfer among the components in the columns.

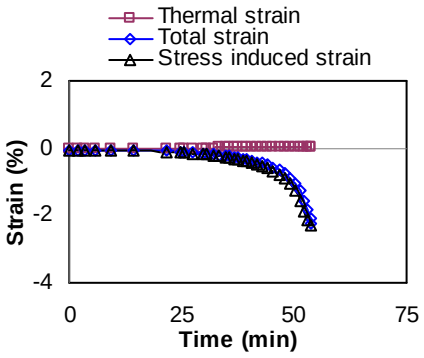

(a) CHS CFDST

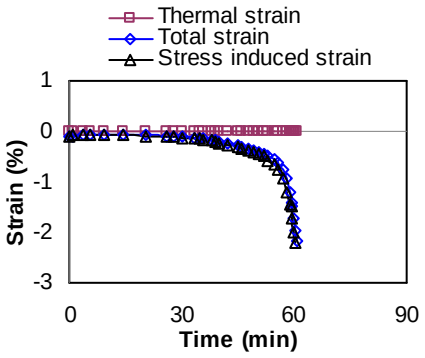

(b) stub CHS CFDST

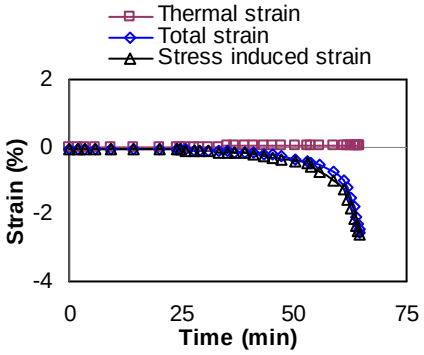

(c) SHS CFDST

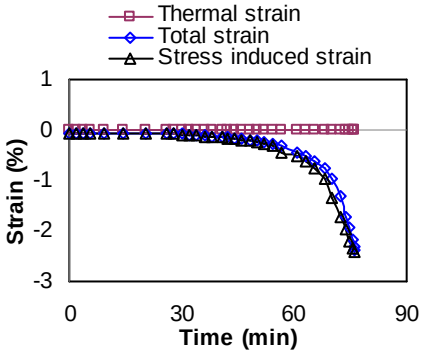

(d) stub SHS CFDST

Figure 7.13 Strain at concrete (Concave side)

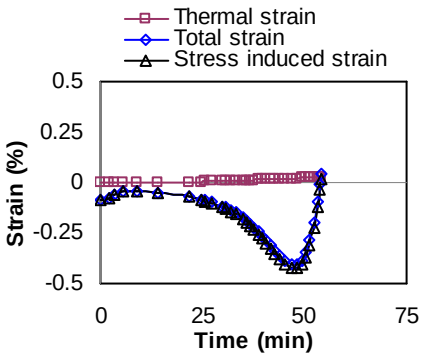

(a) CHS CFDST

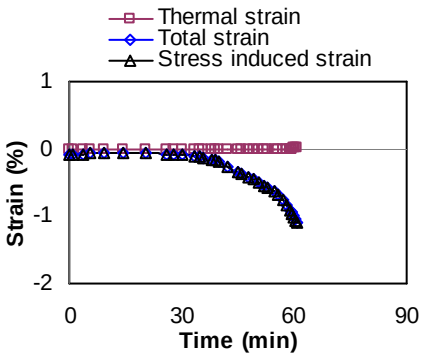

(b) stub CHS CFDST

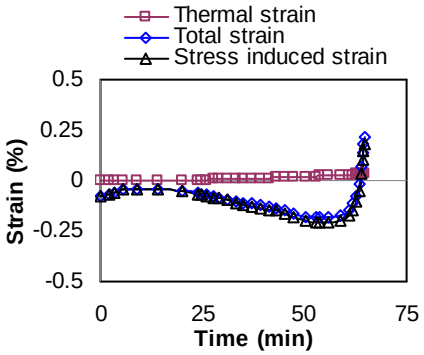

(c) SHS CFDST

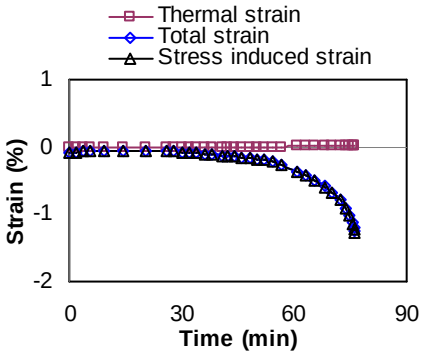

(d) stub SHS CFDST

Figure 7.14 Strain at concrete (Convex side)

7.4.4 Stress and strength

7.4.4.1 Stress and strength of steel tubes

The Mises stresses at the utmost fibres of the concave and convex sides of the outer and inner steel tubes are shown in Figures 7.15 and 7.16. The yield strength of the steel at the corresponding positions is also illustrated. In order to more realistically compare the Mises stresses to the yield strength of the steel, the yield strength of the steel is defined as 0.2% proof stress in the stress-strain relationship.

As can be seen, the Mises stresses in the outer steel tubes increase at the early stage of fire exposure and then decrease gradually until the failure of the columns. There is a drop or fluctuation in the Mises stresses at the convex side of the outer steel tubes of the slender columns when the columns approach fire endurance. This phenomenon is caused by the dramatic increase in the lateral deflection of the columns when they are close to fire endurance. The longitudinal stresses at the convex side of the outer steel tubes in the slender columns change from compression to tension as shown in Figure 7.17.

The Mises stresses in the inner steel tubes decrease in the early stage of fire exposure and then increase moderately until the failure of the columns. Compared to the decline of the Mises stresses in the outer steel tubes, Mises stresses in the inner steel tubes increase more rapidly.

It can be clearly seen in Figure 7.15 that Mises stresses in the outer steel tubes reach the steel yield stress long before the columns reach fire endurance. In other words, yield of the outer steel tubes occurs long before the failure of the columns. However, yield of the inner steel tubes occurs only when the columns are very close to failure.

As shown in Figure 7.17, there is a decrease in the compressive axial stresses in the outer steel tubes at the early stage of fire exposure, and then the stresses increase gradually until the failure of the columns. The compressive axial stresses in the inner steel tubes develop in a way exactly opposite to the outer steel tubes. This implies that part of the load gradually transfers from the outer steel tubes to the inner steel tubes. This load transfer mechanism will be further discussed in a later section.

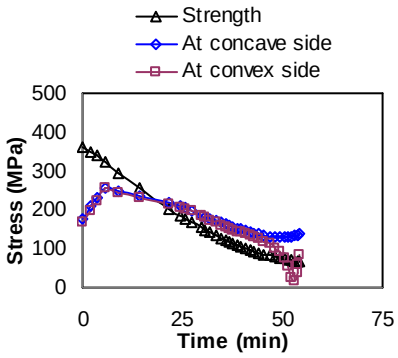

(a) CHS CFDST

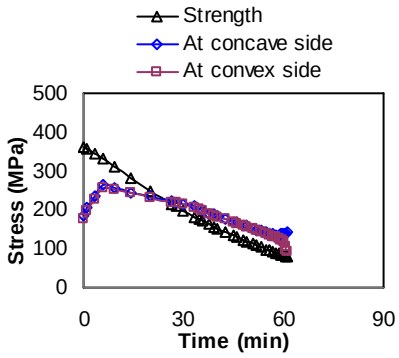

(b) stub CHS CFDST

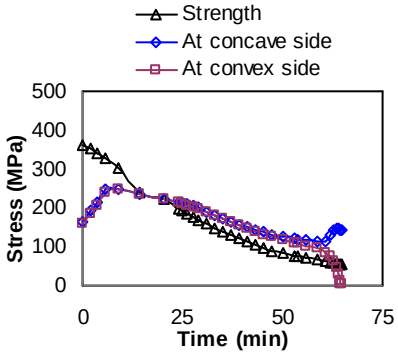

(c) SHS CFDST

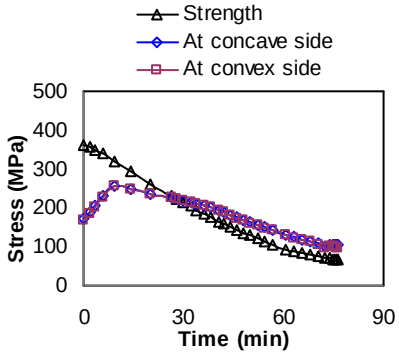

(d) stub SHS CFDST

Figure 7.15 Mises stress and strength of the outer steel tube

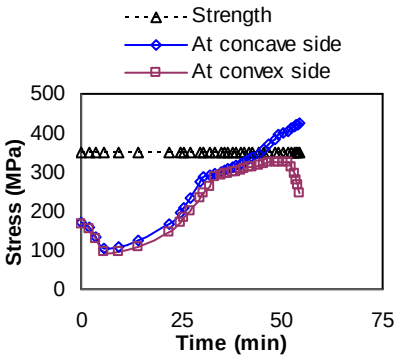

(a) CHS CFDST

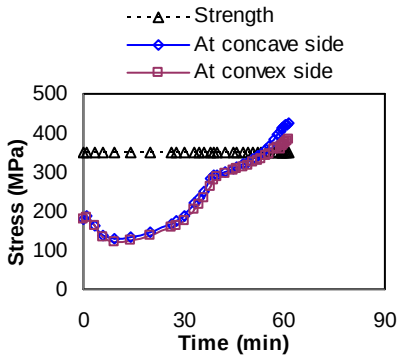

(b) stub CHS CFDST

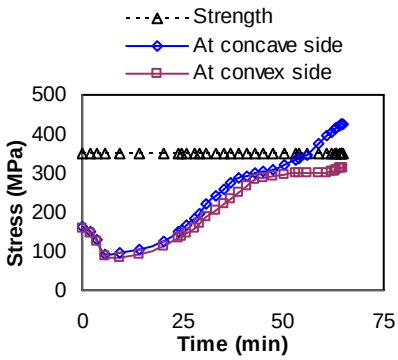

(c) SHS CFDST

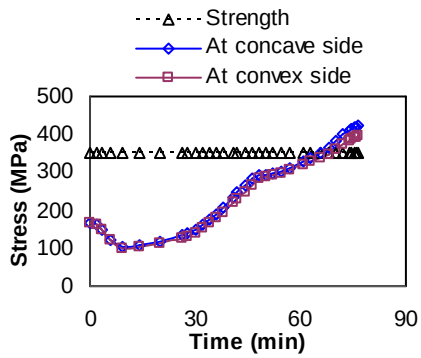

(d) stub SHS CFDST

Figure 7.16 Mises stress and strength of the inner steel tube

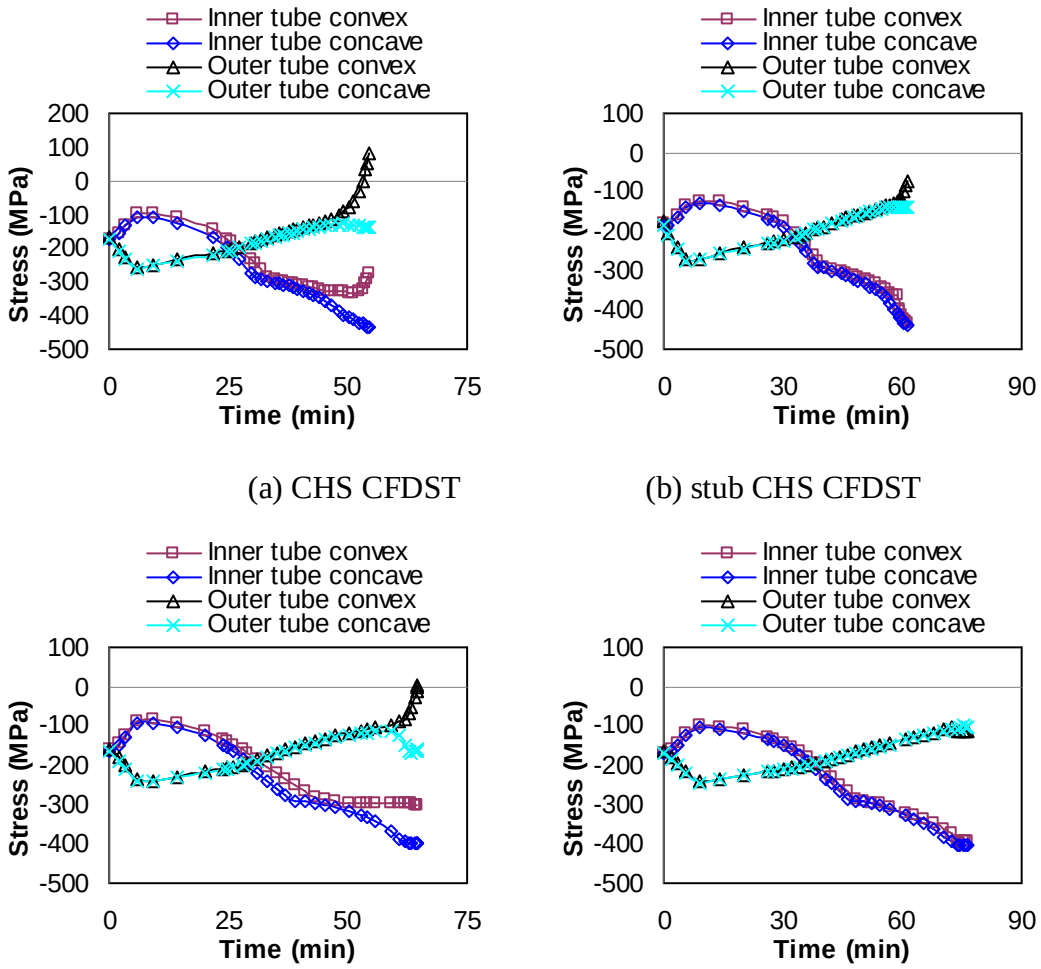

(a) CHS CFDST (b) stub CHS CFDST

(c) SHS CFDST (d) stub SHS CFDST

Figure 7.17 Axial stress in the steel tubes

7.4.4.2 Stress and strength of concrete

Concrete longitudinal stresses at typical points at the concave and convex sides are shown in Figure 7.18. Concrete strength at the corresponding positions is also illustrated. The stress at the convex side becomes tensile for the CFDST slender columns as the columns approach fire endurance. This is caused by the buckling of the slender columns. Generally, the compressive concrete stresses experience a slight decrease at the early stage of fire exposure and then remain relatively stable until the columns are close to failure at which time the stresses increase dramatically for the slender columns or moderately for the stub columns.

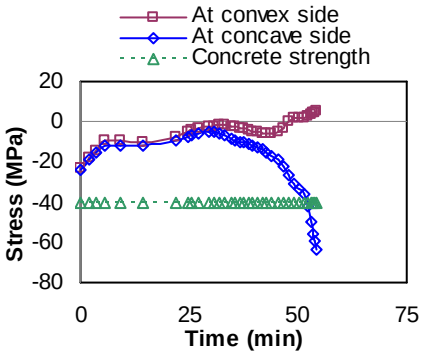

(a) CHS CFDST

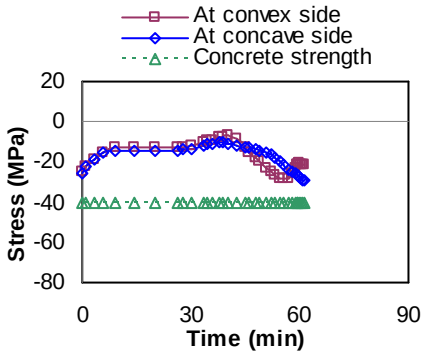

(b) stub CHS CFDST

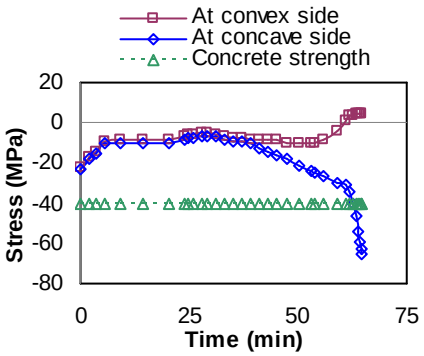

(c) SHS CFDST

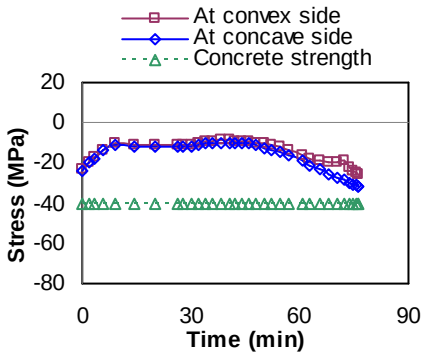

(d) stub SHS CFDST

Figure 7.18 Axial stress and strength of the concrete

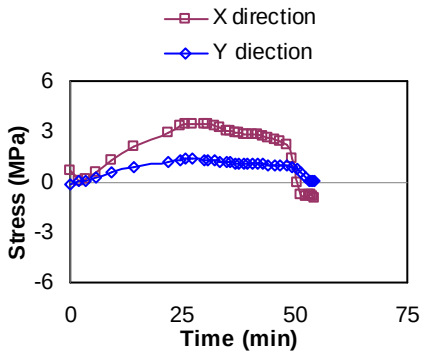

(a) CHS CFDST

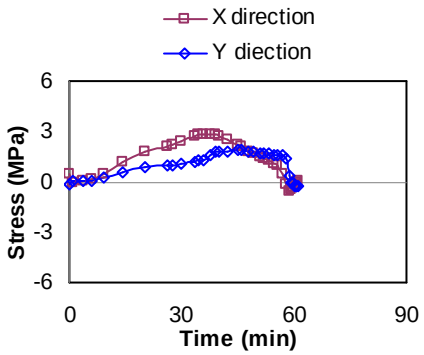

(b) stub CHS CFDST

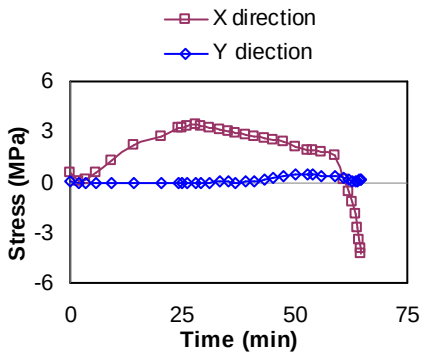

(c) SHS CFDST

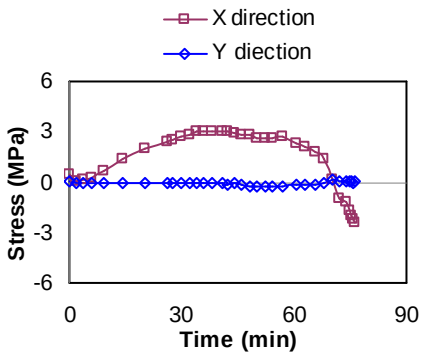

(d) stub SHS CFDST

Figure 7.19 Confinement stress in concrete

The compressive stresses in the concrete of the CFDST stub columns are close to the concrete strength when the columns reach fire endurance, whereas the compressive stresses of the concrete at the concave side in the slender columns are over the concrete strength when the columns are close to failure as shown in Figure 7.19. Normally, concrete can achieve a compressive stress higher than the concrete strength only when the concrete is in a state of multiple-axes compression stress. In order to investigate the effect of the multiple-axes stress on the concrete axial compressive stresses, stresses along two directions perpendicular to the axial direction are shown in Figure 7.19. The orientation of the stresses is illustrated in Figure 7.2, in which x direction corresponds to the radial direction of CHS or the direction perpendicular to the surface of SHS. As can be seen, for most of the fire exposure time the stresses in the concrete along x and y directions are tensile. However, these stresses turn into compression as the columns approach fire endurance which coincides with the concrete axial stresses starting to exceed the concrete strength in the CFDST slender columns. The magnitude of the compressive stresses along x and y directions is minimal for most of the columns. Confinement stresses at such magnitude along the x and y directions cannot offer much assistance for the concrete to achieve an axial stress significantly higher than the concrete strength. However, this contradicts the development of the axial stresses in the CFDST slender columns shown in Figure 7.18 (a) and (c). This phenomenon is most likely caused by the concrete material model in the finite element model.

The material model used in the analysis is the concrete damage plasticity model in ABAQUS (2008). Two damage variables are required in the concrete damage plasticity model, one in compression and the other in tensile, to account for the degradation in the elastic modulus of concrete. These two variables are determined by a series of parameters, such as plastic strain and temperature. In the current simulation, the default values for these two variables have been chosen because data to define these variables at elevated temperatures are unavailable. The default values are independent of other parameters. Therefore, the effect of the plastic straining on the regression of concrete strength has been underestimated. This finally results in the concrete axial stresses being higher than concrete strength even when the confinement on the concrete is weak. The plastic deformation of concrete becomes significant only when the columns are close to fire endurance as shown in Figure 7.13 (a) and (c). In addition, concrete axial stresses reach the strength of the concrete when the CFDST columns are very close to fire endurance. Hence, the use of the default values for the concrete damage variables will

not significantly affect the analytical behaviour of the CFDST columns under fire exposure. As soon as the axial stresses of the concrete reach concrete strength, the concrete can be deemed as failing.

7.4.5 Load sheared by components

Figure 7.20 shows the relationship between percentage of load shared by the components in the CFDST columns and the time of exposure to fire. As expected, there is an obvious load transfer among the components in the CFDST columns. At the early stage of fire exposure, the load shared by the outer steel tubes increases a great deal while the load shared by the concrete and inner steel tubes decreases accordingly. Then the load on the outer steel tubes decreases steadily, accompanied by an increase in the load shared by the concrete and inner steel tubes.

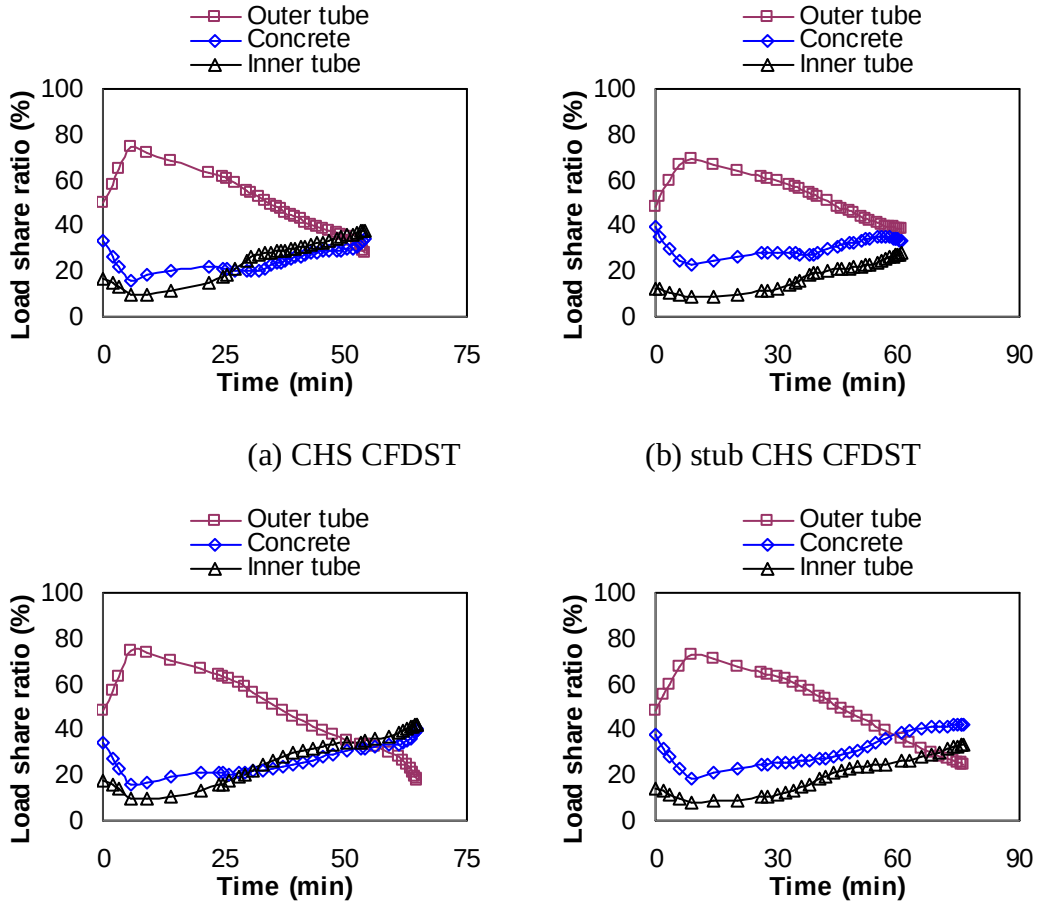

(a) CHS CFDST (b) stub CHS CFDST

(c) SHS CFDST (d) stub SHS CFDST

Figure 7.20 Load shared by components versus fire exposure time

When load is applied on the columns, every component in the CFDST columns is forced to deform consistently in the axial direction. Because the load under fire

condition is much lower than the ultimate capacity of the columns, for example a load level of 0.5 in this analysis, the load shared by each component is approximately determined by the compressive stiffness of the components before fire exposure. As soon as the fire starts, non-uniform temperature distribution arises in the columns. This in turn causes degradation of the material properties and thermal expansion of the components. The outer steel tubes which experience the highest temperature in all the components should deformed most severely due to the rapid loss of strength and stiffness. However, all the components are forced to deform consistently. Some of the load taken by the outer steel tubes has to be removed for the deformation in the outer steel tubes to be maintained at a level consistent with other components. As the concrete and inner steel tubes have less loss of stiffness and strength they take the load removed from the outer steel tubes. Hence, load transfers from the hotter part of the columns, i.e. the outer steel tubes, to the cooler part of the columns, i.e. the concrete and inner steel tubes.

7.5 FAILURE MECHANISM

Failure of structural components under fire exposure is known as a result of deterioration in material mechanical properties and/or thermal stress arising in the components at elevated temperatures. However, for steel-concrete composite columns, i.e. CFST and CFDST columns, failure of the columns in fire exposure does not simply depend on the above-mentioned factors. Another important factor which needs consideration is the composite action in the columns. Even though the composite action brings all components in the columns together to work as a single element to resist the load and the thermal attack of the fire, there is a great difference in the thermal and mechanical responses of each component in the columns. An example to illustrate the differences in the responses of the components is that failure of a component in a CFDST column may not cause failure of the whole column in fire exposure, as other components have not reached their capacities. Therefore, failure of CFDST columns in fire exposure is complex due to a number of actions incorporated in this process. The failure mechanisms of CFDST columns under fire exposure, i.e. factors which control the failure process of CFDST columns and factors which finally trigger the failure of the columns, can be investigated based on the detailed analysis in Sections 7.3 and 7.4 above.

During fire exposure, elevated temperatures in CFDST columns cause variation in the strain, stress, strength, deformation and load share in the components of the columns. The fire endurance of CFDST columns is determined by the relationship of axial deformation versus time to fire. Deformation of the columns is induced by deterioration in the mechanical properties, variation in the stresses and load share in the components. Deterioration in the mechanical properties of the outer steel tubes is far more severe than other components due to the direct fire exposure. The load capacity of the outer steel tubes weakens gradually with the increase in the time of exposure to fire. Part of the load in the outer steel tubes has to transfer to the concrete and the inner tubes. Both Mises stress and yield strength of the outer steel tubes decrease with the increase in the time of exposure to fire. However, the yield strength deteriorates more severely than the Mises stress in the outer steel tubes. Yield of the outer steel tubes occurs as soon as the Mises stress in the outer tubes reaches the yield strength as shown in Figure 7.15. As can be seen, yield of the outer steel tubes occurs long before the failure of the CFDST columns. As this moment, the concrete and inner steel tubes still have the ability to take the load transfer from the outer steel tubes. Stress and load share continue to decrease in the outer steel tubes and increase in the concrete and inner steel tubes. With the increase in the load share in the concrete and inner steel tubes, yield of the inner steel tubes occurs and then leaves the concrete alone to sustain the load transfer from both steel tubes. This soon causes crushing of the concrete. The CFDST columns lose capacity or reach fire endurance when every component in the columns has reached its capacity. Hence, the fire performance of CFDST columns is more affected by the ability of the inner steel tubes together with the concrete to sustain the load transfer from the outer steel tubes.

From the above analysis of the failure process, it is clear that the yield of the inner steel tubes is a key factor which causes the final failure of the columns. The temperatures in the inner steel tubes are lower than those in the concrete and no uniform temperature distribution occurs in the concrete. The concrete as a whole has lost more of its capacity than the inner steel tubes. The inner steel tubes have greater potential to take more load transfer from the outer steel tubes. Therefore, stress in the inner steel tubes will reach yield strength earlier than the concrete reaches its strength, or in other words, the yield of the inner steel tubes occurs earlier than the crush of the concrete.

As discussed in Section 7.3, the failure modes for slender and stub CFDST columns are overall buckling and compression failure respectively. The stress and strain distributions in the slender and stub CFDST columns are different. Yield of the inner steel tubes and crush of the concrete occur in different positions in the slender and stub CFDST columns. As can be seen in Figures 7.16 and 7.18, yield of the inner steel tubes and crush of the concrete occur at the concave side of the slender columns, whereas yield of the inner steel tubes and crush of the concrete occur at the whole section of the inner steel tube and concrete in the stub columns.

7.6 CONCLUSIONS

- Concrete in CFDST columns is an effective thermal insulation for the inner steel tubes and also a heat sink to absorb heat from the outer steel tubes.
- The failure modes for slender and stub CFDST columns are buckling and compression failure respectively. Local buckling of the outer steel tubes occurs in the SHS CFDST columns.
- Both axial and lateral deformation of CFDST columns increase dramatically as the columns approach fire endurance. Lateral deformation is far more severe than axial deformation in the slender columns.
- The outer steel tubes experience more severe straining than the concrete in the inner steel tube. Tensile strains occur at the convex side of the slender columns.
- Stress and strength decrease in the outer steel tubes with the increase in the time of exposure to fire. There is variation in the stress but little change of the strength in the inner steel tubes.
- Yield of the outer steel tubes occurs long before the columns reach fire endurance. Yield of the inner steel tubes occurs when the columns approach fire endurance.
- Stress in the concrete reaches or is near to the strength of the concrete as the columns reach fire endurance.
- There is a load transfer mechanism among the components in CFDST columns. Generally, load transfers from the outer steel tubes to the concrete and inner steel tubes.
- The fire performance of CFDST columns is more affected by the ability of the inner steel tubes together with the concrete to sustain load transfer from the outer steel tubes.
- The yield of the inner steel tubes is a key factor which causes the final failure of the columns.

- The yield of inner steel tubes and crush of the concrete occur at the concave side of the slender columns and the whole section of the stub columns.

Chapter 8

PARAMETRIC STUDIES OF FIRE PERFORMANCE OF CONCRETE-FILLED DOUBLE SKIN STEEL TUBULAR COLUMNS

8.1 INTRODUCTION

The fire performance of CFDST columns has been investigated through fire tests and numerical modelling in the preceding chapters. It can be seen that the fire performance of CFDST columns is complicated due to thermal, structural and composite actions in the columns. Fire performance of the columns is also influenced by a number of parameters, such as size, profile and material properties. Fire tests are the most intuitive methodology to study the fire behaviour of CFDST columns. However, fire tests are very time- and cost- consuming and it is impossible to carry out fire tests to study the effect of a large number of parameters on the fire behaviour of columns. In Chapter 7, several typical CFDST columns were selected for the analysis of fire performance by numerical modelling. This chapter continues to use numerical modelling to further investigate the influence of a number of parameters on the fire performance of the columns.

As discussed in the previous chapters, the fire performance of CFDST columns includes thermal and structural responses. Some of the parameters may affect the thermal response of the columns and in turn influence the structural response, whereas some parameters may affect only the structural response of the columns. Hence, this study is performed in two stages covering the effect of parameters on thermal and structural responses respectively. The parametric studies in this chapter aim to identify parameters which significantly influence the fire behaviour of CFDST columns.

8.2 PARAMETERS FOR ANALYSIS AND THE FE MODEL

The effect of parameters on the thermal and structural responses will be investigated separately in this chapter. Structural response is the consequence of thermal response. However, as structural response does not affect the thermal response, those parameters affecting the thermal response will in turn affect the structural response, but no reverse effect exists. Before the parametric analysis is begun, it is imperative to determine the parameters which potentially affect the thermal and structural responses of CFDST columns.

Temperature elevation in CFDST columns under fire exposure is through heat conduction. Heat transfers to the exterior surface of the columns by radiation and convention and then conducts into the interior part of the columns. Based on this fact, a number of factors which may affect heat conduction and thus temperature distribution in CFDST columns can be identified.

The first group of parameters are related to the geometric size of the columns. For columns under fire exposure, it is generally assumed that fire temperature is uniform along the length of the columns. Therefore, geometric size refers to the cross-sectional size of the columns in the thermal response analysis. The cross-sectional size of the column is determined by the size and thickness of the inner and outer tubes. Alternatively, the perimeter of the outer steel stub, thickness of the concrete and thickness of the tubes may be the parameters to appropriately reflect the cross-sectional size of the columns.

The second type of parameter is the profile of the columns. CFDST columns may consist of different types of steel tubes as inner and outer steel tubes, such as CHS, SHS and RHS. In this study, only two combinations will be investigated, CFDST with CHS and SHS as both inner and outer steel tubes.

The third type of parameter is fire protection. Fire protection is an effective method for the enhancement of the fire resistance of structural components. It is a popular option in the fire safety design of steel and steel-concrete composite structures.

All the parameters which affect the thermal response of the columns will in turn affect the structural response of the columns. Therefore, those parameters selected in the thermal response analysis will be included in the parameters in the structural response analysis.

In addition, a number of parameters will affect only the structural response of the columns. All these parameters can be included in the categories of geometry, material property, load and a combination of geometry and material property. As parameters related to cross- sectional size have been considered in the thermal response analysis, length of the columns is the only geometric parameter which potentially affects the structural response of the columns. Material mechanical properties such as type of

concrete (normal and steel fibre reinforced concrete), strength of the concrete and yield strength of the steel in the inner and outer steel tubes are parameters in the material property category. Load level and load eccentricity are two parameters related to the loading conditions of the columns which may affect the structural response of the columns. The capacities of the inner and outer tubes are parameters which relate to both geometry and material property.

Another parameter potentially affecting the structural response of the columns is the failure mode of the columns. As can be seen in the preceding chapters, the failure mode is buckling for slender columns and compression failure for stub columns. Therefore, the effect of the parameters on stub and slender columns will be investigated separately.

The parameters used in this analysis are summarized in Table 8.1 where a tick against a parameter means the parameter is selected in the analysis. The finite element model used for parametric analysis is the same as that introduced in Chapter 7, i.e. ¼ of the actual columns being used in the modelling and symmetric boundary conditions applied on the symmetric planes. The boundary conditions at the column ends are both pinned. Hence, the effective length is equal to the actual length of the columns. The material thermal and mechanical models in Chapter 6 are used in the analysis.

Table 8.1 Parameters used in the analysis

Parameters	Type of parameter	Effect on thermal response	Effect on structural response
Thickness of concrete	Geometrical	√	√
Perimeter of outer steel tube	Geometrical	√	√
Thickness of outer steel tube	Geometrical	√	√
Thickness of inner steel tube	Geometrical	√	√
Length or slenderness	Geometrical		√
Strength of concrete	Material property		√
Strength of steel in inner steel tube	Material property		√
Strength of steel in outer steel tube	Material property		√
Type of concrete	Material property		√
Fire insulation	Material property	√	√
Load level	Load		√
Load eccentricity	Load		√
Capacity of inner tube	Geometrical & material property		√
Capacity of outer tube	Geometrical & material property		√

8.3 EFFECT OF PARAMETERS ON THERMAL RESPONSE

The thermal response of CFDST columns depends on the cross-sectional size of the columns but is independent of the length of the columns. Hence, it is not necessary to classify the columns into slender and stub columns in the thermal response analysis. Here, two CFDTS columns are used to examine the effect of the parameters on the thermal response of the columns. The dimensions of the columns are shown Table 8.2. When one of the parameters changes, such as the thickness of the outer steel tubes, the other parameters are kept constant in order to investigate the effect of the variable parameter on the thermal response.

Table 8.2 Dimension of CFDST columns for thermal response analysis

No	Outer tube ($D_o \times t_o$) (mm)	Inner tube ($D_i \times t_i$) (mm)
1	CHS1200×40	CHS500×25
2	SHS1200×40	SHS500×25

There are several variables available to quantify the thermal response of CFDST columns, such as temperature distribution, heat flux and heat energy absorbed by the columns. But the only thermal response variable directly related to the structural response of the columns is the temperature distribution in the columns. Hence, temperature distribution in CFDST columns is selected as a variable to quantify the thermal response of the columns. In order to investigate the influence of the parameters on the temperatures in CFDST columns, temperatures at several typical points in each component are output for comparison. The typical points in the components are shown in Figure 8.1. Out-x and Out-I are points at the exterior and interior surfaces of the outer steel tubes, In-X and In-I are points at the exterior and interior surfaces of the inner steel tubes, and C1 and C2 are points at one third of the total concrete thickness.

The typical points at the exterior and interior surfaces of the steel tubes reflect the maximum and minimum temperatures in the tubes. However, two typical points in the concrete are used to give an average temperature distribution in the concrete.

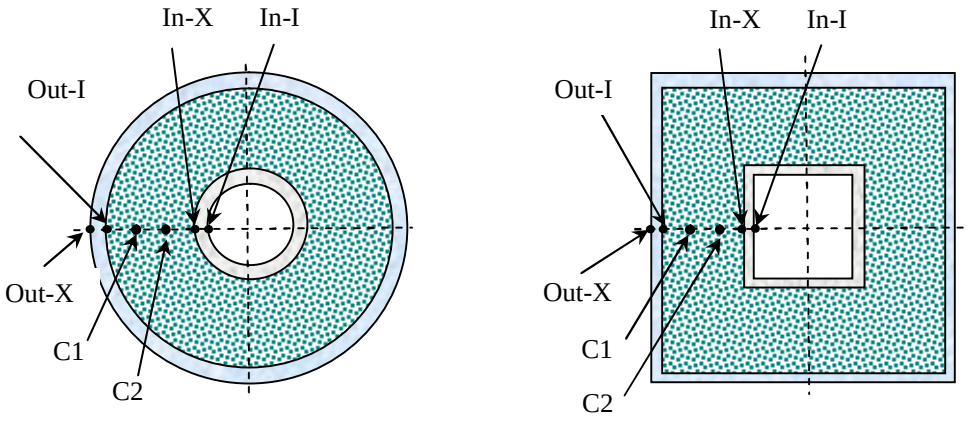

Figure 8.1 Typical points in the components for temperature output

8.3.1 Effect of outer steel tube thickness

The effect of the outer tube thickness on the temperatures in the outer tubes, concrete and inner tubes is shown in Figure 8.2 to 8.4 respectively. As can be seen, variation in the outer tube thickness mainly affects the temperature distribution in the outer steel tubes. Temperatures in the outer steel tubes increase when the diameter (width)-to-thickness ratio of the outer steel tube increases. Such influence is more noticeable when the fire exposure time is less than 60 minutes and becomes weak as time of exposure to fire is over 120 minutes. Variation in the outer tube thickness also has moderate effect on the temperatures in the concrete. However, this parameter has little influence on the temperatures in the inner steel tubes.

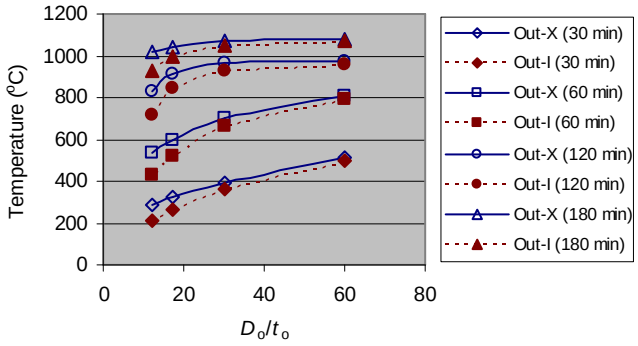

(a) CHS CFDST

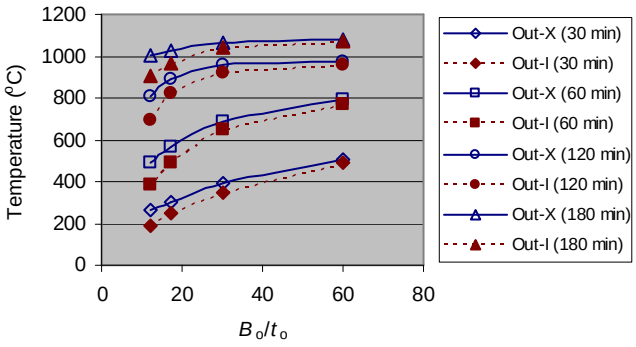

(b) SHS CFDST

Figure 8.2 Influence of the outer tube thickness on the temperatures in the outer tubes

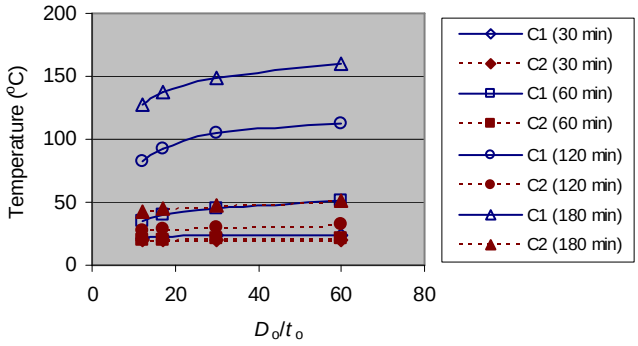

(a) CHS CFDST

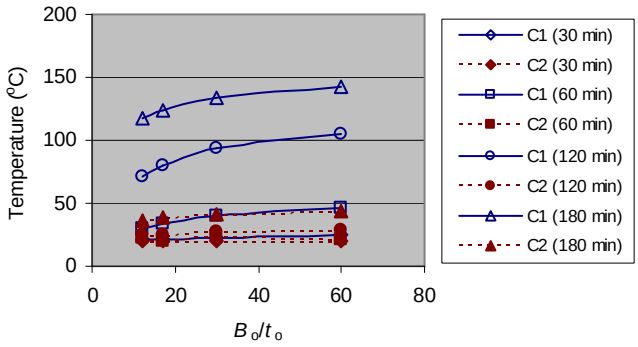

(b) SHS CFDST

Figure 8.3 Influence of the outer tube thickness on the temperatures in the concrete

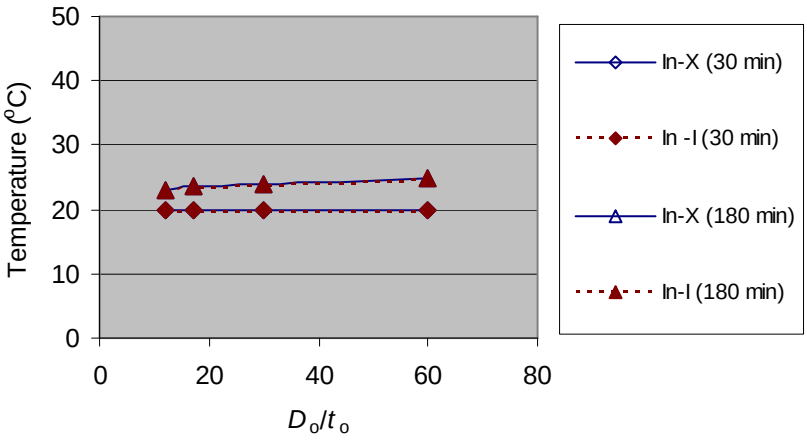

(a) CHS CFDST

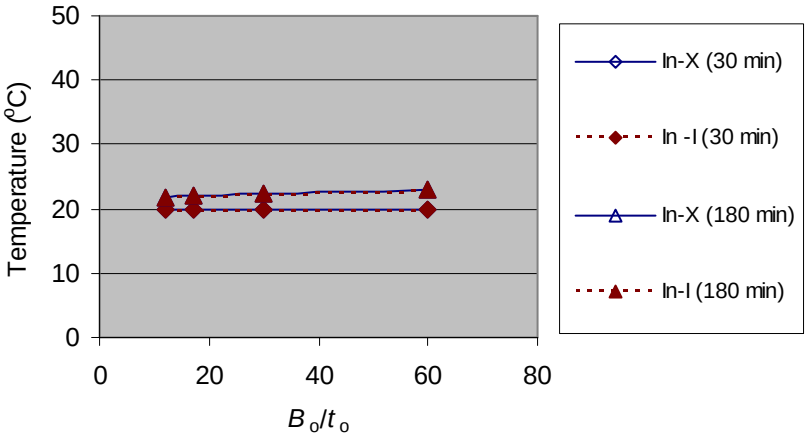

(b) SHS CFDST

Figure 8.4 Influence of the outer tube thickness on the temperatures in the inner tubes

8.3.2 Effect of inner steel tube thickness

The effect of the inner tube thickness on the temperatures in the outer and inner tubes is shown in Figure 8.5 and 8.6 respectively. This parameter has little influence on the temperatures in the outer tubes and has minimal influence on the temperatures in the inner tubes. Temperatures in the concrete are also less influenced by this parameter due to the temperatures in the concrete being between those in the outer and inner tubes. Therefore, the influence of the inner tube thickness on the temperatures in the CFDST columns is negligible.

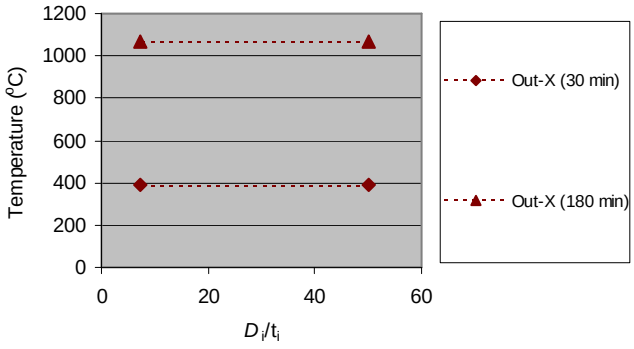

(a) CHS CFDST

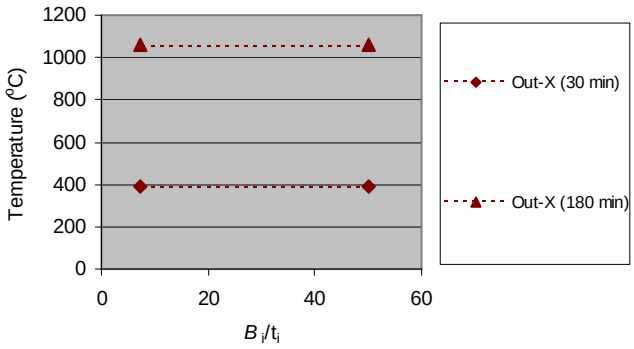

(b) SHS CFDST

Figure 8.5 Influence of inner tube thickness on the temperatures in the outer tubes

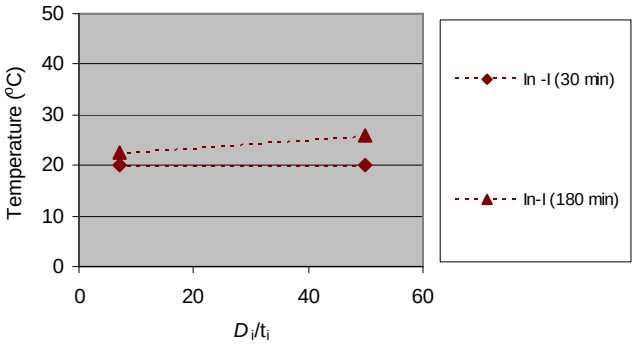

(a) CHS CFDST

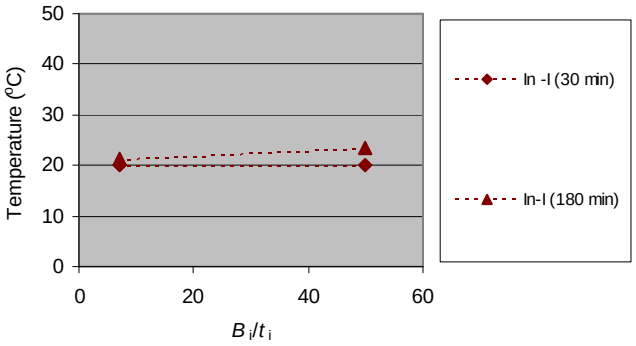

(b) SHS CFDST

Figure 8.6 Influence of inner tube thickness on the temperatures in the inner tubes

8.3.3 Effect of concrete thickness

The influence of cavity ratio on the temperatures in the outer tubes, concrete and inner tubes is shown in Figures 8.7 to 8.9 respectively. Here, cavity ratio is a parameter to represent the concrete thickness in the columns. A higher value of cavity ratio means a thinner concrete thickness. As shown in Figure 8.7, this parameter has minimal influence on the temperatures in the outer tubes. However, it has a significant effect on the temperatures in the concrete and inner tubes as shown in Figures 8.8 and 8.9. Increase in the cavity ratio, i.e. decrease in the concrete thickness, results in an increase in temperatures in the concrete and inner tubes.

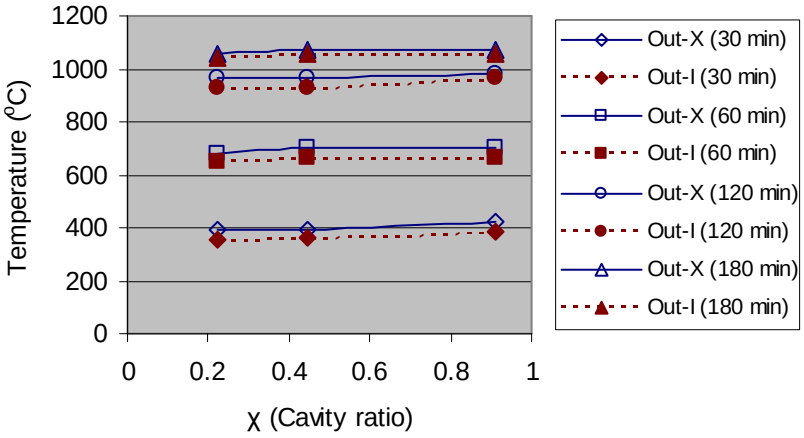

(a) CHS CFDST

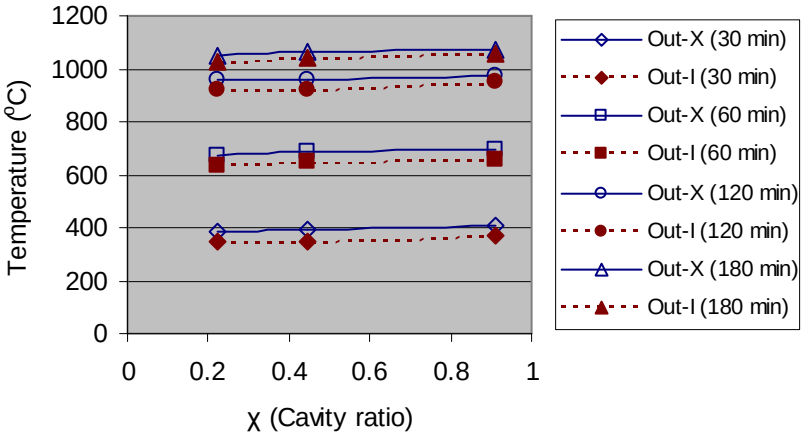

(b) SHS CFDST

Figure 8.7 Influence of concrete thickness on the temperatures in the outer tubes

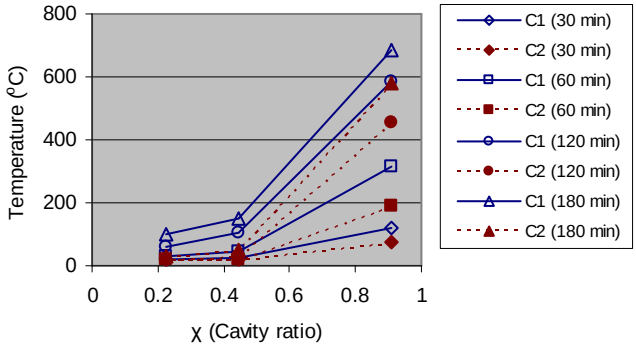

(a) CHS CFDST

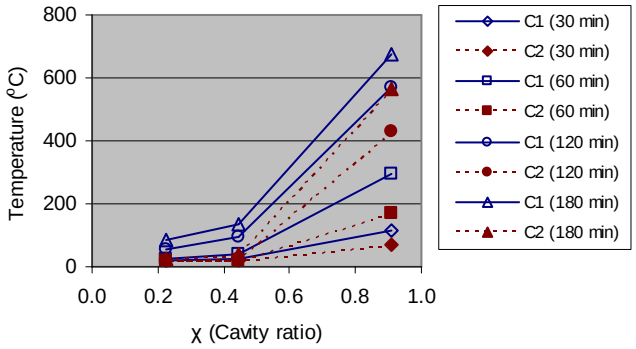

(b) SHS CFDST

Figure 8.8 Influence of concrete thickness on the temperatures in the concrete

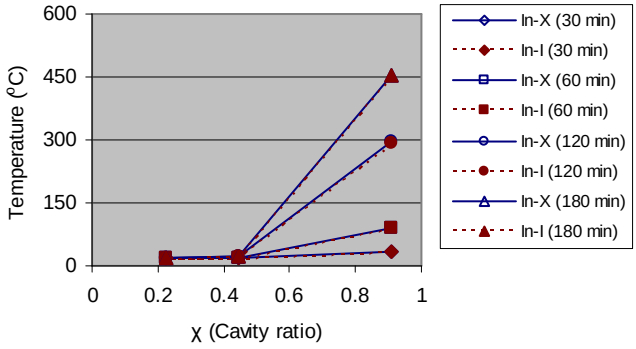

(a) CHS CFDST

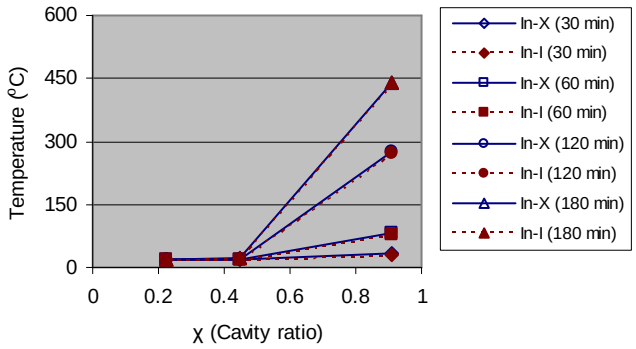

(b) SHS CFDST

Figure 8.9 Influence of concrete thickness on the temperatures in the inner tubes

As discussed in Chapter 7, concrete can serve as heat insulation for the inner tubes in CFDST columns due to its good heat resistance. Therefore, an increase in the thickness of the concrete can result in a decrease in the temperatures of the inner steel tubes and the concrete itself.

8.3.4 Effect of outer tube perimeter

The influence of the outer tube perimeter on the temperatures in the components is shown in Figures 8.10 to 8.12. As can be seen, this parameter has minimal influence on the temperatures in the columns.

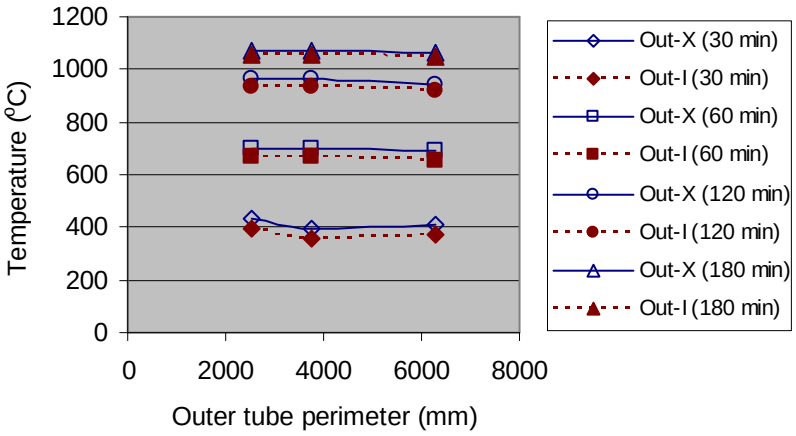

(a) CHS CFDST

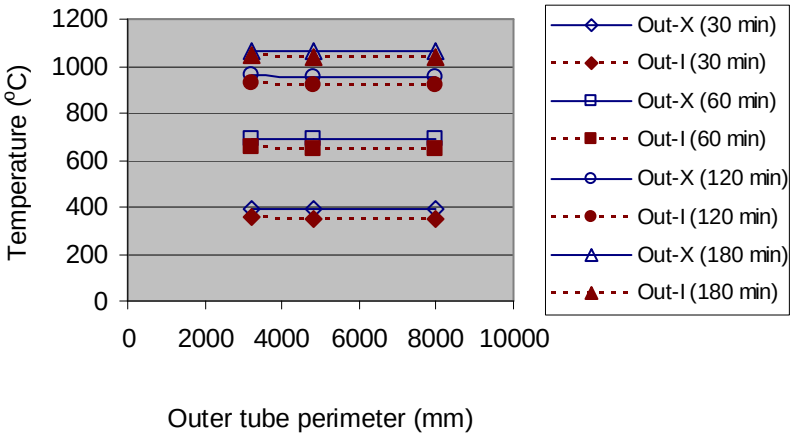

(b) SHS CFDST

Figure 8.10 Influence of perimeter on the temperatures in the outer tubes

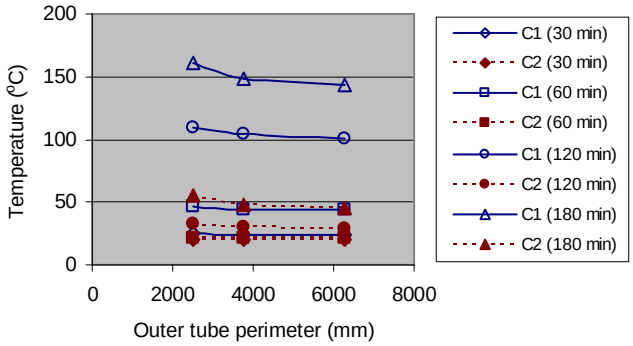

(a) CHS CFDST

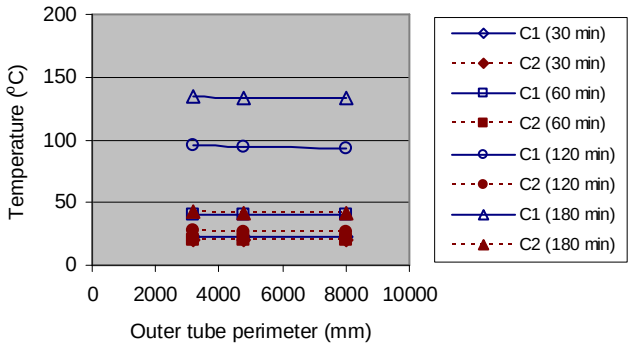

(b) SHS CFDST

Figure 8.11 Influence of perimeter on the temperature in the concrete

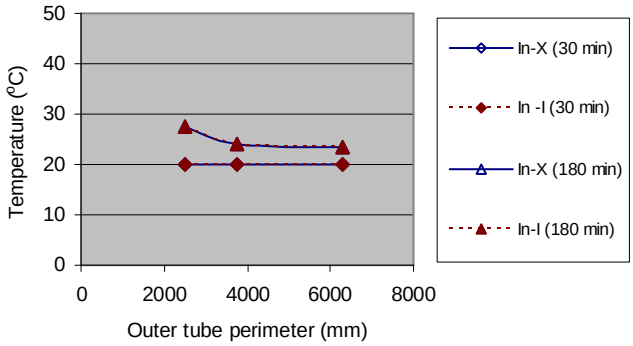

(a) CHS CFDST

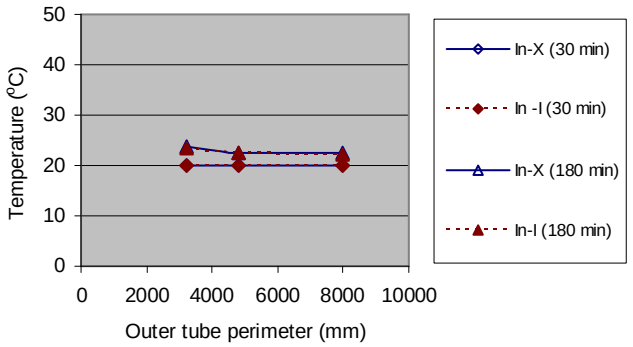

(b) SHS CFDST

Figure 8.12 Influence of perimeter on the temperatures in the inner tubes

In Chapter 3, the perimeter of CFST columns has been identified as a key factor significantly affecting the temperature distribution in the columns. In both CFST and CFDST columns, heat passes through the exterior steel tubes into the interior of the columns. Concrete has much higher heat resistance than steel. Therefore, it is the thickness of the concrete rather than the perimeter of the columns that determines the heat conduction rate in the columns. In CFST columns, the perimeter is proportional to the thickness of the concrete and is actually an index of the concrete thickness in the columns.

8.3.5 Effect of fire protection

The purpose of fire protection systems is to provide thermal insulation for the structural components to delay temperature elevation in them. Here, a fire protection coating used in the fire tests in Chapter 4 is applied to the CFDST columns in Table 8.2 to investigate the effect of fire protection on the temperatures in the columns. The thermal properties of the fire protection coating are the same as those in Chapter 4. The thickness of the coating is 5 mm. The predicted temperatures in each component in the CFDST columns with and without fire protection are shown in Figures 8.13 to 8.15.

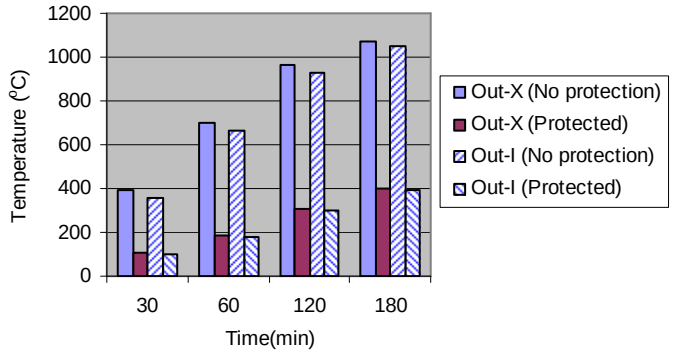

(a) CHS CFDST columns

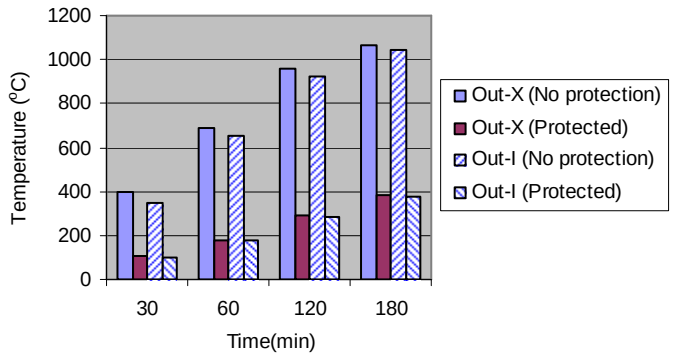

(b) SHS CFDST columns

Figure 8.13 Effect of fire protection on temperatures in outer tubes

As can be seen, fire protection has a significant effect on the temperatures in the outer tubes and concrete. The temperatures drop from about 1100 ^{o}C to 400 ^{o}C in the outer tubes and from about 150 ^{o}C to 80 ^{o}C in the concrete (C1) at 180 minutes of fire exposure when the fire protection coating is used. The outer tubes are shielded from direct fire exposure by the fire protection coating. Therefore, the fire protection coating is more effective in delaying the temperature elevation in the outer tubes than the concrete and inner tubes. Temperatures in the inner tubes are close to ambient temperature up to 180 minutes of fire exposure even when no fire protection is provided. Hence, the fire protection coating has the least influence on the temperatures in the inner tubes.

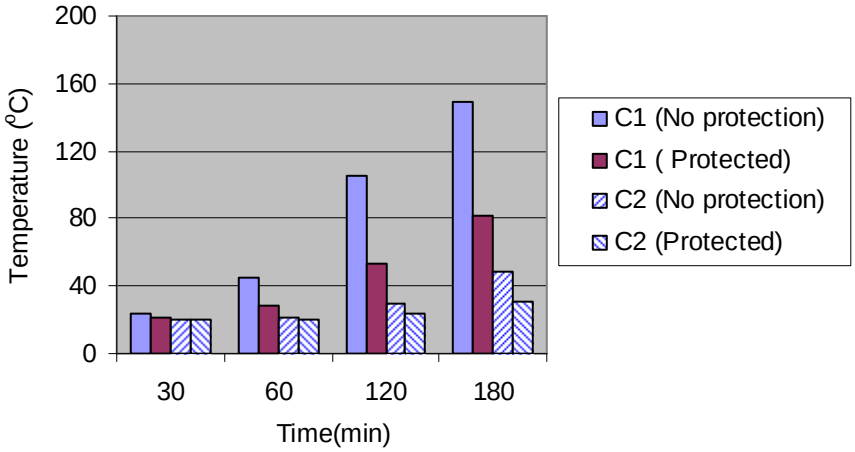

(a) CHS CFDST columns

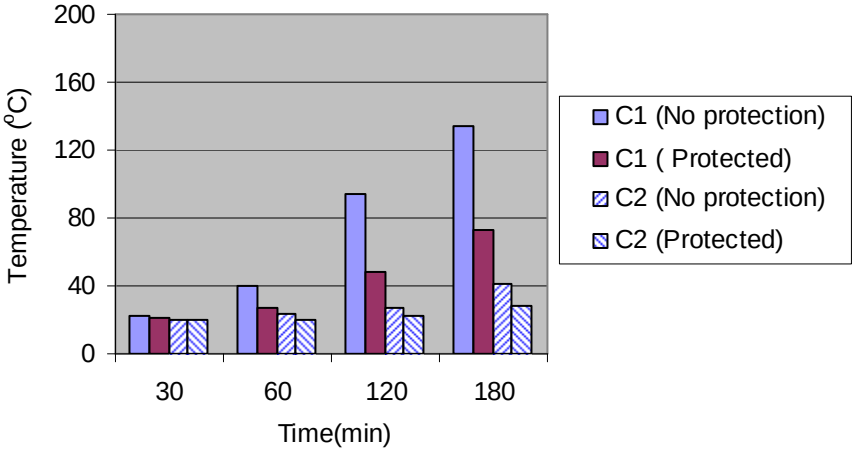

(b) SHS CFDST columns

Figure 8.14 Effect of fire protection on temperatures in concrete

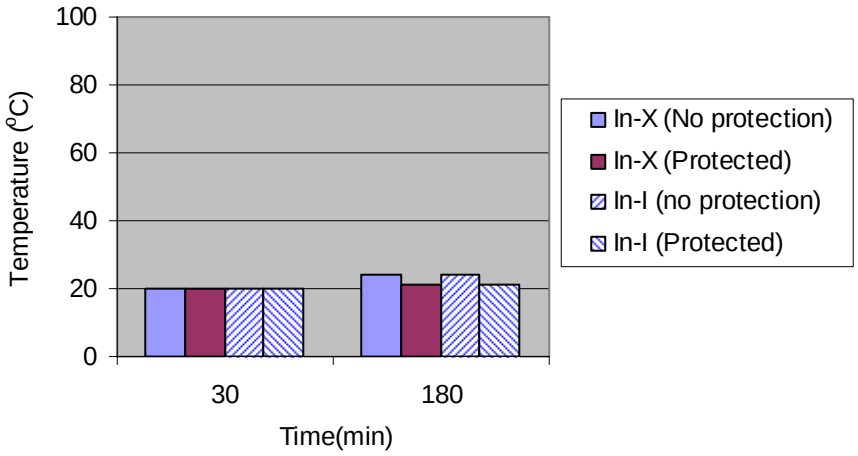

(a) CHS CFDST columns

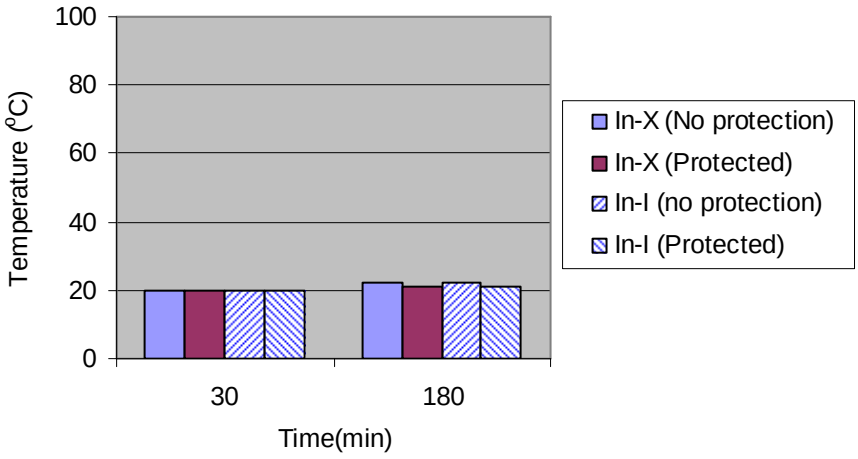

(b) SHS CFDST columns

Figure 8.15 Effect of fire protection on temperatures in inner tubes

8.4 EFFECT OF PERIMETERS ON STRUCTURAL RESPONSE AND FIRE RESISTANCE

A number of parameters affecting the structural response and fire resistance of CFDST columns will be investigated. There are many indicators available to reflect the structural response of CFDST columns in fires, such as axial deformation and stress and strain, but the most relevant to structural fire safety is fire resistance. Hence, fire resistance is chosen here as a comprehensive index to represent the structural response of the columns.

Parameters of the CFDST columns used in the parametric analysis are summarized in Table 8.3.

Table 8.3 Basic parameters for CFDST columns

No	Outer tube ($D_o \times t_o$) (mm)	Inner tube ($D_i \times t_i$) (mm)	Length L (mm)	L/D_o	f_{yo} (MPa)	f_{yi} (MPa)	f_c (MPa)	Load (kN)	Load level	Boundary conditions
1	CHS700×25	CHS300×20	4200	6.0	350	350	40	21945	0.5	Pin-Pin
2	CHS1200×40	CHS500×25	3500	2.9	350	350	40	62990	0.5	Pin-Pin
3	SHS700×25	SHS300×20	4200	6.0	350	350	40	26278	0.5	Pin-Pin
4	SHS1200×40	SHS500×25	3500	2.9	350	350	40	74846	0.5	Pin-Pin

8.4.1 Effect of slenderness

The length to diameter (or width) ratio is used here to represent the slenderness of the columns. Figure 8.16 shows the relationship between fire resistance and length to diameter or width ratio. As shown in the figure, fire resistance of CFDST columns decreases with the increase in the slenderness of the columns. When the length to diameter (or width) ratio is less than five for CHS CFDST (or four for SHS CFDST), the effect of slenderness on the fire resistance is minimal. However, such effect becomes pronounced when the length to diameter (or width) ratio is greater than that value. As can be seen, slenderness has a significant effect on the fire resistance of slender CFDST columns.

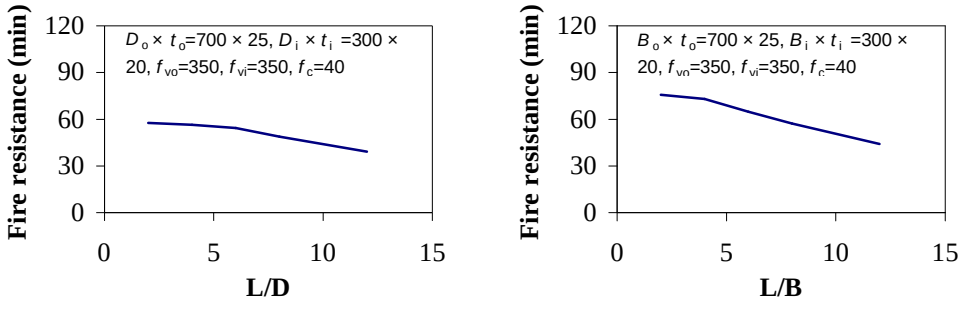

(a) CHS CFDST column (b) RHS CFDST column

Figure 8.16 Effect of slenderness

As discussed in Chapter 7, the failure modes of stub and slender CFDST columns are different. When the length to diameter (or width) ratio is less than a certain value, the

CFDST columns are defined as stub columns which fail with compression failure, whereas when the length to diameter (or width) ratio is greater than this value the CFDST columns are classified as slender columns with a failure mode of overall buckling. Variation in the slenderness or length of the CFDST columns does not affect the thermal response of the columns. In other words, degradation in the strength and stiffness of the concrete and steel in the columns is not affected by variation in the slenderness. Hence, the effect of column slenderness on the fire resistance of the CFDST columns is induced by the difference in the failure modes between the stub and slender columns.

As discussed in Chapter 7, the CFDST stub columns fail under compression due to the yield of the inner steel tubes and crush of the concrete occurring at the cross-section of the columns. As long as the CFDST columns remain as stub columns and fail under compression, the capacity of the columns at elevated temperature is independent of the slenderness of the columns. Therefore, slenderness has little influence on the fire resistance of the stub CFDST columns.

For slender CFDST columns, column capacities are determined by the critical buckling load of the columns. Geometrical non-linearity, i.e. the second order effect, is an important factor influencing the buckling load of slender columns. The second order effect is more pronounced when the slenderness increases. Although the columns are concentrically loaded in this study, an initial straightness imperfection has been considered in the modelling. The initial straightness imperfection is transferred into an initial load eccentricity at both ends of the columns. This value is taken as the straightness tolerance in AS 4100 (2005), the larger value of $L/1000$ or 3 mm, where L is the length of the column in millimetres. Initial eccentricity induced by straightness imperfection is proportional to the length of the columns as the length of the columns is over 3 m. Initial bowing accompanied by the second order effect in the columns results in a decrease in the capacity or fire resistance of the columns at elevated temperature as the slenderness of the columns increases.

8.4.2 Effect of concrete thickness

During analysis of the effect of concrete thickness on the fire resistance of the columns, the diameter or width of the outer CHS or SHS tubes remains unchanged. Variation in concrete thickness is achieved by changing the diameter or width of the inner CHS or

SHS tubes. Cavity ratio is selected as a parameter to represent concrete thickness in the columns. A higher value of cavity ratio represents thinner concrete in a CFDST column. When the cavity ratio becomes zero, the CFDST columns change to a CFST column. Figure 8.17 shows the relationship between the fire resistance and cavity ratio of the CFDST columns. As can be seen in the figure, increase in the cavity ratio or decrease in the concrete thickness generally causes an increase in the fire resistance of the CFDST columns, but such increase is not significant.

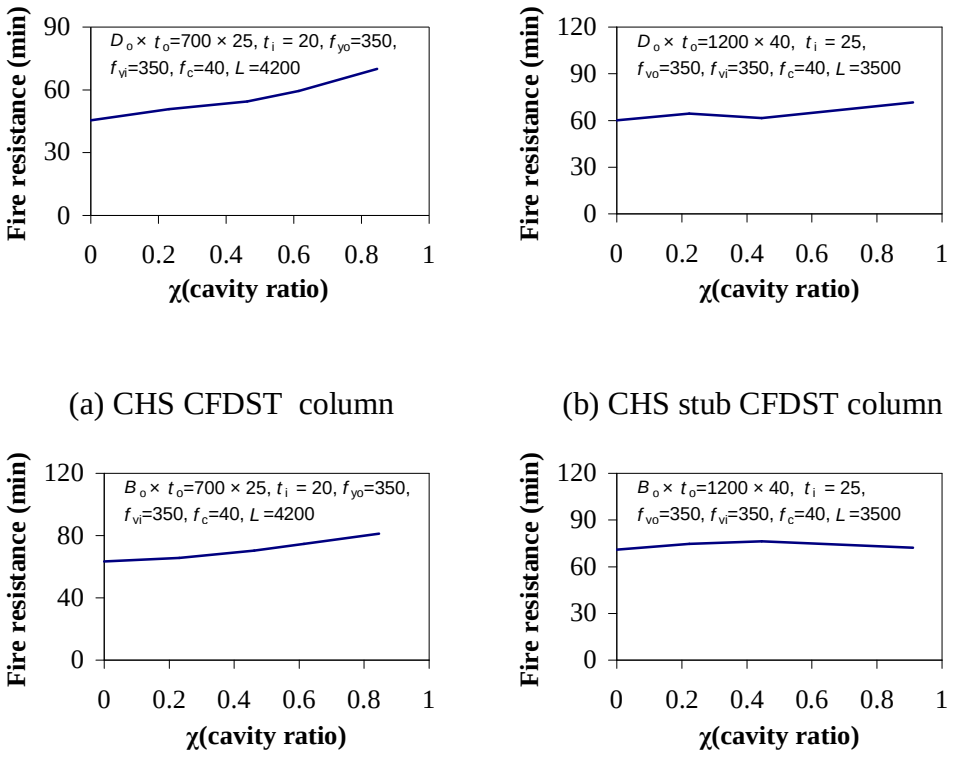

(a) CHS CFDST column (b) CHS stub CFDST column

(c) RHS CFDST column (d) RHS stub CFDST column

Figure 8.17 Effect of concrete thickness

Cavity ratio or concrete thickness has a significant influence on the thermal response or temperature distribution of CFDST columns. From the view point of thermal response, increase in the cavity ratio or decrease in the concrete thickness results in an increase in the temperatures in the CFDST columns and thus has a negative influence on the fire resistance of the columns. However, the trends shown in Figure 8.17 contradict this conclusion. This is due to the variation in the concrete thickness itself also directly affecting the structural response of the columns. Variation in the concrete thickness is achieved by changing the size of the inner tubes, while the size of the outer tubes remains unchanged. Reducing the concrete thickness is equivalent to increasing the size of the inner tubes. This leads to an increase in the capacity of the inner tubes. At the

same time, the concrete can still offer enough insulation to prevent the temperature in the inner tubes increasing too quickly even when the concrete thickness has been reduced. This is beneficial to the structural response of the columns. Hence, variation in the cavity ratio or concrete thickness affects the thermal and structural response of the columns in opposite ways. Finally, the influence of this parameter on the fire resistance of the columns becomes unremarkable as shown in Figure 8.17.

8.4.3 Effect of inner steel tube thickness

Figure 8.18 shows the relationship between fire resistance and inner tube diameter (or width)-to-thickness ratio. In the present study, the diameter or width of the inner steel tubes remains unchanged. Hence, variation in the diameter (or width)-to-thickness ratio is actually induced by the variation in the thickness of the inner steel tubes.

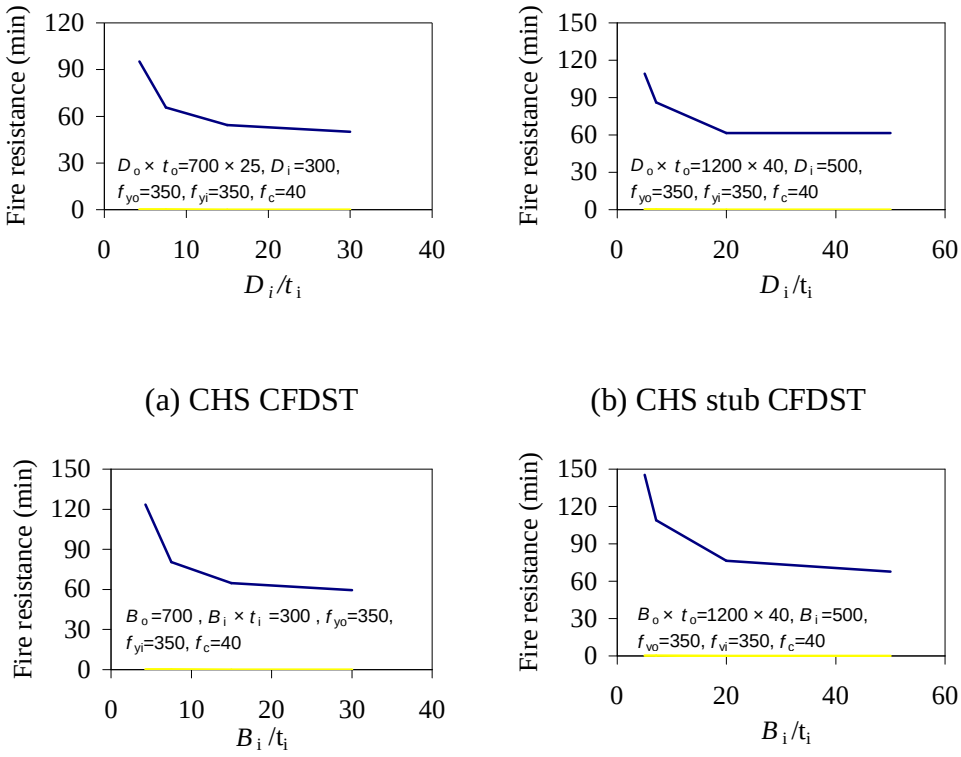

(a) CHS CFDST (b) CHS stub CFDST

(c) RHS CFDST (d) RHS stub CFDST

Figure 8.18 Effect of inner tube thickness on fire resistance

As shown in the figure, the fire resistance of both CFDST slender and stub columns decreases as the diameter (or width)-to-thickness ratio increases or the thickness of the inner steel tubes decreases. The thickness of the inner steel tube has a noticeable influence on the fire resistance of the columns. Such influence is significant when the diameter (or width) ratio is smaller than about 10 for CFDST columns or about 5 for CFDST stub columns. This influence is significant when the diameter (or width) ratio

is less than about 20 for both CFDST columns and stub columns and becomes minimal when the diameter (or width) ratio is greater than about 20.

Inner tube thickness has little influence on the thermal response of the columns, as discussed in the previous section. Hence, variation in inner steel tube thickness affects the fire resistance of the columns through its influence on the structural response of the columns. A decrease in the width-to-thickness ratio or increase in the inner tube thickness results in an increase in the capacity of the inner tubes and thus leads to an increase in the fire resistance. Increasing the thickness of the inner steel tubes is an effective way to enhance the fire resistance of CFDST columns.

8.4.4 Effect of outer steel tube thickness

The effect of outer tube thickness on the fire resistance of the CFDST columns is shown in Figure 8.19. The fire resistance of the columns generally increases with the increase in the diameter (or width)-to-thickness ratio or the decrease in the outer tube thickness. However, the influence of outer tube thickness on the fire resistance of the columns is minimal.

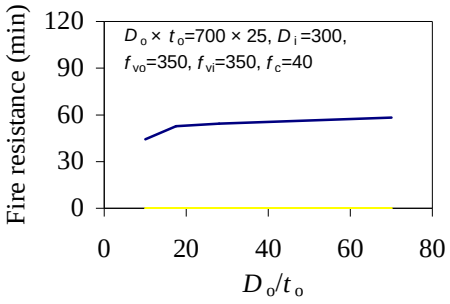

(a) CHS CFDST

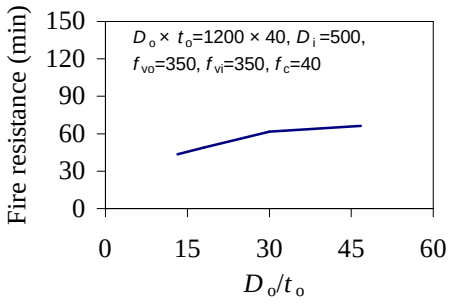

(b) CHS stub CFDST

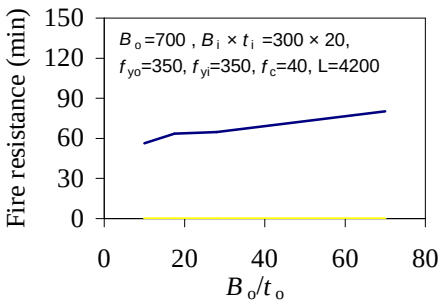

(c) RHS CFDST

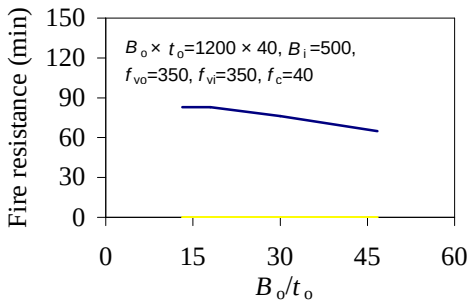

(d) RHS stub CFDST

Figure 8.19 Effect of outer tube thickness on fire resistance

It should be noted that there is a discrepancy in this trend in Figure 8.19 (d). In the square CFDST stub columns, local buckling of the outer tubes occurs at the early stage of fire exposure when the tube thickness becomes too small. This has a negative effect on the fire resistance of the columns.

8.4.5 Effect of outer steel tube perimeter

The effect of outer tube perimeter on the fire resistance of the CFDST columns is shown in Figure 8.20. As can be seen, variation in the outer tube perimeter has a moderate influence on the fire resistance of the CFDST columns. Increase in the outer tube perimeter leads to a moderate increase in the fire resistance of the columns.

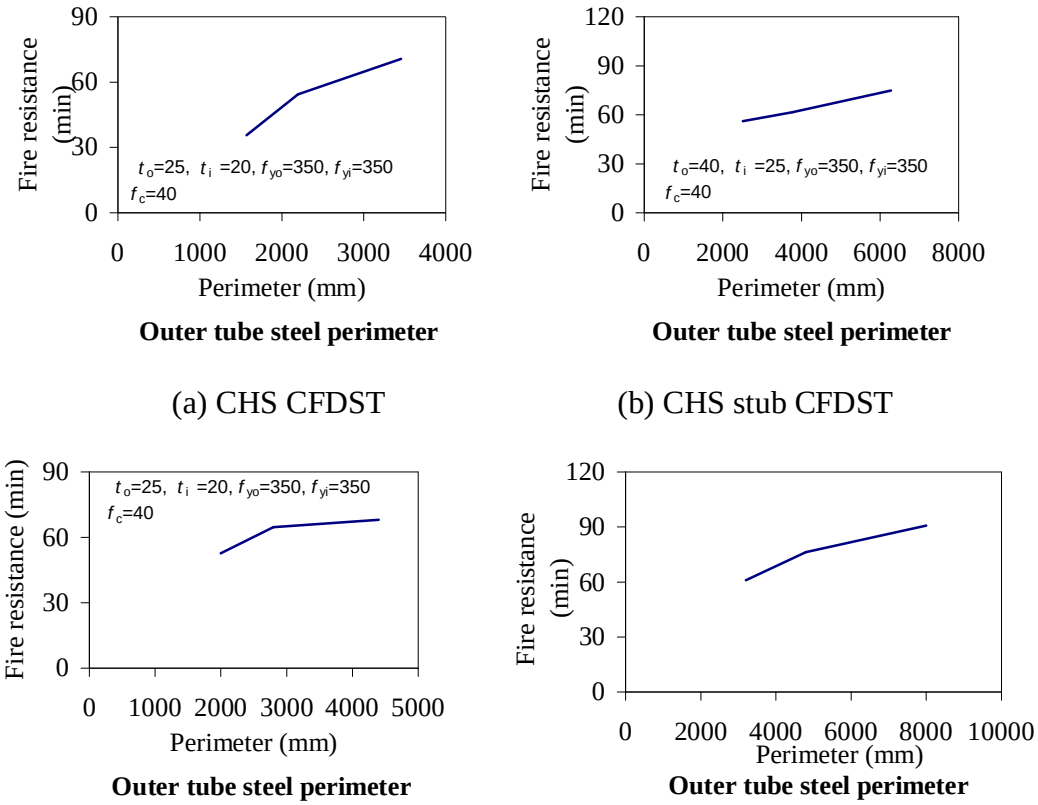

(a) CHS CFDST (b) CHS stub CFDST

(c) RHS CFDST (d) RHS stub CFDST

Figure 8.20 Effect of outer tube perimeter on fire resistance

Variation in the outer tube perimeter has little influence on the thermal response of the columns, as discussed in the preceding section. However, such variation affects the structural response of the columns. Figure 8.21 shows the effect of the outer tube perimeter on the ratios of cross-sectional area of each component to total cross-sectional area of the RHS columns in Figure 8.20 (c). As shown in the figure, an increase in the outer tube perimeter leads to a decrease in the outer tube area and an increase in the

inner tube area. Thus, increase in the outer tube perimeter is beneficial to the structural response and finally the fire resistance of the columns as shown in Figure 8.20.

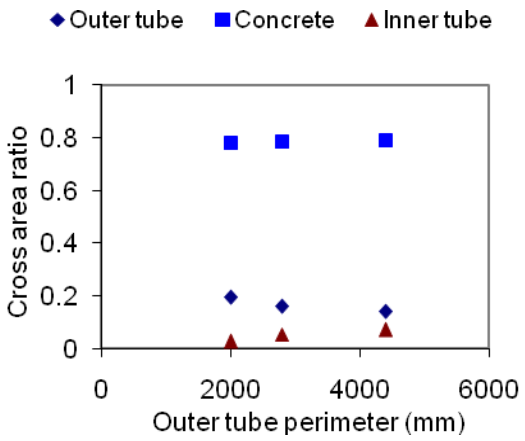

Figure 8.21 Effect of outer tube perimeter on cross-sectional area ratio

8.4.6 Effect of inner steel tube strength

The effect of the yield strength of the inner steel tubes on fire resistance is shown in Figure 8.22.

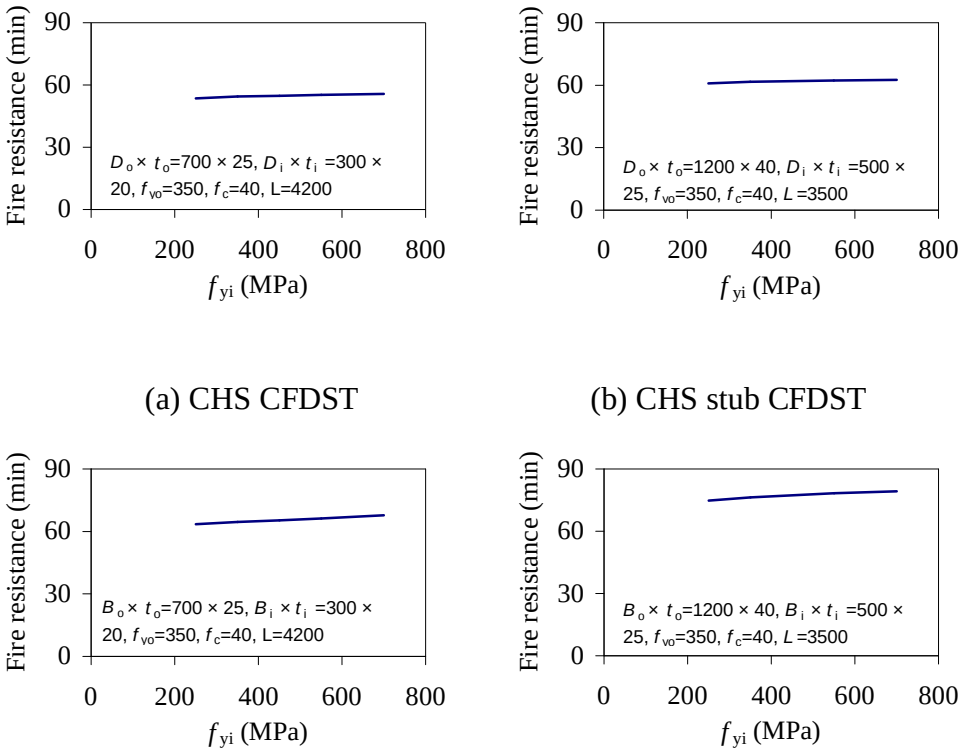

(a) CHS CFDST (b) CHS stub CFDST

(c) RHS CFDST (d) RHS stub CFDST

Figure 8.22 Effect of inner tube steel strength on fire resistance

As can be seen, yield strength of the inner steel tubes has a minimal influence on the fire resistance of the slender and stub CFDST columns when the yield strength changes from 250 to 700 MPa, which is within the normal range of steel yield strength in engineering practice.

8.4.7 Effect of outer steel tube strength

The fire resistance of the CFDST columns decreases with the increase in the outer tube steel yield strength as shown in Figure 8.23. When yield strength of the outer steel tubes change, other parameters, such as the load level, remains constant. As can be seen, variation in the yield strength of the outer steel tubes has a moderate influence on the fire resistance of the columns. The outer tubes will lose capacity quickly when the columns are exposed to fire. Therefore, any attempt to increase the capacity of the outer steel tubes will have a negative effect on the fire resistance of the columns.

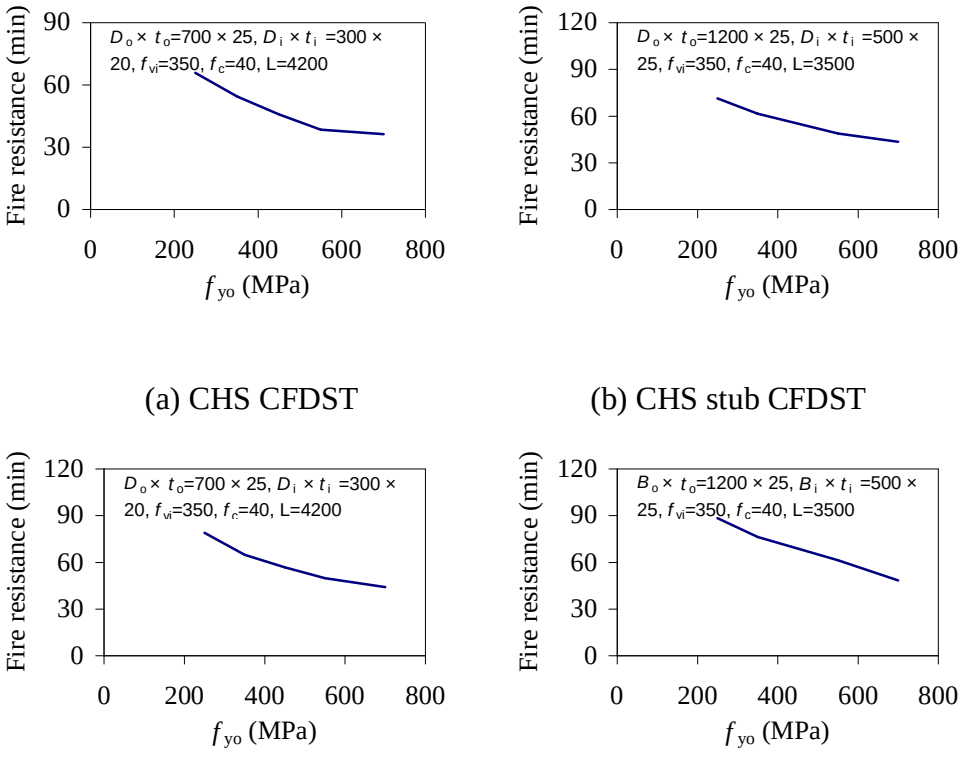

(a) CHS CFDST (b) CHS stub CFDST

(c) RHS CFDST (d) RHS stub CFDST

Figure 8.23 Effect of outer tube steel strength on fire resistance

8.4.8 Effect of concrete strength

The influence of concrete strength on the fire resistance of CFDST columns is shown in Figure 8.24. Fire resistance of the columns increases slightly with the increase in the concrete strength. However, such influence is minimal.

There is a subtle difference in the thermal properties of normal and high strength concrete (Lie, 1992; Kodur, 1998a). As such difference has no significant influence on the thermal response of concrete at elevated temperatures, some design codes use an identical thermal property for both normal and high strength concrete, such as Eurocode 2 (2004). Hence, the effect of concrete strength on the thermal response of CFDST columns can be neglected.

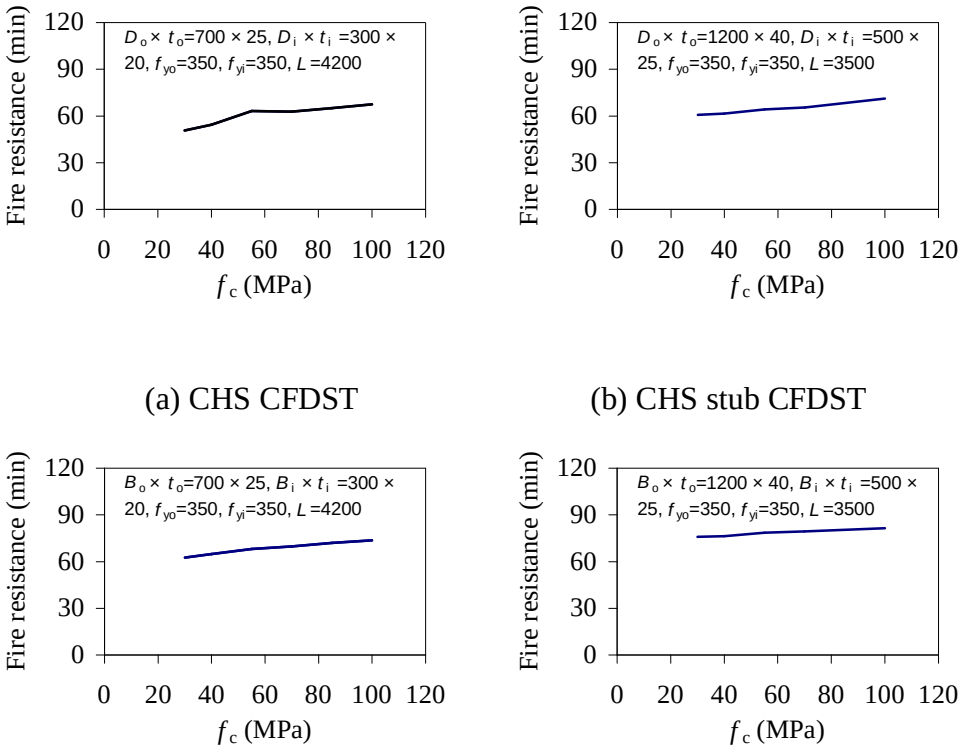

(a) CHS CFDST (b) CHS stub CFDST

(c) RHS CFDST (d) RHS stub CFDST

Figure 8.24 Effect of concrete strength on fire resistance

The increase in the concrete strength causes an increase in the capacity of the concrete and is favourable to the fire resistance of the CFDST columns. However, high strength concrete deteriorates more severely than normal strength concrete at elevated temperature. This difference has been considered in the FE model. Therefore, variation

in concrete strength becomes less influential on the structural response and fire resistance of CFDST columns as shown in Figure 8.24.

8.4.9 Effect of load level

The effect of load level on fire resistance is shown in Figure 8.25. Load level has a significant influence on the fire resistance of CFDST columns. Fire resistance decreases dramatically as the load level increases. Such influence is more pronounced when the load level is smaller than 0.4.

Variation in the load ratio directly affects the stress level in each component in the CFDST columns. The higher the stress level of the components, the less fire exposure time is required to allow the material strength to deteriorate to the stress level. Hence, the fire resistance of the columns decreases drastically when the load ratio increases.

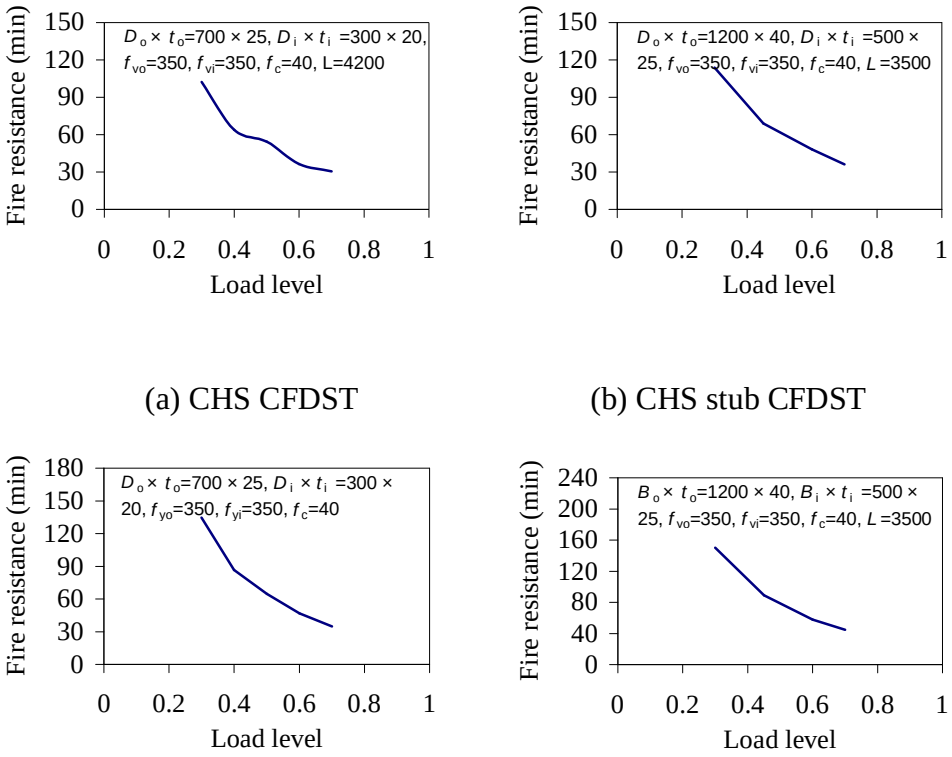

(a) CHS CFDST (b) CHS stub CFDST

(c) RHS CFDST (d) RHS stub CFDST

Figure 8.25 Effect of load level on fire resistance

8.4.10 Effect of load eccentricity

Figure 8.26 shows the effect of the load eccentricity to diameter (or width) ratio on the fire resistance of CFDST columns. As can be seen, there is a tendency for the fire

resistance of the columns to decrease as the load eccentricity increases. However, such influence on the fire resistance is minimal.

Variation in the load eccentricity only affects the structural response and does not affect the thermal response of the columns. The axial load capacity of the columns at ambient temperature decreases as the load eccentricity on the columns increases. Therefore, the absolute axial load values on the columns decrease as eccentricity increases if the load level remains unchanged. Non uniform stress distribution occurs in columns under eccentric load condition. For eccentric load columns, yield or failure of material may occur at the maximum stress position in the cross-section and finally causes the failure of the columns. Hence, an eccentric load column has lower fire resistance ability than the column under concentric load condition if the axial load is the same. At the same time, variation in load eccentricity causes changes in the absolute axial load. These two factors partly counteract each other. Therefore, variation in load eccentricity becomes minimal affecting the fire resistance of the columns.

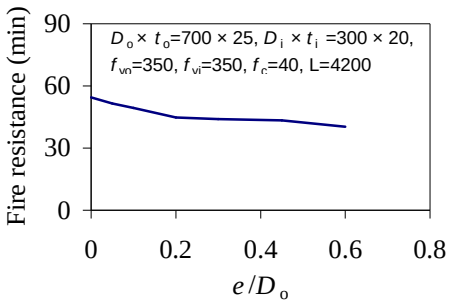

(a) CHS CFDST

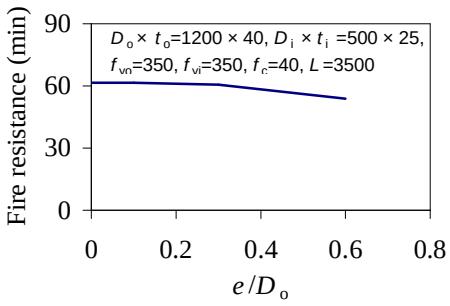

(b) CHS stub CFDST

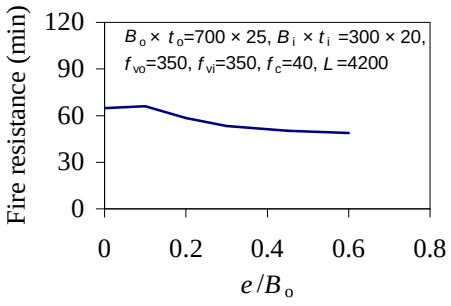

(c) RHS CFDST

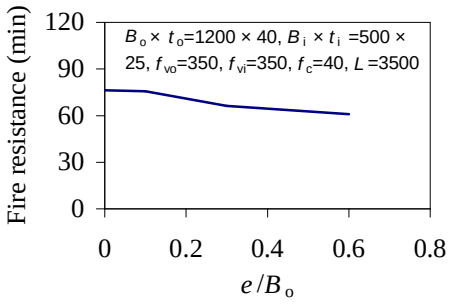

(d) RHS stub CFDST

Figure 8.26 Effect of load eccentricity on fire resistance

8.4.11 Effect of tube capacity

The influence of yield strength and tube wall thickness on fire resistance has been investigated. Here, a further study is carried out to investigate the influence of tube capacity on the fire resistance of the columns. The capacity of the inner and outer tubes depends on the cross-sectional area of the tubes and the yield strength of the tubes. Here, variation in the tube capacity is achieved by changes in the tube wall thickness and yield strength of the tube.

The effect of inner tube capacity on fire resistance is illustrated in Figure 8.27. In the figure, any column at the left hand side has a lower inner tube capacity than one at the right hand side. As can be seen, an increase in the capacity of the inner tube can lead to an increase in the fire resistance of the columns.

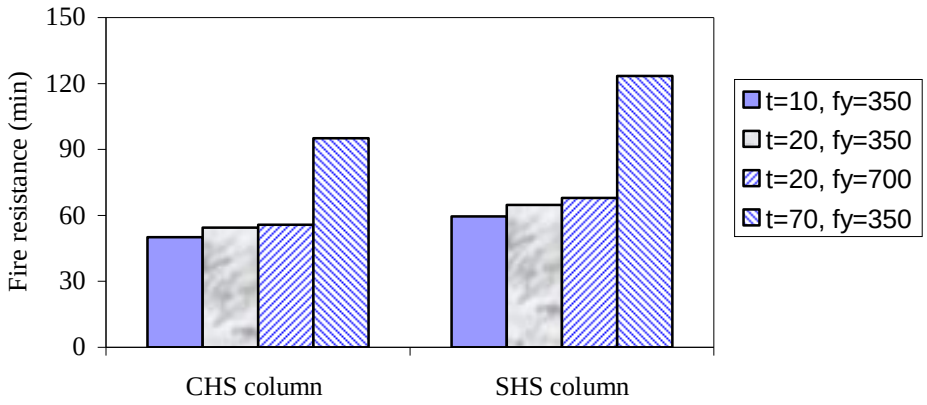

(a) CFDST column

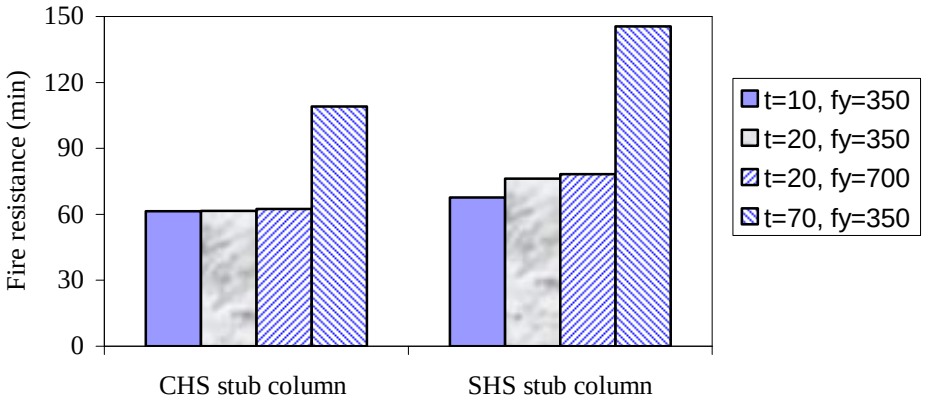

(b) CFDST stub columns

Figure 8.27 Effect of inner tube capacity on fire resistance

Figure 8.28 shows the effect of outer tube capacity on the fire resistance of the CFDST columns. Similarly, any column at the left hand side has a lower inner tube

capacity than one at the right hand side. Generally, an increase in the outer tube capacity leads to a decrease in the fire resistance of the CFDST columns. However, when the tube wall is thick enough, an increase in the outer tube capacity can result in an increase in the fire resistance of the columns. For the SHS CFDST stub columns, local buckling of the outer tube occurs long before the columns reach fire resistance when the tube wall is too thin. The influence of the outer tube capacity on the fire resistance of the SHS CFDST stub columns cannot follow the trend of other columns if the tube wall thickness is too small.

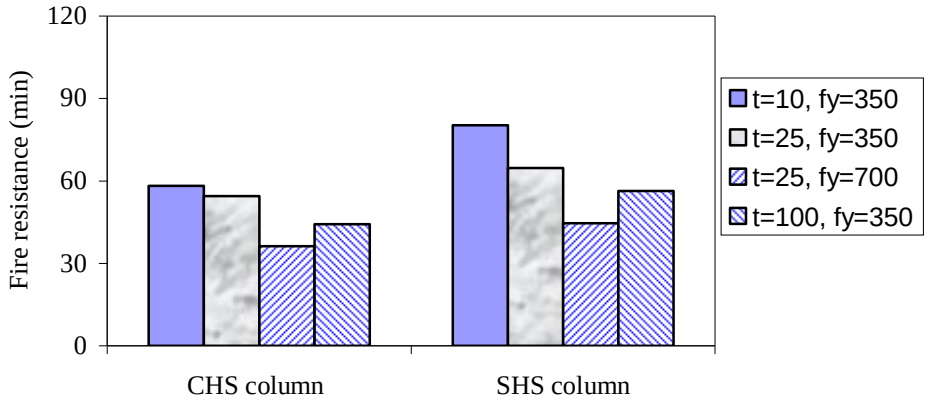

(a) CFDST column

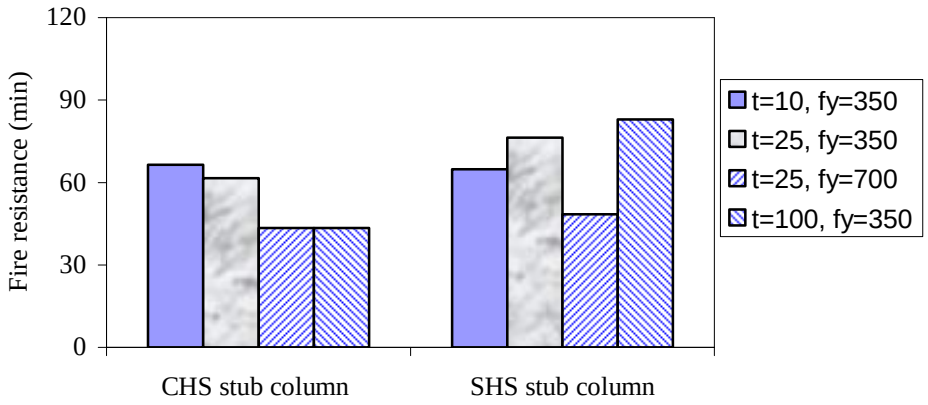

(b) CFDST stub columns

Figure 8.28 Effect of outer tube capacity on fire resistance

8.4.12 Effect of steel fibre reinforced concrete

The comparison of fire resistance between normal and steel fibre reinforced concrete-filled double skin tubular columns is shown in Figure 8.29. CFDST columns filled with steel fibre reinforced concrete can achieve a higher fire resistance compared to the counterpart CFDST columns filled with normal concrete. The difference in the fire

resistance of the columns becomes larger as the load level decreases. The fire resistance of the columns filled with steel fibre reinforced concrete increases by 20 to 30% compared to those filled with normal concrete.

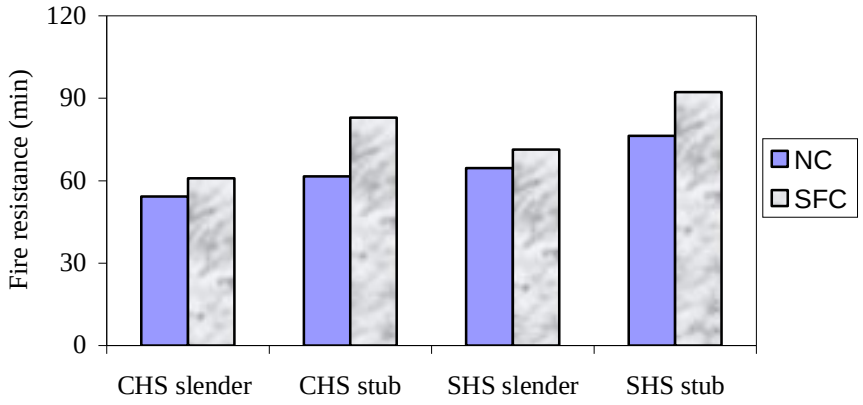

(a) Load level=0.5

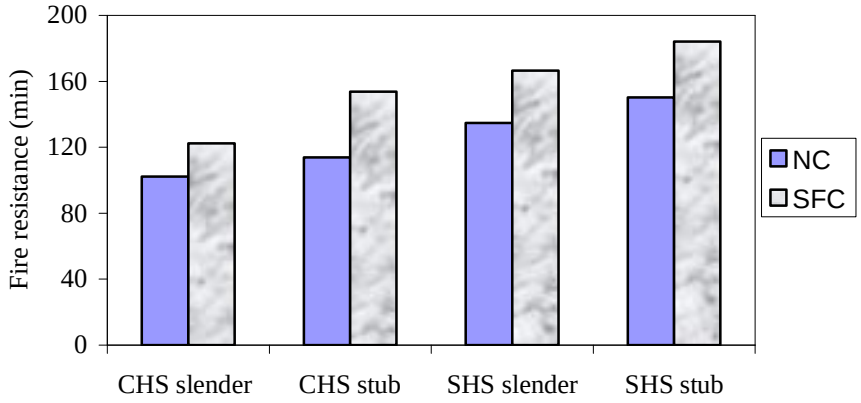

(b) Load level=0.3

Figure 8.29 Effect of steel fibre concrete on fire resistance

As discussed in Chapters 5 and 6, the influence of steel fibre on the concrete mechanical property manifests only at the post-peak stress stage. The load level for columns under fire condition is generally between 0.3 and 0.7, such as 0.5 in the current analysis. Therefore, the use of steel fibre in the concrete may not affect the load share and stress-to-strength ratio in the components before fire exposure starts. The steel fibre in the concrete can effectively prevent cracking of the concrete at post-peak stress stage. Thus, the descending branch of the stress-strain relationship curve declines more gradually for steel fibre reinforced concrete compared to normal concrete. Steel fibre reinforced concrete possesses higher capacity than normal concrete in the post-peak stress stage. Hence, steel fibre reinforced concrete can make a greater contribution than normal concrete to retain the capacity of CFDST columns at elevated temperature. Therefore,

CFDST columns filled with steel fibre reinforced concrete can achieve higher fire resistance.

8.4.13 Effect of fire insulation

The comparison of fire resistance between unprotected and fire insulated CFDST columns is shown Figure 8.30. The fire resistance of the counterpart CFST columns is also shown in the figure for comparison. The fire insulation system is that used in the fire tests introduced in Chapter 4. The thickness of the fire protection coating is 5 mm. As shown in the figure, fire insulation is a very effective way to enhance the fire resistance of CFDST columns. Even when the fire protection coating is only 5 mm, the fire resistance of the columns increases by 500 to 600% compared to unprotected columns. Fire protection can also improve the fire resistance of the counterpart CFST columns. However, the extent of the enhancement in the fire resistance for CFST columns is apparently less than that for the CFDST columns. Here, the fire protection is assumed to be intact until the columns reach fire endurance.

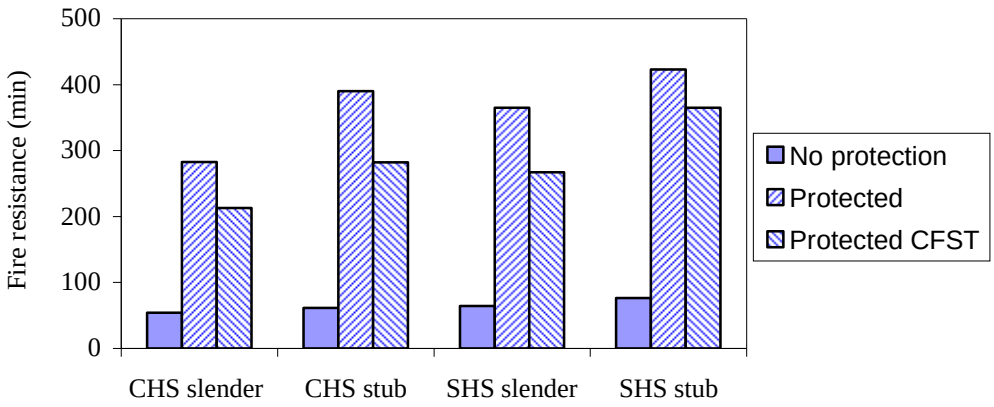

Figure 8.30 Effect of fire protection on fire resistance

The mechanism for fire insulation to improve the fire resistance of the columns is quite simple, that is, to delay temperature elevation in the columns under fire exposure. Hence, deterioration in the mechanical properties in the columns is slowed. Thus, the columns can retain the capacity to resist load for a longer time under fire exposure. The reason why CFDST columns can achieve a higher fire resistance than CFST columns is due to the inner tubes in the CFDST columns being more effective than the core concrete in the CFST columns to resist load.

8.5 CONCLUSIONS

Based on the parametric studies in the fire performance of CFDST columns, the influence of a number of parameters on the fire performance of CFDST can be identified. Several conclusions can be drawn from the parametric studies:

- Concrete thickness is a parameter which has a significant influence on temperature distribution in the concrete and inner tubes in CFDST columns.
- Fire insulation is an effective methodology to retard temperature elevation in the CFDST columns under fire exposure.
- Outer tube thickness and inner tube thickness have no significant influence on the thermal response of CFDST columns.
- Load level is the most important parameter significantly affecting the fire resistance of CFDST columns. Slenderness is another parameter which has a significant effect on the fire resistance of CFDST columns.
- Outer tube strength, inner tube thickness and the perimeter of outer tubes are parameters which have a moderate influence on the fire resistance of CFDST columns.
- Inner tube strength, concrete strength, outer tube thickness and load eccentricity are parameters which have minimal influence on fire resistance.
- Capacity of the steel tubes has a significant effect on the fire resistance of CFDST columns. An increase in the capacity of the inner tube or decrease in the capacity of the outer tube leads to an increase in the fire resistance of the columns.
- The use of steel fibre reinforced concrete in CFDST columns can improve the fire resistance of CFDST columns. The extent of the improvement is about 20% to 30% in the current analysis.
- Fire protection is a very effective way to enhance the fire resistance of CFDST columns. A 5mm thick fire protection coating can lead to the fire resistance of the CFDST columns being increase by 500% to 600% in the current analysis.

Chapter 9

DESIGN GUIDELINES OF CONCRETE-FILLED DOUBLE SKIN TUBULAR COLUMNS FOR FIRE RESISTANCE

9.1 INTRODUCTION

The effects of various parameters on the fire performance of CFDST columns have been studied by finite element modelling in Chapter 8. It can be clearly seen that some of the parameters have minimal influence, whereas some parameters have moderate or significant influence on the fire performance of the columns. Furthermore, the capacity of the inner steel tube has been identified as an important factor in the fire performance of CFDST columns in the analysis of failure mechanisms.

Based on the data and information acquired from the parametric studies and failure mechanism analysis, some design guidelines for fire resistance of CFDST columns can be developed. The design guidelines deal with how to optimize the parameters which significantly influence the fire resistance of the columns. Better fire resistance of CFDST columns can be achieved by implementing the design guidelines in the design procedure.

This chapter first identifies parameters which significantly influence the fire resistance of CFDST columns. Then, design guidelines are developed based on how to appropriately select parameters to enable CFDST columns to achieve better fire resistance performance. Finally, the guidelines are used to design several typical columns for potential use in multistorey buildings. Practical design tables for these columns are also developed.

9.2 PARAMETERS INFLUENCING FIRE RESISTANCE OF CFDST COLUMNS

A finite element model has been proposed and verified to simulate the fire behaviour of CFDST columns under fire exposure in Chapter 6. This model was then used in previous chapters to investigate the failure mechanism of CFDST columns in fire and the influence of a number of parameters on the fire performance of the columns. Several parameters which have a significant influence on the fire resistance of CFDST columns can be identified from the parametric analysis. These parameters are summarized as follows.

- **Load level**

Load level on columns has a significant influence on the fire resistance of CFDST columns. The fire resistance of CFDST columns decreases drastically when the load level of the columns increases. Load level represents the proportion of load to ultimate capacity at ambient temperature, which applies to columns before the temperatures start to increase in the columns under fire exposure. Columns with a higher load level obviously possess less remaining capacity up to the ultimate capacity. Hence, less fire exposure time is required for the degradation of the columns' capacities to the corresponding load level.

- **Capacity of inner steel tube**

As the inner steel tubes in CFDST columns are well insulated by the concrete, temperatures in the inner steel tubes are generally quite low even when the columns reach fire endurance. Therefore, the inner steel tubes fail due to the yield or/and local buckling of the steel tubes with minor influence of elevated temperatures. In addition, inner steel tubes offer an extra load transfer path for CFDST columns under fire exposure other than concrete. Hence, the capacity of inner steel tube in a CFDST column has a significant influence on the fire resistance of the column. An increase in the capacity of the inner steel tube can lead to an increase in the fire resistance of the column.

Change in the capacity of the inner steel tubes can be achieved by altering the inner tube thickness or/and the yield strength of the tube. As can be seen in the parametric studies, alerting the tube thickness is more sensitive than changing the yield strength of the tube. Changing both the tube thickness and yield strength are also very sensitive to the fire resistance of the columns.

- **Use of fire protection system**

A fire protection system is one option to enhance the fire resistance of CFDST columns. Although different types of fire insulation systems are available, the mechanism of the systems is the same, i.e. to delay temperature increase in the columns. For CFDST

columns, the needed thickness of the protection system is less than that for the steel tube alone because of the heat sink provided by the concrete in the columns.

- **Effective length**

As shown in Chapter 8, the fire resistance of CFDST columns decreases as the slenderness of the columns increases. For stub columns, i.e. those for which the slenderness of the columns is smaller than a certain value, the failure mode of the columns under fire exposure is compression failure. The slenderness of the columns has a minor influence on the fire resistance under such a circumstance. However, for slender columns the failure mode is overall buckling. In such a case, the slenderness of the columns has a significant influence on the fire resistance of the columns.

It is well-known that the critical load of slender columns at ambient temperature depends on the geometrical properties and the boundary conditions of the columns. The effective length concept is used to calculate the equivalent length of a column with various boundary conditions to a pined column that has the same buckling load. This concept has also been used for CFST columns under fire exposure to account for the influence of the boundary conditions on the capacity of the columns at elevated temperature.

The columns used for parametric studies in Chapter 8 all have pined boundary conditions. The effective length of columns can be adopted to calculate the slenderness of CFDST columns with boundary conditions other than pined at both ends. Therefore, the influence of slenderness is equivalent to the influence of effective length on the fire resistance of the columns.

- **Capacity of outer steel tube**

In contrast to inner steel tubes, outer steel tubes are the components in CFDST columns directly exposed to fire. Temperatures in the outer steel tubes are much higher than those in the concrete and inner steel tubes. Hence, the outer steel tubes fail due to the yield and/or local buckling of the steel tubes at elevated temperature. The outer steel tubes generally lose capacity far earlier than the columns reach fire endurance. A load transfer mechanism allows load transfer from outer steel tubes to concrete and inner

steel tubes when the outer steel tubes lose capacity. A higher capacity in the outer steel tubes means much load is required to transfer to the concrete and inner steel tubes as the outer steel tubes lose capacity, thus leading to a decrease in the fire endurance of the columns.

Similarly, variation in the capacity of the outer steel tubes can be achieved by changing the tube thickness and/or the yield strength of the outer steel tubes. Change in the yield strength of the outer steel tubes is more sensitive than change in the tube thickness.

- **Perimeter of outer steel tube**

The perimeter of the outer steel tube has a moderate influence in the fire resistance of CFDST columns. An increase in the outer tube perimeter leads to a moderate increase in the fire resistance of the columns.

- **Use of steel fibre reinforced concrete**

The use of steel fibre in concrete can enhance the performance of the concrete. Hence, the fire resistance performance of CFDST columns is enhanced when steel fibre concrete is used. From the data derived from parametric studies, it can be seen that fire resistance increases by about 20% to 30 % when steel fibre concrete is used to replace conventional concrete in CFDST columns. For columns with a lower load level, a higher increase in fire resistance is achieved.

In addition to the above-mentioned parameters which influence the fire resistance of CFDST columns, analysis of the failure mechanism of CFDST columns under fire exposure also offers insights into the fire behaviour of the columns and may lead to the development of design guidelines to enhance fire resistance. It is clear from the failure mechanism analysis that there is a load transfer mechanism in CFDST columns under fire exposure. The outer steel tubes lose capacity long before the columns reach fire endurance. Hence, while the outer steel tubes make less contribution, the inner tubes and concrete make a significant contribution to the fire resistance of the columns. The inner steel tubes have the lowest temperature of all the components. Therefore, the inner steel tubes have the greatest potential to resist load. In order to enable the inner tubes to make a greater contribution, it is important to maintain the temperature in the inner

tubes at a relatively low temperature, far below the critical temperature for the inner tubes alone.

9.3 DESIGN GUIDELINES FOR FIRE RESISTANCE OF CFDST COLUMNS

Parameters which have significant influence on the fire resistance of CFDST columns have been identified in the previous section. Better fire performance of CFDST columns can be achieved by appropriately selecting these parameters during the design procedure. Design guidelines to enable CFDST columns to achieve better fire resistance are proposed as follows:

- CFDST columns can achieve better fire performance than steel tubes alone and than CFST columns if the columns are appropriately designed. Composite action and multiple load transfer paths are the key factors which lead to CFDST columns possessing better fire performance.
- The inner steel tube is the most important component in a CFDST column contributing to the fire performance of the column. Increasing the capacity of the inner tubes is an effective way to increase the fire resistance of CFDST columns.
- The outer steel tube is the most vulnerable component in CFDST columns under fire exposure due to the direct fire exposure of the tube. Reducing the capacity of the outer steel tubes can benefit the fire performance of the columns. This can be achieved by the use of steel tubes with lower yield strength and smaller thickness than outer steel tubes.
- For CFDST columns without fire protection, limiting the load level at a low value is the most effective way to increase the fire resistance of the columns. CFDST columns without fire protection may achieve 1 to 2 h of fire resistance when an appropriate load level is selected.
- For CFDST columns with higher load level or requiring more than 2 h of fire resistance, steel fibre concrete or fire protection should be used. The fire resistance of CFDST can be increased by 20% to 30% when steel fibre concrete is used to replace plain concrete in CFDST. The fire resistance of CFDST with fire protection can reach 3h or more depending on the thickness of the fire protection system.

- The concrete in CFDST columns should be appropriately determined to delay the temperature in the inner tube reaching critical temperature for as long as possible. From the practical standpoint, the minimum thickness of the concrete should be greater than 50 mm so that the concrete can be conveniently placed into the space between the tubes.
- Drain holes must be provided in the outer steel tube to prevent bursting of the steel tubes when steam pressure is generated as water in the concrete transfers into vapour at elevated temperature.

9.4 TYPICAL DESIGN TABLES FOR FIRE RESISTANCE OF CFDST COLUMNS

Design guidelines based on the data from parametric analysis have been proposed for the design of CFDST columns with better fire performance. In this section, these guidelines are used to design some typical CFDST columns for potential use in multistorey buildings. Practical design tables are created accordingly. Due to the variety of parameters which may influence the fire performance of the columns, some of the parameters are pre-determined within the range of typical values in engineering practice in order to reduce the calculations required for the generation of the design tables. It should be noted that the design tables are generated based on data on standard fire temperatures. Hence, they are suitable for the fire resistance design of CFDST columns under standard fire conditions.

The cross-section size of the outer steel tubes is selected as 400 and 500 mm. Columns with cross-section sizes in this range are commonly used in multistorey buildings. A column effective length of 4 m and concrete strength of 40 MPa are selected for the columns. These are typical values for columns in buildings.

Then, the proposed design guidelines are used to design the CFDST columns according to the following procedure.

- **Outer steel tube**

As the outer steel tube is the component making the least contribution to the fire resistance of CFDST columns, values for tube thickness and yield strength should be as

low as possible. Based on this consideration, the yield strength of the outer steel tube is chosen as 250 MPa. The wall thickness of the outer steel tube can be determined by the minimum allowable value to prevent local buckling at ambient temperature as required in design codes for composite columns. Here, Eurocode 4 (2005) is used to determine the minimum wall thickness of the outer tubes. The maximum diameter to wall thickness ratio is $90\frac{235}{f_y}$ for CHS and the height to wall thickness ratio is $52\sqrt{\frac{235}{f_y}}$ for SHS, where f_y is the yield strength. Therefore, the geometric and mechanical properties of the outer steel tubes can be determined as shown in Table 9.1.

Table 9-1Geometric and mechanical properties of outer steel tube

Profile of outer steel tube	$B_o(D_o)\times t_o$ (mm)	f_y (MPa)
CHS	500×6	250
CHS	400×5	250
SHS	500×10	250
SHS	400×8	250

- **Inner steel tube**

As can be seen in the proposed design guidelines, a tube with higher yield strength and greater wall thickness should be selected to enable the columns to achieve better fire resistance performance. Hence, the yield strength of the inner steel tube is chosen as 450 MPa, which is a higher value than structural steel in engineering practice. When selecting an appropriate wall thickness for the inner tube, one factor which should be considered is the size of the tube. The diameter (width)-to-wall thickness of the tube should be within a practical range. The cross-section size of the inner tube must be at least 100 mm smaller than that of the outer tube so that the concrete thickness is greater than 50 mm. Hence, the cross-section sizes of the inner tube should be less than 400 and 300 mm as the sizes of the outer tube are 500 and 400 mm respectively. Considering the possible cross-section of the tubes, the wall thickness of the inner tube is chosen as 20 mm. The diameter (width) to wall thickness ratio is about 15 to 20. This value is generally greater than that of available hot-rolled or cold-formed steel tubes with similar cross-sections, whereas this value is a practical value in engineering applications.

- **Concrete thickness**

The thickness of the concrete should be greater than 50 mm from the standpoint of construction practice. In addition, concrete should offer insulation for the inner steel tube to maintain the temperature in the inner tube much lower than the critical temperature for a certain period of fire exposure. Based on the data in the parametric analysis, a concrete thickness of about 100 mm to 125 mm is appropriate for columns to achieve this goal. Therefore, the diameters (width) of the inner tubes are selected as 250 and 200 mm respectively. The geometric and mechanical properties of the columns and the temperatures in the inner tube at 2h of fire exposure are listed in Table 9.2. As can be seen, the temperature in the inner tube is below 200 ^{o}C after 2h of fire exposure.

Table 9-2 Geometric and mechanical properties of the columns

Profile	$B_o(D_o)\times t_o$ (mm)	$B_i(D_i)\times t_i$ (mm)	L_e (m)	f_{yo} (MPa)	f_{yi} (MPa)	f_c (MPa)	Temperature (^{o}C)
CHS+CHS	500×6	250×20	4	250	450	40	108
CHS+CHS	400×5	200×20	4	250	450	40	196
SHS+SHS	500×10	250×20	4	250	450	40	102
SHS+SHS	400×8	200×20	4	250	450	40	173

- **Use of steel fibre reinforced concrete and fire protection**

The required fire resistance of columns in buildings generally ranges from 1 to 3 h. CFDST columns filled with plain concrete may not meet this requirement in some circumstances. The use of steel-fibre reinforced concrete or fire protection is options to improve the fire performance of the columns. The use of steel-fibre reinforced concrete seems a more attractive solution than the use of fire protection systems as it does not alter the appearance of the columns. However, the extent of the enhancement which steel-fibre reinforced concrete can offer for CFDST columns is generally about 20 to 30% compared to the plain concrete filled CFDST. Therefore, fire protection is necessary when load level is high or high fire resistance performance is needed. The fire protection coating is the same as that introduced in Chapter 5 and the fire protection is assumed to be intact until the columns reach fire endurance.

The CFDST columns shown in Table 9.2 have been designed based on the design guidelines presented in the previous section. The finite element model proposed in Chapter 6 is used to predict the fire resistance of the columns. The data from the

calculation are used to create practical design tables as shown in Table 9.3. In these tables, the load level changes from 0.3, to 0.5 and 0.7 which covers the load levels recommended for steel-concrete composite columns by Twilt et al (1996). The fire resistance of columns is from 1 to 3h. Plain concrete is the first option for the columns to achieve a certain level of fire resistance. If the plain concrete filled CFDST columns cannot achieve a certain level of fire resistance, steel fibre reinforced concrete is chosen as the second option. Fire protection is used as the third option to enable the columns to achieve a certain level of fire resistance if the fire resistance of plain or steel fibre reinforced concrete filled CFDST is not adequate. The fire protection system used here is the fire protection coating presented in Chapter 6. Hence, there are three options for the CFDST columns to achieve a certain level of fire resistance: plain concrete filled CFDST, fibre reinforced concrete filled CFDST and plain concrete filled CFDST with fire protection. These three options are denoted "A" for plain concrete filled CFDST, "B" for fibre reinforced concrete filled CFDST and "C-xx" for plain concrete filled CFDST with fire protection in the tables, in which the digits "xx" in "C-xx" represent the thickness of the fire protection coating in millimetres.

As can be seen in the tables, three optional schemes, CFDST filled with plain concrete, CFDST filled steel fibre reinforced concrete and plain concrete filled CFDST with fire protection, can be chosen for the CFDST columns to achieve a certain level of fire resistance. Plain concrete filled CFDST columns with an outer tube width (or diameter) of 400 to 500 mm can have fire resistance up to 3h if the load level is limited to a low value, i.e. 0.3. The use of steel fibre reinforced concrete to replace plain concrete in CFDST can lead to an increase in the fire resistance of the columns by about 0.5h. Fire protection coating is the most effective way to enhance the fire resistance performance of the columns. It should be noted that the thickness of the fire insulation coating from 5 to 15 mm can enable the columns to achieve 3h of fire resistance, which is much less than the required thickness for steel tube alone, being generally from 20 to 40 mm.

Table 9-3 Fire resistance design table for CFDST columns

(a) CHS 500×6 + 250×20

FR / Load level	60 (min)	90 (min)	120 (min)	150 (min)	180 (min)
0.3	A	A	A	A	A
0.5	A	B	C-5	C-5	C-5
0.7	C-5	C-5	C-5	C-10	C-10

(b) CHS 400×5 + 200×20

FR / Load level	60 (min)	90 (min)	120 (min)	150 (min)	180 (min)
0.3	A	A	A	A	A
0.5	B	C-5	C-5	C-5	C-5
0.7	C-5	C-10	C-10	C-15	C-15

(c) SHS 500×10 + 250×20

FR / Load level	60 (min)	90 (min)	120 (min)	150 (min)	180 (min)
0.3	A	A	A	A	A
0.5	A	A	B	C-5	C-5
0.7	C-5	C-5	C-5	C-5	C-10

(d) SHS 400×8 + 200×20

FR / Load level	60 (min)	90 (min)	120 (min)	150 (min)	180 (min)
0.3	A	A	A	A	A
0.5	A	A	B	C-5	C-5
0.7	C-5	C-5	C-5	C-10	C-15

9.5 CONCLUSIONS

Several conclusions can be drawn from the study presented in this chapter:

- Parameters which have significant influence on the fire resistance performance of CFDST columns have been identified. These parameters include load level, capacity of inner steel tube, the use of fire protection, effective length, capacity of outer steel tube, perimeter of outer steel tube and the use of steel fibre reinforced concrete.
- Design guidelines have been developed based on the appropriate selection parameters to enable the columns to achieve a certain level of fire resistance.
- The design guidelines are used to design several typical CFDST columns for potential use in multistorey buildings and the corresponding practical design tables are developed. This procedure can be used to develop practical design tables or diagrams which cover a wide range of parameters.

Chapter 10

CONCLUSIONS

10.1 CONCLUSIONS

This thesis presents extensive experimental and numerical simulation studies of the fire behaviour of SCC-filled CFDST columns. The primary aim of the research is to improve knowledge and understanding of the fire performance of SCC-filled CFDST columns and provide guidance for the design of fire resistance in CFDST columns.

Prior to studying SCC-filled CFDST columns, an investigation was conducted into the fire performance of SCC-filled CFST stub columns by standard fire tests and finite element modelling. The investigation was a preparation for the further study of SCC-filled CFDST columns subjected to fire and aimed to understand how SCC affects the fire performance of composite columns. Then, a series of standard fire tests were carried out for SCC-filled CFDST columns and stub columns. A total of six columns and 16 stub columns were prepared for standard fire tests. The observations and data from the fire tests were used to investigate the fire behaviour and the effects of several factors on fire resistance performance. In addition, methods to improve fire resistance performance, i.e. fire protection and steel fibre reinforced SCC, were examined. In order to comprehensively study the fire behaviour of CFDST, a finite element model was developed to simulate the thermal and structural responses of CFDST under fire exposure. This numeral model was verified by the results obtained from the fire tests. The finite element model was adopted to obtain data which cannot be measured in fire tests, such as stress, strain and load share in the components, in order to investigate the failure mechanisms of the columns in fire conditions. Parameters likely to affect the thermal and structural responses of CFDST columns were discussed. A parametric study was carried out to identify key parameters which significantly affect fire resistance performance with the aid the finite element model. Finally, guidance on the appropriate selection of parameters for CFDST to achieve better fire resistance performance was developed. Several typical CFDST columns were designed based on the developed guidelines to show how to use the guidelines to design CFDST columns to achieve a certain level of fire resistance and practical design tables were developed accordingly.

Some conclusions which can be drawn from the outcomes of the current research are summarized as follows.

1. The fire behaviour of SCC-filled CFST stub columns is similar to that of conventional concrete filled columns due to the steel tube providing confinement of the concrete to prevent spalling and disaggregation of the SCC. Composite action is a key factor to help the columns achieve better fire performance. An obvious load transfer mechanism between the steel tube and concrete is revealed through numerical analysis. The yield of the steel tube occurs earlier than the columns reach fire resistance and is a major cause of failure of the columns. As soon as the steel tube yields, the concrete becomes the dominant component to resist most of the load.

2. The standard fire tests show that the limiting temperature of the outer tube in CFDST columns is higher than that of the tube alone and that of the tube in CFST columns. In terms of the limiting temperature, CFDST columns have better fire resistance than unfilled steel tube and CFST. The limiting temperature in CFDST columns depends on the load level and probably on the different combination of outer and inner steel tubes. Concrete offers good insulation for the inner tubes so that the temperatures in the inner tubes are as low as 450 ^{o}C for the CFDST columns and 200 ^{o}C for the stub columns as the columns reach fire resistance. This indicates that the inner tubes do not fail due to the influence of elevated temperature. The mass of the concrete, namely the concrete thickness and perimeter of the outer tube, is a major factor affecting the temperature distribution in the columns.

3. Fire test results show that composite action exists in the CFDST columns under fire exposure. The interaction of the concrete and the steel tubes has a significant influence on the fire performance of the SCC-filled CFDST columns. The steel tubes provide confinement of the concrete in the columns to prevent spalling and disaggregation of the SCC at elevated temperatures, as in the case of SCC-filled CFST stub columns. At the same time, the concrete offers strong support to the outer steel tubes to change the failure mode of the tubes. However, less support is provided to the inner tubes by the concrete and thus the inner tubes fail in a way similar to an unfilled tube. Load transfer in the components of the columns is another demonstration of composite action in the columns. The outer steel tubes reach limiting temperature far earlier than the columns reach fire endurance. Hence, other components in the columns take the load originally borne by the outer tubes to maintain the columns as a whole element to resist load until the failure of the columns.

4. Several approaches to enhance the fire resistance performance of CFDST columns have been trialled in fire tests. The first approach is to use fire protection at the exterior surface of the outer tubes to delay temperature elevation in the columns. The use of 10 mm fire protection coating in the columns can lead to the columns achieving a fire resistance of more than 2.5h, whereas for unfilled steel tube the coating thickness is required to be 40 mm to achieve the same fire resistance. Hence, thinner fire protection coating is required for CFDST columns than for the unfilled steel tubes if the same fire resistance is anticipated. Another approach is to use fibre reinforced concrete. Stub column test results show that the use of steel fibre reinforced concrete can increase the fire resistance of the columns. The extent of the increase in the fire resistance depends on the load level and the concrete mass. The use of both steel and polypropylene fibres does not further enhance the fire resistance performance of the columns compared to the use of steel fibres only.

5. A finite element model to simulate the thermal and structural responses of the CFDST columns in fires has been proposed. A concrete mechanical property model for core concrete in CFDST has also been proposed. This model comprehensively considers the material and geometric non-linearity and interaction of tubes and concrete. Detailed data on the thermal and structural responses of the total columns or each component can be obtained to further investigate the fire behaviour of the columns.

6. Detailed data from numerical modelling further prove that concrete provides good insulation for the inner tubes and also serves as a heat sink to delay the temperature increase in the outer tube. The non-uniform temperature distribution and the differences in the material properties of steel and concrete result in variations in the stress, strength, strain and capacity in the components during the process of fire exposure. Mises stress in the outer steel tubes rises at the early stage of fire exposure and then decreases until the column reaches fire resistance. In contrast, the axial stress in concrete and the Mises stress in the inner tubes drop briefly at the beginning of fire exposure and then both values increase steadily. Such variation in the stress states in the components causes changes in the load share in the components accordingly. This clearly indicates the load transfer mechanism in the columns. The outer steel tube is the first component which loses its capacity.

Nevertheless, the columns may still have capacity to sustain load even with the yield of the outer tubes. Yield of the inner steel tube is the major cause of failure of the columns. The concrete becomes almost the sole component to resist load and crushes soon after the inner tube yields. Hence, the ability of the inner tubes is the key factor affecting the fire resistance behaviour of CFDST columns.

7. A parametric study has been conducted to analyse the influence of a number of parameters on the fire performance of CFDST columns. Among these parameters, it has been found that load level, capacity of inner tube, fire protection, effective length, capacity of outer tube, perimeter of the outer tube and the use of steel fibre reinforced concrete have significant or moderate influence on the fire resistance performance of CFDST columns.

8. Guidelines for the appropriate selection of parameters to enable CFDST columns to achieve better fire resistance performance are proposed. The key points in the guidelines are to increase the capacity of the inner tube, reduce the capacity of the outer tube and maintain a reasonable concrete thickness to decrease the temperature in the inner tube. Steel fibre reinforced concrete or fire protection are options for columns which need higher fire resistance performance. Practical fire resistance design tables are developed for several columns of potential use in multistorey buildings.

10.2 SUGGESTIONS FOR FUTURE STUDY

The basic fire performance of SCC-filled CFDST columns has been understood through the standard fire tests and finite element modelling undertaken in this research. A number of suggestions for further study are listed in the following section, which if investigated, may lead to improved understanding of the fire performance of CFDST and provide a practical fire resistance design methodology for CFDST.

1. Extension of the practical design tables for fire resistance design of several CFDST columns to general tables to cover a wide range of CFDST in engineering applications, or the generation of other practical diagrams or formulations for the fire resistance design of CFDST columns.
2. Investigation of the relevance of the fire performance of CFDST columns under standard fire conditions to real fire conditions. Differences in fire conditions result

in differences in the thermal response and finally affect the structural response of CFDST columns. This can be achieved by comparing the fire performance of CFDST columns under typical compartment fires and standard fire conditions. The final purpose is to establish the methodology for the use of the outcomes from standard fire tests to represent the fire performance of CFDST columns in real fire conditions.

3. Investigation of the influence of constraints on the fire resistance performance of CFDST columns. The boundary conditions for columns in the current research are either fixed or pinned and an effective length concept is used to consider the difference in the column end boundary conditions. However, boundary conditions of CFDST columns in buildings may involve complex constraints rather than the simple fixed or pinned conditions. Hence, the influence of constraints on fire resistance performance needs to be understood.
4. Investigation of the possibility of developing environmental friendly SCC, e.g. by reducing Portland cement and increasing fly ash to reduce CO_2 release or by utilizing recycled aggregate from earthquake waste to save natural resources.

REFERENCES

1. ABAQUS, 2008, *ABAQUS Analysis User's Manual*, (Providence: SIMULIA).
2. ACI, 2007, *Self-Consolidating Concrete*, 237R-07, (Farmington: ACI).
3. AIJ, 1997, *Recommendations for Design and Construction of Concrete Filled Steel Tubular Structures*, (Tokyo: Architectural Institute of Japan).
4. AISC-LRFD, 1999, *Load and Resistance Factor Design Specification for Structural Steel Buildings*, (Chicago: American Institute of Steel Construction).
5. Anchor R., Malhotra H. and Purkiss J., 1986, Desigm of Structures Against Fire. Edited by R. Anchor, H. Malhotra and J. Purkiss, In *Proceedings of International Conference on Design of Structures Against Fire*. (Birmingham: Elsevier Applied Science Publishers).
6. Anderberg Y., 1988, Modelling steel behaviour, *Fire Safety Journal*, 13(1), pp 17-26.
7. Anderberg Y. and Thelandersson N., 1976, *Stress and deformation characteristics of concrete at high temperatures Bulletin 54*, (Lund: Lund Institute of Technology).
8. SCA, 2002, *Self-compacting Concrete: Recommendations for Use*, (Sweden: Swedish Concrete Association).
9. AS-1530-4, 2005, *Method for Fire Tests on Building Materials, Components and Sub-structures-Part 4: Fire Resistance Test of Element of Construction*, (Sydney: Standards Australia).
10. AS 1163, 1991, *Structural Steel Hollow Sections, AS 1163*. (Sydney: Standards Australia).
11. AS 1391, 2007, *Metallic Materials - Tensile Testing at Ambient Temperature*. (Sydney: Standards Australia).
12. AS 4100, 1998, *Steel Structures*, AS 4100. (Sydney: Standards Australia).
13. ASTM E119-88, 1995, *Standard Methods of Fire Tests of Building Constructions and Materials*, (Philadelphia: ASTM).
14. Bailey C., 2002, Holistic behaviour of concrete buildings in fire, *Proceedings of the Civil Engineering, Structures and Buildings* 152(3), pp 199-212.
15. Bailey C., 2006a, *Nominal fire*. http://www.mace.manchester.ac.uk/.

16. Bailey C., 2006b, One stop shop in structural fire engineering. http://www.mace.manchester.ac.uk/.
17. Bazant Z. and Kaplan M., 1996, *Concrete at High Temperature: Material Properties and Mathematical Models*, (Essex: Longman Group Limited).
18. Bennetts I D, 2002, Design of steel structures under fire conditions, *Progress in Structural Engineering and Materials*, 4(1), pp 6-17.
19. BHP Research, 1991, *Modelling of Concrete-filled Columns in Fire, BHPR/ENG/R/91/031/PS69*, (Melbourne: BHP Research).
20. Blontrock H. and Taerwe L., 2002, Exploratory spalling tests on self compacting concrete, In the *Proceedings of the 6th International Symposium on Utilization of High Performance Concrete*, (Leipzig), pp. 659-666.
21. Bonen D. and Shah S.P., 2005, Fresh and hardened properties of self-consolidating concrete, *Progress in Structural Engineering and Materials*, 7(1), pp 14-26.
22. Bostrom L., 2002, *The Performance of some Self-compacting Concretes when Exposed to Fire*, (Sweden: Swedish National Testing and Research Institute).
23. BS5400, 1979, *Concrete and Composite Bridge: Part 5*, (London: British Standards Institute).
24. British Steel Tubes and Pipes, 1990, *Design for SHS Fire Resistance to BS5950: Part 8*, (London: British Steel Tubes and Pipes).
25. British Steel, 1990, *SHS Design Manual for Concrete-Filled Columns, Part 2: Fire Resistance Design*, (London: British Steel).
26. British Steel & Sweden Technology Centre, 1999, *The Behaviour of Multi-storey Steel-framed Buildings in Fire*, (Moorgate: British Steel & Sweden Technology Centre).
27. Brouwers H.J.H. and Radix H.J., 2005, Self-compacting concrete: Theoretical and experimental study, *Cement and Concrete Research*, 35(11), pp 2116-2136.
28. BSI, 1990, *Structural Use of Steelwork in Building, Part 8, Code of Practice for Fire Resistance Design*, (London: BSI).
29. CEB-FIP, 1993, CEB-FIP Model Code 1990, (London: Thomas Telford Ltd.).
30. Chen, J. and Young, B., 2006, Corner properties of cold-formed steel sections at elevated temperatures, *Thin-Walled Structures*, 44(2), pp 216-223.
31. Chen J. and Young B., 2006a, Stress-strain curves for stainless steel at elevated temperatures, *Engineering Structures*, 28(2), pp 229-239.

32. Chen J. and Young B., 2007, Experimental investigation of cold-formed steel material at elevated temperatures, *Thin-Walled Structures*, 45(1), pp. 96-110.
33. Chen J., Young B. and Uy B., 2006, Behavior of high strength structural steel at elevated temperatures, *Journal of Structural Engineering*, ASCE, 132(12), pp 1948-1954.
34. Cheng F.P., Kodur V.K.R. and Wang T.C., 2004, Stress-strain curves for high strength concrete at elevated temperatures, *Journal of Materials in Civil Engineering*, 16(1), pp 84-90.
35. CIDECT, 1988, *Fire Resistance of Hollow Section Composite Columns of Small cross-sections*, CIDECT Research Project 15G, Final Report.
36. CIDECT, 1990, *Fire Tests on Cleat Connections to Concrete-filled RHS Columns*, CIDECT Research Project 15H, Final Report.
37. CIDECT, 1998, *Design Charts for the Fire Resistance of Concrete-filled HSS Columns under Centric Loading*, CIDECT Research Project 15J, Final Report.
38. CIDECT, 2000, *Fire Resistance of Hollow Section Composite Columns with High Strength Concrete Filling*, CIDECT Research Project 15P-12/00, Final Report.
39. CIDECT, 2004a, *Improvement and Extension of the Simple Calculation Method for Fire Resistance of Unprotected Concrete-filled Hollow Columns*, CIDECT.
40. CIDECT, 2004b, *Improvement and Extension of the Simple Calculation Method for Fire Resistance of Unprotected Concrete-Filled Hollow Columns*, CIDECT Research Project 15Q, Final Report.
41. Corbett G.G., Reid S.R. and Al-Hassani S.T.S., 1990, Resistance of steel-concrete sandwich tubes to penetration, *International Journal of Impact Engineering*, 9(2), pp 191-203.
42. Corus, 2006, http://www.corusconstruction.com/en/company/business_units/bi-steel_home, Corus Group.
43. DBI13-51, 2003, *Technical Specification for Concrete-Filled Steel Tubular Sstructures*, (Fuzhou: The Construction Department of Fujian Province).
44. Dehn F., Holschemacher K. and Weibe D., 2000, *Self-compacting Concrete (SCC) Time Development of the Material Properties and the Bond Behaviour*, (Leizig: University of Leipzig).
45. Ding J. and Wang Y.C., 2006, The behaviour of rotationally restrained concrete filled tubular columns in fire, in the *Proceedings of the 11th International Symposium on Tubular Structures*, edited by Packer J.A. and Willibald S, (London: Taylor & Francis Group), pp. 417-424.

46. Ding, J. and Wang, Y.C., 2008, Realistic modelling of thermal and structural behaviour of unprotected concrete filled tubular columns in fire, *Journal of Constructional Steel Research*, 64(10), pp 1086-1102.
47. Domone, P.L., 2006, Self-compacting concrete: An analysis of 11 years of case studies. *Cement & Concrete Composite*, 28(2), pp. 197-208.
48. ECCS, 1988, *Fire Safety of Steel Structures, Technical Note, Calculation of the Fire Resistance of Centrally Loaded Composite Steel-concrete Columns Exposed to the Standard Fire*, ECCS-Technical Committee 3.
49. ECCS, 1983, *European Recommendations for the Fire Safety of Steel Structures*, ECCS.
50. ECS 24, 1990, Regulation of Application Technology of Fire Resistive Coating for Steel Structure, (Beijing: China Association for Engineering Construction Standarzation). [in Chinese]
51. EFNARC, 2002, *Specification and Guidelines for Self-compacting Concrete*, European Federation of National Trade Associations, (UK: EFNARC).
52. Elchalakani M., Zhao X.L. and Grzebieta R., 2002, Tests on concrete-filled double-skin (CHS outer and SHS inner) composite short columns under axial compression, *Thin-Walled Structures*, 40(5), pp 415-441.
53. Ellobody E. and Young B., 2006, Design and behaviour of concrete-filled cold-formed stainless steel tube columns, *Engineering Structures*, 28(5), pp. 716-728.
54. Ellobody E. and Young B., 2006a, Nonlinear analysis of concrete-filled steel SHS and CHS columns, *Thin-Walled Structures*, 44(8), pp. 919-930.
55. Ellobody E., Young B. and Lam D., 2006, Behaviour of normal and high strength concrete-filled compact steel tube circular stub columns, *Journal of Constructional Steel Research*, 62(7), pp. 706-715.
56. Eurocode 2, 2004, *Design of Concrete Structures:Part 1.2 General Rules-Structural Fire Design, EN-1992-1-2:2003*, (Brussels: European Committee for Standardization).
57. Eurocode 3, 2005, *Design of Steel Structures:Part 1.2 General Rules-Structural Fire Design, EN-1993-1-2:2005*, (Brussels: European Committee for Standardization).
58. Eurocode 4, 2005, *Design of Steel and Concrete Composite Structures: Part 1.2 General Rules: Structural Fire Design*, (Brussels: European Committee for Standardization).

59. Florian K., 2006, *Dissemination of Fire Safety Engineering Knowledge*, http://www.arcelor.com/sections/DIFISEK/UK/DIFISEK_UK.html.
60. Gabriel A. K., 2000, Effect of fire on concrete and concrete structures, *Progress in Structural Engineering and Materials*, 2(4), pp 429-447.
61. Galambos T.V., 2000, Recent research and design developments in steel and composite steel-concrete structures in USA, *Journal of Constructional Steel Research*, 118(11), pp 3036-54.
62. Ge H.B. and Usami T., 1992, Strength of concrete-filled thin-walled steel box columns: experiment, *Journal of Structural Engineering, ASCE*, 118(11), pp 3036-3054.
63. Gho W.M. and Liu D., 2004, Flexural behaviour of high-strength rectangular concrete-filled steel hollow sections. *Journal of Constructional Steel Research*, 60(11), pp 1681-1696.
64. Ghojel J., 2004, Experimental and analytical technique for estimating interface thermal conductance in composite structures elements under simulated fire conditions, *Experimental Thermal and Fluid Science*, 28(4), pp. 347-354.
65. Grunewald S. and Walraven, J.C., 2001, Parameter-study on the influence of steel fibers and coarse aggregate content on the fresh properties of self-compacting concrete, *Cement and Concrete Research*, 31(12), pp 1793-1798.
66. Han L.H., 1998, Fire resistance of concrete filled steel tubular columns, *Advances in Structural Engineering*, 2(1), pp 35-39.
67. Han L.H., 2000, Fire resistance of concrete filled steel tubular beam-columns in China-state of the art. In *Proceedings of the Conference: Composite Construction in Steel and Concrete IV*, Banff, Alta, Canada, American Society of Civil Engineers, pp. 793-803.
68. Han L.H., 2001, Fire performance of concrete filled steel tubular beam-columns, *Journal of Constructional Steel Research*, 57(6), pp 695-709.
69. Han L.H., 2007, *Concrete-filled Structure, Theory and Practice (Second Edition)*, (Beijing: Science Press) (in Chinese).
70. Han L.H. and Huo J.S., 2003, Concrete-filled hollow structural steel columns after exposure to ISO-834 fire standard, *Journal of Structural Engineering, ASCE*, 129(1), pp 68-78.
71. Han L.H. and Yao G.H., 2004, Experimental behaviour of thin-walled hollow structural steel (HSS) columns filled with self-consolidating concrete (SCC), *Thin-Walled Structures*, 42(9), pp 1357-1377.

72. Han L.H. and Zhao X.L., 2003, Recent developments in concrete filled steel tubular structures in China, in *Proceedings of the International Conference of Advanced in Structures*, edited by Hancock G.J., Bradford M.A., Wilkinson T.J., Uy B. and Rasmussen K.J.R, (Rotterdam: Balkema), pp 907-913.
73. Han L.H., Huo J.S. and Wang Y.C., 2007, Behavior of steel beam to concrete-filled steel tubular column connections after exposure to fire, *Journal of Structural Engineering, ASCE*, 133(6), pp 800-814.
74. Han L.H., Tao Z., Huang H. and Zhao X.L., 2004, Concrete-filled double skin (SHS outer and CHS inner) steel tubular beam-columns, *Thin-Walled Structures*, 42(9), pp 1329-1355.
75. Han L.H., Xu L. and Zhao X.L., 2003a, Tests and analysis on the temperature field within concrete filled steel tubes with or without protection subjected to a standard fire, *Advances in Structural Engineering*, 6(2), pp 121-133.
76. Han L.H., Yang Y.F. and Xu L., 2003b, An experimental study and calculation on the fire resistance of concrete-filled SHS and RHS columns, *Journal of Constructional Steel Research*, 59(4),pp 427-452.
77. Han L.H., Yao G.H. and Zhao X.L., 2005, Tests and calculations for hollow structural steel (HSS) stub columns filled with self-consolidating concrete (SCC), *Journal of Constructional Steel Research*, 61(9), pp 1241-1269.
78. Han, L. H., Yao, G. H. & Tao Z. Behaviour of concrete-filled steel tubular members subjected to combined loading, *Thin-walled Structures*, 2007; 45(6),600-19.
79. Han L.H., Lu H., Yao G.H. and Liao F. Y., 2006, Further study on the flexural behaviour of concrete filled steel tubes, *Journal of Constructional Steel Research*, 62(69), pp 554-565.
80. Han L.H., Huang H., Tao Z. and Zhao X.L., 2006, Concrete-filled double skin steel tubular (CFDST) beam-columns subjected to cyclic bending, *Engineering Structures*, 28(12), pp 1698-1714.
81. Han L.H., Xu L. and Zhao X.L., 2003d, Tests and analysis on the temperature field within concrete filled steel tubes with or without protection subjected to a standard fire, *Advances in Structural Engineering*, 6(2), pp 121-133.
82. Han L.H., Zhao X.L., Yang Y.F. and Feng J.B., 2003c, Experimental study and calculation of fire resistance of concrete-filled hollow steel columns, *Journal of Structural Engineering, ASCE*, 129(3), pp 346-356.

83. Harmathy T.Z., 1978, Design to Cope with Fully Development Fires, In *Design of Buildings for Fire Safety*, Edited by Smith E.E. and Harmathy T.Z., (Boston: ASTM), pp. 198-276.
84. Harper C.A., 2004, *Handbook of Building Materials for Fire Protection*, (New York: McGraw-Hill).
85. Hass R., 1991, *On Realistic Testing of the Fire Protection Technology of Steel and Concrete Supports-Translation of BHP/NL/T/1444*, (Melbourne: BHP Research).
86. Holschemacher K. and Klug Y., 2002, *A Database for the Evaluation of Hardened Properties of SCC*, (Leipzig: University of Leipzig).
87. Huang C.S., Yeh Y.K., Liu H.T., Tsai K.C., Weng S.H. and Wu M.H., 2002, Axial load behavior of stiffened concrete-filled steel columns, *Journal of Structural Engineering, ASCE*, 128(9), pp 1222-1230.
88. Hwang S.-D., Khayat K.H. and Bonneau O., 2006, Performance-based specifications of self-consolidating concrete used in structural applications, *ACI Materials Journal*, 103(2), pp 121-129.
89. ISO-834, 1999, *Fire Resistance Tests:Elements of Building Construction*, (Geneva: International Organization for Standardization).
90. Johann M.A., Albano L.D., Fitzgerald R.W. and Meacham B.J., 2006, Performance-based structural fire safety, *Journal of Performance of Constructed Facilities*, 20(1), pp 45-53.
91. JSCE, 1999, *Recommendations and Materials: Recommendations for Construction of Self-compacting Concrete*, (Tokyo: Japan Society of Civil Engineers), pp. 417-437.
92. Karlsson B. and Quintiere J., 2000, *Enclosure Fire Dynamics*, (London: CRC Press).
93. Khoury G.A., 1995, Strain components of nuclear-reactor-type concretes during first heat cycle, *Nuclear Engineering and Design*, 156(1-2), pp 313-21.
94. Khoury G.A., Dias W.P. and Sullivan P.J.E., 1986, Deformation of concrete and cement paste loaded at constant temperatures from 140 to 724^{o}C, *Materials and Structures*, 19(110), pp 97-104.
95. Kim D.K., Chio S.M. and Chung K.S., 2000, Structural characteristics of CFT columns subjected fire loading and axial force, in the *Proceedings of 6th ASCCS Conference*, Los Angeles, pp. 271-278.

96. Klingsch W., 1985, New development in fire resistance of hollow section structures, in the *Proceedings of Symposium on Hollow Structural Sections in Building Construction*, (Chicago: ASCE), pp. 1-34.
97. Klingsch W., 1991, Optimization of cross section of steel composite columns, in the *Proceedings of the Third International Conference on Steel-Concrete Composite Structures*, Fukuoka, Japan, pp. 99-105.
98. Kodur V.K.R., 1997, Behaviour of high strength concrete-filled steel columns exposed to fire, In the *Proceedings of the Annual Conference of the Canadian Society for Civil Engineering*, (Montreal: Canadian Society for Civil Engineering), pp. 183-192.
99. Kodur V.K.R., 1998, Design equations for evaluating fire resistance of SFRC-filled HSS columns, *Journal of Structural Engineering, ASCE*, 124(6), pp 671-677.
100. Kodur V. K. R., 1998a, Performance of high strength concrete-filled steel columns exposed to fire, *Canadian Journal of Civil Engineering*, 25, pp.975-81.
101. Kodur V.K.R., 1999, Performance-based fire resistance design of concrete-filled steel columns, *Journal of Constructional Steel Research*, 51(1), pp 21-36.
102. Kodur V. Guildlines for fire resistant design of concrete-filled steel HSS columns-State-of-the-art and research needs. *International Journal of Steel Structures* 2007; 7(3): 173-172.
103. Kodur V. and McGrath R., 2003, Fire endurance of high strength concrete columns, *Fire Technology*, 39(1), pp 73-87.
104. Kodur V.K.R., 2005, Achieving fire resistance through steel concrete composite construction, in the *Proceedings of the Structures Congress and Exposition*, (New York: American Society of Civil Engineers), pp. 529-534.
105. Kodur V.K.R. and Lie T.T., 1996, Fire resistance of circular steel columns filled with fiber-reinforced concrete, *Journal of Structural Engineering, ASCE*, 122(7), pp 776-782.
106. Kodur V.K.R. and Lie T.T., 1997, Evaluation of fire resistance of rectangular steel columns filled with fibre-reinforced concrete, *Canadian Journal of Civil Engineering*, 24(3), pp 339-349.
107. Kodur V.K.R. and MacKinnon D.H., 1998, Simplified design of concrete-filled hollow structural steel columns for fire endurance, *Journal of Constructional Steel Research*, 46(1-3), pp 298-298.

108. Kodur V.K.R. and Mackinnon D.H., 2000, Design of concrete-filled hollow structural steel columns for fire endurance, *Engineering Journal, AISC*, 37(1), pp 13-24.
109. Kodur V.K.R., Wang T.C. and Cheng F.P., 2004a, Predicting the fire resistance behaviour of high strength concrete columns, *Cement and Concrete Composite*, 26(3), pp 141-153.
110. Kodur V.K.R., Cheng F.P., Wang T.C. and Sultan M.A., 2003, Effect of strength and fibre reinforcement on fire resistance of high-strength concrete columns. *Journal of Structural Engineering ASCE*, 129(2), pp. 253-59.
111. Kvedaras A.K. and Sapalas A., 1999, Research and practice of concrete-filled steel tubes in Lithuania, *Journal of Constructional Steel Research*, 49(2), pp 197-212.
112. Lawson R.M., 2001, Fire engineering design of steel and composite buildings, *Journal of Constructional Steel Research*, 57(12), pp 1233-1247.
113. Li L.Y. and Purkiss J., 2005, Stress-strain constitutive equations of concrete material at elevated temperatures, *Fire Safety Journal*, 40(7), pp 669-686.
114. Lie T.T., 1992, *Structural Fire Protection: ASCE Manuals and Reports on Engineering Practice No. 78*, (New York: ASCE).
115. Lie T.T., 1994, Fire resistance of circular steel columns filled with bar-reinforced concrete, *Journal of Structural Engineering, ASCE*, 120(5), pp 1489-1509.
116. Lie T.T. and Chabot M., 1990, Method to predict the fire resistance of circular concrete filled hollow steel columns, *Journal of Fire Protection Engineering*, 2(4), pp 111-128.
117. Lie T.T. and Stringer D.C., 1992, *Evaluation of the Fire Resistance of Reinforced Concrete Columns with Rectangular Cross-section*, NRC-CNRC Internal Report No. 601.
118. Lie T.T. and Chabot M., 1992a, *Experimental Studies on the Fire Resistance of Hollow Steel Columns Filled with Plain Concrete*, NRC-CNRC Internal Report No. 611.
119. Lie T.T. and Chabot M., 1992b, *Experimental Studies on the Fire Resistance of Hollow Steel Columns Filled with Plain Concrete*, NCRC.
120. Lie T.T. and Stringer D.C., 1994, Calculation of the fire resistance of steel hollow structural section columns filled with plain concrete, *Canadian Journal of Civil Engineering*, 21(3), pp 382-385.

121. Lie T.T. and Irwin, R.J., 1995, Fire resistance of rectangular steel columns filled with bar-reinforced concrete, *Journal of Structural Engineering, ASCE*, 121(5), pp 797-805.
122. Lie T.T. and Kodur V.K.R., 1996a, Fire resistance of steel columns filled with bar-reinforced concrete, *Journal of Structural Engineering, ASCE*, 122(1), pp 30-36.
123. Lie T.T. and Kodur V.K.R., 1996b, Thermal and mechanical properties of steel-fibre-reinforced concrete at elevated temperatures, *Canadian Journal of Civil Engineering*, 23(2), pp 511-517.
124. Lie T.T. and Kodur V.K.R., 1997, Performance-based design methods for fire resistance. Structures, In the *Proceedings of ASCE Congress*, (New York: ASCE), pp. 523-528.
125. Lie T.T. and Caron S.E., 1988, *Fire Resistance of Hollow Steel Columns Filled with Silicious Aggregate Concrete: Test Results*, NRC-CNRC Internal Report, No. 570.
126. Lie T.T. and Chabot M., 1998, *Fire Resistance of Hollow Steel Columns Filled with Carbonate Aggregate Concrete: Test Results*, NRC-CNRC Internal Report No. 573.
127. Lin M.L. and Tasi K.C., 2005, Mechanical behaviour of double-skinned composite steel tubular columns, in the *Proceedings of the First International Conference on Steel & Composite Structures*, Pusan, Korea.
128. Lu, H., Zhao, X.L. and Han, L.H., 2005. Temperatures distribution in self-compacting concrete columns, in *Proceedings of the 4th Australasian Congress on Applied Mechanics,* (Institute of Materials Engineering Australasia Ltd: Melbourne) pp. 81-86.
129. Lu H., Zhao X.L. and Han L.H., 2006, Fire resistance of SCC filled square hollow structural sections, In *Proceedings of the 11th International Symposium and IIW International Conference on Tubular Structures*, edited by Packer J.A. and Willibald S, (London: Taylor & Francis Group) pp. 403-410.
130. Lu, H., Zhao, X.L. and Han, L.H., 2009, Fire behaviour of high strength self-consolidating concrete filled steel tubular stub columns. *Journal of Constructional Steel Research,* 65(10-11), pp. 1995-2010.

131. Margaret L., 1986, The behaviour of a fire, in *the Proceedings of the International Conference on Design of Structures Against Fire*, (London: Elsevier Applied Science Publishers).
132. Meacham B.J., 1997, Introduction to performance-based fire safety analysis and design with applications to structural fire safety, in the *Proceedings of the ASCE Structures Congress*, (New York: ASCE), pp. 529-533.
133. Montague P., 1975, A simple composite construction for cylindrical shells subjected to external pressure, *Journal of Mechanical Engineering and Science*, 17(2), pp: 105-113.
134. Nakanishi K., Kitada T. and Nakai H., 1999, Experimental study on ultimate strength and ductility of concrete filled steel columns under strong earthquake, *Journal of Constructional Steel Research*, 51(3), pp 297-319.
135. Narayanan R., 1998, *Steel-concrete Composite Structures: Stability and Strength*. (London: Elsevier Applied Science).
136. Nehdi M. and Ladanchuk J.D., 2004, Fiber synergy in fiber-reinforced self-consolidating concrete, *ACI Materials Journal*, 101(6), pp 508-517.
137. Nethercot D.A., 2004, *Composite Constructuion*. (New York: Taylor & Francis).
138. Nishiyama I and Morino S, 2004, US-Japan cooperative earthquake research program on CFT structures: achievement on the Japanese side, *Progress in Structural Engineering and Materials*, 6(1), pp 39-55.
139. Noumowe A., Carre H., Daoud A. and Toutanji H., 2006, High-strength self-compacting concrete exposed to fire test, *Journal of Materials in Civil Engineering*, 18(6), pp 754-758.
140. O'Meagher A.J., Bennetts I.D., Hutchinson G.L. and Stevens L.K., 1991, *Modelling of HSS Columns Filled with Concrete in Fire*, BHPR/ENG/R/91/031/PS69.
141. Okada T., Yamaguchi T., Sakumoto Y. and Keira K., 1991, Load heat tests of full-scale columns of concrete-filled tubular steel structure using fire-resistant steel for buildings, in the *Proceedings of the Third International Conference on Steel-Concrete Composite Structures*, Fukuoka, Japan, pp. 101-106.
142. Okamura H., 1997, Self-compacting high-performance concrete, *Concrete International*, 19(7), pp 50-54.
143. Okamura H. and Ouchi M., 2003, Self-compacting concrete, *Journal of Advanced Concrete Technology*, 1(1), pp 5-15.

144. Omoto T. and Ozawa K., 1999, *Recommendation for Self-compacting Concrete*, (Tokyo: Japan Society of Civil Engineers).
145. Ouchi M., Osterberg T., Hallberg S. E., Lwin M., 2003, Applications of self-compacting concrete in Japan, Europe and the United States, In the *Proceedings of* the *3rd International Symposium on High Performance Concrete*, Orlando, Florida, USA, pp. 20.
146. Outinen J., Kesti J. and Makelainen P., 1997, Fire design model for structural steel S355 based upon transient state tensile test results, *Journal of Constructional Steel Research*, 42(3), pp 161-169.
147. Patterson N.L., Zhao X.L., Wong B.M., Ghjel J. and Grundy P., 1999, Elevated temperature testing of composite columns, In: *Advances in Steel Structures*, Edited by Cheng S.L. and Teng J.G., Oxford, pp. 1074-1054..
148. Persson B., 2001, A comparison between mechanical properties of self-compacting concrete and the corresponding properties of normal concrete, *Cement and Concrete Research*, 31(2), pp 193-198.
149. Persson B., 2004, Fire resistance of self-compacting concrete. *Materials and Structures*, 37(273), pp 575-584.
150. Phan L.T. and Carino N.J., 1998, Review of mechanical properties of HSC at elevated temperature, *Journal of Materials in Civil Engineering*, 10(1), pp 58-64.
151. Plank R.J., 2000, The performance of composite-steel-framed building structures in fire, *Progress in Structural Engineering and Materials*, 2(2), pp 179-186.
152. Poh K.W., 1997, General stress-strain equation, *Journal of Materials in Civil Engineering*, 9(4), pp 214-217.
153. Poh K.W., 1998, General creep-time equation, *Journal of Materials in Civil Engineering*, 10(2), pp 118-120.
154. Purkiss J., 1986, Heat temperature effects, in the *Proceedings of the International Conference on Design of Structures Against Fire*. (London: Elsevier Applied Science Publishers).
155. Purkiss J.A., 2007, *Fire Safety Engineering: Design of Structures* (Second Edition) (Oxford: Elsevier Ltd).
156. Ramberg W. and Osgood W., 1943, *Description of Stress Strain Curves by Three Parameters, Technical Note No. 902*, (Washington DC: National Advisory Committee for Aeronautics).
157. Reinhardt H.W. and Stegmaier M., 2006, Self-consolidating concrete in fire, *ACI Materials Journal*, 103(2), pp 130-135.

158. Renaud C., Aribert J.M. and Zhao B., 2003, Advanced numerical model for the fire behaviour of composite columns with hollow steel sections, *Steel and Composite Structures*, 3(2), pp 75-95.
159. Sakumoto Y., Okada T., Yoshida M. and Tasaka S., 1994, Fire resistance of concrete-filled, fire-resistant steel-tube columns, *Journal of Materials in Civil Engineering*, 6(2), pp 169-184.
160. Sakumoto Y. and Saito H., 1995, Fire-safe design of modern steel buildings in Japan, *Journal of Constructional Steel Research*, 33(1-2), pp 101-123.
161. Schneider U., 1986, Modelling of concrete behaviour at high temperatures, In *Proceedings of the International Conference on Design of Structures Against Fire*, Edited by: Anchor R.D., Malhotra H.L. and Purkiss J.A., (London: Elsevier Applied Science Publishers), pp. 53-69.
162. Schutter G.D., 2005, *Guidelines for Test Fresh Self-compacting Concrete*, TESTING-SCC.
163. Shanmugan N.E. and Lakshmi B., 2001, State of the art report on steel-concrete composite columns, *Journal of Constructional Steel Research*, 57(10), pp 1041-80.
164. Skarendahl A. and Petersson O., 2001, *State-of-the-art Report of RILEM Technical Committee 174-SCC, Self-Compacting Concrete*, RILEM.
165. SFPE, 2002, *SFPE Handbook of Fire Protection Engineering*, (Quincy: The Society of Fire Protection Engineering).
166. Su N., Hsu K.C. and Chai H.W., 2001, A simple mix design method for self-compacting concrete, *Cement and Concrete Research*, 31(12), pp 1799-1807.
167. Su N. and Miao B., 2003, A new method for the mix design of medium strength flowing concrete with low cement content, *Cement and Concrete Composites*, 25(2), pp 215-222.
168. Tan K.H. and Tang C.Y., 2004, Interaction model for unprotected concrete filled steel columns under standard fire conditions, *Journal of Structural Engineering, ASCE*, 130(9), pp 1405-1413.
169. Tao Z. and Han L.-H., 2006, Behaviour of concrete-filled double skin rectangular steel tubular beam-columns, *Journal of Constructional Steel Research*, 62(7), pp 631-646.
170. Tao Z., Han L.H. and Wang Z.B., 2005, Experimental behaviour of stiffened concrete-filled thin-walled hollow steel structural (HSS) stub columns, *Journal of Constructional Steel Research*, 61(7), pp 962-983.

171. Tao Z., Han L.H. and Zhao X.L., 2004, Behaviour of concrete-filled double skin (CHS inner and CHS outer) steel tubular stub columns and beam-columns, *Journal of Constructional Steel Research*, 60(8), pp 1129-1158.
172. Tao Z., Han L.H., 2003, Tests and mechanics model for concrete-filled double skin steel tubular stub columns. In *Proceedings of the International Conference on Advances in Structures*: Edited by Hancock G., Bradford, M.A., Wilkinson and T.J., Uy B., Rasmussen K.J.R., (Netherlands: A.A. Balkema Publishers), pp. 899-905.
173. Teng J.G., Yu T., Wong Y.L. and Dong S.L., 2006, Hybrid FRP-concrete-steel tubular columns: Concept and behaviour, *Construction and Building Materials*, 21(4), pp 846-854.
174. The Concrete Centre, 2004, *Concrete and Fire: Using Concrete to Achieve Safe, Efficient Buildings and Structures*, (Camberley: The Concrete Centre).
175. Thomas I.R. and Bennetts I.D., 1992, Developments in the design of steel structures for fire, *Journal of Constructional Steel Research*, 23(1-3), pp 295-312.
176. TR-63, 2003, *Interim Guideline for the Use of Self-consolidating Concrete in Precast/Prestressed Concrete*, PCI Interim SCC Guidelines TR-63, pp. 148.
177. Twile L., Hass R., Klingsch W., Edwards M. and Dutta D., 1996, *For Structural Hollow Sections Exposed to Fires*, (Köln: TUV-Verlag).
178. Twilt L., 1988, Strength and deformation properties of steel at elevated temperatures: Some practical implications, *Fire Safety Journal*, 13(1), pp 9-15.
179. Usmani A.S. and Lamont S., 2004, Key events in the structural response of a composite steel frame structure in fire, *Fire and Materials*, 28(2-4), pp 281-297.
180. Uy B., 1995, Bradford MA. Local buckling of cold formed steel in composite structural elements at elevated temperatures. *Journal of Constructional Steel Research*. 34(1), pp.53-73.
181. Uy B. and Patil S.B., 1996, Concrete filled high strength steel box columns for tall buildings: behaviour and design. *Structural Design of Tall Buildings*, 5(2), pp 75-94.
182. Uy B., 1998, Local and post-local buckling of concrete filled steel welded box columns, *Journal of Constructional Steel Research*, 47(1-2), pp 47-72.
183. Uy B., 2001, Strength of short concrete filled high strength steel box columns. *Journal of Constructional Steel Research*, 57(2), pp 113-134.
184. Vachon M., 2002, ASTM puts self-consolidating concrete to the test, *Standardization News*, 30(7), pp 34.

185. Varma A.H., Ricles J.M., Sause R. and Lu L.-W., 2004, Seismic behavior and design of high-strength square concrete-filled steel tube beam columns. *Journal of Structural Engineering, ASCE*, 130(2), pp 169-179.
186. Wang, Y.C., 1990, The effect of structural continuity on the fire resistance of concrete filled columns in non-sway frames. *Journal of Constructional Steel Research.* 50(2), pp.177-97.
187. Wang Y.C., 1997, Some considerations in the design of unprotected concrete-filled steel tubular columns under fire conditions, *Journal of Constructional Steel Research*, 44(3), pp 203-223.
188. Wang Y.C., 1999, The effect of structural continuity on the fire resistance of concrete filled columns in non-sway frames, *Journal of Constructional Steel Research*, 50(2), pp 177-197.
189. Wang Y.C., 2000, A simple method for calculating the fire resistance of concrete-filled CHS columns, *Journal of Constructional Steel Research*, 54(3), pp 365-386.
190. Wang Y.C., 2003, *Steel and Composite Structures: Behaviour and Design for Fire Safety*, (London: Spon Press).
191. Wang Y.C., 2005, Performance of steel-concrete composite structures in fire, *Progress in Structural Engineering and Materials*, 7(2), pp. 86-102.
192. Wang Y.C. and David J.M., 2003, An experimental study of the fire performance of non-sway loaded concrete-filled steel tubular columns assembles with extend end plate connections, *Journal of Constructional Steel Research*. 59(7), pp. 819-838.
193. Wang Y.C. and Kodur V.K.R., 2000, Research toward use of unprotected steel structures, *Journal of Structural Engineering, ASCE*, 126(12), pp 1442-1450.
194. Wang Y.C. and Orton A. H., 2008, Fire resistance design of concrete filled tubular steel columns, *The Structural Engineer*, 7(October), pp. 40-45.
195. Wei S., Mau S.T., Vipulanandan C. and Mantrala S.K., 1995a, Performance of new sandwich tube under axial loading: Analysis, *Journal of Structural Engineering, ASCE*, 121(12), pp 1815-1821.
196. Wei S., Mau S.T., Vipulanandan C. and Mantrala S.K., 1995b, Performance of new sandwich tube under axial loading: Experiment, *Journal of Structural Engineering, ASCE*, 121(12), pp 1806-1814.
197. Wright H., Oduyemi, T. and Evans H.R., 1991, The experimental behaviour of double skin composite elements, *Journal of Constructional Steel Research*, 19(2), pp 111-132.

198. Xiao Y., He W.H. and Choi K.K., 2005, Confined concrete-filled tubular columns, *Journal of Structural Engineering, ASCE,* 131(3), pp 488-497.
199. Yagishita F., Kitoh H., Sugimoto M., Tanihira T. and Sonoda K., 2000, Double-skin composite tubular columns subjected to cyclic horizontal force and constant axial force, in *the Proceedings of the 6th ASCCS Conference,* pp. 497-503.
200. Young B. and Ellobody E., 2006, Experimental investigation of concrete-filled cold-formed high strength stainless steel tube columns. *Journal of Constructional Steel Research*, 62(5), pp 484-492.
201. Yu T.T., 2006, Flexural behavior of hybrid FRP-concrete-steel double-skin tubular members, *Journal of Composites for Construction*, 10(5), pp 443-452.
202. Zeng J.L., Tan K.H. and Huang Z.F., 2003, Primary creep buckling of steel columns in fire, *Journal of Constructional Steel Research*, 59(8), pp 951-970.
203. Zhao X.L. and Grzebieta R., 2002, Strength and ductility of concrete filled double skin (SHS inner and SHS outer) tubes, *Thin-Walled Structures*, 40(2), pp 199-213.
204. Zhao X.L., Han B. and Grzebieta R.H., 2002a, Plastic mechanism analysis of concrete-filled double-skin (SHS inner and SHS outer) stub columns, *Thin-Walled Structures*, 40(10), pp 815-833.
205. Zhao X.L., Grzebieta R. and Mlchalakani M., 2002b, Tests of concrete-filled double skin CHS composite stub columns, *Steel and Composite Structures: An International Journal*, 2(2), pp 129-146.
206. Zhao X.L. and Han L.H., 2006, Double skin composite construction, *Progress in Structural Engineering and Materials*, 8(3), pp 93-102.
207. Zhao, X.L., Wilkinson, T. and Hancock, G.J., 2005, Cold-formed tubular members and connections, (Oxford: Elsevier Science).
208. Zhao, X.L., Tong, L.W. and Wang, X.Y., 2010, CFDST stub columns subjected to large deformation axial loading, *Engineering Structures*, in press.
209. Zhou F. and Young B., 2008, Tests of concrete-filled aluminium stub columns, *Thin-Walled Structures,* 46(6), pp. 573-583.
210. Zhou F. and Young B., 2009, Concrete-filled aluminium circular hollow section column tests, *Thin-Walled Structures,* 47(11), pp. 1272-1280.